NASA CR-145136

SCOUT NOZZLE DATA BOOK

by

S. Shields

DECEMBER 1976

Prepared Under Contract No. NAS1-12500 Task R-52 by

VOUGHT CORPORATION
Dallas, Texas

for

NASA

National Aeronautics and
Space Administration

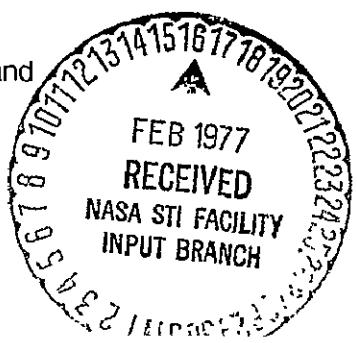

SCOUT NOZZLE DATA BOOK

By S. Shields

Prepared Under Contract No. NAS1-12500 Task R-52 by

VOUGHT CORPORATION
Dallas, Texas

for

NASA

National Aeronautics and
Space Administration

FOREWORD

This document is a technical program report prepared by the Vought Systems Division, LTV Aerospace Corporation, under NASA Contract NAS1-12500. The program was sponsored by the SCOUT Project Office of the Langley Research Center with Mr. W. K. Hagginbothom as Technical Monitor.

The author wishes to acknowledge the contributions of Mr. R. A. Hart in the area of Material Process and Fabrication and the SCOUT propulsion personnel in supplying reports and other documentation as well as their efforts in reviewing the various sections of this document.

Pages i and ii are blank.

TABLE OF CONTENTS

TABLE OF CONTENTS (Continued)

TRIDENT NOZZLES DATA

TABLE OF CONTENTS (Continued)

LIST OF FIGURES

LIST OF FIGURES (Continued)

LIST OF FIGURES (Continued)

LIST OF TABLES

LIST OF TABLES (Continued)

SUMMARY

This report summarizes available analyses and material property information relevant to the design of four rocket motor nozzles currently incorporated in the four solid propellant rocket stages of the NASA SCOUT launch vehicle. The nozzles covered in this report include those for the following motors:

First Stage	-	Algol IIIA
Second Stage	-	Castor IIA
Third Stage	-	Antares IIA
Fourth Stage	-	Altair IIIA

Separate sections for each nozzle provide complete data packages. Appendix C includes information on the Antares IIB motor which had limited usage as an alternate motor for the third stage.

Projected SCOUT payload requirements necessitate maximum utilization of the performance and structure capability inherent in the SCOUT propulsion system, i.e., maximum motor and nozzle performance and minimum inert weight within the existing SCOUT vehicle envelope. Several high energy propellants are currently under development in the solid propellant rocket industry and the effect of using these propellants in SCOUT motors is being studied. The most recent motor development program using these high energy propellants is the U.S. Navy's Trident (C-4) Program. The results of the Trident nozzle material screening, selection and design implementation are included in this study. A review of those designs and the related nozzle development program is used as the basis for recommending possible design improvements for SCOUT motor nozzles within existing SCOUT vehicle constraints.

Two appendices summarize previous SCOUT nozzle studies. Appendix A summarizes SCOUT nozzle materials, drawings, geometry and specifications. An industry survey of new material developments was made. The materials were compared and evaluated for possible application to

SCOUT nozzle designs. Appendix B selected several promising materials. Two X-259 motors were used to test two development nozzle designs. The results of that study and related analyses are included in the appendix.

The results of finite element analyses of each SCOUT motor nozzle are included in this report. Material properties used in each analysis are also presented (Tables IV, X, XV, XX and XXX). Reliable material properties, particularly at elevated temperature, are difficult to obtain and often differ significantly for identical materials from different sources. In addition, there are significant differences in loading and heating rates between a motor firing and laboratory tests. Time at temperature is also important for phenolic laminates. These problems were discussed with each SCOUT motor vendor and an approximate assessment of the accuracy of each nozzle stress analysis was made and are included in this report.

Appendix A summarizes an investigative study by VSD of nozzle materials. Material properties in that Appendix (Figures A-1.1 through A-6.9) were considered to be the most reliable values available at that time (1969). More recent tests (1971, Table XXXI) show a strong dependency on heating rate for coefficient of thermal expansion values of two phenolic laminates. This property linearly affects calculated stress and strain values in the finite element analysis.

SCOUT
NOZZLES DATA

INTRODUCTION

The nozzles described in this section are those for the rocket motors currently used in the SCOUT propulsion system, as follows:

Stage	Motor
First	Algol IIIA
Second	Castor IIA
Third	Antares IIA
Fourth	Altair IIIA

Antares IIA and IIB nozzles have been used on third stage motors. The throat size of the IIB nozzle is smaller, resulting in higher motor pressure and increased performance. Several material changes were also made in the IIB nozzle design. Alternate first (Algol IIC) and fourth (Altair IIA) stage motors, as well as a fifth stage motor, Alcyone IA, have also been used on SCOUT but were not included in the present study because of their infrequent usage. Details of the Antares IIB nozzle are presented in Appendix C.

In addition to nozzle descriptions and geometry, complete information on nozzle thermal and pressure environment is included. From existing analyses critical temperature and stress distributions are summarized. The material properties which were used in those analyses are included in each motor section. Minimum margins of safety and maximum temperatures are noted. Measured thermocouple data from static tests and flight conditions and post test erosion data are included. A brief history of development and service life problems experienced for each nozzle are summarized.

ALGOL IIIA

Background. - Algol IIIA is the SCOUT vehicle first stage booster motor. The previous Algol IIB nozzle had an RVA monolithic graphite throat. In addition to differences in the steel housing, the graphite throat was replaced by a graphite phenolic tape wrapped insert in the Algol IIC to provide greater structural reliability. Other changes included use of a silica phenolic throat insulator and a forward insulator made in two parts using a carbon phenolic tape wrapped section just forward of the insert. The only difference between the Algol IIC nozzle and the Algol IIIA nozzle is a slightly smaller throat diameter in the Algol IIC. These two nozzles were the first SCOUT motors to use a tape wrapped graphite phenolic throat insert. The Algol IIIA nozzle geometry and materials are shown in Figures 1 and 2. Table I lists alternate qualified materials for each component in this nozzle.

Performance Data. - The SCOUT first stage motor has a maximum expected operating pressure (MEOP) of 6.7×10^6 N/m^2 (970 psi) and a flame temperature of 3366°K (5600°F). The propellant is a PBAN composite with 17% aluminum. Motor performance parameters which affect the nozzle environment are summarized in Table II. Time dependent variations in chamber pressure are shown in Figure 3.

Drawings and Specifications. - Table III lists the Algol IIIA nozzle drawing and material specifications. Component fabrication procedures for this motor are described by Kaiser Aerospace and Electronic Corporation Production Routing Orders (PRO No.). These PRO's reference Production Illustrations (PI No.) for detailed process steps such as temperature, pressure and machining operations.

Material Description. - Each material used in the Algol IIIA nozzle is described in this section. Vendor process specifications and applicable procedures are summarized in Table III and Figure 4 to describe the manufacturing operations and sequence of nozzle assembly. The materials used in this nozzle were selected on the basis of previous usage in similar environment, their good elevated temperature characteristics, availability and cost. Reliability and performance have been demonstrated by two development and three qualification ground firing tests and nine successful flights to date.

Elevated temperature dependent material properties are shown for the Algol IIIA nozzle materials in Table IV. The data for most materials is available up to 700°F but rather limited at higher temperatures. In the case of reinforced plastics such as graphite, carbon and silica phenolic laminates, the properties of the materials change significantly due to carbonization of the resin. The materials have entirely different characteristics in this state at elevated temperature as compared to the original material condition. This process is dependent on length of time at the elevated temperatures and only limited information is available in this area.

Temperature dependent material properties for each of the Algol III materials are shown in Table IV. A brief description of each material follows.

4S 5232 (forward entrance insulation) is a silica fabric impregnated with a silica filled MIL-R-9299 phenolic resin. The current vendor designation for this material is 4S 4132. The reinforcement is Sil-Temp 84, Astrosil 84 or Refrasil C-100-48.

MX 4926 or FM 5072 (aft entrance insulation) is a carbon fabric impregnated with a high temperature phenolic resin containing carbon reinforcement. The resin is a MIL-R-9299 Type II phenolic, the carbon fabric is Hitco CCA2, polycarbon CSA or Union Carbide VCK.

MXG 175 or FM 5014 (throat insert and exit cone insulation) is a graphite fabric impregnated with a high temperature phenolic resin. The fabric reinforcement is Hitco GI550 and the high temperature phenolic resin used is Evercoat CE-201 for MXG 175 and MIL-R-9299 for FM 5014.

MX 2600 (throat insulation and exit cone insulation) is a silica fabric impregnated with a high temperature phenolic resin containing silica reinforcement. The phenolic resin must meet specification MIL-R-9299, Type II phenolic resin. The silica fabric is Sil Temp 84 or Hitco C100-48. The reinforcement, or filler, is silica dioxide of 98% purity.

Epon 815 is an epoxy resin, used with curing agent A, to impregnate the glass cloth and roving in the exit cone overwrap. The resin cures at room temperature.

HT 424 is a high temperature epoxy-phenolic film adhesive that meets the requirements of MIL-A-5090, Type III structural adhesive. It is a gray film, moderately tacky with a glass fabric reinforcement. Assemblies may be bonded at pressures ranging from contact to 100 psi depending on the applications. The adhesive curing temperature is $439^{\circ}K \pm 5^{\circ}$ ($330^{\circ}F \pm 10^{\circ}$) and cure time is 30 minutes at temperature.

Epon 913 is a two-part epoxy adhesive consisting of a light gray thixotropic paste (Part A) and a dark amber liquid curing agent (Part B). The adhesive is prepared by thoroughly mixing 100 parts of Part A with 12 parts of Part B. It combines long pot life with the ability to cure at mild temperatures in a relatively short time.

Properties of plastic laminates are closely related to resin content and density. Volatile content and percent filler are useful for acceptance criteria. These (vendor) values are tabulated below for each of the nozzle materials.

Material	Resin solids %		Resin filler, %		Volatiles, %		Flow, %	
	Min	Max	Min	Max	Min	Max	Min	Max
MX 2600	29	33	6	10	3	7	-	-
MX 4926	31.5	36.5	-	-	4	8	1.0	-
FM 5072	34	(Typ.)	-	-	-	4	-	-
MXG 175	31	37	-	-	2	8	3	20
FM 5014	31	37	-	-	-	4	-	-
4S 5232	31	37	-	-	-	7	-	-

The following thermal and physical properties were used in the Algol IIIA analysis and were obtained from References (1) and (2). Lap shear strength values for two adhesives, HT 424 and 913, are given below. A third adhesive, 815 with curing agent A, is used to impregnate the glass cloth prior to applying the filament overwrap on the exterior of the exit cone. No physical properties were presented in the above references for this material.

Adhesives

Material	Vendor	Bond Thickness, M	Lap Shear Strength, N/m^2				
			Room Temperature	395°K (250°F)	533°K (500°F)	672°K (750°F)	811°K (1000°F)
HT 424	Bloomingdale Rubber Co.	$.378 \times 10^{-3}$ (.015 in)	13.8×10^6 (2000 psi)	11.0×10^6 (1600)	8.27×10^6 (1200)	6.21×10^6 (900)	4.48×10^6 (650)
913	Hysol Corp.	$.126 \times 10^{-3}$ (.005) to $.505 \times 10^{-3}$ (.020 in)	13.8×10^6 (2000 psi)	2.76×10^6 (400)	----	----	----

Fabrication and Process.- The fabrication and inspection procedures are summarized for each component of the Algol IIIA nozzle in Figure 4. That figure briefly summarizes the fabrication procedures and quality inspections for each nozzle component. Process quality control tests are summarized in Table V.. Test specimens are obtained from rings cut off of the end of the cured component.

Thermal Data

The nozzle thermal analysis included the entrance cone, throat insulator, throat, and exit cone. The Algol IIIA flight nozzle was designed to satisfy the following thermal design criteria (Reference 1).

Component	Ablated Depth Safety Factor	Maximum External Surface Temperature ^{o}K
Aft Closure	1.75	345 ($160^{o}F$)
Nozzle	1.50	395 ($250^{o}F$)

Char and Erosion. - The ablation analysis shows that all components meet the required safety factor on ablation depth. The greatest amount of ablation occurs in the silica phenolic entrance cone where a maximum of 0.04 m (1.57 in) is removed. The maximum throat ablation depth is 0.0127 m (0.50 in.), the maximum ablation in the graphite cloth exit cone region is 0.00535 m (0.21 in.) just aft of the insert and the maximum ablated depth in the silica phenolic exit cone is 0.00918 m (0.36 in.) just aft of the graphite phenolic liner. The ablation and char profiles at burnout are shown in Figure 5.

Temperature Distribution. - The temperatures for all regions of the steel nozzle housing never exceed $330^{o}K$ ($150^{o}F$). Ten stations are identified in Figure 1. At each of these stations the transient temperature distributions through the thickness are shown in Figures 6 through 15 at several times throughout the 81 second firing duration. From the analysis it was concluded that the nozzle is thermally adequate and meets all thermal and ablation criteria.

Structural Analysis

The following components were analyzed by Chemical Systems Division of United Technology Corporation (Reference 2):

Steel nozzle housing

Entrance insulation

Throat insert package

Exit cone

Adhesive bonds

The steel housing was analyzed by means of a computer method which employed finite length axisymmetric rings with compatible edge displacements. This analysis established the required boundary conditions at the nozzle attach flange in the nozzle finite element analysis. Margins of safety for the shell structure were also determined from this analysis; but these are known to be conservative because no allowance was made in the calculations for stiffness of the insulators. The throat finite element model is shown in Figure 16.

The entrance insulation, throat insert package and exit cone were analyzed using a finite element stress analysis computer program capable of handling orthotropic axisymmetric solids. The combined effects of temperature distributions and pressure were considered at two times, t + 0 seconds and t + 55 seconds. Degradation of material properties due to heating was incorporated into the analysis and margins of safety calculations were made. A structural analysis of the nozzle assembly for proof pressure was also performed.

Loads. - Motor pressure loads used in the structural analysis of the nozzle are defined by the pressure history curve shown in Figure 3 for the 311°K (100°F) motor.

The nozzle proof test pressure is 2.908×10^6 N/m^2 (422 psi); the steel housing proof test pressure is 5.52×10^6 N/m^2 (800 psi).

Jet vane loads are not included in the nozzle analysis since these are reported by LTV to have no effect on the nozzle structure. Vibration and acceleration forces are not included in the structural analysis.

Environment. - The temperature distributions determined in the nozzle during motor operation at various times from thermal analysis were incorporated into the structural analysis of the primary components of the nozzle. Storage environment has no impact on the nozzle structural analysis.

Factors of Safety. - The required factors of safety for this nozzle are as follows:

Limit load: anticipated load on structure

Design yield load: 1.15 x limit load

Design ultimate load: 1.36 x limit load

A factor of safety of 1.36 was used for combined pressure and thermal loads. A factor of 1.0 was used for proof test stresses. Margins of safety are defined as follows for this condition. Limit stresses are maximum calculated stresses from expected pressure and thermal loads.

$$M.S. = \frac{\text{Material Ultimate Stress}}{\text{F.S. x Limit Stress}} - 1$$

Results of Analyses. - For flight load conditions the structural analysis showed adequate strength in all components and bond lines. Minimum margin of safety in nozzle components was 0.03 in the graphite phenolic insert. This was based on a factor of safety of 1.36 applied to combined pressure and thermal stresses. Relatively low margins of safety, based on static analysis which assume linear elastic theory, are considered acceptable for plastic laminates due to their apparent plastic behavior at elevated temperature and demonstrated past reliability. Calculated margins of safety for all components for two flight conditions and for proof test conditions are listed in Table VI.

Estimated Accuracy of the Algol IIIA Nozzle Analysis. - The analysis of this nozzle was performed by means of a finite element computer program for orthotropic axisymmetric solids. This nozzle differed from the previous SCOUT first stage motor, Algol IIB, mainly in the substitution of graphite phenolic laminate material in place of the previous ATJ graphite throat. In the Algol IIIA nozzle analysis (Reference 2) margins of safety were based exclusively on comparisons of maximum uniaxial stresses with design allowable uniaxial material strength. A minimum margin of safety of 0.03 for radial tension was determined in the graphite phenolic insert late in firing. To date there have been 18 successful firings of this nozzle, indicating a successful design with apparent conservatism in the relatively low calculated margin of safety.

The same vendor performed an analysis of expected accuracy of the Altair IIIA nozzle (see section titled "Parametric Variance Study" in the Altair IIIA section of this report). Although the "probability of no cracking" approach used for the graphite insert of that nozzle was also applied to the carbon phenolic retainer, such application is highly conservative. Plastic laminates, particularly at elevated temperatures, exhibit large plastic, non-linear elongation prior to failure. This is particularly beneficial when the principal stresses are due to thermal gradients. This inherent quality is the principal reason that a graphite phenolic insert was selected for the Algol IIIA motor nozzle. The 3-sigma variance of carbon phenolic at 1370^{o}K (2003^{o}F) was calculated (Reference 4) for standard inspection requirements to be 92% for stress and 19% for strength. These variances were calculated for use with typical probability methods assuming standard distributions. For these variances the probability of success for the Altair IIIA nozzle was determined to be 1.0 (Reference 4). The same probability of success may also be considered applicable to the Algol IIIA nozzle.

Problem Areas. - The present SCOUT first stage motor nozzle has experienced no problems during static firing or flights. Only two possible problem areas were analyzed during development and qualification

phases: (1) local bond failure at the forward edge of the throat insulation to steel shell interface; and (2) "frothing" of the leak detector fluid on the surface of the insert during leak tests.

Structural analysis of the nozzle for the 800 psi proof pressure condition predicted local unbond between insert and overwarp for a distance of approximately 0.0205 M (0.8 in) from the leading edge. Three nozzles were proof tested to this level during development. Ultrasonic inspection indicated local unbond at the leading edge of the insulation to steel shell interface on all three nozzles. Two of these motors were static fired successfully, and the third was sectioned. After firing, the two development nozzles were also sectioned but no nozzle degradation could be detected as a result of the previous local unbond condition. Maximum length of unbond was measured at .033 M (1.8 in).

A proof pressure level of 355 psi produces the same radial deflection at the local "unbond area" as would occur during flight. The selected proof pressure of 422 psi for the nozzle provides a suitable overtest and is used for production nozzles. Subsequently, fifteen Algol IIIA nozzles have been proof tested at 2.91×10^6 N/m^2 (422 psi) with no indications of unbond. Of these nozzles, nine have been used on successful SCOUT flights.

Proof pressure levels for the Algol IIIA motor included:

Motor case = 7.357×10^6 N/m^2 (1067 psi)

Nozzle steel shell = 5.516×10^6 N/m^2 (800 ± 20 psi)

Nozzle assembly = 2.91×10^6 N/m^2 (422 ± 5 psi)

Stresses at the leading edge of the bondline for the nozzle pressure proof test are compared below with stresses computed for the two flight conditions analyzed for limit conditions.

Condition	Pressure N/m^2		Bondline Stress N/m^2	
Proof Test	2.91×10^6	(422 psi)	4.209×10^6	(625 psi)
Ignition	5.171	(750 psi)	1.921	(280 psi)
Burnout	3.965	(575 psi)	-4.22	(-612 psi)

The proof test arrangement is shown schematically in Figure 17.

"Frothing" was a term designating the formation of small bubbles in the leak detection fluid which covered the surface of the insert. The result resembled a thin layer of shaving cream and was explained as being a result of normal porosity of the graphite phenolic material and residual internal pressure from the proof pressure test done prior to the 0.15×10^6 N/m^2 (22 psi) leak test. No damage to the insert could be detected as a result of this porosity. In most instances, if the low pressure leak test were performed at least 8 hours after the proof test, no frothing occurred.

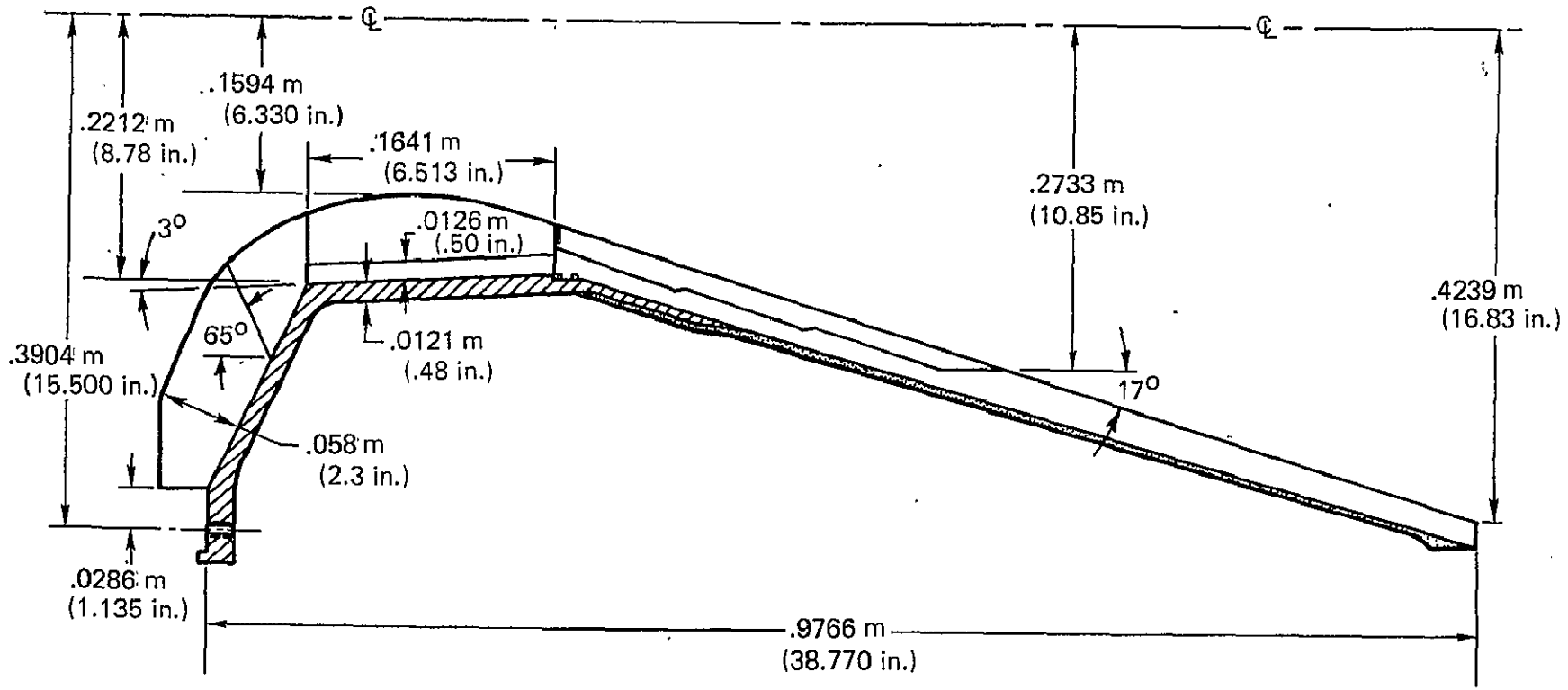

FIGURE 1. – ALGOL IIIA NOZZLE GEOMETRY

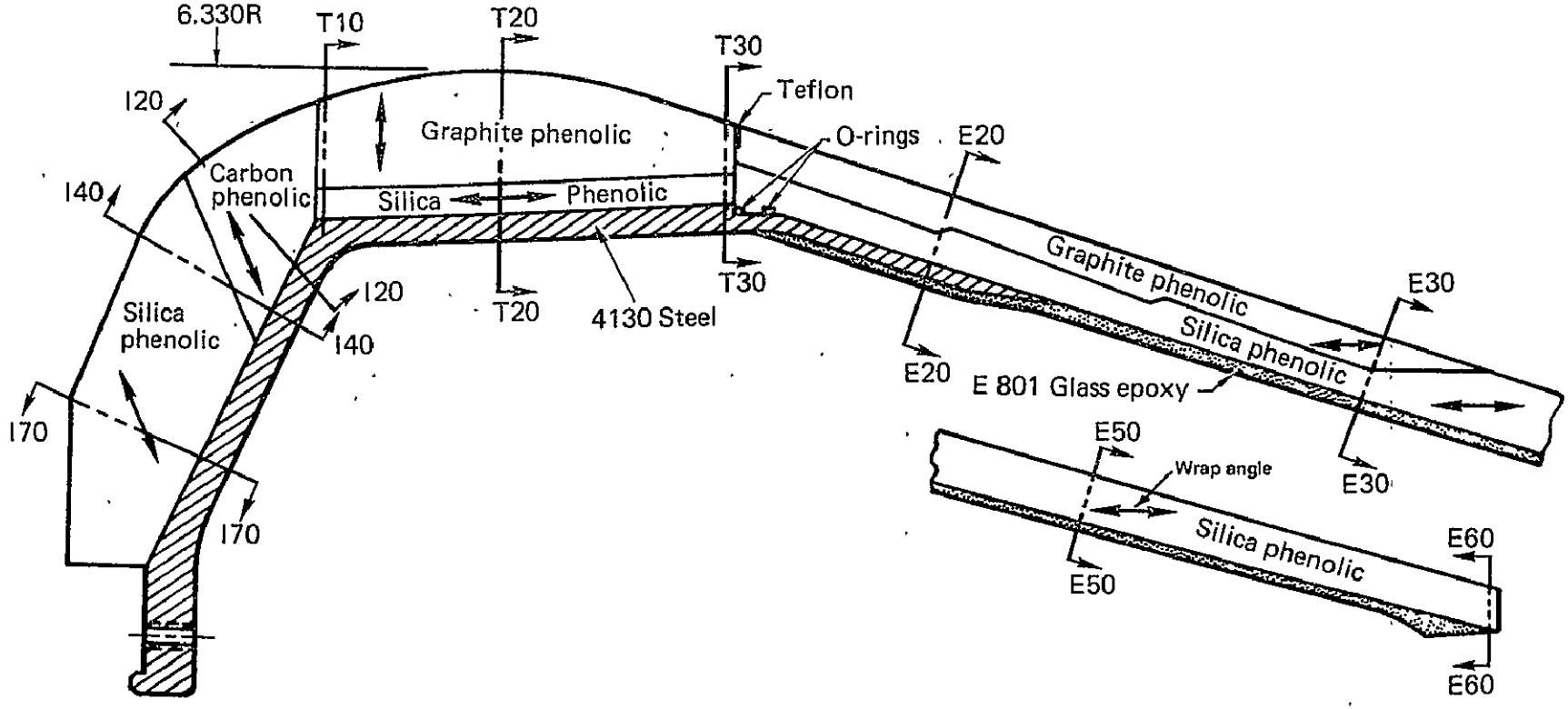

FIGURE 2. – ALGOL IIIA NOZZLE MATERIALS

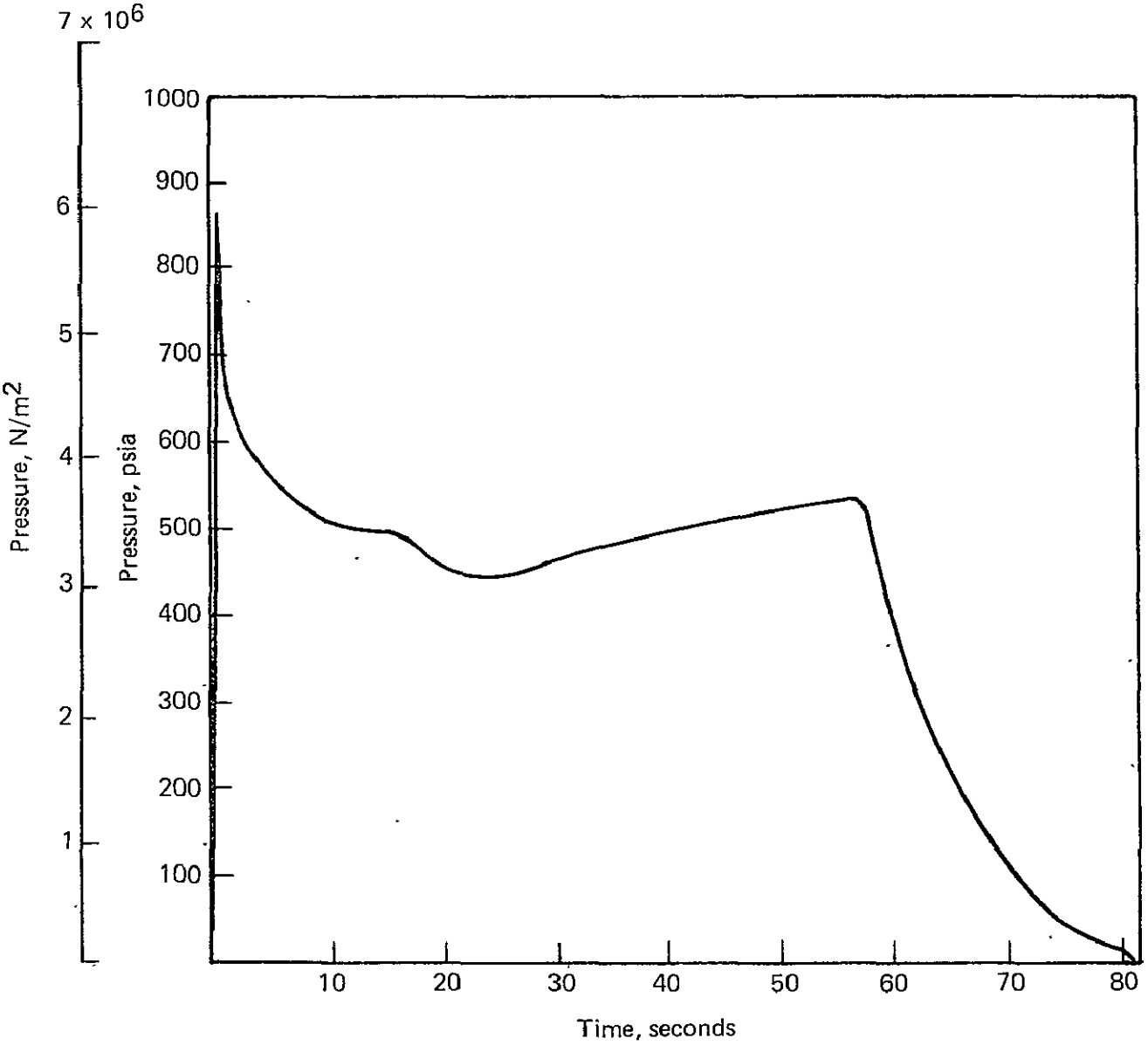

FIGURE 3. – ALGOL IIIA PRESSURE VS TIME

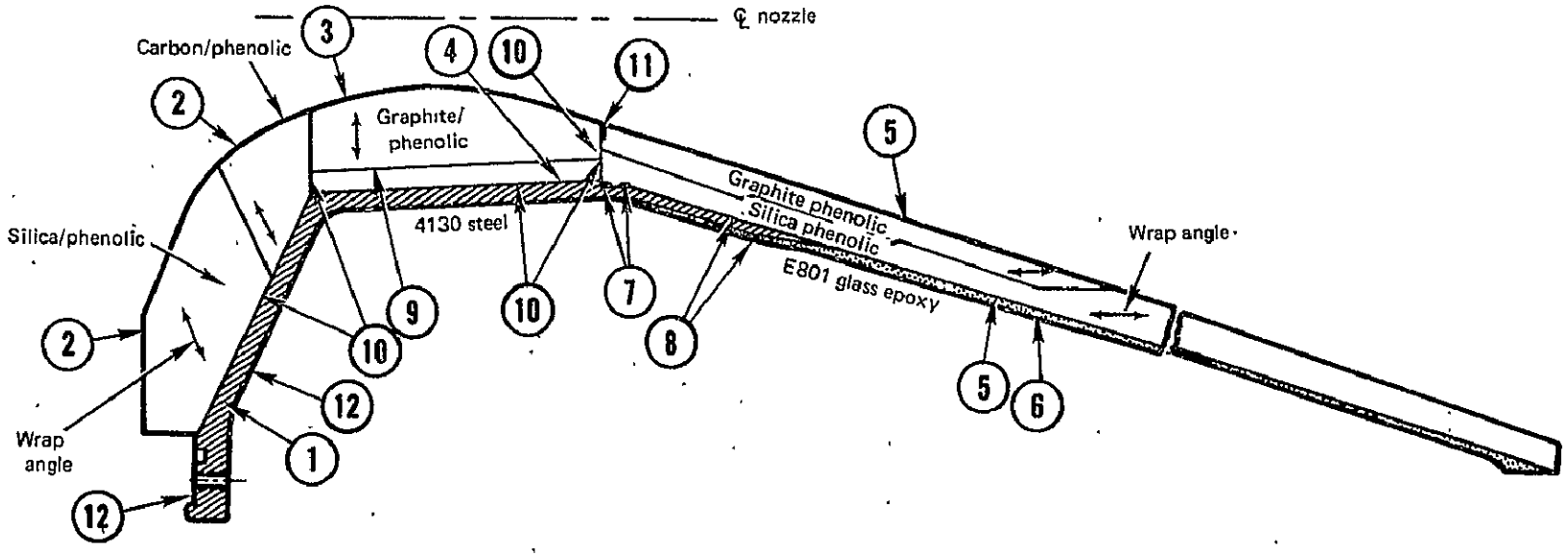

Item no	Name	Material	Fabrication/inspection
1	Steel housing	4130 steel per Mil-S-6758 cond E	The housing is machined from a 4130 steel die forging supplied in the normalized and tempered condition. The following typical properties were obtained from tensile specimens removed from 21 forged housings. FTU, 112 KSI FTY, 88 KSI % elongation — 20 Each forging is inspected for defects by wet continuous magnetic particle inspection per MIL-I-6868 using fluorescent particles. The machined housing is hydrostatic tested at 800 psi for 2-3 minutes before it is assembled with a nozzle assembly.
2	Entrance insulation	Silica/phenolic tape per 4 MDS 40722 Class I, Type II and carbon/phenolic tape per SEO 116 Type II	The entrance insulation is fabricated from two tape-wrapped materials: silica/phenolic cloth (4S 5232) in the higher area ratio region and carbon/phenolic cloth (MX 4926) in the relatively severe lower area region immediately forward of the throat insert. Both materials were tape-wrapped at $65 + 2^{0}$ to the nozzle centerline. They are debulked, hydroclave cured at 1000 psi and post cured in an open air oven as a composite unit, and then machined to a configuration for bonding to the nozzle housing. An alcohol wipe test and radiographic inspections are used to determine the existance of any external or internal defects in the cured composite.

FIGURE 4. — ALGOL IIIA FABRICATION AND INSPECTION

Item no	Name	Material	Fabrication/inspection
3	Throat insert	Graphite/phenolic tape per 4 MDS 40721 Class I, Type II	The throat insert is fabricated from a graphite/phenolic tape (MXG175) that is wrapped 90° to the centerline of the nozzle. The part is then bagged and cured in a hydroclave at 1000 psi. After cure the part is removed from the bag and post cured in an open air oven The throat insert is machined to a configuration for bonding and then inspected by alcohol wipe for surface delaminations and radiographic inspected for internal defects. After final assembly the throat is machined to the drawing contour.
4	Throat insulation	Silica/phenolic tape per 4 MDS 40722 Class I, Type II	The throat insulation is fabricated from silica/phenolic tape (MX2600) which is wrapped at 3° ± 1° to the nozzle centerline. The part is then bagged and hydroclave cured at 1000 psi. The cured part is machined to configuration for bonding and inspected for surface defects by the alcohol wipe method. Radiographic inspection is also employed to examine the part for any internal defects.
5	Exit cone insulation	(Forward) graphite/phenolic tape per 4 MDS 40721 Class I, Type I (overwrap) silica/phenolic tape per 4 MDS 40722 Class I, Type I	The forward exit cone insulation is fabricated from graphite/phenolic tape (MXG175) that is wrapped parallel ±2° to the nozzle centerline The wrapped part is bagged and partially cured in a hydroclave at 1000 psi. The O D. is then machined to profile for overwrapping with silica/phenolic (MX2600). The MX2600 is tape wrapped at± 2° to the nozzle centerline over the graphite/phenolic forward insulation. The composite is then debulked, and cured in a hydroclave at 1000 psi. the cured exit cone insulation is alcohol wipe inspected for surface defects and radiographic inspected for internal defects. No cracks or delaminations are allowed.
6	Exit cone overwrap	Glass fabric 1584-volan finish and E801 Glass roving	Four layers of glass fabric cloth (1584-volan) impregnated with epoxy resin Epon 815/curing agent A are applied to be OD surface of the exit cone. The assembly is vacuum bagged, cured and then overwrapped with E801 glass roving that is fed through a bath of 815 epoxy resin/A curing agent. The filament wound exit cone is oven cured and then tap tested to inspect the bond line between the exit cone insulation, housing and composite overwrap. No debonds are allowed.
7	O-ring	O-ring per MIL-R-25897, Type I Class I (ARP 568-283)	O-rings are molded from viton rubber (Fluorocarbon elastomer) and are installed to provide a seal against possible gas leakage. The forward o-ring is used to prevent adhesive from flowing along the steel housing during assembly operations so that the aft o-ring can function as a gas seal.
8	Adhesive	Epoxy resin EPON 815 with curing agent A	This epoxy system is used for impregnating the glass fabric cloth and the E801 glass roving during the exit cone overwrap operation
9	Adhesive	Epoxy-phenolic resin aluminum filled, on glass cloth, HT 424	Elevated temperature curing adhesive used to bond graphite/phenolic throat (MXG175) to silica/phenolic (MX2600) throat insulation.
10	Adhesive	Epon 913 epoxy	Room temperature curing epoxy adhesive used to bond the entrance insulation throat assembly and exit cone insulation to 4130 steel housing. Bond line thickness controlled to .005 to .020 inches EPON 913 is also used to bond the throat assembly to both the entrance insulation and the exit cone insulation The bond line between the housing and the entrance insulation and throat assembly is ultrasonic inspected for debonds.
11	Spacer ring	Teflon	The teflon spacer ring is inserted between the throat insert and exit cone insulation during assembly of the nozzle. The teflon ablates during motor firing to provide a separation or expansion joint between the throat and exit cone.
12	Protective finish	Zinc chromate primer per MIL-P-8585, color T Corrosion preventative compound per MIL-C-16173, Grade 2.	Applied to all non-mating external surfaces of steel housing. Applied to all internal and mating surfaces of steel housing.

FIGURE 4. – ALGOL IIIA FABRICATION AND INSPECTION – Concluded

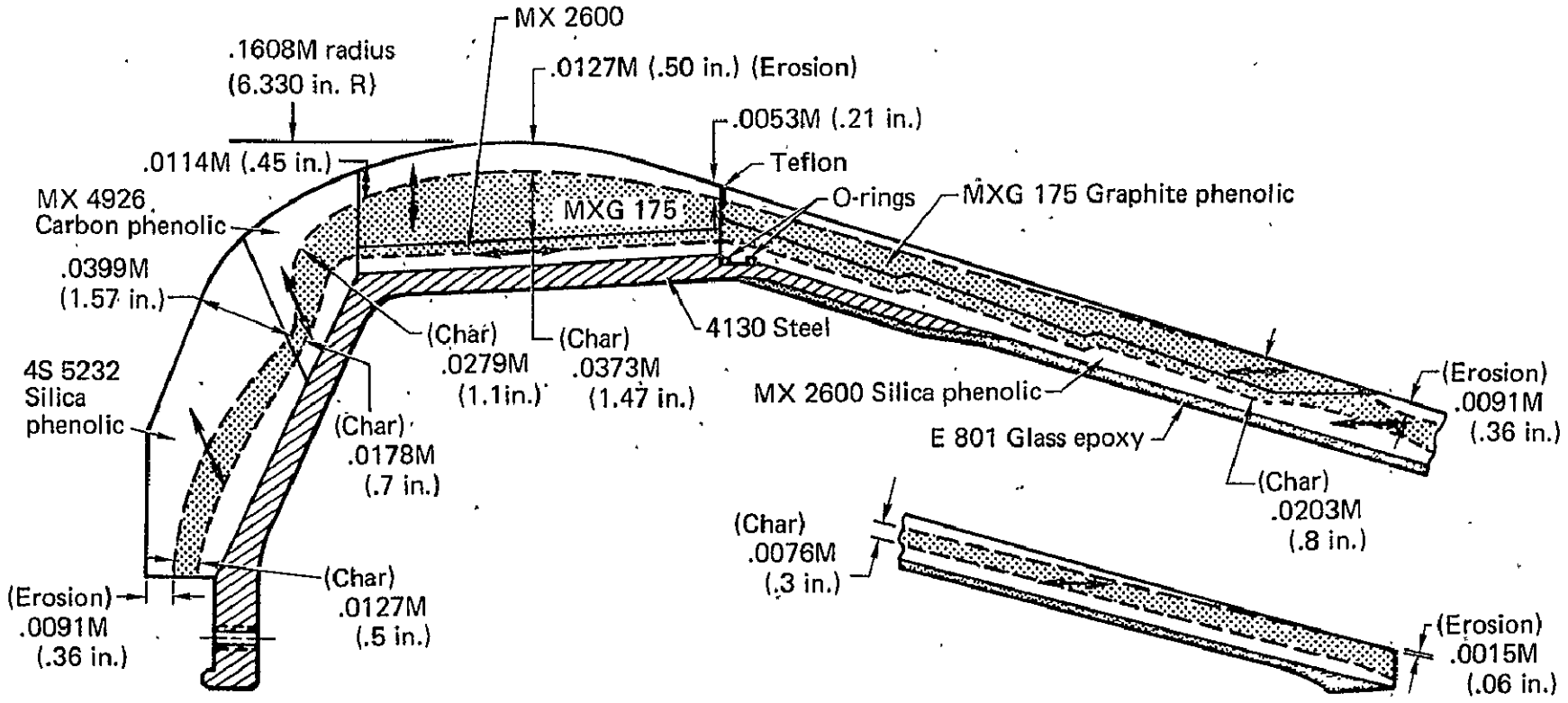

Reference 1

FIGURE 5. – ABLATION AND CHAR PROFILES

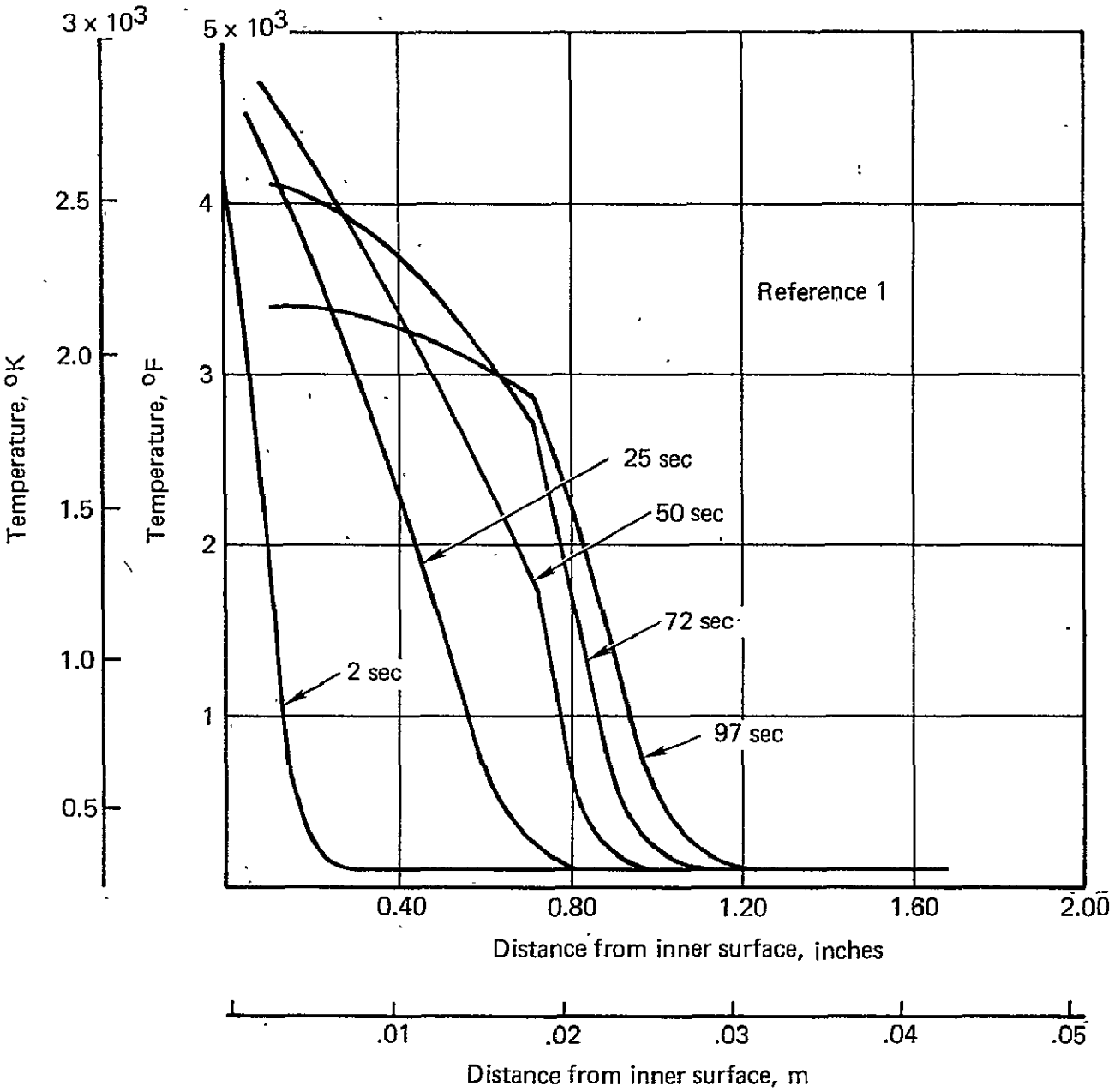

FIGURE 6. – EXIT CONE TEMPERATURES AT STATION E 20
(See Figure 2 for section location)

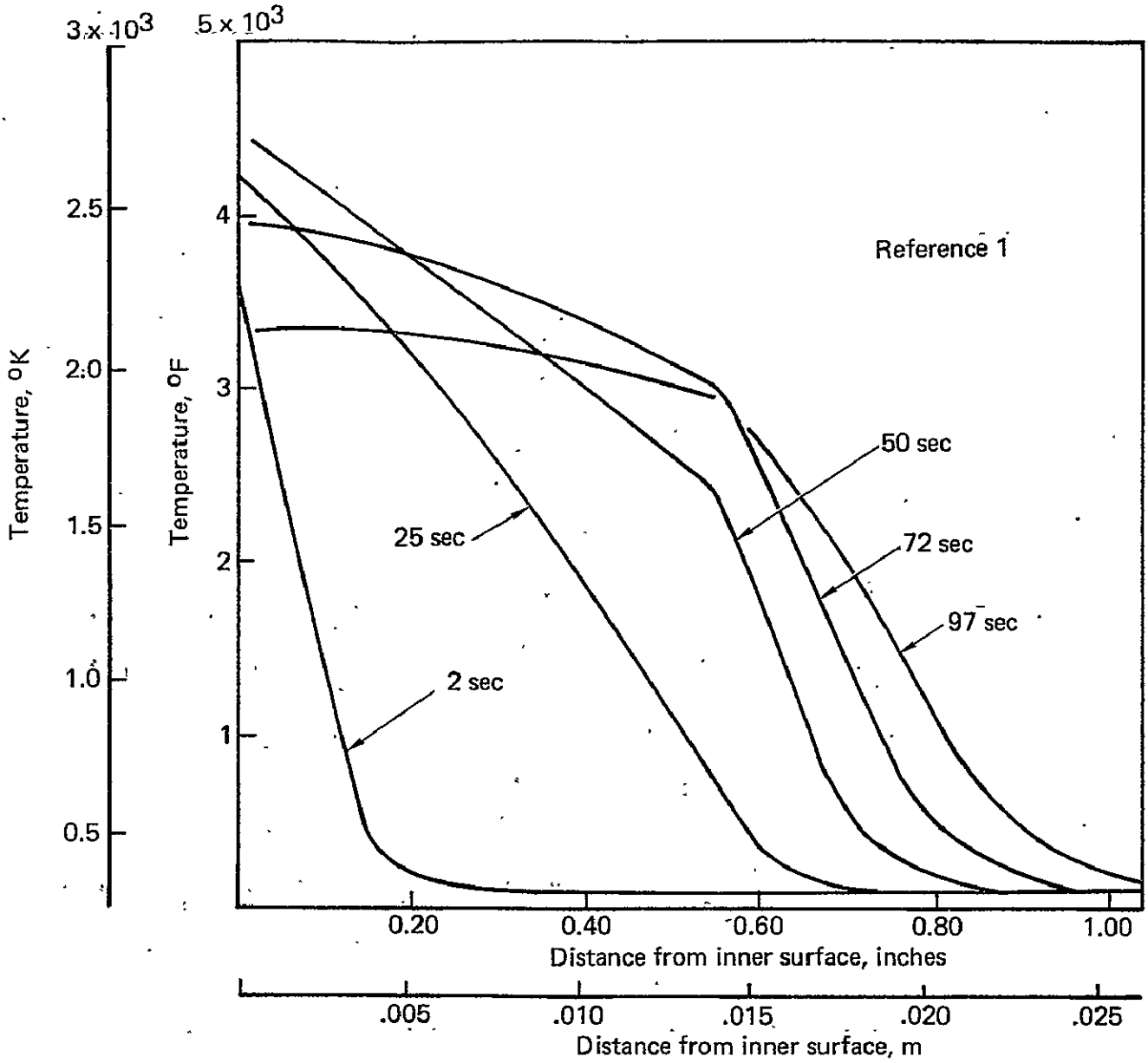

FIGURE 7. – EXIT CONE TEMPERATURES AT STATION E 30
(See Figure 2 for section location)

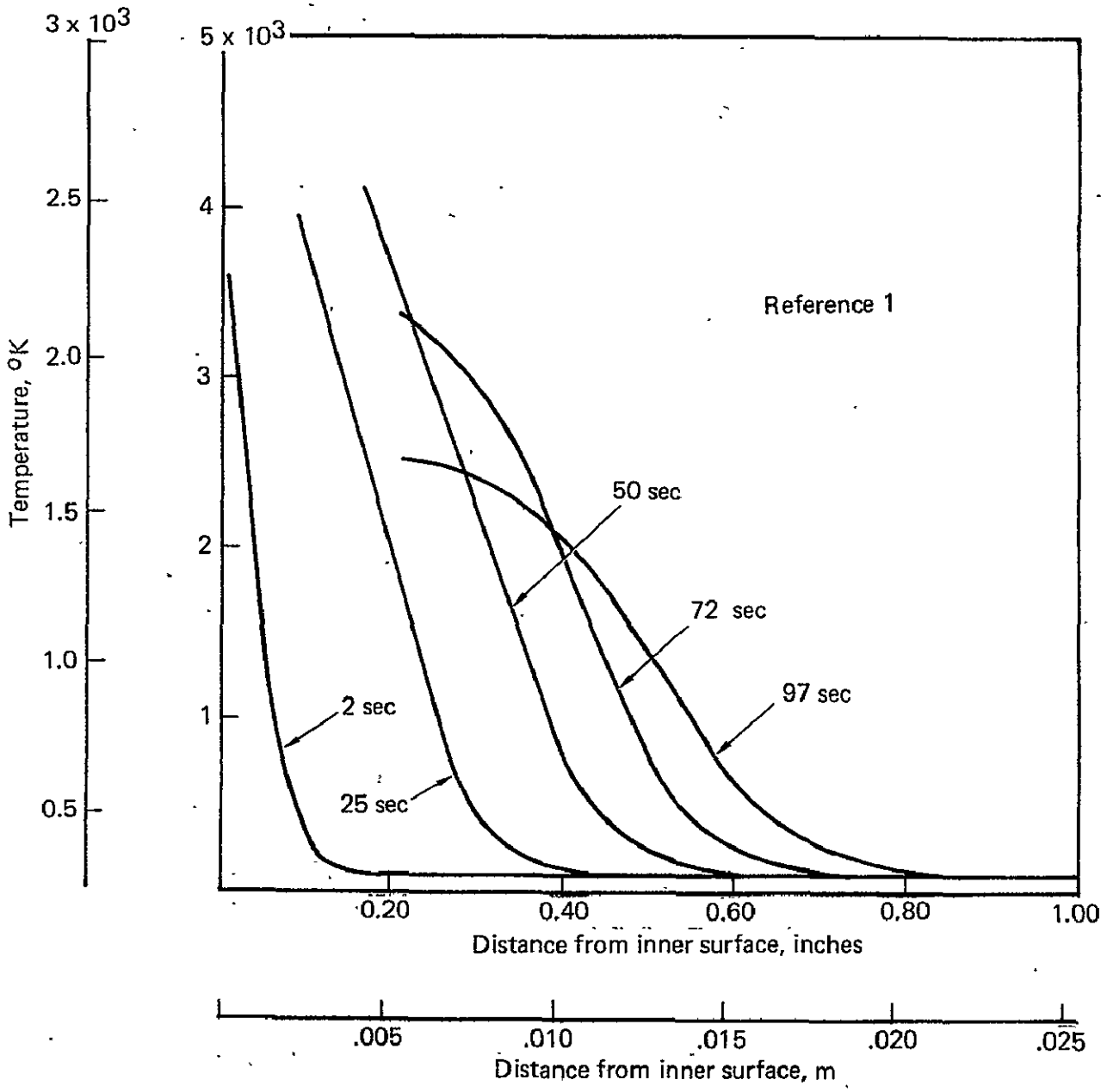

FIGURE 8. — EXIT CONE TEMPERATURES AT STATION E 50

(See Figure 2 for section location)

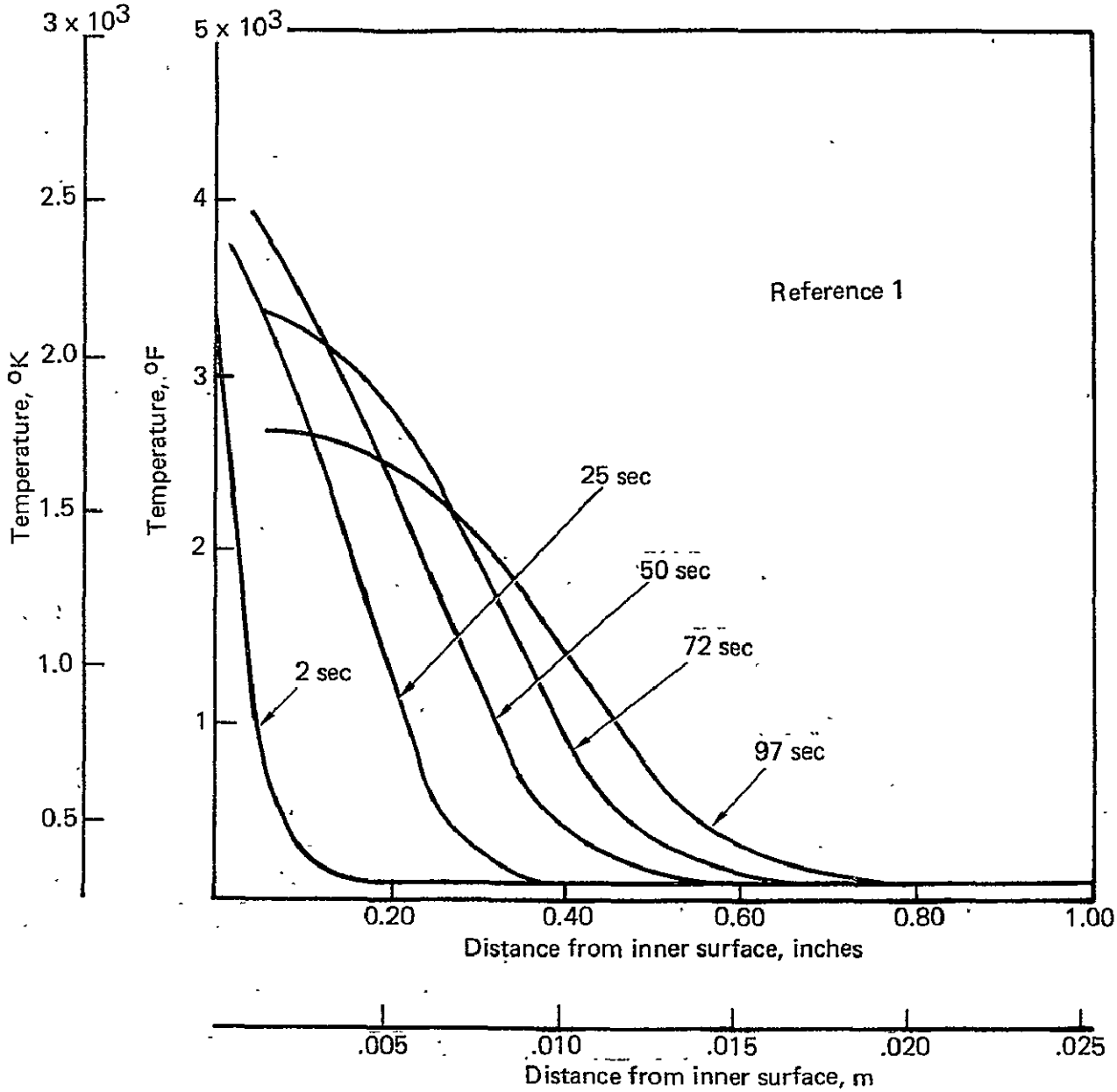

FIGURE 9. – EXIT CONE TEMPERATURES AT STATION E 60

(See Figure 2 for section location)

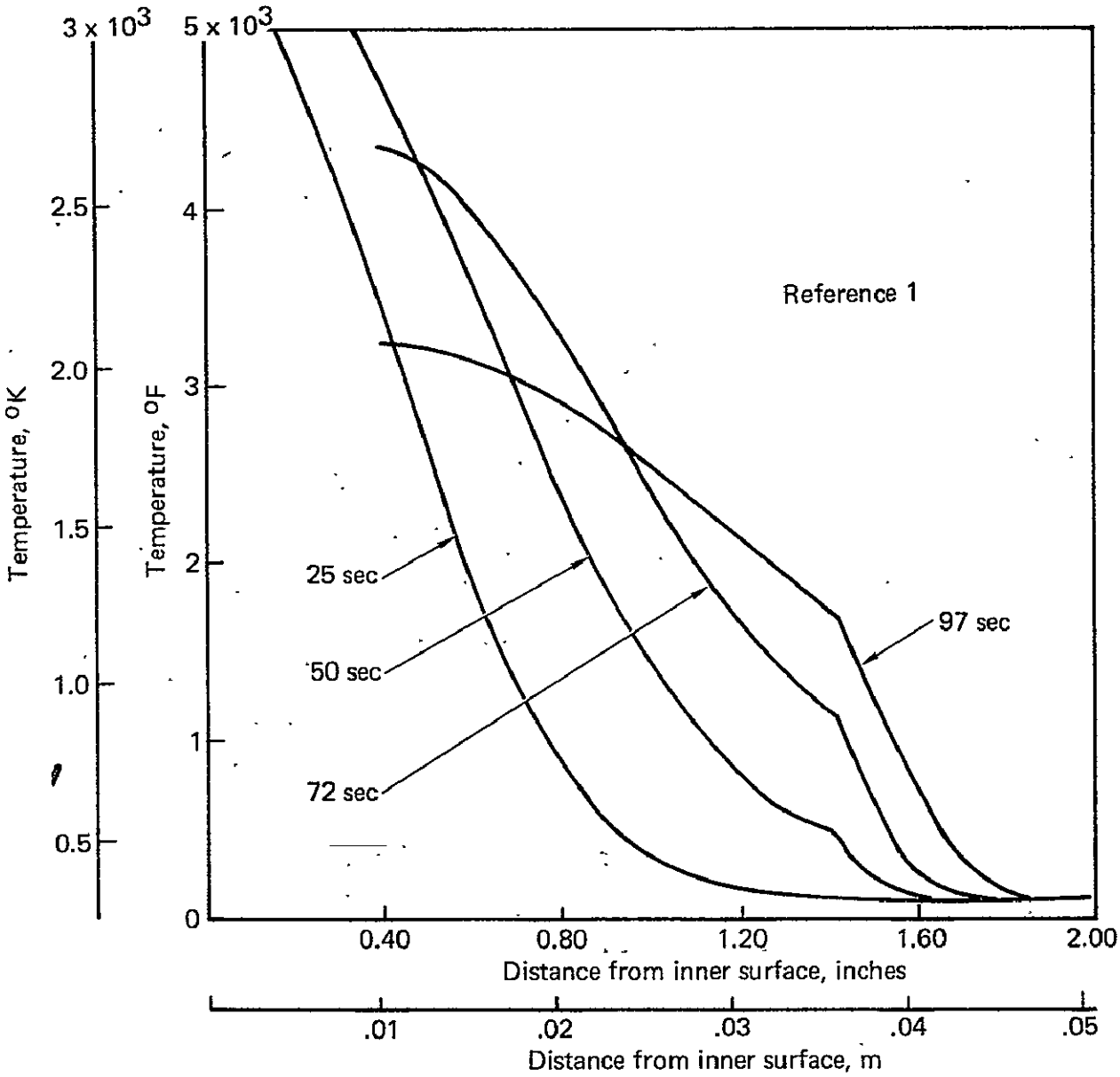

FIGURE 10. – INSERT TEMPERATURES AT STATION T10

(See Figure 2 for section location)

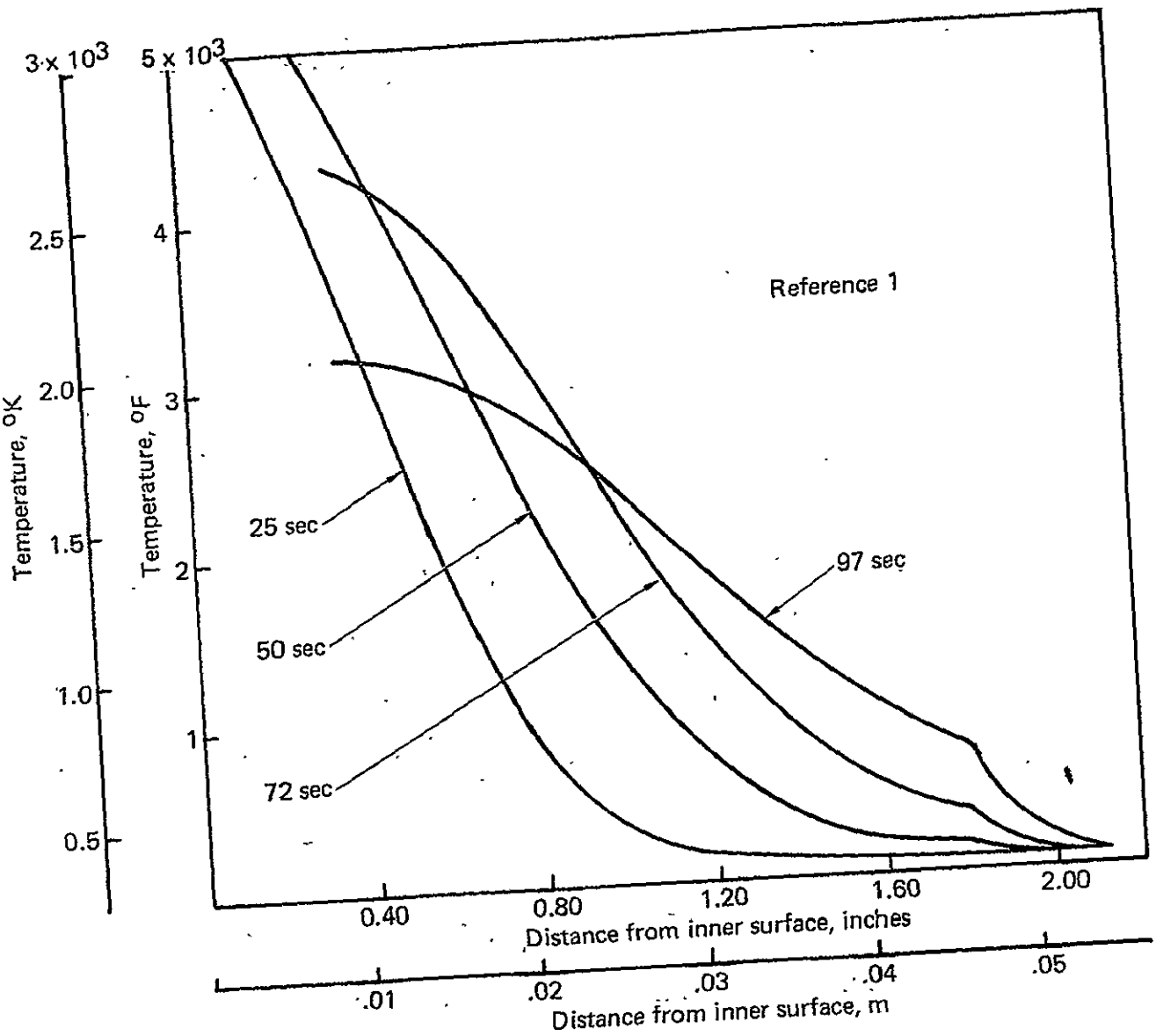

FIGURE 11. – INSERT TEMPERATURES AT STATION T20

(See Figure 2 for section location)

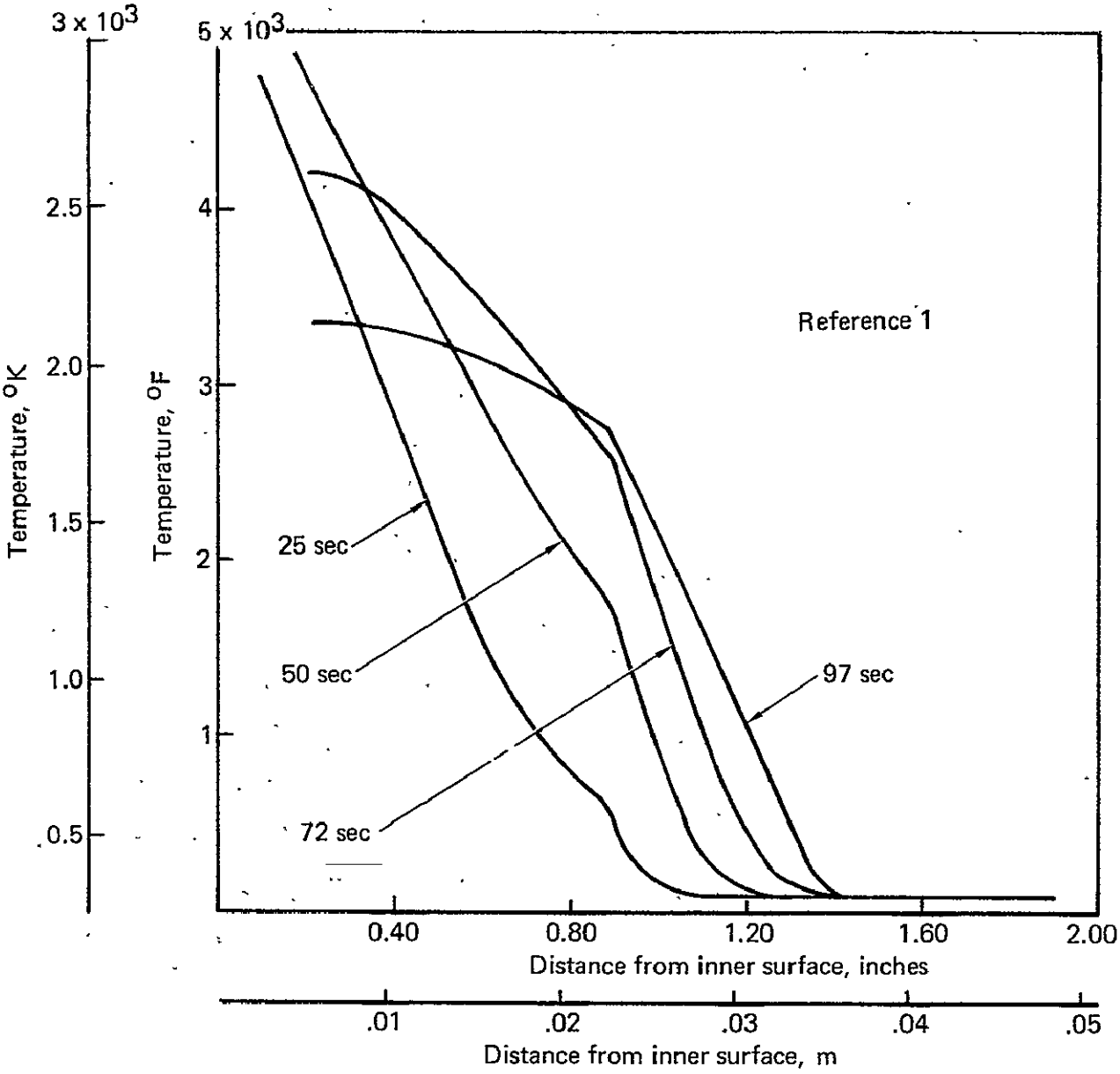

FIGURE 12. – INSERT TEMPERATURES AT STATION T 30

(See Figure 2 for section location)

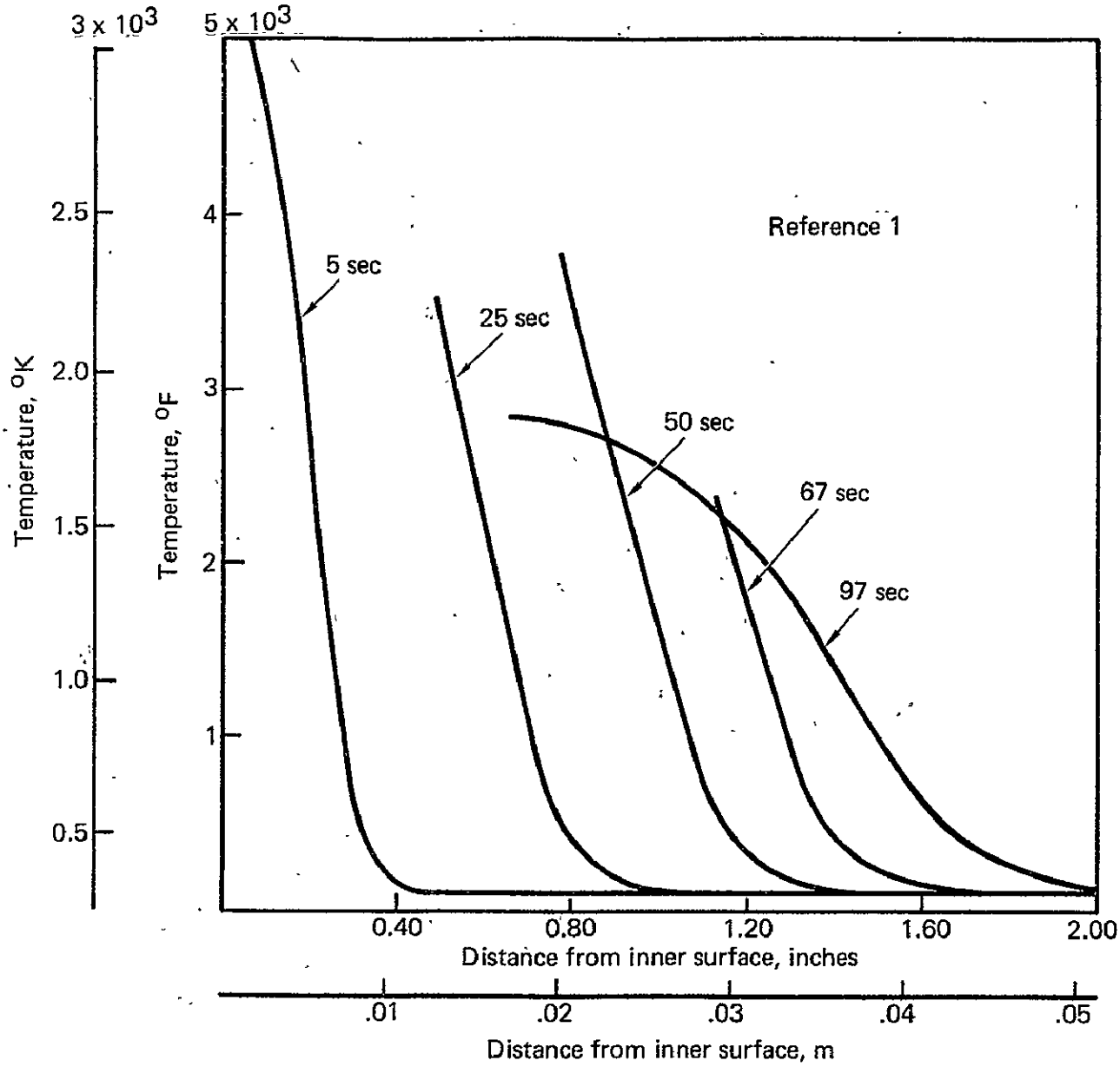

FIGURE 13. – FWD INSULATOR TEMPERATURES AT STATION I 20

(See Figure 2 for section location)

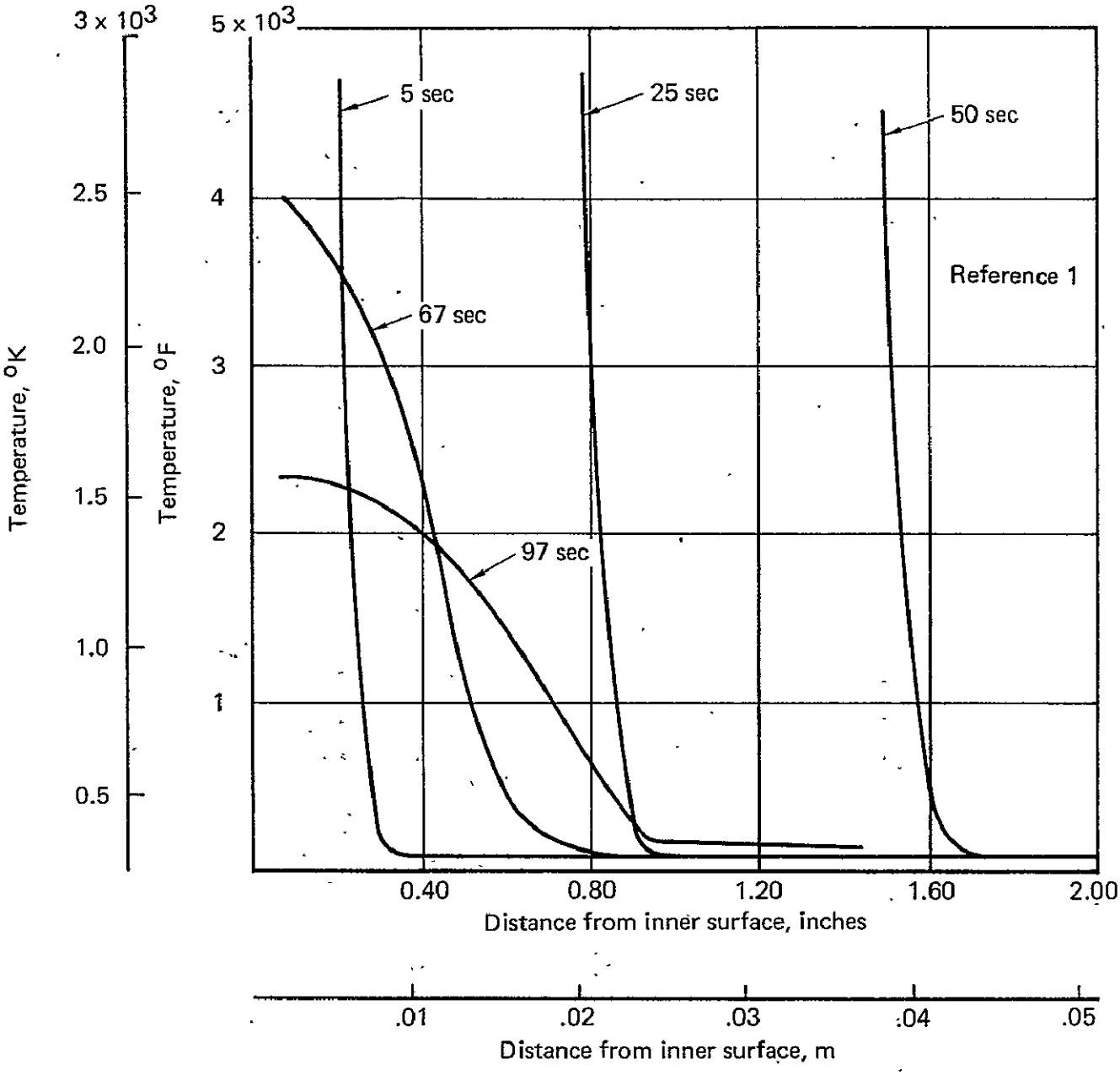

FIGURE 14. – FWD INSULATOR TEMPERATURES AT STATION 1.40

(See Figure 2 for section location)

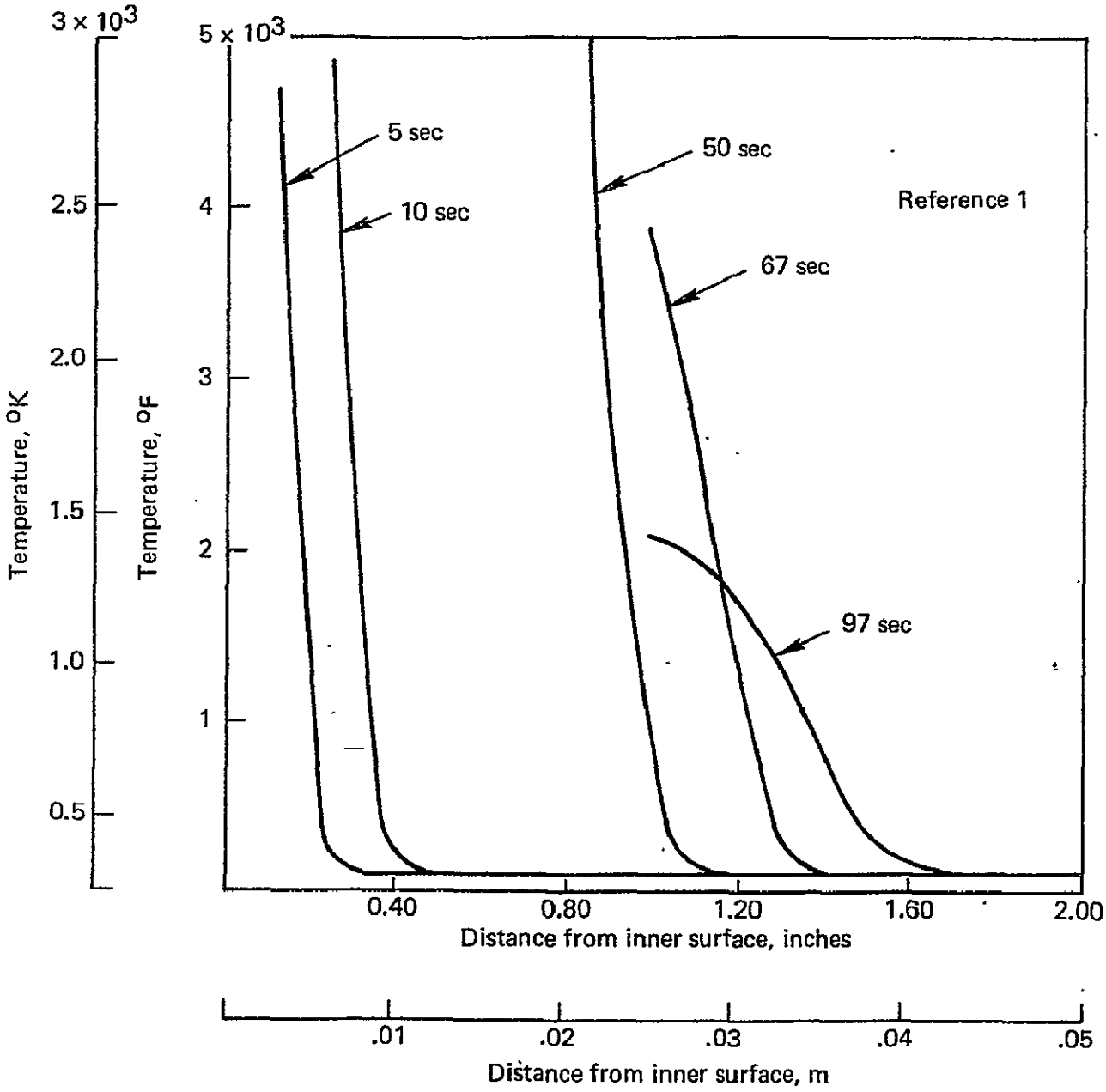

FIGURE 15. – FWD INSULATOR TEMPERATURES AT STATION I 70

(See Figure 2 for section location)

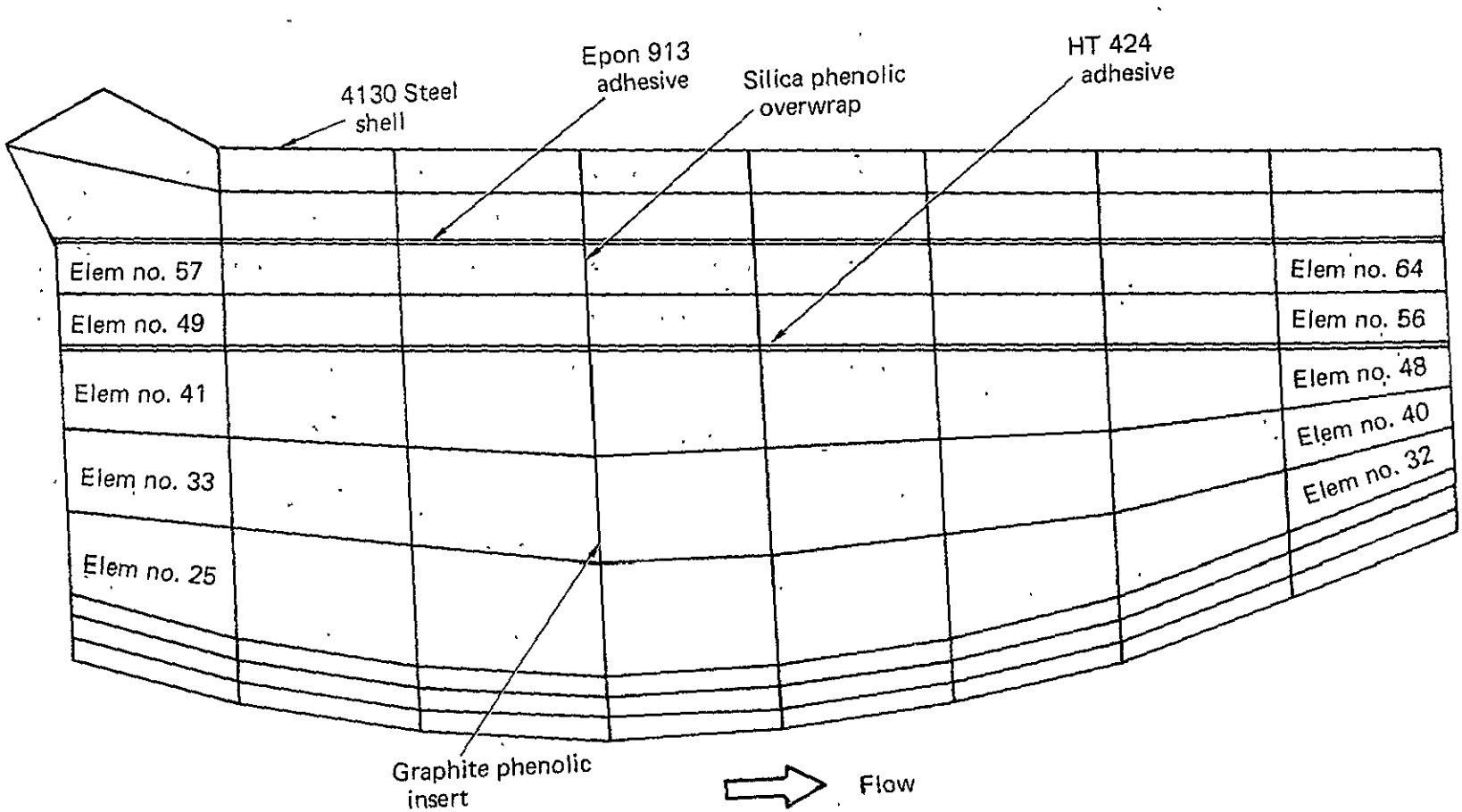

FIGURE 16. – ALGOL IIIA THROAT MODEL

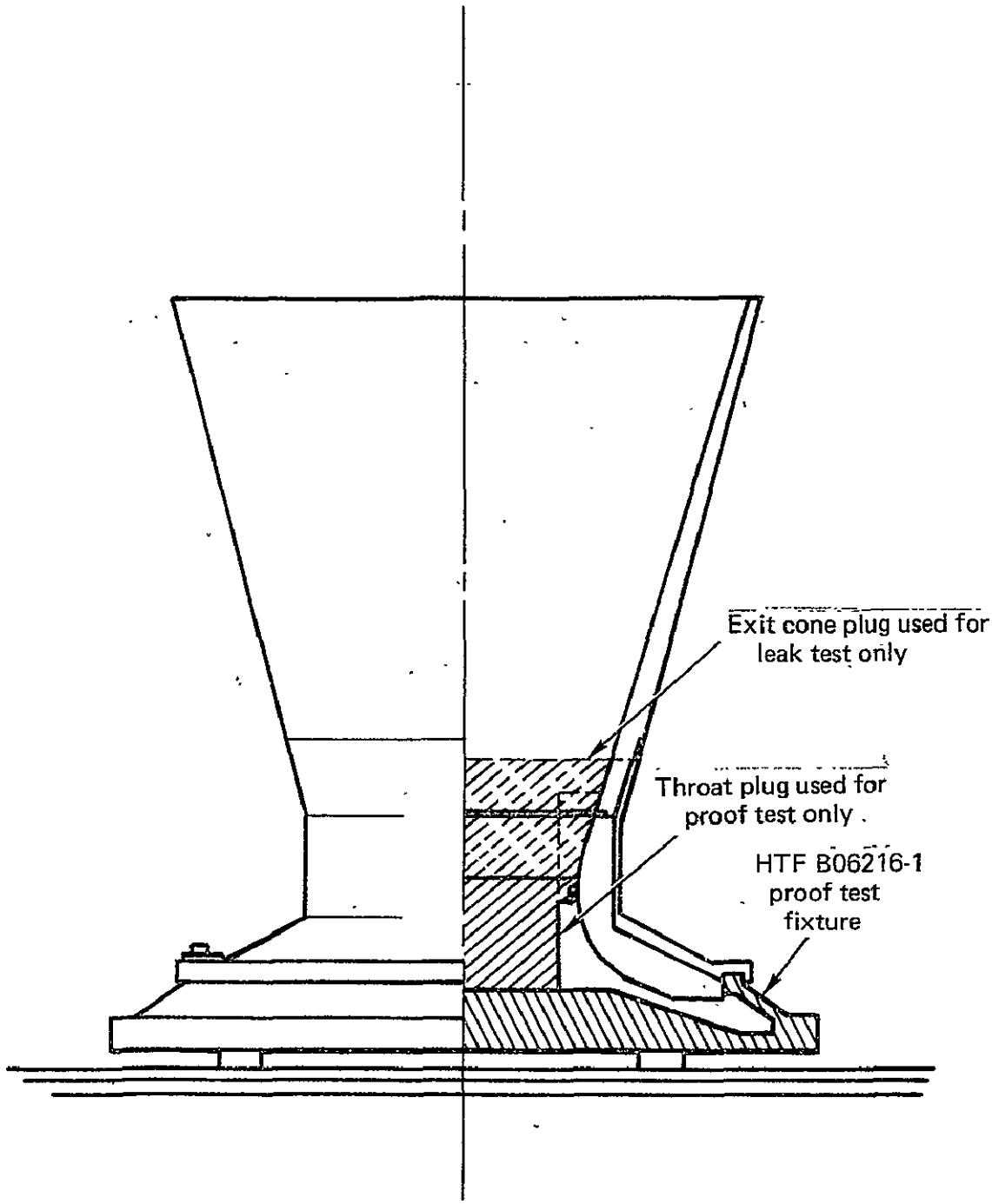

FIGURE 17. – NOZZLE PROOF TEST AND LEAK CHECK ARRANGEMENT

TABLE I. – ALGOL IIIA NOZZLE MATERIALS

Component	Material	Vendor designations	UTC procurement specification
Housing	4130 steel, cond. E	None	MIL-S-6758
Fwd entrance insulation	Silica phenolic	4S-5232 (Hexcel Corp)	4 MDS-40722
Aft entrance insulation	Carbon phenolic	MX 4926 (U. S. Polymeric) FM 5072 (Fiberite)	SE 0116
Throat insert	Graphite phenolic	MXG 175 (U. S. Polymeric) FM 5014 (Fiberite)	4MDS-40721
Throat insulation	Silica phenolic	MX 2600 (U. S. Polymeric)	4MDS-40722
Exit cone insulation (forward)	Graphite phenolic	MXG 175 (U. S. Polymeric)	4MDS-40721
Exit cone insulation (overwrap)	Silica phenolic	4S-5232 (Hexel Corp) MX 2600 (U. S. Polymeric)	4MDC-40722
Aft closure	Silica phenolic	4S-5232 (Hexcel Corp) MX2600 (U. S. Polymeric)	4MDS-40722
Exit cone overwrap	E801 glass roving	Glass roving	Owens/Corning TP 238
O-ring	Viton rubber	ARP 568-283	MIL-R-25897
Adhesive	Epon 815 resin	Epoxy	Commercial grade
Adhesive	Epoxy phenolic	Epoxy phenolic	UTC SE 0084
Adhesive	Epon 913	Epoxy	UTC SE 0084
Spacer ring	Teflon	Teflon	AMS 3651

TABLE II. – ALGOL IIIA MOTOR CHARACTERISTICS

Propellant property	Type/Designation	Motor performance	
Propellant designation	UTP-3096C	Avg web thrust vacuum, N	432000 (98400 lb)
Propellant type	Aluminized composite	Total motor weight, kg	14181 (31236 lb)
Grain configuration	Cylindrical 4 pointed star	Consumed weight, kg	12827 (28253 lb)
Propellant gas properties: (chamber)		Propellant weight, kg	12706 (27986 lb)
		Specific impulse vacuum (sec)	259.6
Specific heat ratio (γ)	1.18	Total burn time (sec)	72.3 (@ 298°K)
C_p, cal/gm-°K	0.439 (sec)	Web burn time (sec)	56.7(2)
Molecular weight	20.11	Pressure, web time avg, N/m^2	3.47 x 10^6 (503 psi)
C*, m/sec	1537 (5035 f/sec)	MEOP, N/m^2	6.68 x 10^6 (970 psi)
Flame temp, °K	3366 (5600°F)	Proof pressure, N/m^2	Case: 7.35 x 10^6 (1) (1067 psi) Nozzle: 2.91 x 10^6 (422 psi)

(1) Case proof test uses 20:1 water and water soluble oil pressurized at 1.38 x 10^6 N/m^2/min (200 psi/min) to 7.425 x 10^6 N/m^2 (1077 ± 10 psig) for 2 to 3 minutes.
Nozzle shell proof test uses 20:1 water and soluble oil at 1.38 x 10^6 N/m^2/min (200 psi/min) to 5.515 x 10^6 N/m^2 (800 ± 20 psig) for 2 to 3 minutes.
Nozzle assembly proof test uses nitrogen gas pressurized at 1.38 x 10^6 N/m^2/min (200 psi/min) to 2.91 x 10^6 N/m^2 (422 ± 5 psig). Pressure is reduced to .1515 x 10^6 N/m^2 (22 ± 2 psig) for 5 to 8 minutes. Leaks are not allowed.

(2) Conditioned at 298°K.

Reference 13.

TABLE III. – ALGOL IIIA NOZZLE DRAWINGS AND MATERIAL SPECIFICATIONS

Number	Title
Dwg B06216	Nozzle, rocket motor
Spec 4MDS 40721	Tape, graphite cloth, phenolic resin impregnated
Spec 4MDS 40722	Tape, high-silica cloth, phenolic resin impregnated
Spec 4MDS 40752	Cloth, graphite
Spec 4MDS 40753	Cloth, glass, high silica content
Spec SE0084	Adhesive bonding, reinforced plastic material to metal
Spec SE0091	Cloth, carbon
Spec SE0116	Tape, carbon cloth, phenolic resin impregnated

TABLE IV. – ALGOL IIIA NOZZLE MATERIAL PROPERTIES

Material: silica phenolic (MX 2600 or 4S5232)

		300°K R.T.	395°K (250°F)	533°K (500°F)	811°K (1000°F)	1366°K (2000°F)	1922°K (3000°F)	2478°K (4000°F)
Thermal conductivity, cal/m-hr-°K x 10^3 (B-in./ft^2-hr-°F)	With lam. 45°	.32 (3)	.35 (3)	.43 (3)	.86 (7)	1.55 (13)	1.93 (16)	2.25 (18)
	Against lam.	.24 (2)	.29 (2)	.32 (3)	.43 (4)	.99 (8)	1.21 (14)	2.4 (18)
Coeff of thermal exp M/M-°K x 10^{-6} (in/in.-°F) x 10^{-6}	With lam.	6.7 (3.7)	6.7 (3.7)	6.7 (3.7)	6.7 (3.7)	6.7 (3.7)	6.7 (3.7)	6.7 (3.7)
	Against lam.	–	–	–	–	–	–	–
Modulus of elasticity N/m^2 x 10^9 (psi x 10^6)	With lam.	17.9 (2.6)	15.8 (2.3)	13.8 (2)	10.3 (1.5)	5.5 (.8)	5.5 (.5)	–
	Against lam.	–	–	–	–	–	–	–
Tensile ult strength N/m^2 x 10^6 (psi x 10^3)	With lam.	96 (14)	79 (11.5)	55 (8)	–	–	–	–
	Against lam.	68 (10)	56 (8.2)	39 (5.7)	–	–	–	–
Interlaminar shear strength N/m^2 x 10^6 (psi x 10^3)		19.3 (2.8)	–	–	–	–	–	–
Specific heat cal/gm-°K		.23	.26	.29	.47	.49	.5	.5
Poisson's ratio, μ		–	–	–	–	–	–	–

Reference 1, 2

TABLE IV. – ALGOL IIIA NOZZLE MATERIAL PROPERTIES-Continued

Material: carbon phenolic (MX 4926)

		300°K R.T.	395°K (250°F)	533°K (500°F)	811°K (1000°F)	1366°K (2000°F)	1922°K (3000°F)	2478°K (4000°F)
Thermal conductivity, cal/m-hr-°K x 10^3 (B-in./ft^2-hr-°K)	With lam.	1.33 (10.7)	1.35 (10.9)	1.42 (11.5)	1.80 (14.5)	3.34 (27)	6.30 (50)	9.7 (77)
	Against lam.	–	–	–	–	–	–	–
Coeff. of thermal exp. M/M-°K x 10^{-6} (in./in.-°F x 10^{-6})	With lam.	–	10.1 (5.6)	8.5 (4.7)	2.0 (1.1)	1.1 (0.6)	2.2 (1.2)	3.8 (2.1)
	Against lam.	–	16.9 (9.4)	28.9 (16)	3.6 (2.0)	3.5 (1.4)	3.4 (1.9)	3.1 (1.7)
Modulus of elasticity N/m^2 x 10^9 (psi x 10^6)	With lam.	17.2 (2.5)	19.3 (2.8)	15.1 (2.2)	11.0 (1.6)	9.6 (1.4)	3.4 (0.5)	3.4 (0.5)
	Against lam.	12.4 (1.8)	9.0 (1.3)	6.2 (0.9)	5.5 (0.8)	4.1 (0.6)	4.1 (0.6)	4.1 (0.6)
Tensile ult strength N/m^2 x 10^6 (psi x 10^3)	With lam.	124 (18)	107 (15.5)	86 (12.5)	65 (9.5)	52 (7.5)	41 (6)	41 (6)
	Against lam.							
Interlaminar shear strength N/m^2 x 10^6 (psi x 10^3)		19 (2.8)	15 (2.2)	10 (1.5)	2.8 (0.4)	2.8 (0.4)	2.8 (0.4)	2.8 (0.4)
Specific heat cal/gm -°K		.23	.27	.28	.475	.49	0.5	0.5
Poisson's ratio, μ		–	–	–	–	–	–	–

Reference 1, 2

TABLE IV. – ALGOL IIIA NOZZLE MATERIAL PROPERTIES–Concluded

Material: graphite phenolic (MXG 175 or FM 5014)

		300°K R.T.	395°K (250°F)	533°K (500°F)	811°K (1000°F)	1366°K (2000°F)	1922°K (3000°F)	2478°K (4000°F)
Thermal conductivity, cal/m-hr-°K×10^3 (B-in./ft^2-hr-°F)	With lam.	3.28 (26)	3.34 (27)	3.67 (30)	4.36 (35)	5.9 (48)	7.64 (61)	9.9 (80)
	Against lam.	1.15 (9)	1.15 (9)	1.22 (9)	1.6 (13)	3.28 (27)	5.78 (47)	8.83 (71)
Coeff of thermal exp. M/M-°K x 10^{-6} (in./in.-°F×10^{-6})	With lam.	–	12.6 (7)	7.2 (4)	1.8 (1)	1.8 (1)	1.8 (1)	2.7 (1.5)
	Against lam.	–	23.4 (13)	−14.4 (−8)	.9 (.5)	3.6 (2)	3.6 (2)	3.6 (2)
Modulus of elasticity N/m^2 x 10^9 (psi x 10^6)	With lam.	13.1 (1.9)	11.0 (1.6)	8.3 (1.2)	0.7 (1)	2.75 (0.4)	2.4 (0.35)	2.1 (0.3)
	Against lam.	2.8 (0.4)	2.1 (0.3)	1.4 (0.2)	0.7 (0.1)	0.35 (0.05)	0.35 (0.05)	0.35 (0.05)
Tensile ult strength N/m^2 x 10^6 (psi x 10^3)	With lam.	55 (8)	45 (6.5)	34 (5)	20 (3)	13 (1.9)	13 (1.9)	13 (1.9)
	Against lam.	5.1 (0.74)	5.0 (0.73)	4.3 (0.63)				
Interlaminar shear strength N/m^2 x 10^6 (psi x 10^3)		13 1.85	10 1.52	7.5 1.10	2.8 0.4	1.6 0.24	1.6 0.24	1.6 0.24
Specific heat cal/gm-°K		0.23	0.32	0.37	0.43	0.48	0.5	0.5
Poisson's ratio, μ		–	–	–	–	–	–	–

Reference 1, 2

TABLE V. — IN-PROCESS TESTS

Component	Material	Type test	No. specimens	Requirements
Exit cone liner	Silica/phenolic	Tensile	3	55.1×10^6 N/m^2 (8000 psi)
	Silica/phenolic	Specific gravity	6	1.68
	Silica/phenolic	Residual volatiles	3	3% max.
	Graphite/phenolic	Tensile	3	55.1×10^6 N/m^2 (8000 psi)
	Graphite/phenolic	Specific gravity	6	1.37
	Graphite/phenolic	Residual volatiles	3	3% max
	Graphite/silica interface	Flexural	3	82.8×10^6 N/m^2 (12000 psi)
Entrance insulation	Silica/phenolic	Tensile	3	55.1×10^6 N/m^2 (2600 psi)
		Specific gravity		1.68
Throat	Graphite/phenolic	Interlaminar shear	4	19.0×10^6 N/m^2 (8000 psi)
	Graphite/phenolic	Tensile (hoop direction)	4	62.1×10^6 N/m^2 (9000 psi)
	Graphite/phenolic	Specific gravity	3	1.37
	Graphite/phenolic	Residual volatiles	3	3% max
Bond strength exit cone to steel housing	913 Epoxy adhesive with 410 stainless steel adherents	Lap shear	4	16.6×10^6 N/m^2 (2400 psi)
Bond strength throat to throat insulation	HT 424 Adhesive with 410 stainless steel adherents	Lap shear	4	13.8×10^6 N/m^2 (2000 psi)
Bond strength throat assembly and entrance insulation to steel housing	913 Epoxy adhesive with 410 stainless steel adherents	Lap shear	4	13.8×10^6 N/m^2 (2000 psi)

Reference 20

TABLE VI. – ALGOL IIIA NOZZLE STRESS SUMMARY

Condition/location	Failure mode	Ultimate stress $N/m^2 \times 10^6$	Allowable stress $N/m^2 \times 10^6$	Margin of safety
A. Firing, t + 0 seconds				
1. Aft closure insulation, silica-phenolic	Shear	5.9 (854 psi)	19.3 (2800 psi)	+2.28
2. Entrance cap, carbon-phenolic	Shear	5.07 (737)	19.3 (2800)	+2.80
3. Throat insert, graphite-phenolic	Axial tension	2.53 (367)	5.11 (740)	+1.02
4. Throat insert, silica-phenolic	Shear	5.25 (762)	19.3 (2800)	+2.67
5. Exit cone, graphite-phenolic	Shear	1.67 (242)	17.9 (2600)	+9.7
6. Exit cone, silica-phenolic	Radial tension	1.18 (169)	6.9 (1000)	+4.92
7. Exit cone, glass over-wrap	Hoop tension	5.43 (787)	896.0 (130000)	High (3)
8. Nozzle steel housing	Hoop tension	357.0 (51760)	620.0 (90000)	+0.74
9. Throat to shell adhesive bond	Shear	5.34 (775)	13.8 (2000)	+1.58
10. Throat to shell adhesive bond	Tension	2.63 (381)	17.9 (2000) (1)	+5.3
B. Firing, t + 55 seconds				
1. Aft closure insulation, silica-phenolic	Hoop tension	14.7 (2139 psi)	67.0 (9700 psi)	+3.53
2. Entrance cap, carbon-phenolic	Normal tension	6.45 (936)	6.7 (1000)	+0.07
3. Throat insert, graphite-phenolic	Radial tension	30.8 (4472)	31.7 (4600)	+0.03
4. Throat insert, silica-phenolic	Normal tension	3.13 (453)	5.0 (720)	+0.59
5. Exit cone, graphite-phenolic	Axial tension	5.18 (752)	13.1 (1900)	+1.53
6. Exit cone, silica-phenolic	Shear	16.2 (2345)	18.3 (2600)	+0.13
7. Exit cone, glass over-wrap	Hoop tension	37.8 (5488)	896.0 (130000)	High
8. Nozzle steel housing	Hoop tension	289.0 (41820)	620.0 (90000)	+1.16
9. Throat to shell adhesive bond	Shear	5.2 (753)	13.8 (2000)	+1.66
10. Throat to shell adhesive bond	Compression	−5.74 (−833)	–	–

(1) Assumed allowable.

Reference 2

TABLE VI. – ALGOL III NOZZLE STRESS SUMMARY – Concluded

Condition/location	Failure mode	Limit stress $N/m^2 \times 10^6$	Allowable stress $N/m^2 \times 10^6$	Margin of safety
C. Prooftest, $P = 2.91 \times 10^6$ N/m^2 (422 psi)				
1. Aft closure insulation, silica-phenolic	Normal tension	2.52 (366 psi)	6.90 (1000 psi)	+2.73
2. Entrance cap, carbon-phenolic	Shear	3.10 (451)	19.3 (2800)	+6.22
3. Throat insert, graphite-phenolic	Axial tension	2.00 (291)	5.10 (740)	+2.54
4. Throat insert, silica-phenolic	Normal tension	3.23 (470)	6.90 (1000)	+2.13
5. Exit cone, graphite-phenolic	Normal tension	.31 (45)	5.10 (740)	+16.4
6. Exit cone, silica-phenolic	Shear	1.42 (207)	19.3 (2800)	+13.5
7. Exit cone, glass over-wrap	Hoop tension	.03 (5)	896.0 (130000)	High
8. Nozzle steel housing	Hoop tension	134.0 (19470)	620.0 (90000)	+4.63
9. Throat to shell adhesive bond	Shear	5.96 (866)	13.8 (2000)	+2.31
10. Throat to shell adhesive bond	Tension	5.85 (850)	13.8 (2000) (1)	+2.06
D. Steel sheel prooftest, $P = 5.65 \times 10^6$ N/m^2 (820 psi)				
1. Throat shell	Hoop tension	255.0 (37000)	620.0 (90000	+1.43
2. Conical aft closure	Hoop tension	331.0 (48000)	620.0 (90000	+0.88

(1) Assumed allowable

Reference 2

CASTOR IIA

Background. - This solid propellant motor was developed for the National Aeronautics and Space Administration as the second stage of the NASA SCOUT vehicle. This is the only SCOUT motor in which the nozzle exit cone is used as an interstage load-carrying structural component. The same motor but with a similar, shortened, canted nozzle is also used on Delta vehicles. In over 77 SCOUT flights since recertification in 1963 there have been no failures. Castor nozzle geometry and materials are shown in Figures 18 and 19. Table VII lists alternate qualified materials for each nozzle component.

Performance Data. - The Castor IIA (TX-354-3) motor has a maximum expected operating pressure (MEOP) of 5.509×10^6 N/m^2 (799 psi) and a flame temperature of 3589°K (6000°F). This motor uses a carboxyl-terminated polybutadiene propellant, TP-H7036, having 20% aluminum content and 60% ammonium perchlorate oxidizer. Motor performance parameters are summarized in Table VIII. Figure 20 shows the nominal chamber pressure variation throughout firing. There have been numerous flights of this SCOUT motor and as a result the pressure curve is well defined. Values are normally averaged after every ten flights.

Drawings and Specifications. - Castor IIA nozzle drawings and specifications are shown in Table IX.

Material Description

The Castor II nozzle materials are described below. Temperature dependent physical and mechanical properties are included in Table X.

4130 Steel nozzle housing is machined from an AISA 4130 steel forging normalized to 620×10^6 N/m^2 (90,000 psi) heat treat.

ATJ Graphite (Throat Insert). - This is an extremely fine grained, $.15 \times 10^{3}$ M (.006 in.) diameter grain size, high strength graphite. It is fabricated by molding to an average density of 1.73 gm/cc. The molding operations produce a preferred orientation of the graphite particles which give rise to "with grain" and "across grain" properties. It can be machined to very close limits and sharp detail with fine surface finish.

RPD41 (Throat Insert Insulation). - This is a pre-impregnated felt tape manufactured from a long spinning grade Chrysotile asbestos fiber carded into ASTM Grade AAAA felt and impregnated with a high temperature phenolic resin. Low thermal conductivity, low thermal diffusivity and good mechanical properties make RPD41 an excellent material for structural insulators.

4030-190 (Entrance Insulation). - This is a molded glass phenolic material that protects the forward edge of the insert. The material consists of chopped glass roving that is impregnated with a high temperature phenolic resin (Fiberite HT-460). The chopped glass roving uses fiber lengths from 0.5 to 1.0 inch.

MX 2600 (Exit Cone Insulation). - This is a silica fabric impregnated with a high temperature phenolic resin containing silica reinforcement. The phenolic resin must meet specification MIL-R-9299 Type II, phenolic resin. The silica fabric is Sil Temp 84 or Hitco C100-48. The reinforcement, or filler, is silica dioxide of 98% purity. Alternate materials FM 5504 and FM 5067, are similar and may also be used for exit cone insulation.

Polyurethane nozzle closure is machined from a molded high density polyurethane foam and bonded in the exit cone with a silicone rubber adhesive. The nozzle closure fractures on motor ignition at a pressure of approximately $.31 \times 10^{6}$ N/m^{2} (45 psi).

Fabrication and Process. - Fabrication and inspection procedures are summarized for each component of the Castor IIA nozzle in Figure 21. That figure briefly summarizes the fabrication procedures and quality inspections for each nozzle component.

Thermal Data

The thermal data for the Castor IIA motor was obtained from a static test (Motor 22) in altitude test cells at the Arnold Engineering Development Center (AEDC) in Tullahoma, Tennessee. The data presented was obtained in firing Castor IIA (TX354-3) nozzles and reported in reference 3.

These two motors, 5 and 22, were tested as part of the Preliminary Flight Rating Test program and were heavily instrumented with strain gages and thermocouples. Similar results were obtained from both motors and the data presented from motor 22 is considered typical for the Castor IIA nozzle.

Char and Erosion. - Figure 22 shows a graphical presentation of a Castor IIA motor nozzle which indicates the char and erosion depths at each location. This figure also shows the station numbers which are utilized in Table XI to present measured char and erosion depths at selected locations.

Temperature Distribution. - The Castor IIA motor was fired for 39.06 seconds. Figure 23 presents the exterior temperatures 60 seconds after the start of firing of the motor, including a 20.94 second soak period. The temperatures indicate that, during the firing of the motor and the short soak period duration after the firing, the exterior surfaces outboard of the throat insert remain near initial temperatures. The exit cone, due to its thinner construction, attains slightly higher temperatures. All temperatures presented will increase significantly as the soak period is extended. At 20.94 seconds in soak, none of the exterior temperatures attained their peak values.

Figure 24 presents the analytically determined isotherms at 10 seconds after ignition as obtained by a 2-dimensional transient thermal analysis. At approximately 10 seconds after ignition the maximum thermal gradient occurs in the ATJ nozzle insert.

Figure 25 presents the analytically determined isotherms at 35 seconds after ignition as obtained by analysis. At 35 seconds maximum temperatures are attained in the ATJ nozzle insert.

Structural Analysis

This nozzle was analyzed by Thiokol Corporation, Huntsville Division (reference 3). Nozzle attach fittings and steel exit cone structure were analyzed by hand methods for maximum flight and ground handling loads. Nozzle design ultimate pressure was assumed to be $.6475 \times 10^6$ N/m^2 (940 psi) which represented a factor of safety of 1.3 over the original MEOP value of 4.91×10^6 N/m^2 (713 psi). Since that time the MEOP value has been increased to 5.5×10^6 N/m^2 (799 psi), but, due to the relatively high calculated margins of safety of the steel components it was not considered necessary to redesign these parts for a higher ultimate pressure. The insert thermoelastic analysis used nominal pressure values shown in Figure 20.

An insert analysis (reference 3) was performed in 1968. The methodology used at that time required assumptions of isotropic properties and rigid bond lines. These assumptions affect to some extent the accuracy of the results presented herein and the method of calculating margins of safety.

Loads. - Pressure distributions along the insert are plotted for different times after ignition in Figure 26. These limit pressures were used in the thermoelastic analysis.

Nozzle proof test pressure is 4.14×10^6 N/m^2 (600 psi). This test checks the bond line integrity at the outboard edge of the insert. Test fixture arrangement is shown in Figure 27.

Factors of Safety. - The analyses performed were based on the following required factors of safety and design loads.

Limit Load: Anticipated maximum load on structure.

Design Ultimate Load (Shear & Bending) = 1.5 x Limit Load

Design Ultimate Load (Compression & Tension) = 1.8 x Limit Load

Design Ultimate Stress (Thermal Environment) = 1.0 x Limit Load

$$\text{Margin of Safety} = \frac{\text{Ultimate Strength}}{\text{Design Ultimate Load}} - 1$$

$$\text{Factor of Safety} = \frac{\text{Design Ultimate Load (Stress)}}{\text{Limit Load (Stress)}}$$

Results of Analyses. - Margins of safety for the attach bolts and steel shell are tabulated in Table XII. A minimum margin of safety of .22 occurs under combined bending and axial loads in the flange attach bolts and a minimum margin of .52 in the nozzle exit cone area.

A thermoelastic analysis of the throat insert and adjacent surrounding insulation and nozzle body (without exit cone) was performed in 1969 (reference 3). The model was assumed to be linearly elastic, isotropic and homogeneous due to the limitations of the then available computer method. Results of this analysis shown in Figures 28 and 29 indicated negative margins of safety which were not consistent with the long successful nozzle history during which no cracked inserts have ever been noted. Figure 30 shows the stress strain behavior of ATJ graphite at elevated temperatures based on material characterization tests. This figure was used by Thiokol to obtain more realistic stress distributions in the inserts by use of secant moduli. The approach used was to take the calculated strain based on the linear elastic analysis and read the associated stress from the proper curve in Figure 30. These reduced stresses are plotted in Figures 31 and 32. The material temperature dependent allowables are superimposed on these figures. Comparison of allowable versus actual stresses in these figures indicates acceptable margins of safety. Quantitative values of margins of safety do not result directly from this method of evaluation. For example, at location A in Figure 28 the margin of safety may be obtained as follows:

$$M.S. = \frac{2800}{2000} - 1 = +0.4$$

Estimated Accuracy of the Castor IIA Nozzle Analysis. - Estimates of expected accuracy of the structural analysis were made for the Castor IIA nozzle. Ignition strains can be predicted within about 10%. Under these conditions materials tend to behave elastically due to high loading rate and the materials are still at essentially room temperature. Somewhat larger errors normally result for calculated stresses due to

variations in moduli of elasticity of component materials, but proper characterization, screening and inspection of materials can restrict the error for the ignition condition to about 29% for graphites, and somewhat higher for laminates due to their orthotropic characteristics.

Stresses and strains which occur later in firing are more difficult to predict accurately due mainly to the non-linear behavior of materials at elevated temperature and inherent errors in material characterization at higher temperatures. Proper modelling of surface recession, use of non-linear theory or similar iterative procedures and careful attention to material interfaces permit reasonable assessment of critical stresses and strains for this condition. For the Castor IIA nozzle, total errors are believed to be within 35%. The most important factor in a nozzle analysis is proper modelling of the complex structure including bond lines and boundary conditions. In one instance in which only these last two factors were varied, stresses differed by 500% although identical environments and material properties were used.

Problem Areas. - During the Castor IIA development program the exit cone insulation assembly processing was changed to permit this component to be molded and then bonded into the steel exit cone structure. This was done to provide greater bond reliability and to eliminate a cure shrinkage problem which existed when the insulation was molded in place. This change resulted in greater erosion resistance. The exit cone insulation fabrication technique was also changed from a rosette lay-up to a tape wrap procedure. During the long successful history of SCOUT usage there have been no flight or static test failures of this nozzle.

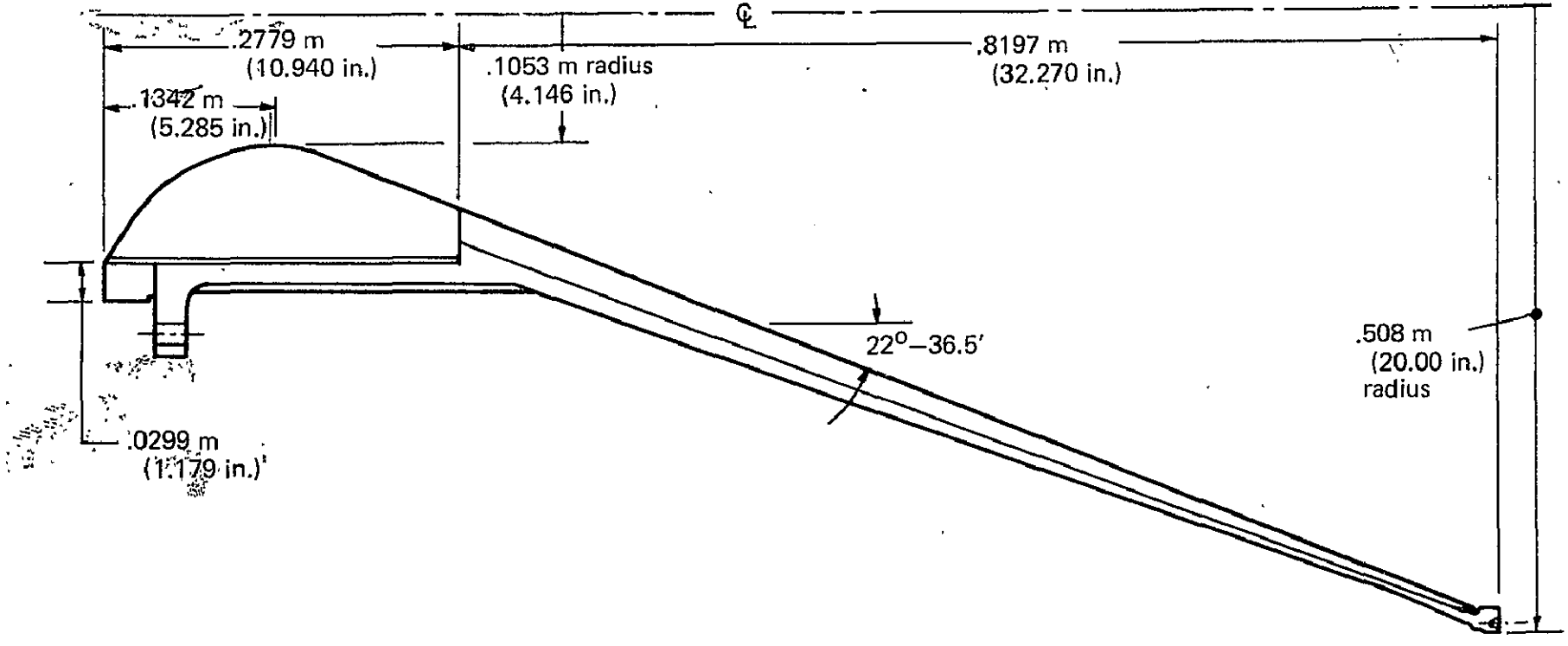

FIGURE 18. – CASTOR IIA NOZZLE GEOMETRY

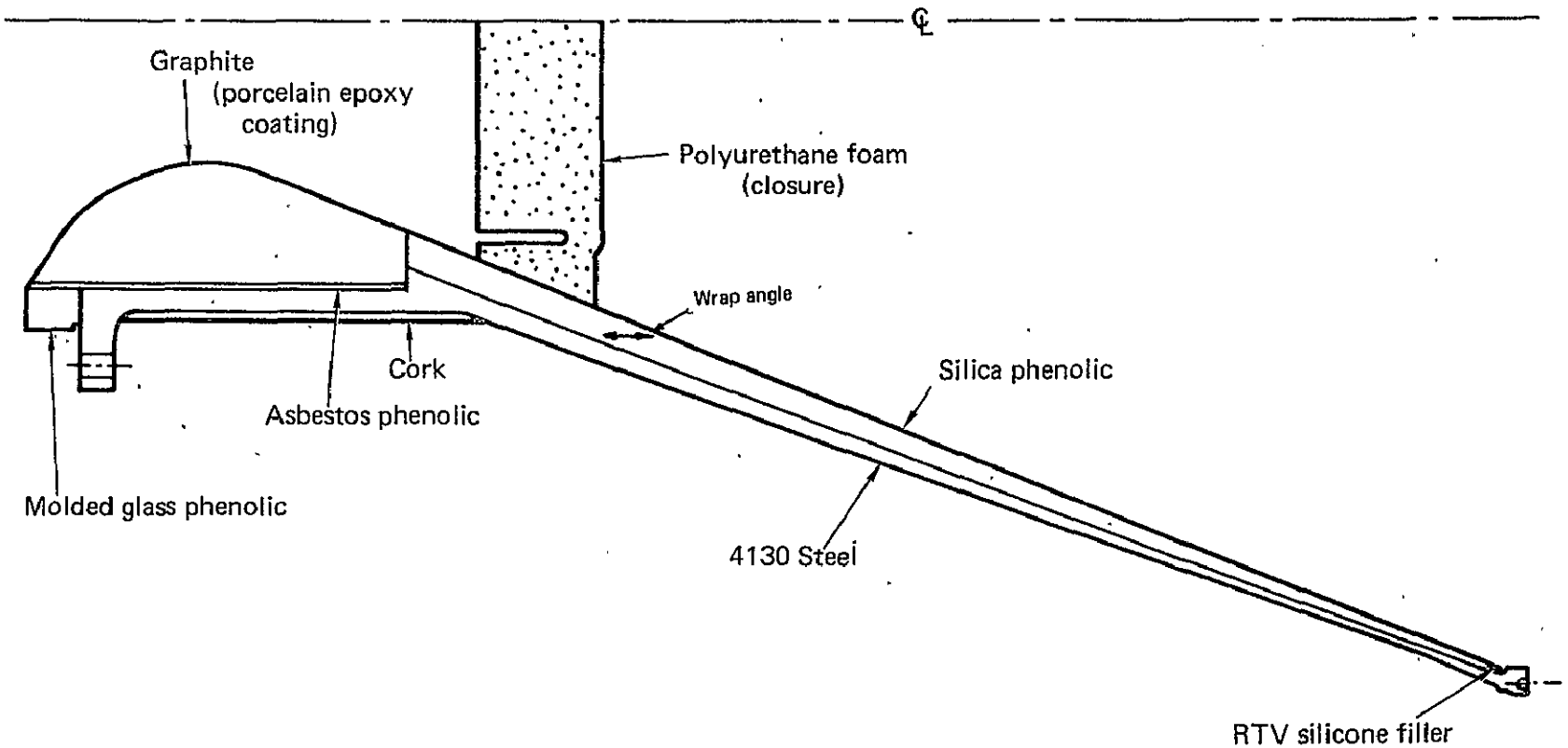

FIGURE 19. – CASTOR IIA NOZZLE MATERIALS

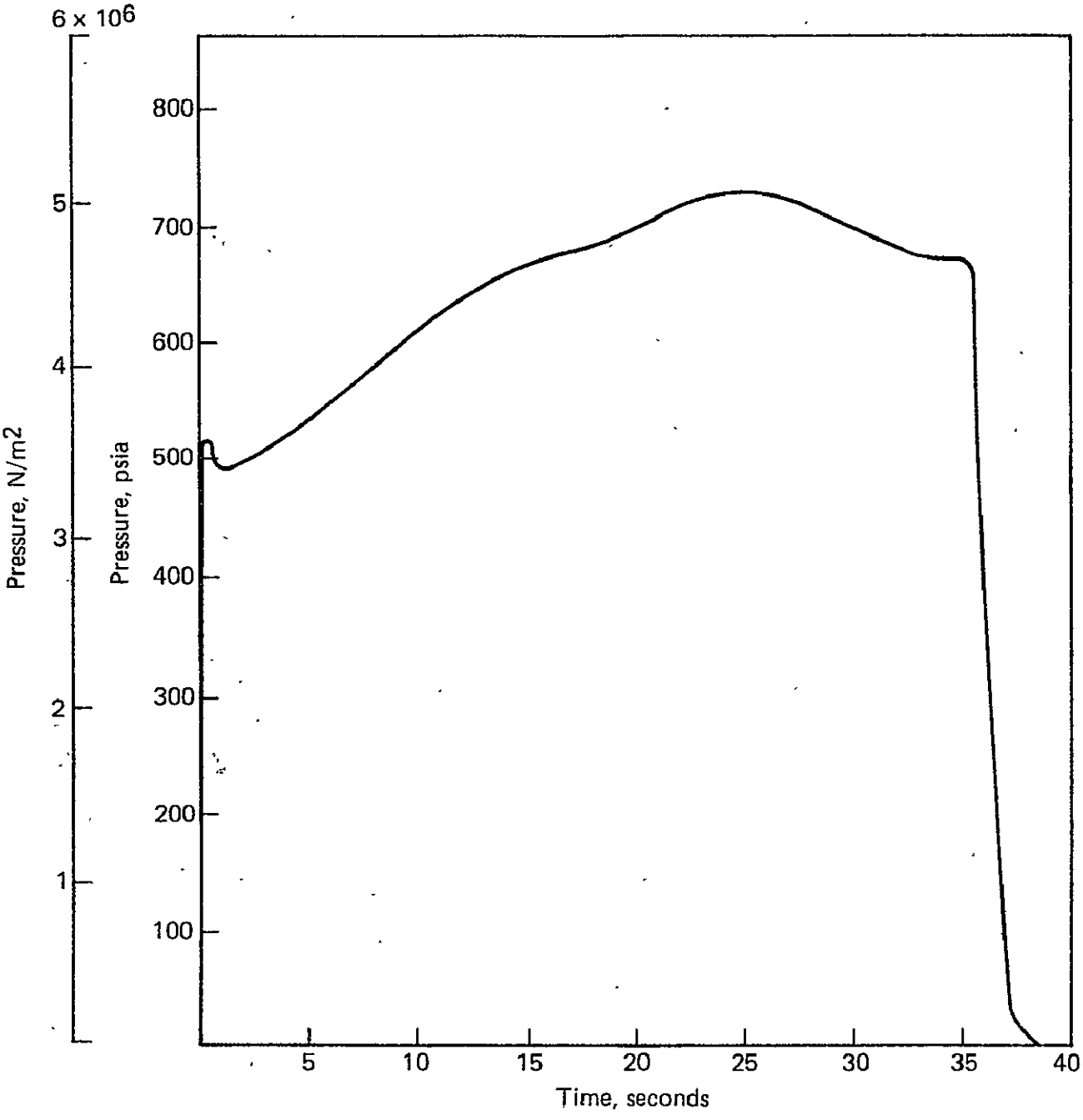

FIGURE 20. – CASTOR IIA PRESSURE VS TIME

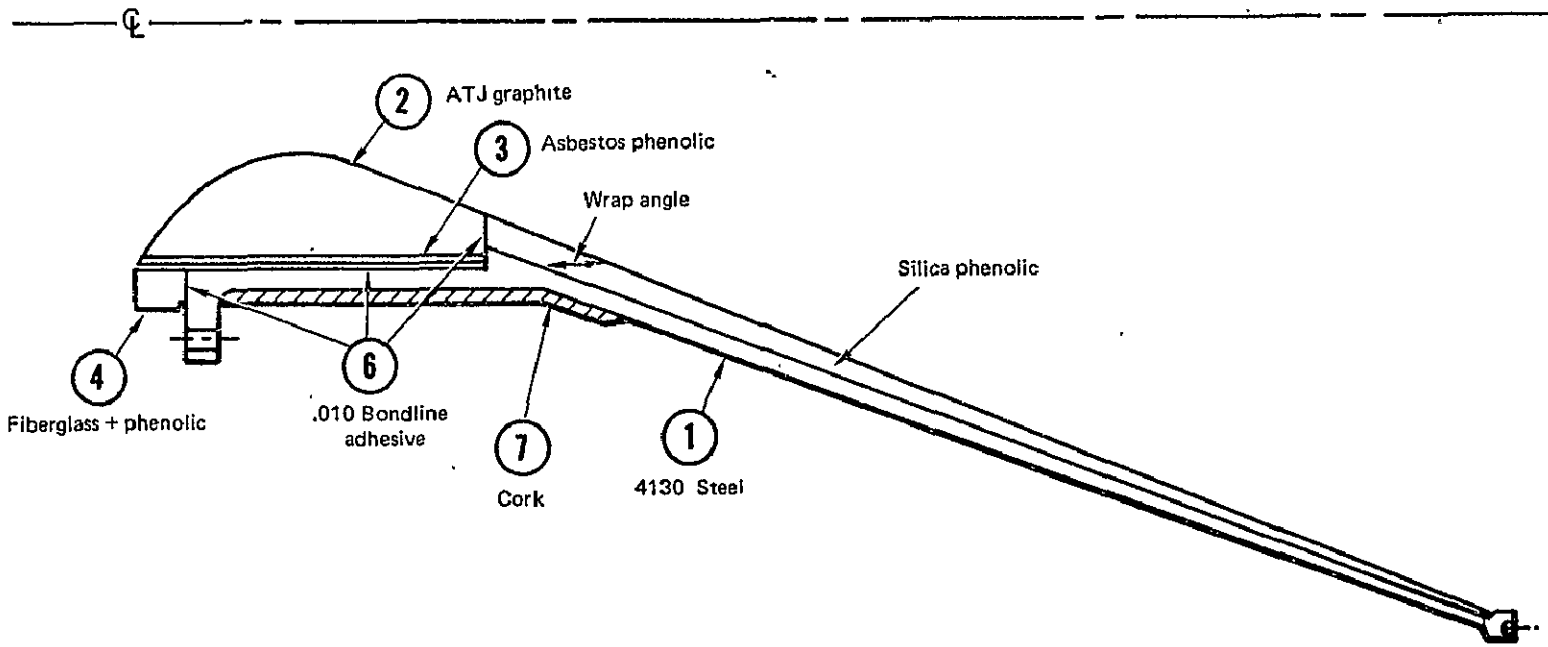

Item No.	Name	Material	Fabrication/Inspection
1	Nozzle body	4130 Steel per MIL-S-6875, cond D.	The nozzle body is machined from a normalized AISI 4130 steel forging having a tensile strength of 620×10^6 N/m^2 (90,000 psi). The nozzle body serves as a mating component between the first and second stages of the Scout vehicle. It also incorporates a flange for bolting to the motor case. Threads are provided in the exit area to mate with the separation diaphragm. The nozzle forging is radiographically inspected for internal defects. Bare steel surfaces are protected from corrosion by an epoxy primer coating or corrosion preventive MIL-C-11796, class 3.
2	Throat insert	ATJ Graphite	The nozzle throat insert is machined from ATJ graphite manufactured by the National Carbon Co. It is a fine grain, essentially flaw-free, molded polycrystalline graphite which has a maximum grain size of .006 inch, a moderately high strength, and a typical specific gravity of 1.72 gm/cc. The throat insert is radiographically and visually inspected for internal and external defects. After final nozzle assembly the graphite throat surface is coated with porcelain epoxy paint (protex 225) to seal the graphite surface for the nozzle pressure test.
3	Throat insulation	Asbestos phenolic tape per SP 319, type II, class 2.	The asbestos phenolic tape (RPD41) is tape wrapped parallel to the nozzle centerline over the outside diameter surface of the ATJ throat insert, previously coated with a polysulfide adhesive (TA-L703), and then cured at a temperature of 408° to 450°K (275 to 350°F) for 6 hours in an air oven.

FIGURE 21.- CASTOR II A FABRICATION AND INSPECTION — Continued

Item No.	Name	Material	Fabrication/Inspection
4	Forward insulation	Glass phenolic molding per TCC SP-262, type I, class 1.	The forward entrance insulation is fabricated by compression molding a chopped glass fiber material impregnated with a high temperature phenolic resin (fiberite 4030-190 compound) in a steel mold. The glass phenolic molding is cured in the mold and then removed and post cured in an air oven. Visual and radiographic inspections are performed on the molding for surface and internal defects. The specific gravity of each molding is also determined.
5	Exit cone insulation	Silica phenolic tape per TCC SP521, type II, class A, comp 1 or 2.	The exit cone insulation is made from a high silica phenolic tape (FM 5067 or MX 2600) which is tape wrapped on a steel mandrel with the wrap angle parallel to the nozzle centerline. The part is vacuum bagged and cured at 428°K (310°F) in a hydroclave at 6.9 x 10^6 N/m^2 (1000 psi). Post cure of the insulation is performed in an air oven at 350°F. In process test specimens are removed from a prolongation of the exit cone insulation prior to hydroclave cure for percent volatiles and percent flow determinations. A tag end specimen from the cured wrap is tested for resin content, specific gravity and barcol hardness as a quality control check on the process. Visual inspection is performed to make sure that part is free from delaminations, blisters and evidence of water leakage during hydroclave cure. The exit cone insulation is bonded to the steel nozzle body with RTV88 silicone adhesive and cured at room temperature for a minimum of 24 hours.
6	Adhesive	TA-L721 polysulfide per TCC SP-17	The forward insulation and throat insert assembly are bonded to the steel nozzle body with TA-L721 polysulfide adhesive. All bonding surfaces are lightly sanded and cleaned with methylene chloride before the adhesive is applied to the mating surfaces. The parts are assembled and cured in a bonding fixture at room temperature for 24 hours or for 2 hours at 350°K (170°F). Upon completion of cure the nozzle assembly is machined to the engineering drawing configuration.
7	External insulation	Armstrong 2755 insulcork	The nozzle assembly is covered with a .008 m (.312 in.) thick layer of armstrong 2755 cork on the exterior surface of the nozzle throat region. The cork extends from the flange aft for 13 inches. RTV 88 silicone rubber adhesive or HYSOL EA 934 epoxy adhesive is used to bond the cork to the steel body. The cork is painted with EC 2241 protective coating which is a synthetic rubber base paint that provides fungus growth protection to the cork insulation.

FIGURE 21. – CASTOR II A FABRICATION AND INSPECTION – Concluded

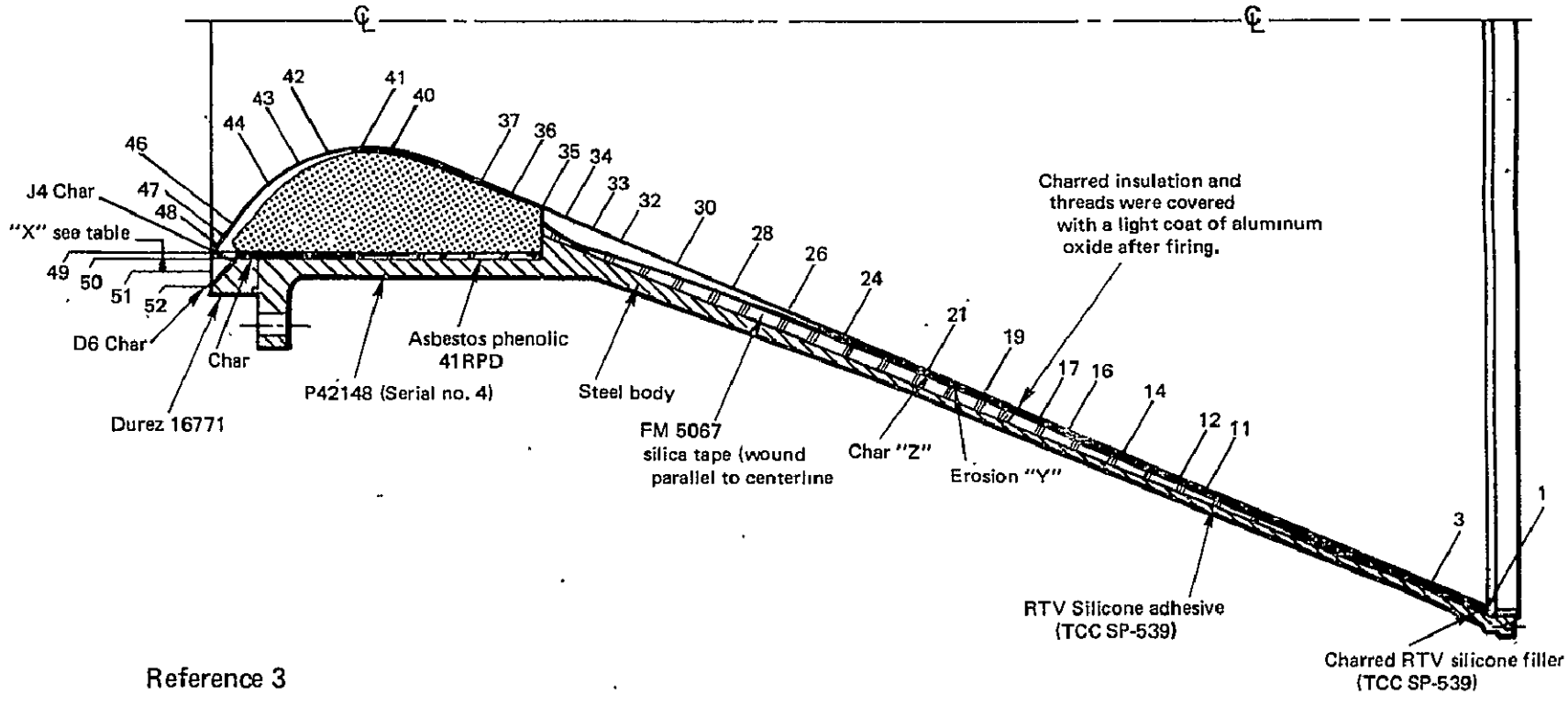

Reference 3

FIGURE 22. – CHAR AND EROSION PROFILE, MOTOR NO. 22

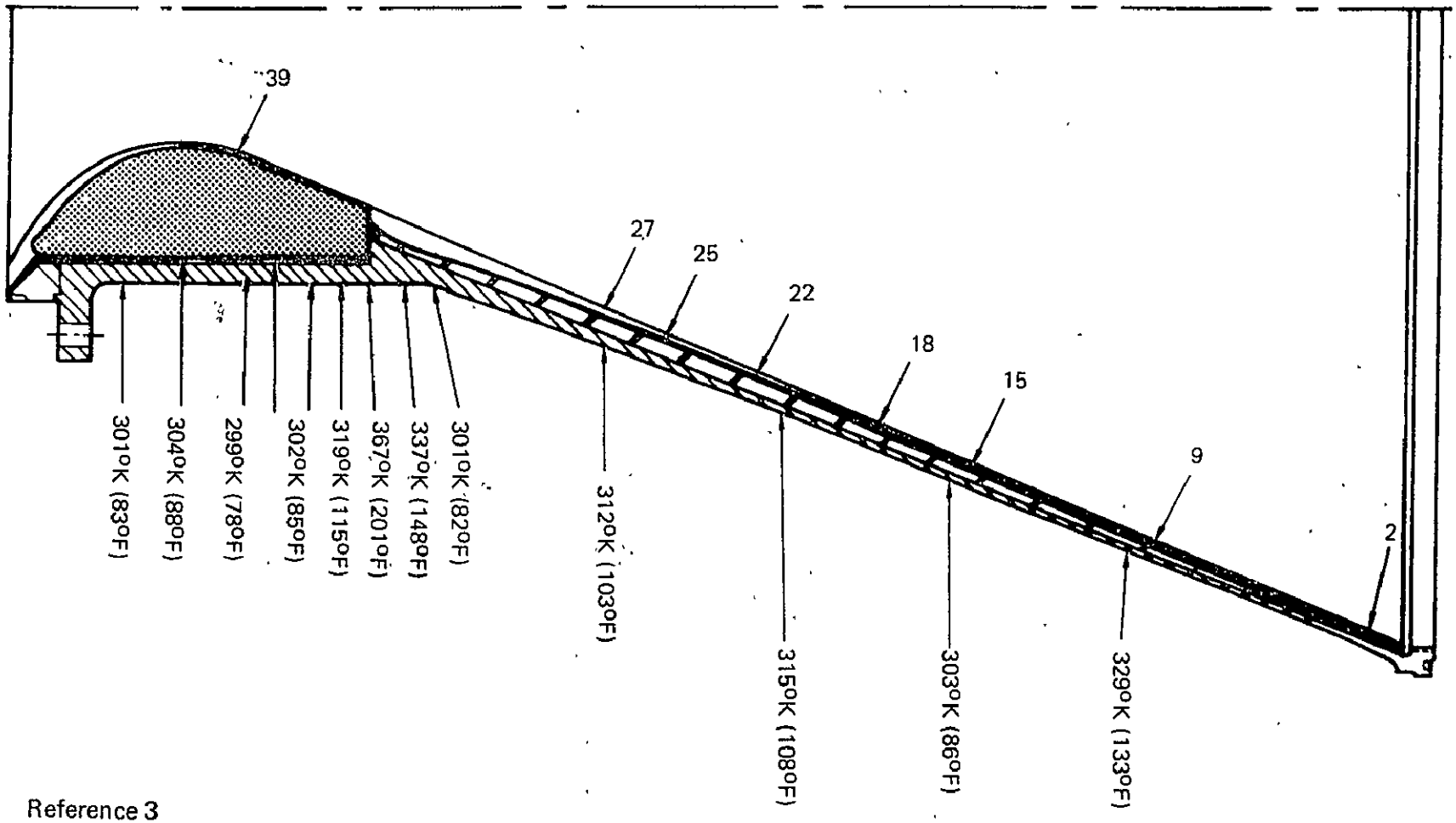

Reference 3

FIGURE 23. – TYPICAL EXTERIOR TEMPERATURES OF MOTOR NO. 22 AFTER A 39.06 SEC FIRING AND A 20.94 SEC SOAK PERIOD

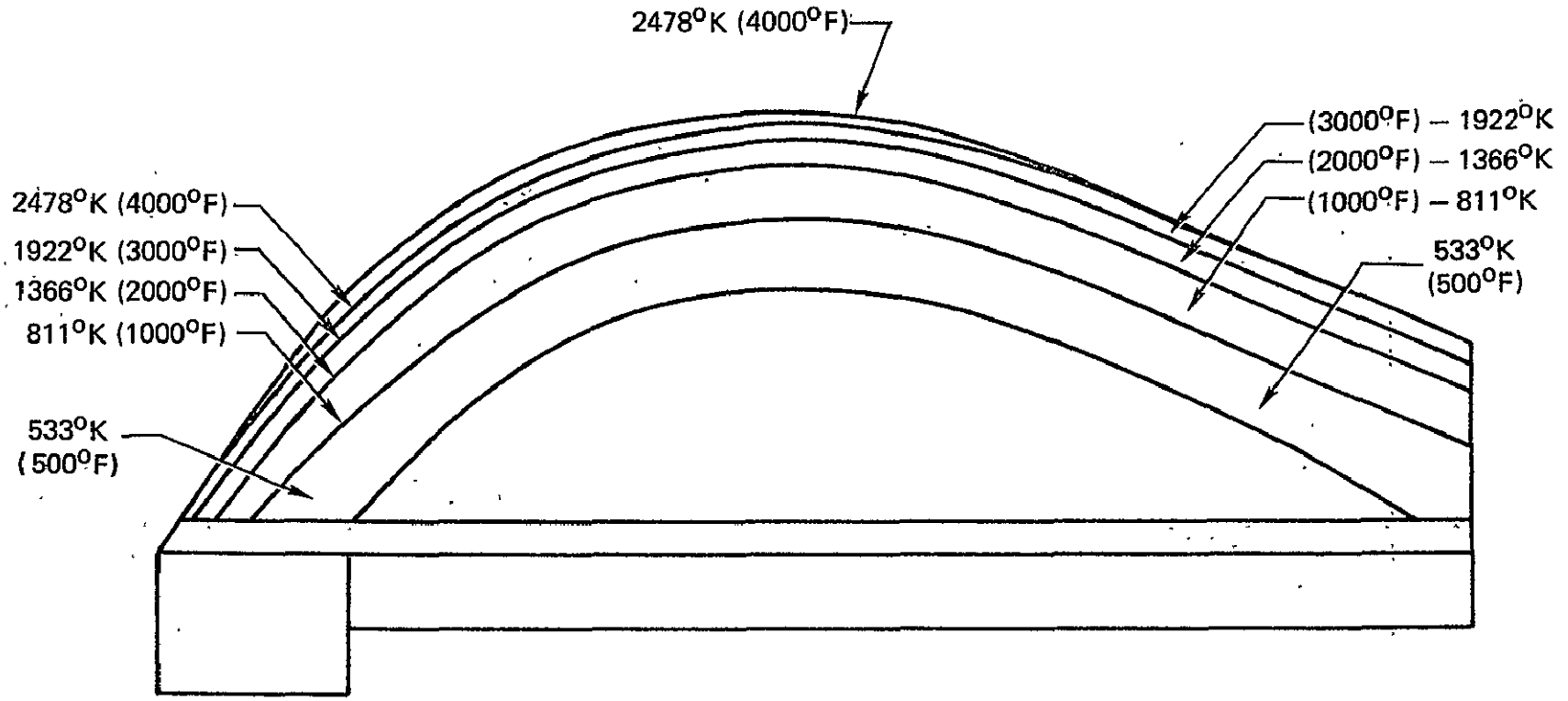

FIGURE 24 – NOZZLE INSERT ISOTHERMS AT 10 SECONDS AFTER IGNITION

Reference 3

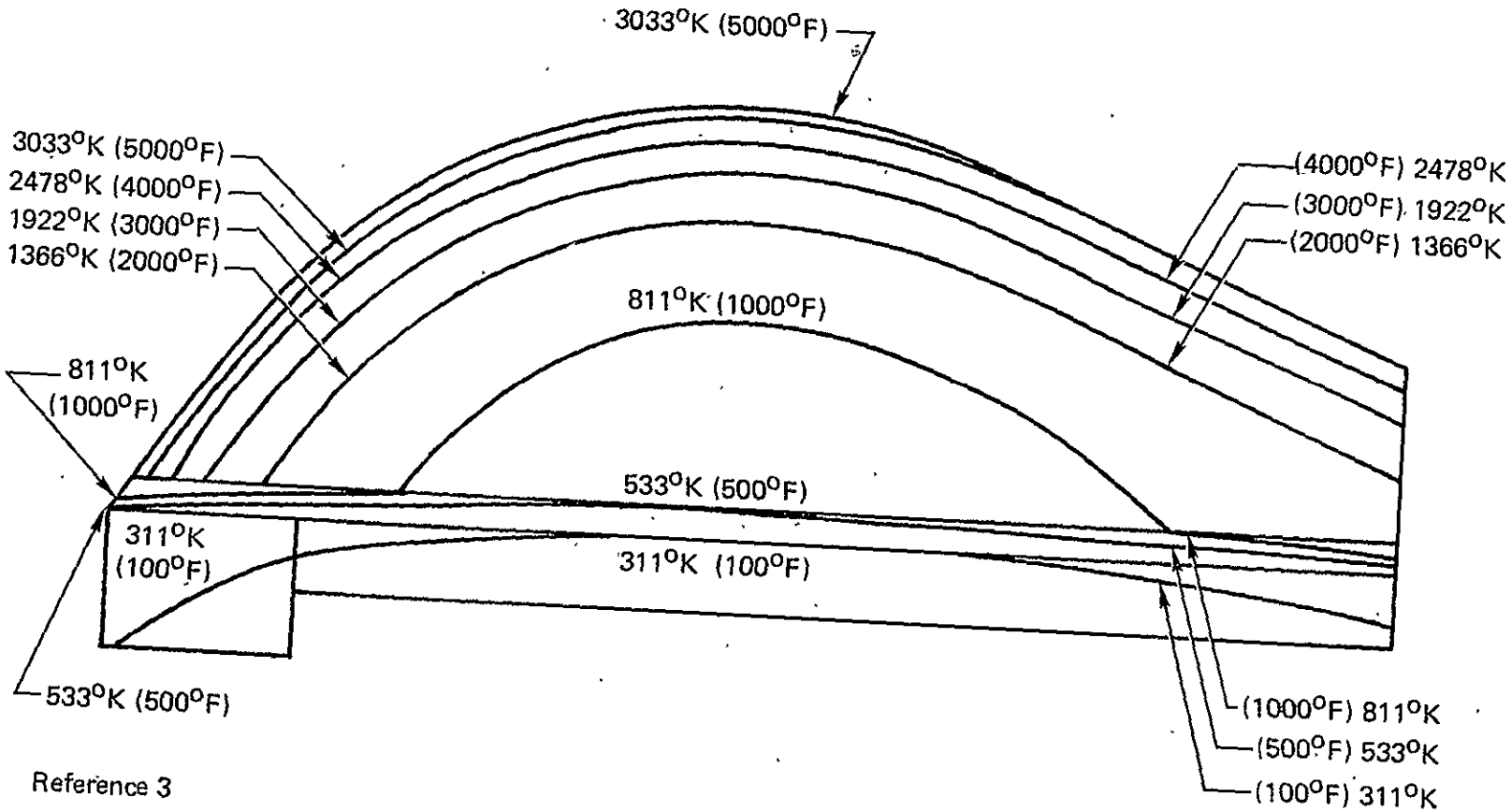

Reference 3

FIGURE 25. – NOZZLE INSERT ISOTHERMS AT 35 SECONDS AFTER IGNITION

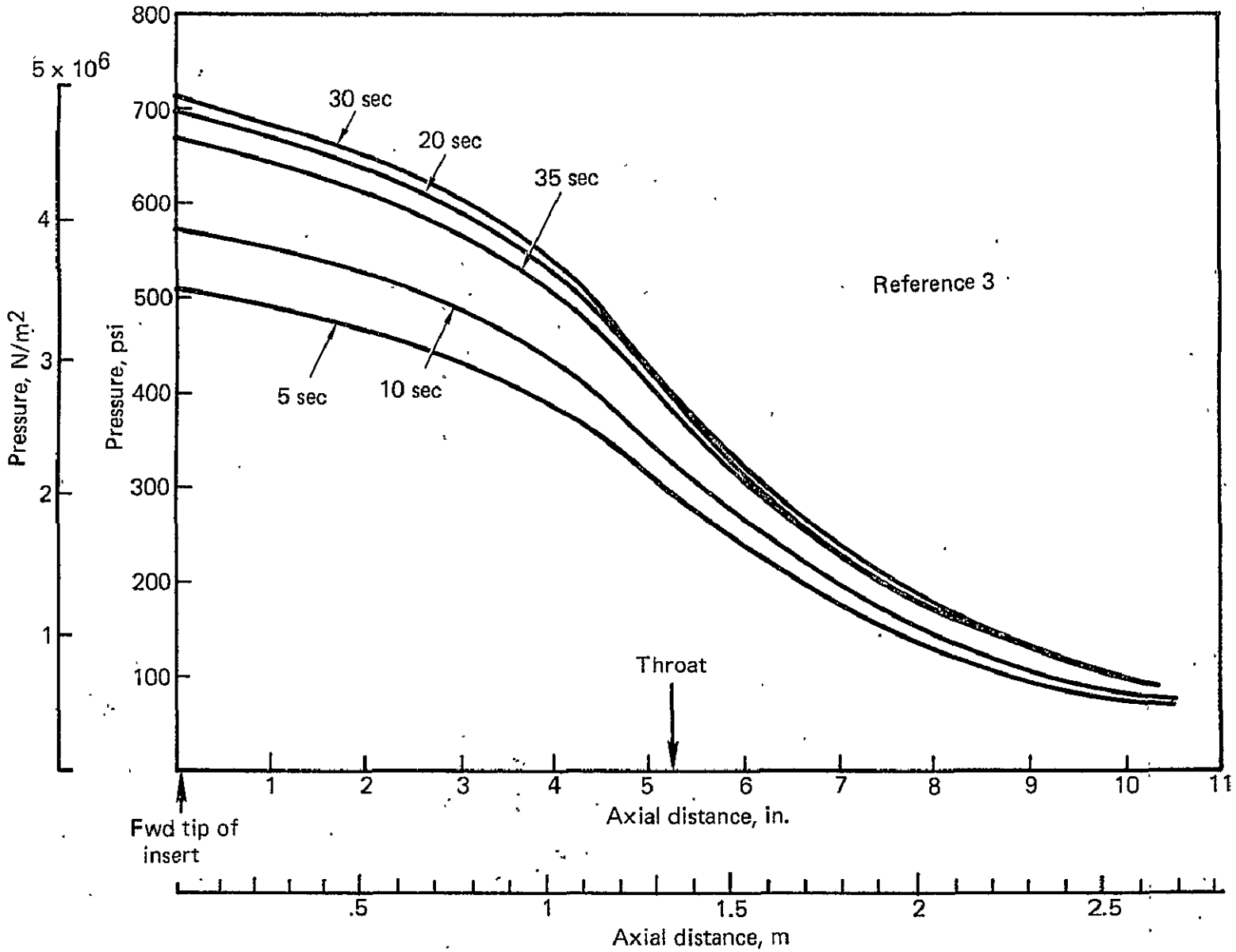

FIGURE 26. – PRESSURE DISTRIBUTIONS ALONG THE INSERT

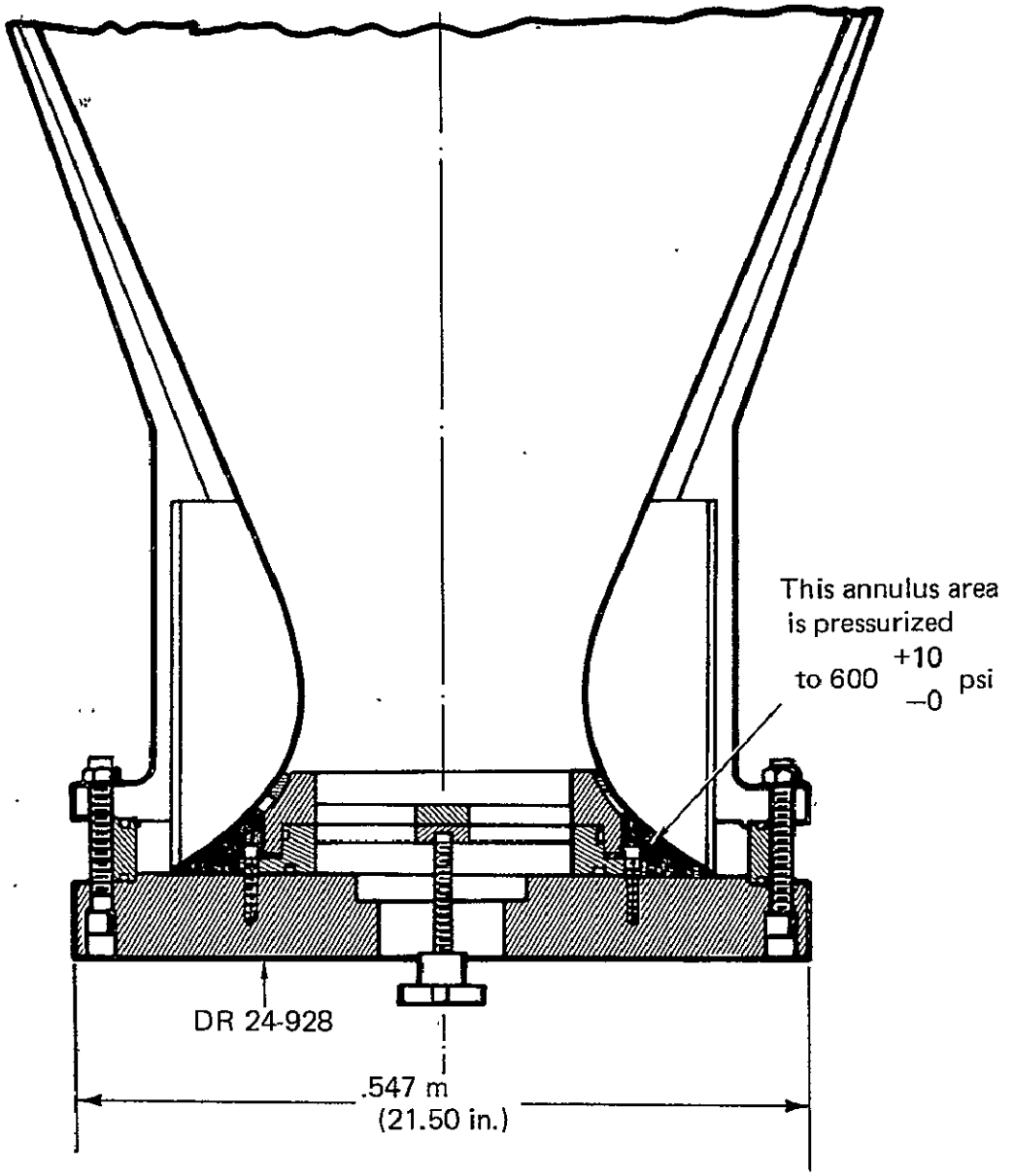

FIGURE 27. — PROOF TEST ARRANGEMENT

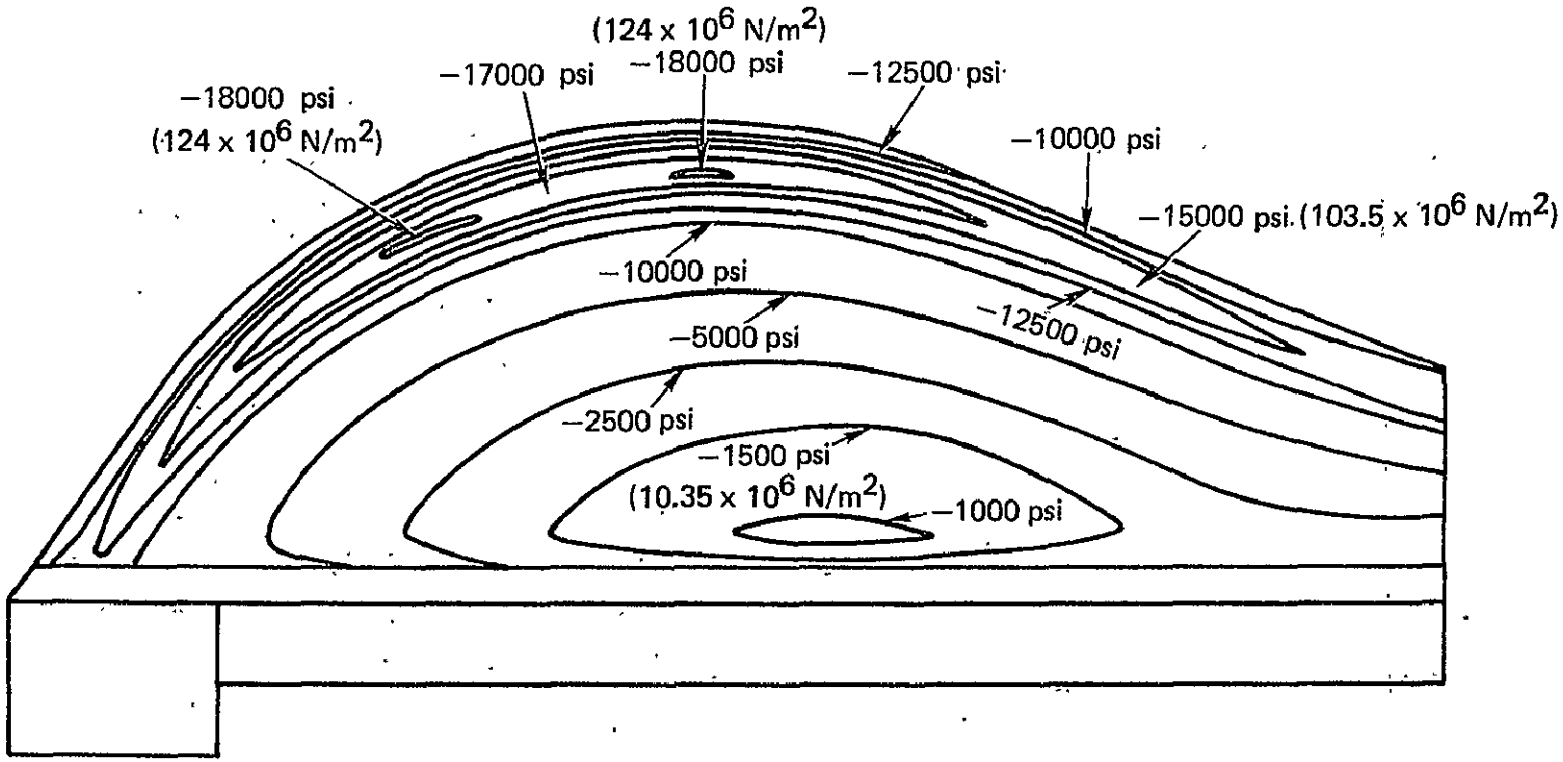

Reference 3

FIGURE 28. — CONTOURS OF HOOP STRESSES BASED ON INITIAL MODULUS FOR TIME EQUAL 35 SECONDS

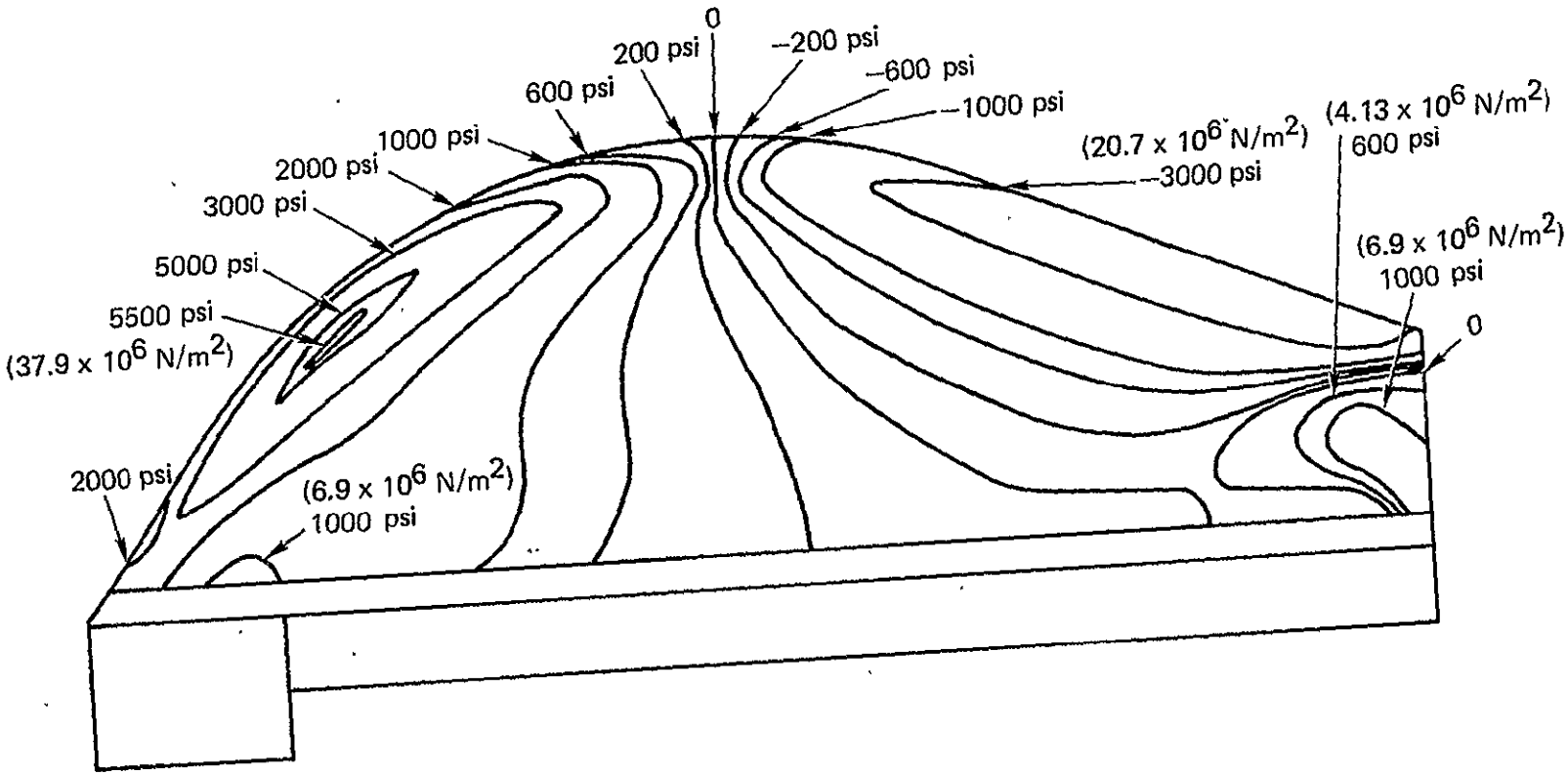

Reference 3

FIGURE 29. — CONTOURS OF SHEAR STRESSES BASED ON INITIAL MODULUS FOR TIME EQUAL 30 SECONDS

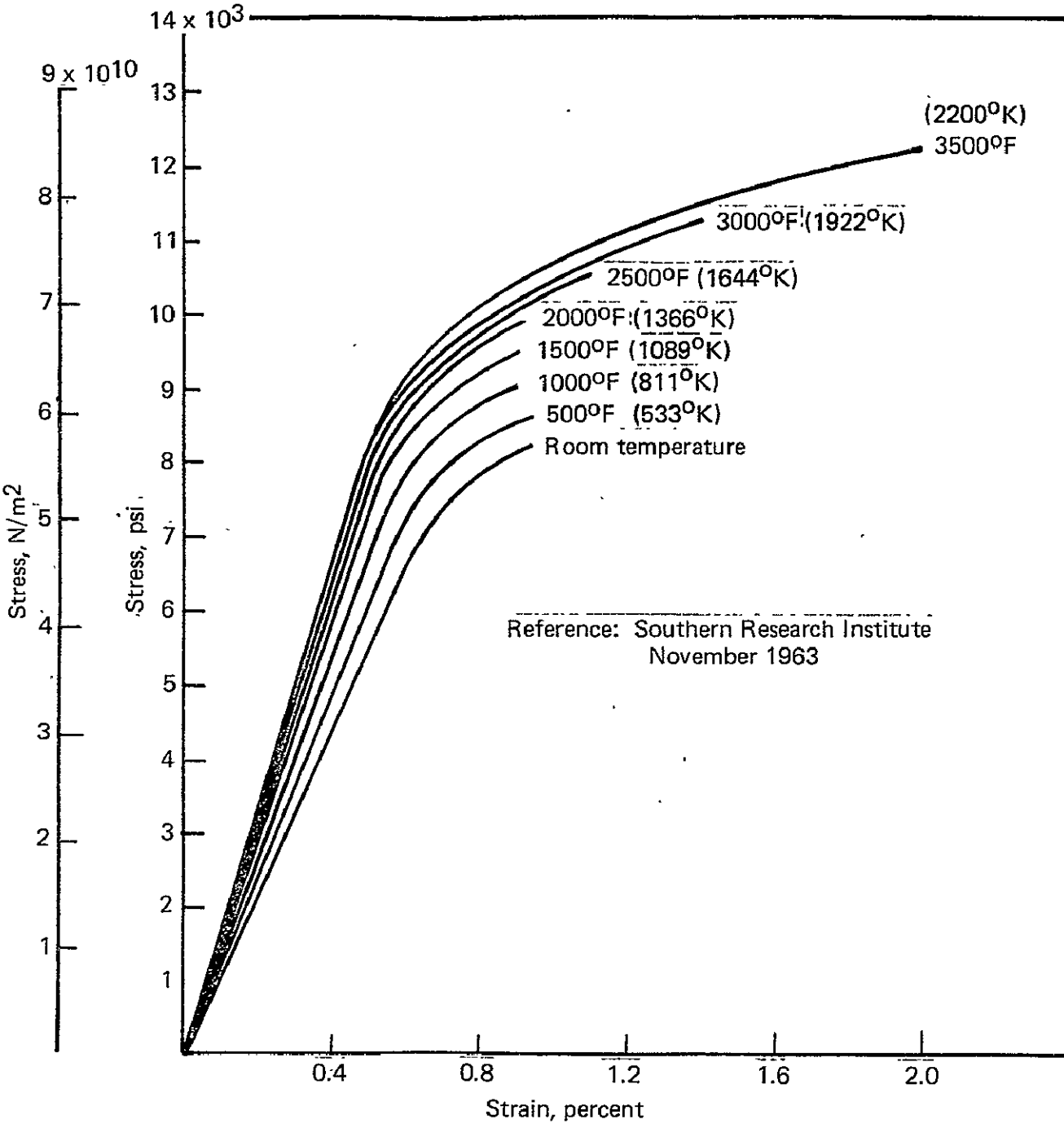

FIGURE 30. – ESTIMATED STRESS-STRAIN CURVES FOR ATJ GRAPHITE LOADED IN COMPRESSION WITH THE GRAIN

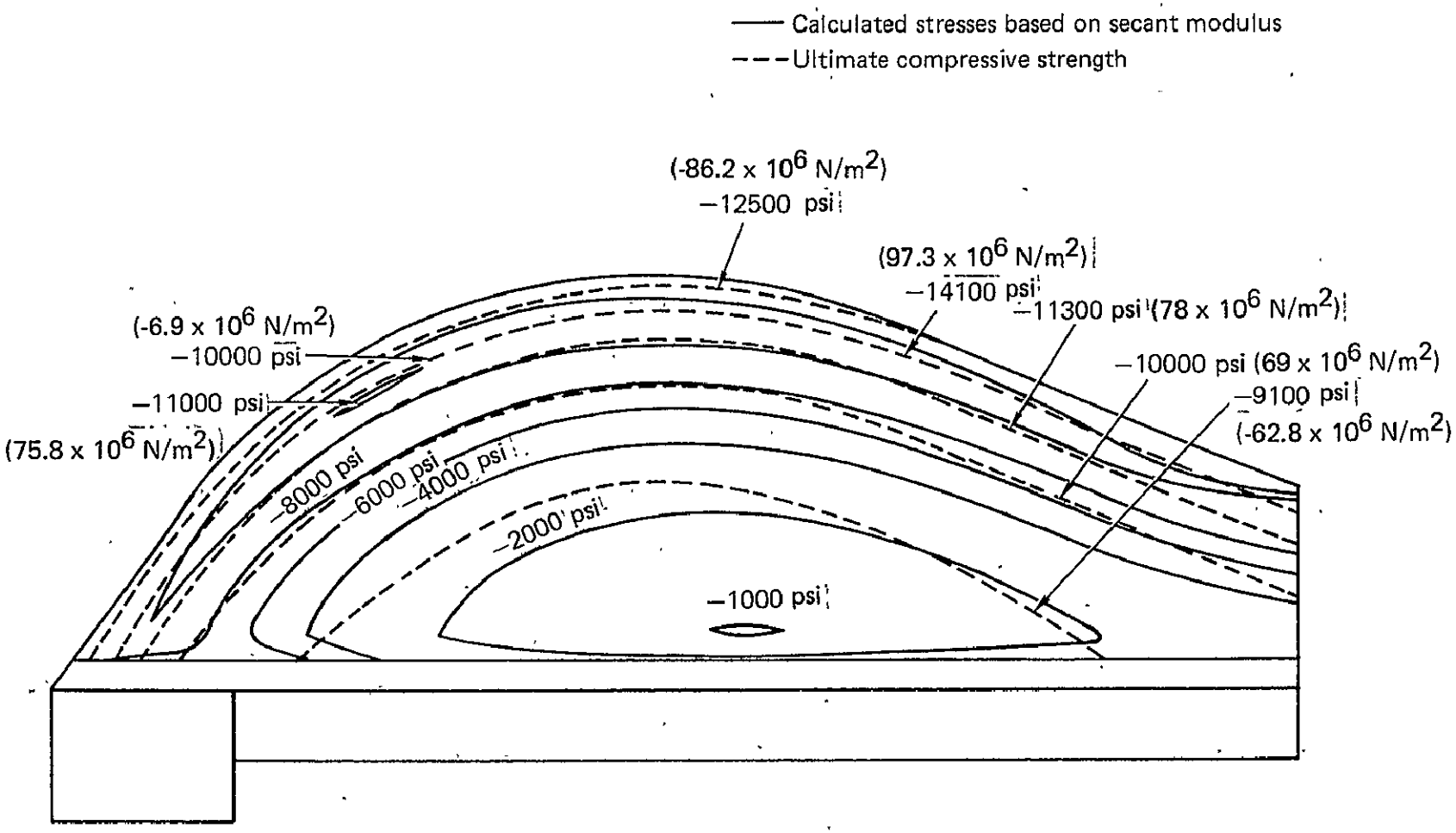

Reference 3

FIGURE 31. – COMPARISON OF CALCULATED HOOP COMPRESSIVE STRESSES TO ULTIMATE COMPRESSIVE STRENGTH OF ATJ GRAPHITE MEASURED WITH THE GRAIN

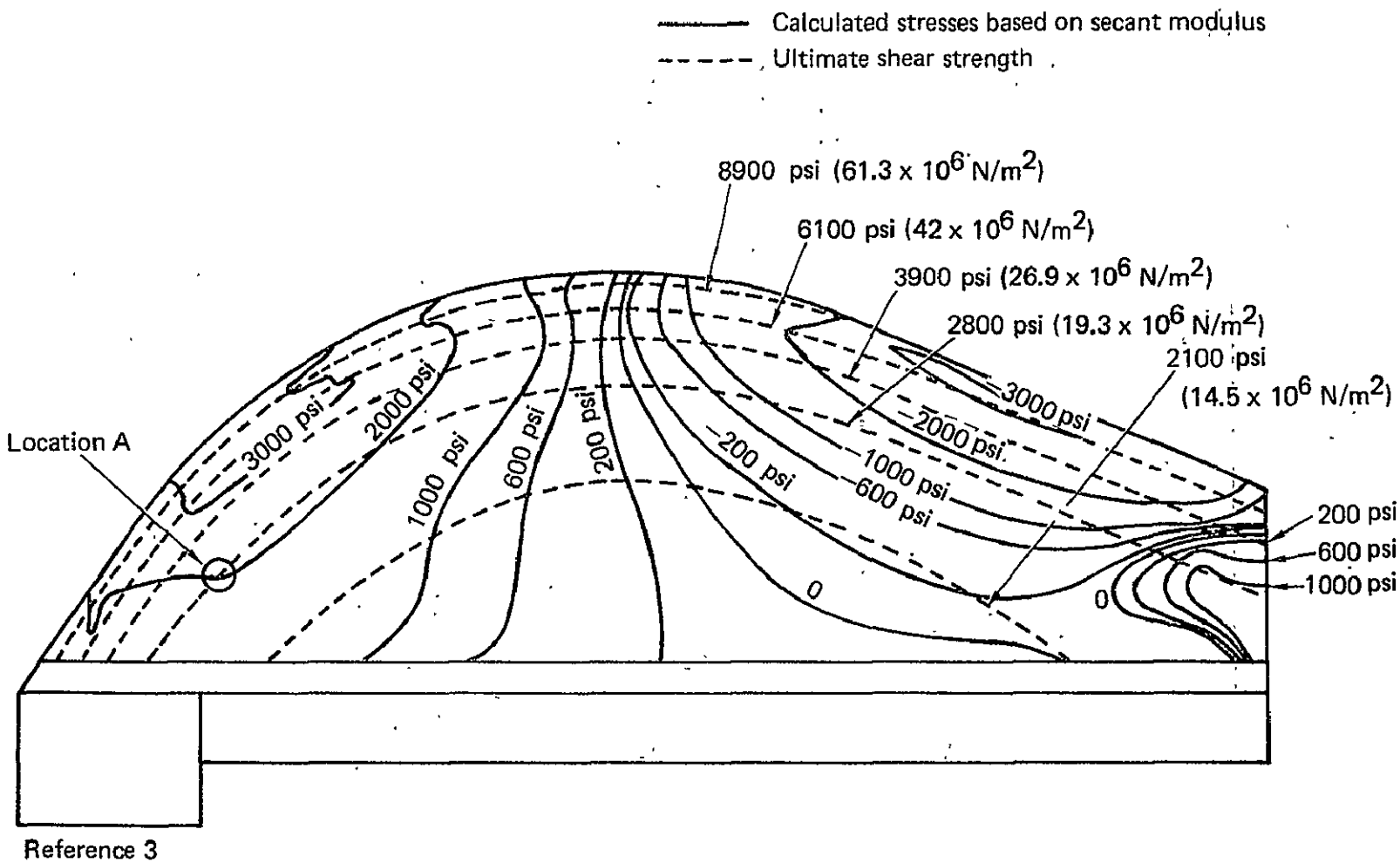

FIGURE 32. – COMPARISON OF CALCULATED SHEAR STRESSES TO ULTIMATE SHEAR STRENGTH OF ATJ GRAPHITE MEASURED WITH THE GRAIN

TABLE VII – CASTOR IIA NOZZLE MATERIALS

Component	Material	Alternate designation	TC Procurement specification
Throat insert	Graphite	ATJ	SP-537
Throat insert coating	Porcelain epoxy	—	MIL-C-22750 Type I, clear
Throat insert insulation	Asbestos phenolic	RPD 41	SP 319 Type II, Class 2
Entrance insulation	Molded glass phenolic	FM 4030–190	SP 262 Type I, Class 1
Exit cone insulation	Silica phenolic	FM 5504 FM 5067 MX 2600	SP 521 Type II, Class A composition 1 or 2
Nozzle body	Steel	AISI 4230	MIL-S-6758 Cond. D
Adhesives	Polysulfide Silicone Polysulfide Epoxy	TA L-703 RTV 88 TA L-721 EA 934	SP-408-D Commercial grade TCC SP-17-C Commercial grade
External insulation	Cork	—	Armstrong Cork Co. No. 2755
Closure	Polyurethane foam	—	SP 192, type II

TABLE VIII. – CASTOR IIA MOTOR CHARACTERISTICS

Propellant property	Type/Designation	Motor performance	
Propellant designation	TP-H 7036	Avg. web thrust, vacuum, N	274708 (61760 lb)
Propellant type	Aluminized composite	Total motor weight, kg	4429 ± 7 (9756 ± 16 lb)
Grain configuration	Cylindical bore with 2 circumferential slots.	Consumed weight, kg	3757 ± 8 (8275 ± 18 lb)
Propellant gas properties: (chamber)		Propellant weight, kg	3732 ± 7 (8220 ± 16 lb)
		Specific impulse vacuum (sec)	281.9
Specific heat ratio (γ)	1.16	Total burn time (sec)	39.
C_p, cal/gm–^oK	0.476	Web burn time (sec)	35.9
Molecular weight	30.3	Pressure, web time average, N/m^2	4.46×10^6 (647.8 psia)
C*, m/sec	1591 (5210 f/sec)	MEOP, N/m^2	5.509×10^6 (799 psi)
Flame temp, ^oK	3589 (6000^oF)	Proof pressure, N/m^2	4.14×10^6 (600 psi)

Reference 14.

TABLE IX. – CASTOR IIA NOZZLE DRAWINGS AND MATERIAL SPECIFICATIONS

TC dwg no.	Title
CR 40441	Insulation
DR 40464	Insert
DR 40465	Insert Assembly
FR 40749	Nozzle body
R41993	Insulation
R42148	Nozzle assembly
R42653	Closure (flight)
R42741	Nozzle assembly, insulation
R42919	Disc (nozzle closure fitting)
TC spec no.	**Title**
SP 17	Adhesive composition TA-L721
SP 113	Identification of parts
SP 193	Resin, epoxy
SP 203	Asbestos floats
SP 245	Liquid polymer, polysulfide, type I
SP 262	Molding compound
SP 319	Resin impregnated felt
SP 332	High silica fabric
SP 338	Mixed imine curing agent
SP 408	Adhesive composition, polysulfide polymer
SP 451	Nozzle closure
SP 521	Resin impregnated high silica fabric
SP 524	Nozzle exit cone insulation
SP 531	Nozzle exit cone insulation
SP 537	Nozzle insert
SP 555	Molded plastic components
SP 561	Model specification, motor, rocket, solid propellant

TABLE X. – CASTOR IIA NOZZLE MATERIAL PROPERTIES

Material: ATJ Graphite

		300°K R. T.	395°K (250°F)	533°K (500°F)	811°K (1000°F)	1366°K (2000°F)	1922°K (3000°F)	2478°K (4000°F)
Thermal Conductivity cal/m-hr-°K x 10^4 (B-in/ft^2-hr-°F)	With Grain	8.26 (667)			5.96 (481)	4.0 (323)	3.38 (273)	2.86 (232)
	Against Grain							
Coeff. of Thermal exp. M/m-°K x 10^{-6} (in/in-°F x 10^{-6}	With Grain	2.46 (1.37)			3.43 (1.9)	2.08 (1.15)	4.32 (2.40)	4.87 (2.70)
	Against Grain							
Modulus of Elasticity N/m^2 x 10^9 (psi x 10^6)	With Grain	7.6 (1.1)			9.3 (1.35)	10.7 (1.55)	11.4 (1.66)	9.2 (1.34)
	Against Grain							
Compression ult. Strength N/m^2 x 10^6 (psi x 10^3)	With Grain	58.0 (8.4)			62.4 (9.05)	69.0 (10.0)	78.0 (11.3)	9.72 (14.1)
	Against Grain							
Shear strength N/m^2 x 10^6 (psi x 10^3)	With Grain	10.3 (1.5)			14.1 (2.05)	19.3 (2.8)	26.9 (3.9)	42.0 (6.1)
Specific heat cal/gm-°K		0.17			0.39	0.46	0.49	0.51
Poisson's Ratio, μ		.10			.11	.12	.11	.13

Reference 3

TABLE X. – CASTOR IIA NOZZLE MATERIAL PROPERTIES – Continued

Material: Glass phenolic (low density) 4030–190

		300°K R. T.	395°K (250°F)	533°K (500°F)	811°K (1000°F)	1366°K (2000°F)	1922°K (3000°F)	2478°K (4000°F)
Thermal Conductivity cal/m-hr-°K x10³ (B-in/ft²-hr-°F)	With Lam.	.26 (2.1)			.32 (2.6)	.33 (2.7)	.47 (3.8)	1.32 (10.7)
	Against Lam.	.38 (3.1)			.55 (4.5)	.68 (5.5)	1.08 (8.8)	2.13 (17.3)
Coeff. of Thermal Exp., M/m-°K x 10⁻⁶ (in/in-°F x 10⁻⁶)	With Lam.							
	Against Lam.							
Modulus of Elasticity N/m² x 10⁹ (psi x 10⁶)	With Lam.							
	Against Lam.							
Tensile Ult. Strength N/m² x 10⁶ (psi x 10³)	With Lam.							
	Against Lam.							
Interlaminar Shear strength N/m² x 10⁶ (psi x 10³)								
Specific Heat cal/gm-°K		.190			.438	.484	.495	.498
Poisson's Ratio, μ								

Reference 3

TABLE X. – CASTOR IIA NOZZLE MATERIAL PROPERTIES – Concluded

Material: RPD41 Asbestos phenolic

Reference 3

		300°K R. T.	395°K (250°F)	533°K (500°F)	811°K (1000°F)	1366°K (2000°F)	1922°K (3000°F)	2478°K (4000°F)
Thermal Conductivity, cal/m-hr-°K x 10^3 (B-in/ft^2-hr-°F)	With Lam.	.59 (4.8)						.32 (2.6)
	Against Lam.							
Coeff. of Thermal Exp. M/m-°K x 10^{-6} (In/in-°F x 10^{-6})	With Lam.	19 (10.5)	13.5 (7.5)	8.3 (4.6)	2.16 (1.2)	.36 (.2)		
	Against Lam.							
Modulus of Elasticity N/m^2 x 10^9 (psi x 10^6)	With Lam.	22.1 (3.2)				12.9 (1.88)	1.0 (.15)	
	Against Lam.							
Tensile Ult. Strength N/m^2 x 10^6 (psi x 10^3)	With Lam.							
	Against Lam.							
Interlaminar Shear strength N/m^2 x 10^6 (psi x 10^3)								
Specific Heat Cal/6m -°K		.29						.29
Poisson's Ratio, μ								

TABLE XI. – CHAR AND EROSION PROFILE (MOTOR NO. 22)

Material	Station[1]	"X"		Erosion "Y"		Char "Z"		Exp ratio
		M	in.	M	in.	M	in.	
Exit insulation	1	0.0	0.00	.00102	.04	.00635	.25	21.191
	3	.0508	2.00	.00102	.04	.00533	.21	19.542
	11	.2540	10.00	.00102	.04	.00559	.22	13.562
	12	.2794	11.00	.00127	.05	.00457	.18	12.872
	14	.3302	13.00	.00152	.06	.00457	.18	11.586
	16	.3810	15.00	.00178	.07	.00457	.18	10.345
	17	.4064	16.00	.00229	.09	.00381	.15	9.766
	19	.4572	18.00	.00279	.11	.00356	.14	8.643
	21	.5080	20.00	.00406	.16	.00381	.15	7.589
	24	.5842	23.00	.00533	.21	.003302	.13	6.130
	26	.6350	25.00	.00610	.24	.00305	.12	5.259
	28	.6858	27.00	.00762	.30	.00254	.10	4.424
	30	.7366	29.00	.01041	.41	.00178	.07	3.689
	32	.7874	31.00	.01321	.52	.00178	.07	3.004
	33	.8128	32.00	.01600	.63	.00178	.07	2.703
	34	.8382	33.00	.01448	.57	.00152	.06	2.404
Graphite	35	.8636	34.00	.0076	.03	–	–	2.150
	36	.8890	35.00	.00203	.08	–	–	1.868
	37	.91443	36.00	.00330	.13	–	–	1.605
	40	.9906	39.00	.00330	.13	–	–	1.022
	41	1.0160	40.00	.00356	.14	–	–	1.010
	42	1.0414	41.00	.00483	.19	–	–	1.088
	43	1.0668	42.00	.00635	.25	–	–	1.282
	44	1.0922	43.00	.00838	.33	–	–	1.660
	46	1.1227	44.20	.00762	.30	–	–	2.633
	47	1.1278	44.40	.00635	.25	–	–	2.880
	48	1.1328	44.60	.01524	.60	–	–	3.113
Asbestos	49	1.1392	44.85	.01880	.74	–	–	3.113
Molded glass phenolic	50	0.0	–	.01905	.75	.00610	.24	3.538
	51	.0114	0.45	.01041	.41	.00356	.14	3.957
	52	.02388	0.94	.00000	.00	.00254	.10	4.424

[1]See Figure 22 for station location.

Reference 3

TABLE XII. – CALCULATED MARGINS OF SAFETY IN STEEL COMPONENTS

Component	Conditions	Bending stress $N/m^2 \times 10^6$ (psi)	Axial stress $N/m^2 \times 10^6$ (psi)	FBU $N/m^2 \times 106$ (psi)	FTY $N/m^2 \times 106$ (psi)	M. S.
Nozzle EC	Flight	471. (68300)	31.4 (4541)	807. (117000)	413. (60000)	.52
Nozzle EC	Ground handling	251. (36370)	0	807. (117000)	—	2.21
Attach	Conditions	Bending load m–N (in–lb)	Axial load N (lb)	F_{Bolt} N (lb)	P_{Ult} N (lb)	M. S.
7/16 Dia.	Flight	$.163 \times 10^6$ (1.44×10^6)	667000 (150000)	49500 (11132)	60500 (13600)	.22

Reference 3

ANTARES IIA

Background. - Antares IIA is the SCOUT third stage motor and is also used in other scientific programs. The X-259-B3 (Antares IIA) motor has had over 200 successful firings in its production history. It is lightweight by design, but motor and nozzle components have relatively high factors of safety and have exhibited high reliability. Nozzle geometry and materials are shown in Figures 33 and 34. Table XIII lists alternate qualified materials for each nozzle component.

Performance Data. - The Antares IIA motor has a maximum expected operating pressure (MEOP) of 2.87×10^6 N/m^2 (416 psi) and a flame temperature of 3802°K (6384°F). The propellant is CYI-75, a modified double-base composite with 20.5% aluminum. Motor characteristics and performance are summarized in Table XIV. Chamber pressure variation during firing is plotted in Figure 35. Chamber pressure versus time is measured during every SCOUT mission, and after every ten flights the pressure curve values are averaged and the curve updated if necessary. Due to the large number of flights for this motor, the motor pressure history curve is well characterized.

Drawings and Specifications. - Table XVI lists the Antares IIA nozzle drawing and material specifications. Component assembly procedures for this motor are described by Standard Operating Procedures.

Material Description. - Temperature dependent material properties of component materials for the Antares IIA nozzle are shown in Table XV. These materials are described below.

RPD-150 is a general purpose molding compound of long spinning grade chrysotile asbestos fibers, grade AAAA, impregnated with a high temperature phenol-formaldehyde resin, B staged and then mascerated into a molding compound. The material may be molded at pressures of 13.78×10^6 N/m^2 (2000 psi) and greater at temperatures between 408 to 436°K (275 to 325°F) Post cure is recommended to obtain optimum properties.

ATJ Graphite is an extremely fine grained, $.15 \times 10^{-3}$M (.006 in) diameter grain size, high strength graphite. It is fabricated by molding to an average density of 1.73 gm/cc. The molding operations produce a preferred orientation of the graphite particles which give rise to "with grain" and "across grain" properties. It can be machined to very close limits and sharp detail with fine surface finish.

MX 2630A is a graphite fabric impregnated with a high temperature phenolic resin containing refractory reinforcement. The graphite fabric is WCA grade woven as a plain (square)weave. The graphite fabric resin is a MIL-R-9299 Type II phenolic. The filler in the resin is composed of refractory zirconia fines which pass through a 325 mesh screen.

MX 2600 is a silica fabric impregnated with a high temperature phenolic resin containing silica reinforcement. The phenolic resin must meet specification MIL-R-9299, Type II phenolic resin. The silica fabric is Sil Temp 84 or Hitco C100-48. The reinforcement, or filler, is silica dioxide of 98% purity.

Tayloron PA-6 is an asbestos paper impregnated with a high temperature phenolic resin that conforms to MIL-R-9299, Type II, Class 2. The asbestos paper is Microasbestos paper supplied by the John Mansville Corporation.

ECG140-801 (filament wound glass rovings) is impregnated with Epon 828 resin system and B-staged at room temperature and cured at 311°K (100°F) for 4 hours and then at 344°K (160°F) for 2 hours.

Armstrong A-2 is a white epoxy adhesive that has a low coefficient of thermal expansion, making it quite suitable for bonding ceramic type materials. It has excellent wetting properties and it also provides exceptionally strong bonds to rigid materials such as phenolics. Activator A or curing agent A offers short time room temperature cures. The adhesive is prepared by mixing 4 parts of curing agent A to 100 parts of A-2 epoxy resin. Bond lap shear strength at room temperature is 2900 psi. No elevated temperature data is available.

The following percentages of solids, resins, and volatiles for the plastic laminate nozzle materials were obtained from vendor catalogs and are used as acceptance criteria at room temperature.

Material	Resin solids %		Resin filler %		Volatiles %	
	Min	Max	Min	Max	Min	Max
RPD-150	38	43	-	-	3	12
MX 2630A	36	40	-	-	3	7.5
MX 2600	29	33	6	10	3	7
Tayloron PA-6	41	47	-	-	7	12

Fabrication and Process. The fabrication and inspection procedures are summarized for each component of the Antares IIA nozzle in Figure 36. That figure briefly summarizes the fabrication procedures and quality inspections for each nozzle component.

Thermal Data

Temperature Distribution. - Complete thermal analyses for this nozzle are not available at either VSD or the nozzle vendor (HI). The most complete temperature data is found in Reference (4). Isotherm maps were obtained from that reference and are presented in Figures 37 through 40.

These figures show temperature distributions at 5, 10, 20 and 34 seconds after ignition. These isotherms represent interpolated temperature data between adjacent nodes. For this reason the shape of the curves at the insert to overwrap interface may be only approximate. This would account for the differences in this region between these curves and those obtained for the Antares IIB (Figures C-6 through C-8).

Due to the 20.5% concentration of aluminum in the CYI-75 propellant, the high chamber radiative heat flux causes maximum surface temperatures on the ATJ insert to occur forward of the throat despite higher convective heat transfer coefficients in the throat area. Maximum thermal gradients occur early in firing. A maximum insert temperature of 3760°K (6300°F) occurs at 34 seconds, which is about burnout time for this motor. ATJ throat average erosion rate was calculated to be 6.9×10^{-5} m/sec (2.75 mils/sec). Erosion was ignored in the thermal and stress analyses.

An instrumented exit cone was tested under simulated altitude conditions using motor S/N HIB-203. A similar firing under sea level conditions for motor S/N HIB-103A had previously exhibited higher temperature for the exit cone (see Figure 41). In both tests the exit cone was surrounded by an insulating shield between the exit cone and surrounding fiberglass transition section which normally connects SCOUT second and third stage motors. For comparison, exit cone temperatures from a similar simulated altitude test are shown for an Antares IIB motor. The lower temperatures for that motor are due to the (approximately 8 seconds) shorter firing time.

Structural Analysis

No formal thermoelastic analysis has been published specifically for the Antares IIA nozzle. However, minimum margins of safety for this nozzle were calculated to establish relative comparisons among the FW-4S, X-254 and the Antares IIA nozzles (reference 4). Only results for the ATJ graphite insert were published in that reference. A similar analysis at

5 seconds by VSD yielded equivalent results, and also included calculated margins of safety and stress distributions for the overwrap support ring. Results of both analyses are included in this section. Two other analyses investigated the reliability of the RPD-150 overwrap ring and those results are also summarized.

Loads. - Chamber pressure is plotted in Figure 35. At early firing times when thermoelastic stresses are maximum, chamber pressure is 2.31×10^6 N/m^2 (335 psi). Pressure distribution around the nozzle is plotted in Figure 42. Nozzle proof test pressure is 3.275×10^6 N/m^2 (475 psi); MEOP is 2.87×10^6 N/m^2 (416 psi).

Factors of Safety. - The required factors of safety for this nozzle are as follows:

Limit Load: Anticipated loads, pressures and temperatures

Design Yield Load: 1.15 x MEOP

Design Ultimate Load: 1.3 x Limit Loads

Proof Pressure: 1.14 x MEOP (no yield)

Factor of Safety: Ultimate stress capability/Limit stress

Results of Analyses. - Two analyses were performed to investigate the reliability of the RPD-150 asbestos phenolic retainer ring, but the models used were not representative of the Antares IIA flight configuration. The first analyses (by Hercules, Incorporated, reference 5) used a Graphitite G-90 insert. This X259-C2 nozzle is similar in geometry but is subjected to higher pressure than the Antares IIA. Insufficient thermal data was published to calculate allowables in the critical areas, but maximum calculated stresses are shown below for comparison.

Component	Maximum Principal Stress	
	N/m^2	(psi)
Overwrap	41.34×10^6	(6000)
G-90 Insert	23.43	(3400)
Exit Cone Liner	6.20	(900)
Exit Cone Insulation	55.12	(8000)

From this analysis it was concluded by the analyst that the retainer ring would successfully withstand its expected environment even if a circumferential crack existed to a depth of 50 percent of the part thickness.

A second (VSD) analysis of the overwrap considered only cool-down stresses in an intermediate configuration (Figure 43) of the molded asbestos phenolic and the aluminum adapter ring. A maximum calculated principal tensile stress of 29.3×10^6 N/m^2 (4252 psi) did not explain the persistent problem of cracked rings during processing (F_{TU} = 9 ksi).

A thermoelastic computer (SAAS II) analysis of the nozzle was also performed by VSD using available thermal contours from Reference (4). The first iteration calculated relatively high axial tensile stresses across the bond line at the aft edge of the ATJ insert. Temperatures at 5 seconds exceed 811°K (1000°F) along most of this bondline. This would cause thermal degradation of the epoxy resin adhesive in that area. Therefore, a final iteration assumed an ineffective bond along the aft edge of the ATJ insert. Results of that analysis are shown in Figures 44 through 46 and are summarized below. The bondline interface between the insert and the asbestos phenolic overwrap experienced compressive stresses at this time due to early heating of the insert while the overwrap is still relatively cool. Maximum computer stresses and resulting factors of safety at 5 seconds are listed below ($F.S. = F_{TU} / \sigma_{max}$) for the VSD nozzle analysis.

Component	σ_{Hoop} $N/m^2 \times 10^6$ (psi)	Temp. ^oK (^oF)	F_{TU} N/m^2 (psi)	F.S.
ATJ Insert	4.08 x 10^6 (592)	950 (1250)	26.18 x 10^6 (3800)	5.4
Overwrap (Char Layer)	9.03 (1311)	332 (138)	62.01 (9000)	0.69*

Component	σ_{Axial} N/m^2 (psi)	Temp. ^oK (^oF)	F_{TU} N/m^2 (psi)	F.S.
ATJ Insert	15.85 x 10^6 (2301)	1172 (1650)	20.67 x 10^6 (3000)	1.3
Overwrap	8.94 (1298)	950 (1250)	20.67 (3000)	2.3

* Local negative margin in the hot char layer is considered acceptable.

The maximum stresses and associated factors of safety for the ATJ graphite insert reported in the UTC analysis of Reference (4) are shown below:

Time =	3 Sec.	5 Sec.	10 Sec.
Max. Hoop Stress N/m^2 (psi)	13.3 x 10^6 (1928)	10.55 x 10^6 (1530)	No tension
Temperature, ^oK (^oF)	671 (750)	950 (1250)	
Tensile Allowable, N/m^2 (psi)	31.1 x 10^6 (4500)	32.4 x 10^6 (4700)	
Factor of Safety	2.33	3.07	
Max. Axial Stress, N/m^2 (psi)	12.0 x 10^6 (1742)	11.5 x 10^6 (1670)	6.6 x 10^6 (959)
Temperature, ^oK (^oF)	671 (750)	811 (1000)	1033 (1400)
Tensile Allowable, N/m^2 (psi)	31.1 x 10^6 (4500)	31.7 x 10^6 (4600)	32.8 x 10^6 (4750)
Factor of Safety	2.59	2.85	4.95

In the following table, maximum insert hoop and axial stresses from the two nozzle analyses are compared using tensile allowables from the VSD analysis at 5 seconds. The most critical axial stresses compare well; the differences in the less critical hoop stresses may be attributed to a combination of methodology, thermal physical properties and temperature inputs.

	Reference (4)	VSD Analysis
Max. Hoop Stress, N/m^2 (psi)	10.55×10^6 (1530)	4.08×10^6 (592)
Temperature, ^oK (^oF)	950 (1250)	950 (1250)
Tensile Allowables, N/m^2 (psi)	26.18×10^6 (3800)	26.18×10^6 (3800)
Factor of Safety	2.5	5.4
Max. Axial Stress, N/m^2 (psi)	11.5×10^6 (1670)	15.85×10^6 (2301)
Temperature, ^oK (^oF)	811 (1000)	1172 (1650)
Tensile Allowables, N/m^2 (psi)	20.0×10^6 (2900)	20.67×10^6 (3000)
Factor of Safety	1.7	1.3

The reliable performance history of the ATJ graphite insert appears to be a result of the relatively high factors of safety for this component throughout firing. Postfire examinations of the asbestos phenolic overwrap have never shown cracked or other serious discrepancies in these rings. The local high stress region shown in Figure 45 is apparently relieved due to a high strain capability of the plastic laminate at elevated temperature. This is typical for such materials and reflects some degree of conservation in most elastic analysis methods.

Estimated Accuracy of the Antares IIA Nozzle Analysis. - The preceeding section (Results of Analyses) illustrates potential differences when two analyses are performed for the same nozzle but using different models and different sources of material physical properties. Differences of 100% are not uncommon, although a better comparison would probably have resulted for this nozzle from use of computed temperature

distributions rather than use of relatively inaccurate isotherm data for thermal inputs in the VSD analysis.

The Antares IIA motor has had a long successful history without any nozzle failures. Due to its consistently satisfactory performance, and because this motor is currently being phased out of the SCOUT system no detailed thermoelastic analysis has been performed. Therefore, a definitive estimate of analysis accuracy cannot be made for this nozzle.

Problem Areas. - Most of the problems encountered with this nozzle have been minor and have been associated with the RPD-150 asbestos phenolic overwrap material. Despite these problems this nozzle has never experienced a failure during firings.

The asbestos phenolic overwrap ring is hygroscopic and sensitive to its surrounding environment. In addition, no satisfactory manufacturing process has been found to eliminate periodic cracked rings. This has been a persistent cost and schedule problem but has not affected the demonstrated nozzle reliability. A design review of this problem was concluded in February 1967 without solving the problem completely. However, since that date there have been five X259-A3, thirty X259-B3, and one X259-B4 successful SCOUT flights with no ring failures.

Four nozzle retainer rings were rejected in 1970 due to unbond between the asbestos phenolic overwrap ring and the aluminum nozzle attach ring. This was attributed to silicone oil contamination during fabrication. That problem was resolved successfully.

During the same year subscale char motor tests were used to qualify the retainer ring manufactured by a new vendor. These tests indicated excessive erosion rates, but it was established by firing data (HIB-204) that the char motor results were conservative and no real problems were present.

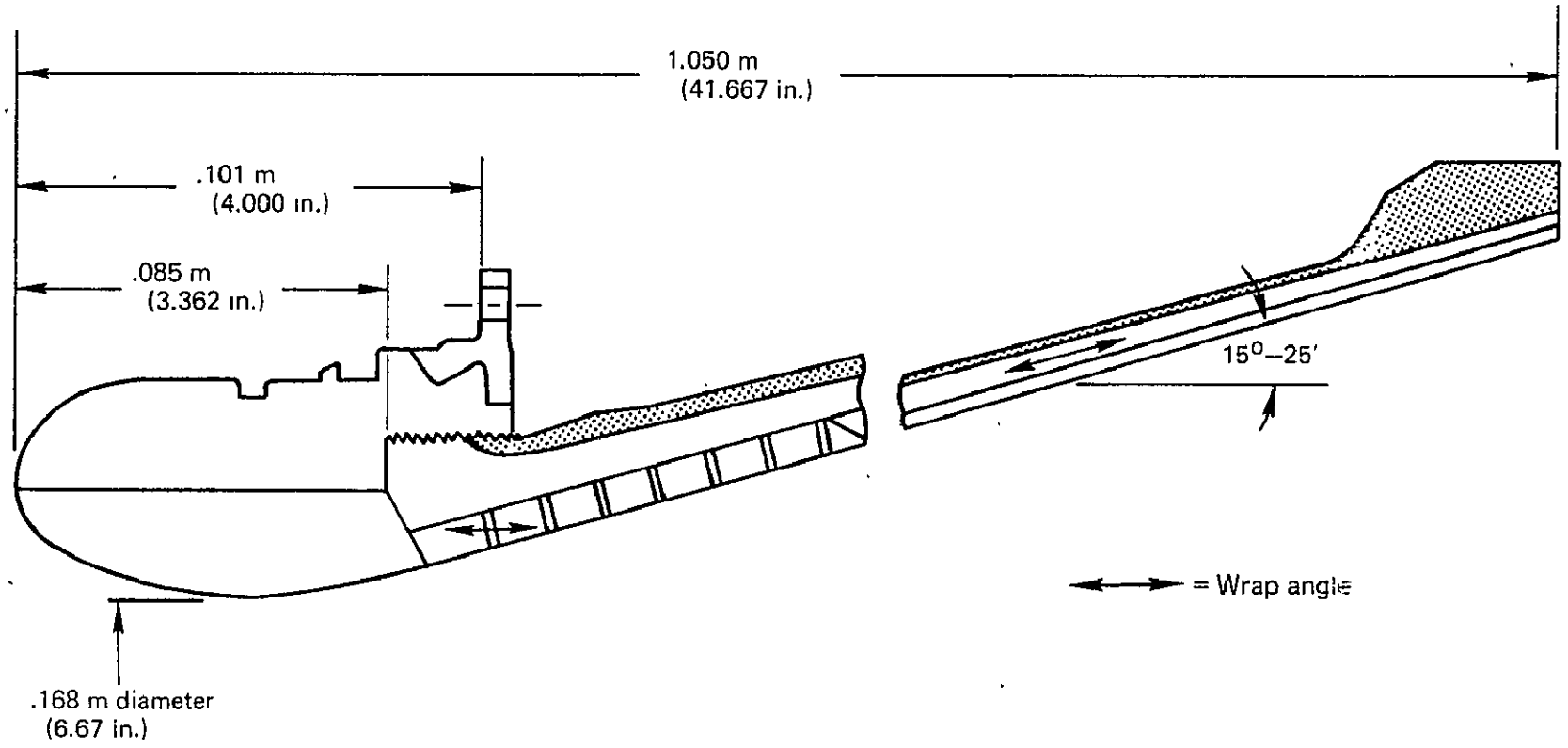

FIGURE 33. – ANTARES IIA NOZZLE GEOMETRY

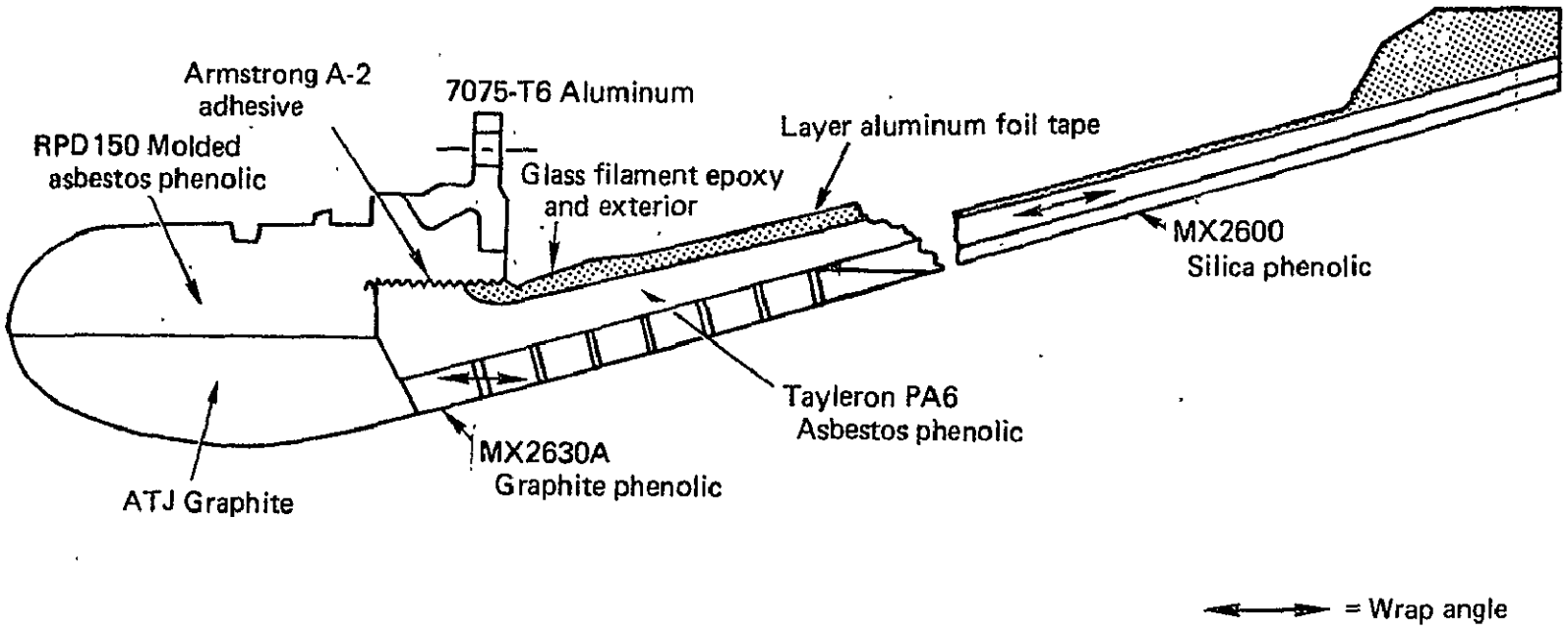

FIGURE 34. – ANTARES IIA NOZZLE MATERIALS

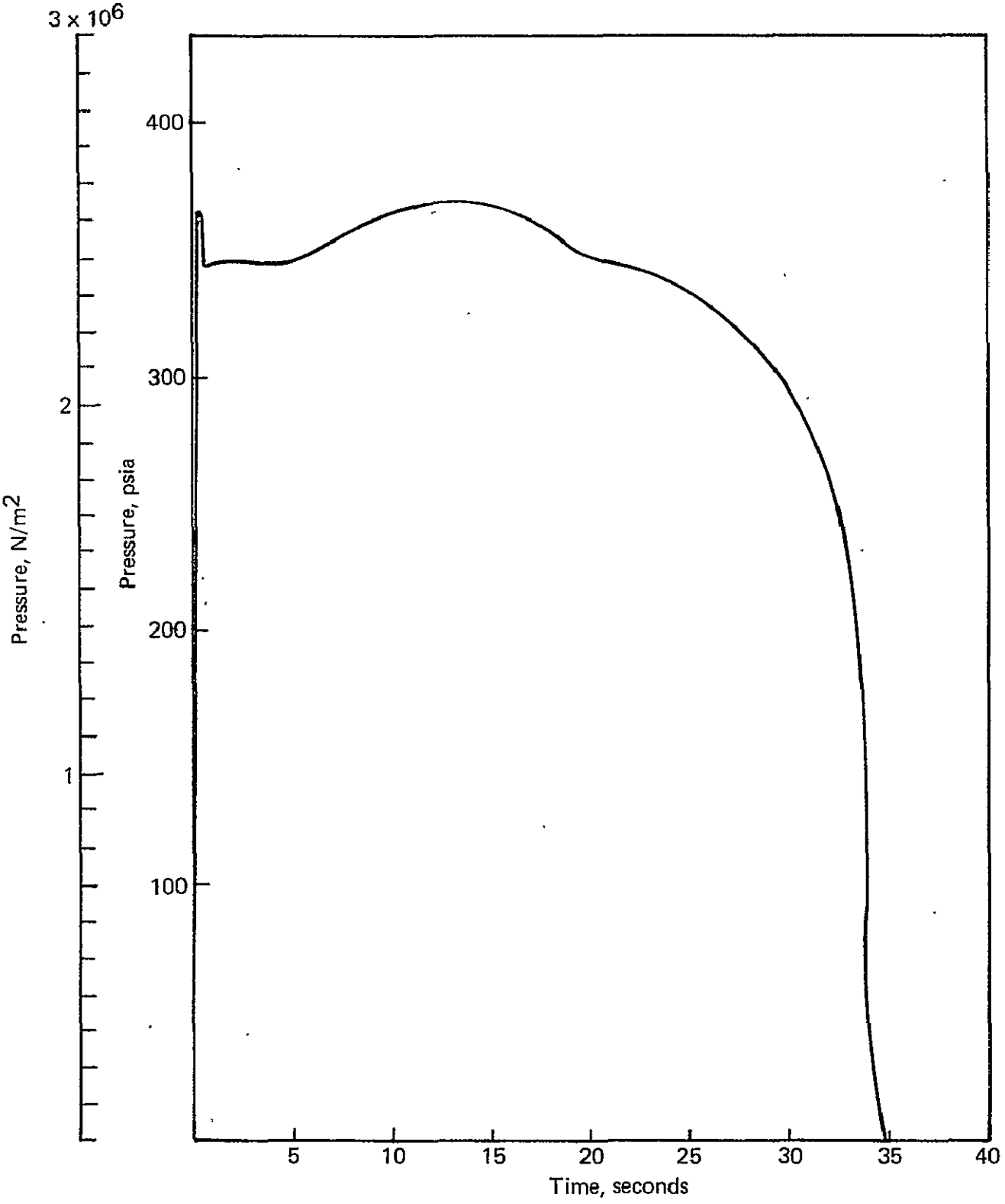

FIGURE 35. — ANTARES IIA PRESSURE VS TIME

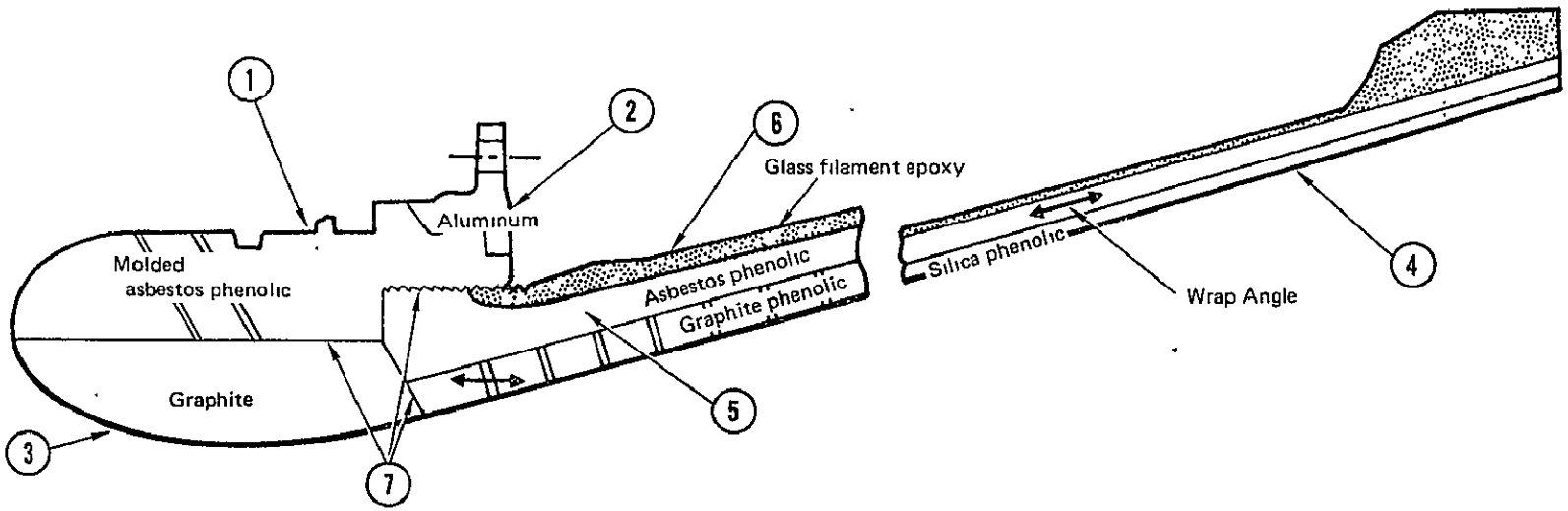

Item	Name	Material	Fabrication/inspection
1	Throat insert retainer ring molding	RPD 150 Asbestos phenolic per HS 259-2-166	The RPD 150 asbestos phenolic throat insert retaining ring and the 7075-T6 nozzle attach ring (item 2) are molded into an assembly in a hydraulic press using the following procedure. A weighed amount of macerated RPD 150 asbestos phenolic fiber is compressed in a cylindrical die at room temperature, ejected from the mold and preheated to 367°K (200°F) in a dielectric oven and then placed into a 423°K (300°F) preheated molding die. The 7075-T6 attach ring is also preheated to 423°K (300°F) and placed on top of the heated preform of RPD 150 just prior to closing the mold. The two materials are cured at 423°K (300°F) at a pressure of 39.4 x 10^6 N/m^2 (5700 PSI). After ejection from the mold the assembly is post cured for 80 hours at 423°K (300°F) in an air oven. The molded assembly is visually and radiographically inspected for external and internal defects. All molded assemblies are final machined to drawing configuration. Two rows of (30) .000166 m (1/16") diameter holes equally spaced around the circumference are drilled through the retainer ring 45° to the nozzle centerline.
2	Nozzle attachment ring	7075-T6 Ring forging per QQ-A-367	The ring forging is ultrasonically inspected for internal defects prior to machining into an attach ring. The machined attach ring is dye penetrant inspected prior to use in the retainer ring molding operation.
3	Throat insert	ATJ graphite per HS 259-1-205	The ATJ graphite throat inserts are machined out of a .227 mx .505 mx .605 m (9" X 20" X 24") block of molded ATJ graphite. The inserts are machined so that the "with grain" direction of the graphite is normal to the centerline of the bore. Radiographic inspection is performed on each machined graphite insert to determine its acceptability for use in a nozzle assembly.

FIGURE 36. — ANTARES II A FABRICATION AND INSPECTION

Item	Name	Material	Fabrication/Inspection
4	Exit cone liner Forward Aft	MX 2630A Graphite phenolic tape per HS 259-1-97, Type II MX 2600 Silica phenolic tape per HS 259-1-195, Type II	The exit cone liner is fabricated from two tape wrapped materials. graphite phenolic cloth (MX 2630A) in the forward portion and silica phenolic (MX 2600) in the aft portion. The two materials are tape wrapped parallel to the nozzle centerline on a common mandrel, vacuum bagged and partially cured in a hydroclave at 6.2 x 10^6 N/m^2 (900 psi). The partially cured assembly is then coated with phenolic resin (MIL-R-9299 Class 2, Type II) and over-wrapped with asbestos phenolic paper (Tayloron PA—6) parallel to the liner surface. This assembly is hydroclave cured at 6.2 x 10^6 N/m^2 (900 psi) and then post cured in an oven. A ring of graphite phenolic is removed from the exit cone during facing operations for a density measurement test. 00158 M (1/16 in.) diameter holes are drilled in the graphite phenolic material to the asbestos phenolic interface to permit outgassing of volatile material during motor firing. 48 longitudinal grooves are equally spaced circumferentially in the PA-6, covered with acetate tape and overwrapped with glass filament epoxy for additional venting of outgassing volatiles.
5	Exit cone liner backup insulation	Tayloron PA-6 asbestos phenolic per HS 259-1-111	
6	Exit cone outer shell	Filament wound glass rovings, ECG 140-801 per HS 259-1-211 181 Glass cloth, thalco glass per MIL-C-9084, Type VIII	The exit cone is covered with one layer of glass cloth (MIL-C-9084, Type VIII) impregnated with epon 828/ Metaphenylene diamine resin system and "B" staged at room temperature for 6-12 hours One ply of glass roving using the same epoxy resin system is wound circumferentially over the exit cone. After "B" staging for 6-12 hours, a second ply of glass rovings is wrapped over the exit cone and again "B" staged for 6-12 hours at room temperature The large end of the exit cone is built up of alternate layers of glass cloth and circumferential winding plies The exit cone is then oven cured for 4 hours at 311°K (100°F) followed by 2 hours at 344° K (160°F) One layer of Y9040 aluminum foil tape is bonded over the exit cone exterior surface to minimize heat radiation to the surrounding vehicle structure.
7	Adhesive	Armstrong A-2 epoxy with curing agent A per HS 259-1-186, Comp 4	The exit cone is machined and then bonded to the throat insert retainer molding using Armstrong A-2 epoxy with curing agent A. The assembly is oven cured at 325°K (125°F) for one hour. A thin layer of A-2 epoxy/curing agent A adhesive is applied to the I.D. surface of the retainer ring molding and similarly cured This operation is performed to seal off the vent holes to prevent adhesive from extruding into them during bonding of the graphite throat insert. The ATJ graphite throat insert is bonded into the retainer ring/exit cone assembly using A-2/curing agent A epoxy adhesive and cured at 325°K (125°F) for one hour. The bonding surfaces of both the asbestos phenolic retainer ring and the ATJ graphite throat insert are alcohol wipe inspected prior to bonding. The graphite throat is also inspected by the fluorescent penetrant method.

FIGURE 36. — ANTARES II A FABRICATION AND INSPECTION — Concluded

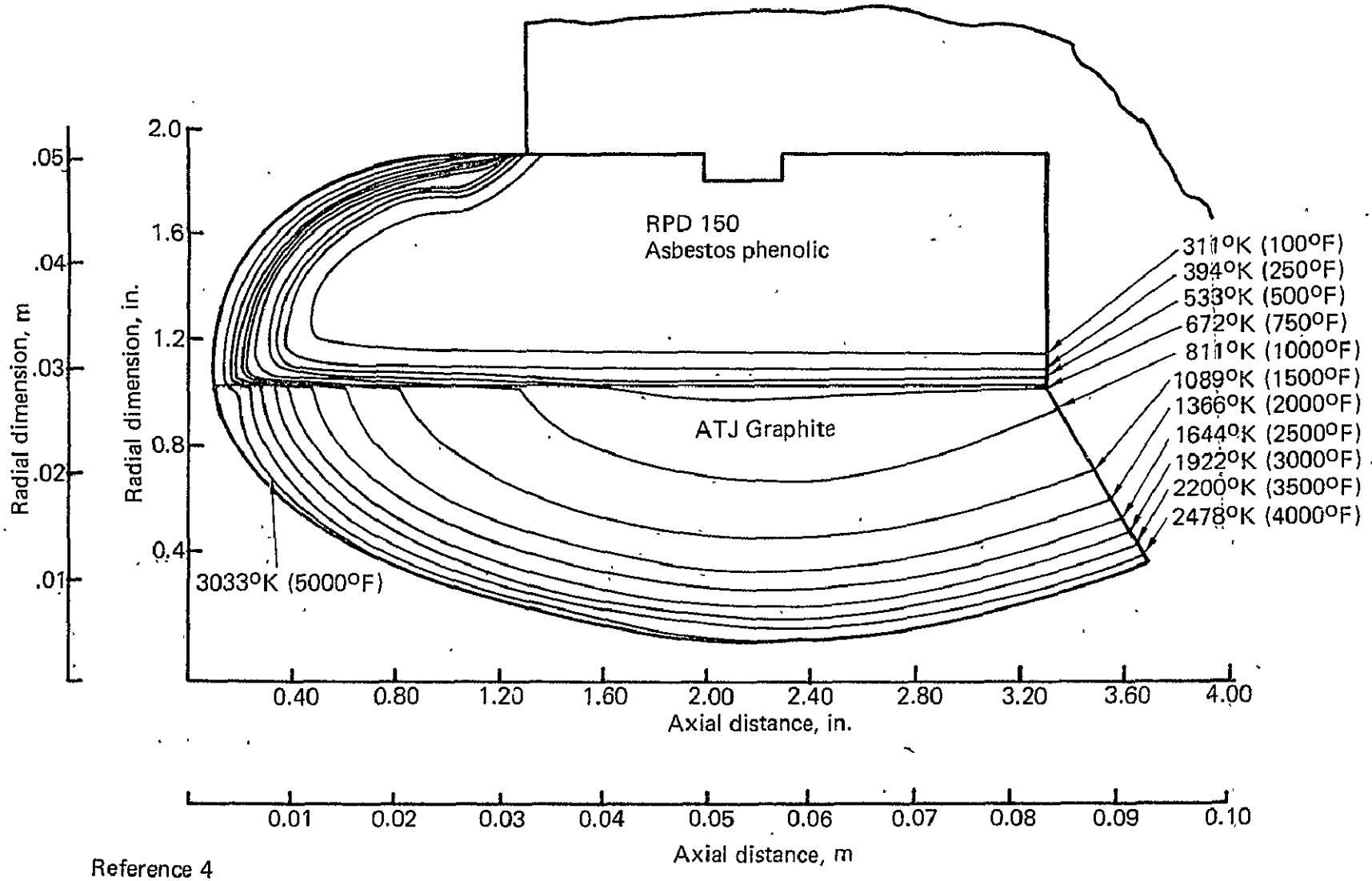

Reference 4

FIGURE 37. – TEMPERATURE DISTRIBUTION AT 5 SECONDS

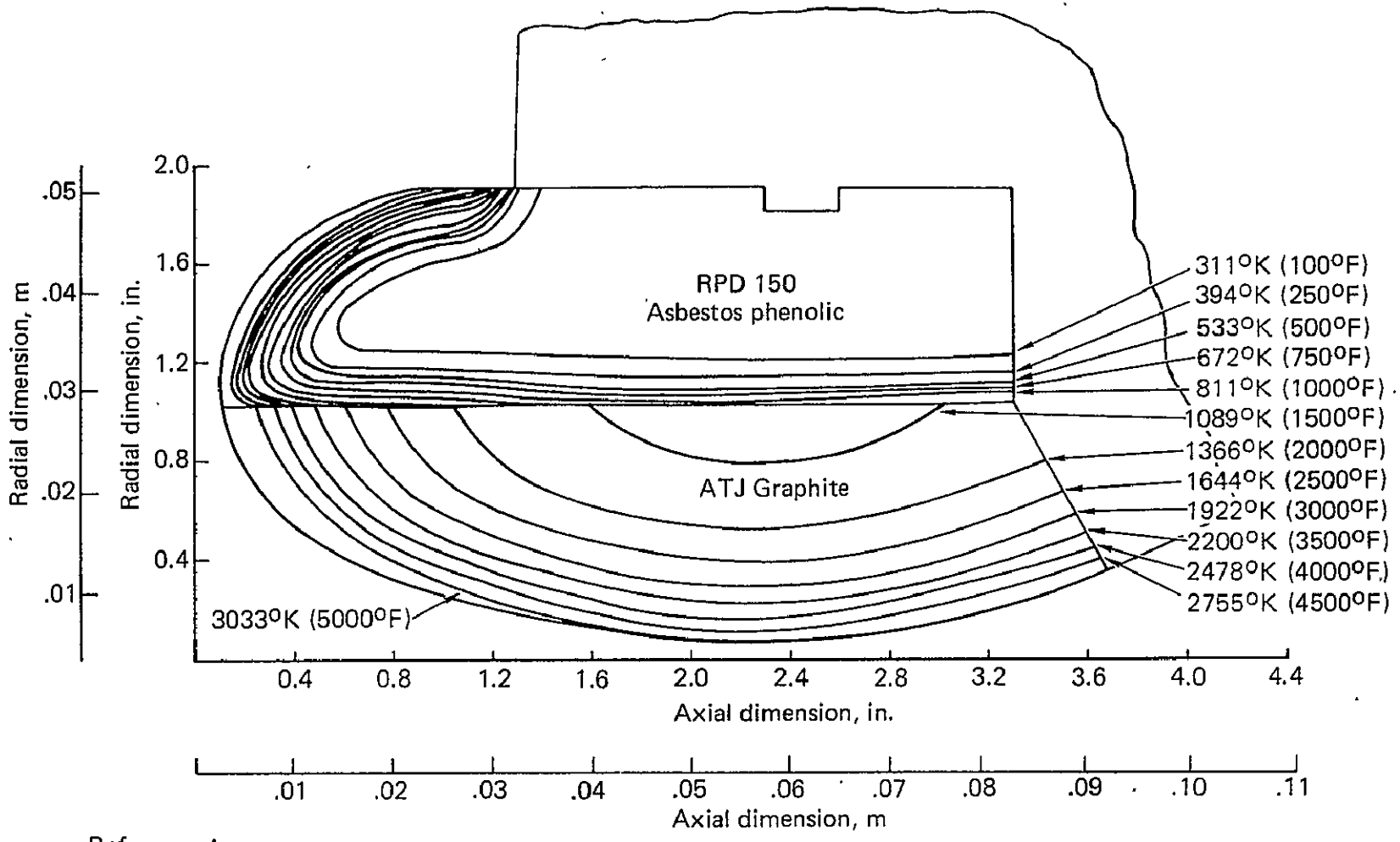

Reference 4

FIGURE 38. – TEMPERATURE DISTRIBUTION AT 10 SECONDS

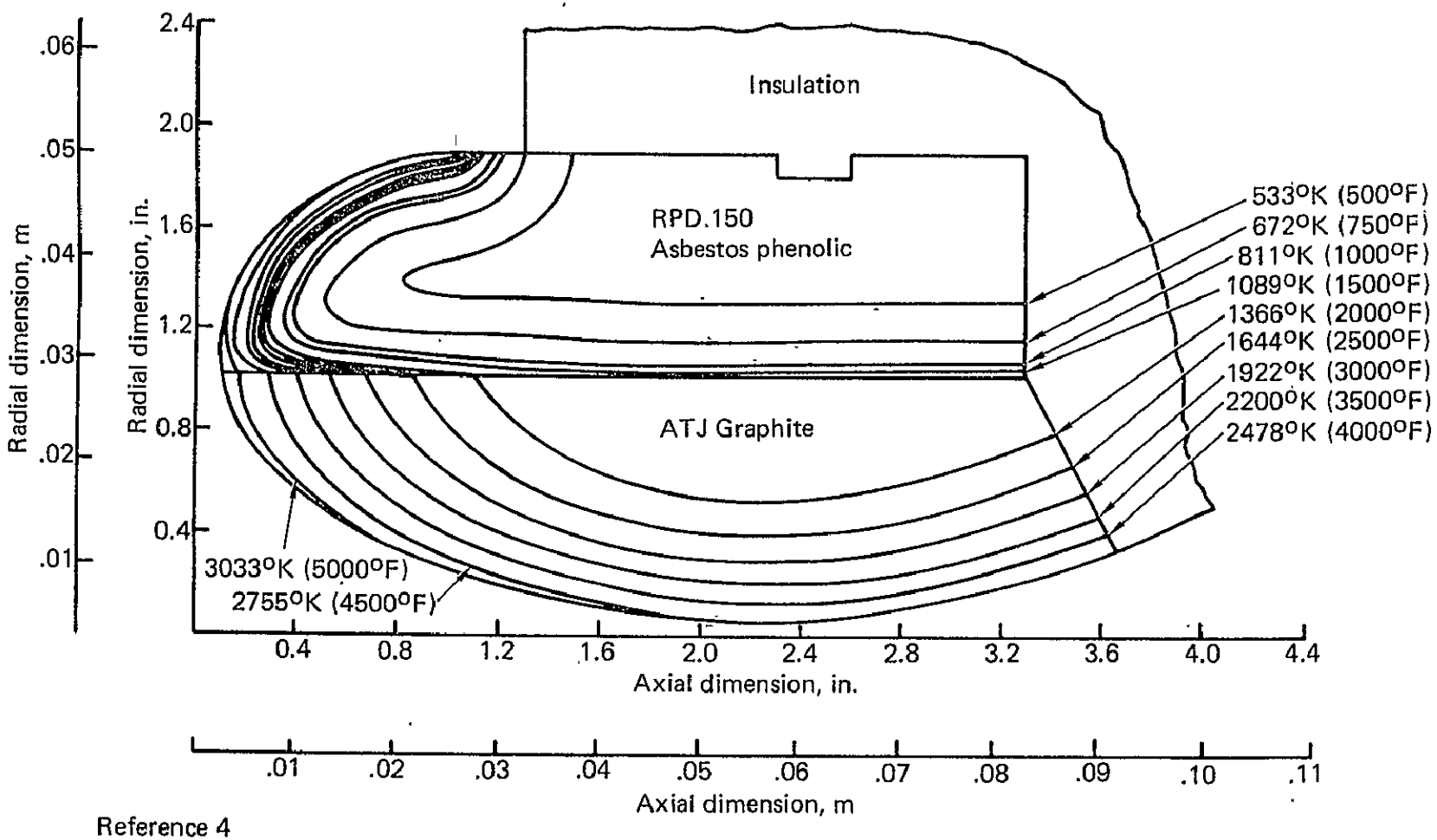

Reference 4

FIGURE 39. — TEMPERATURE DISTRIBUTION AT 20 SECONDS

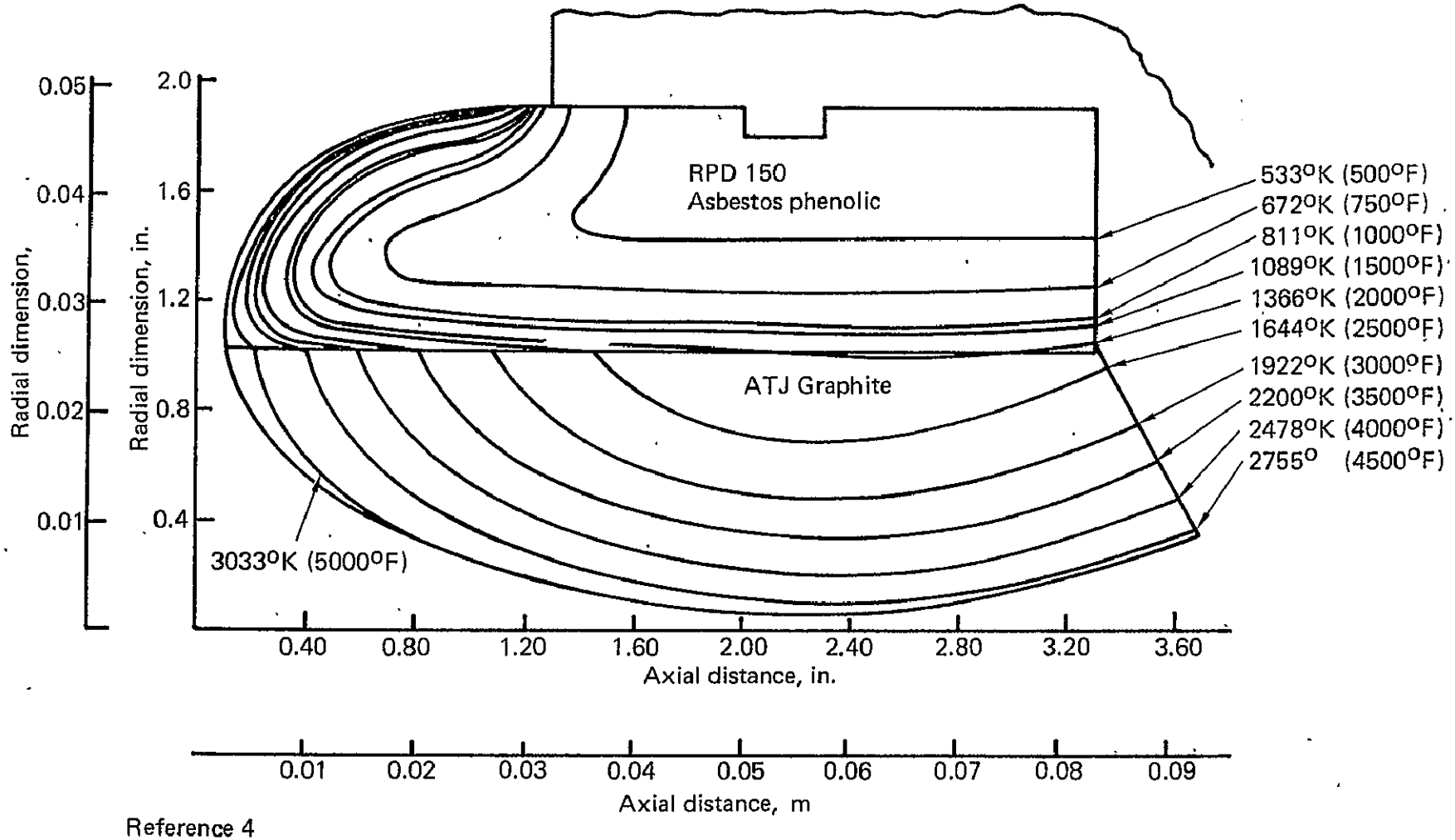

Reference 4

FIGURE 40. – MAXIMUM TEMPERATURES AT 34 SECONDS

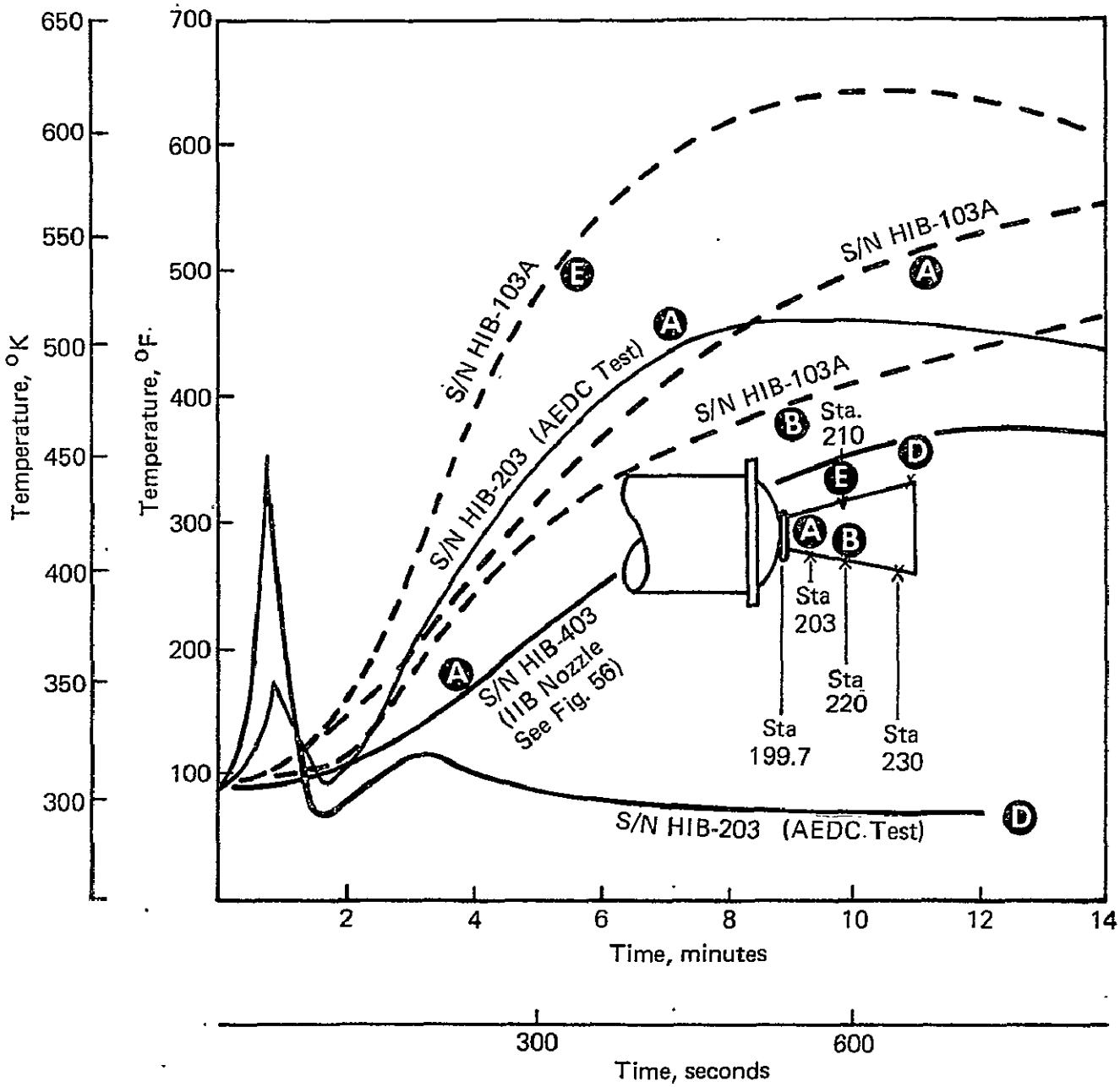

Reference 21
Reference 22

FIGURE 41. – EXIT CONE EXTERNAL TEMPERATURES

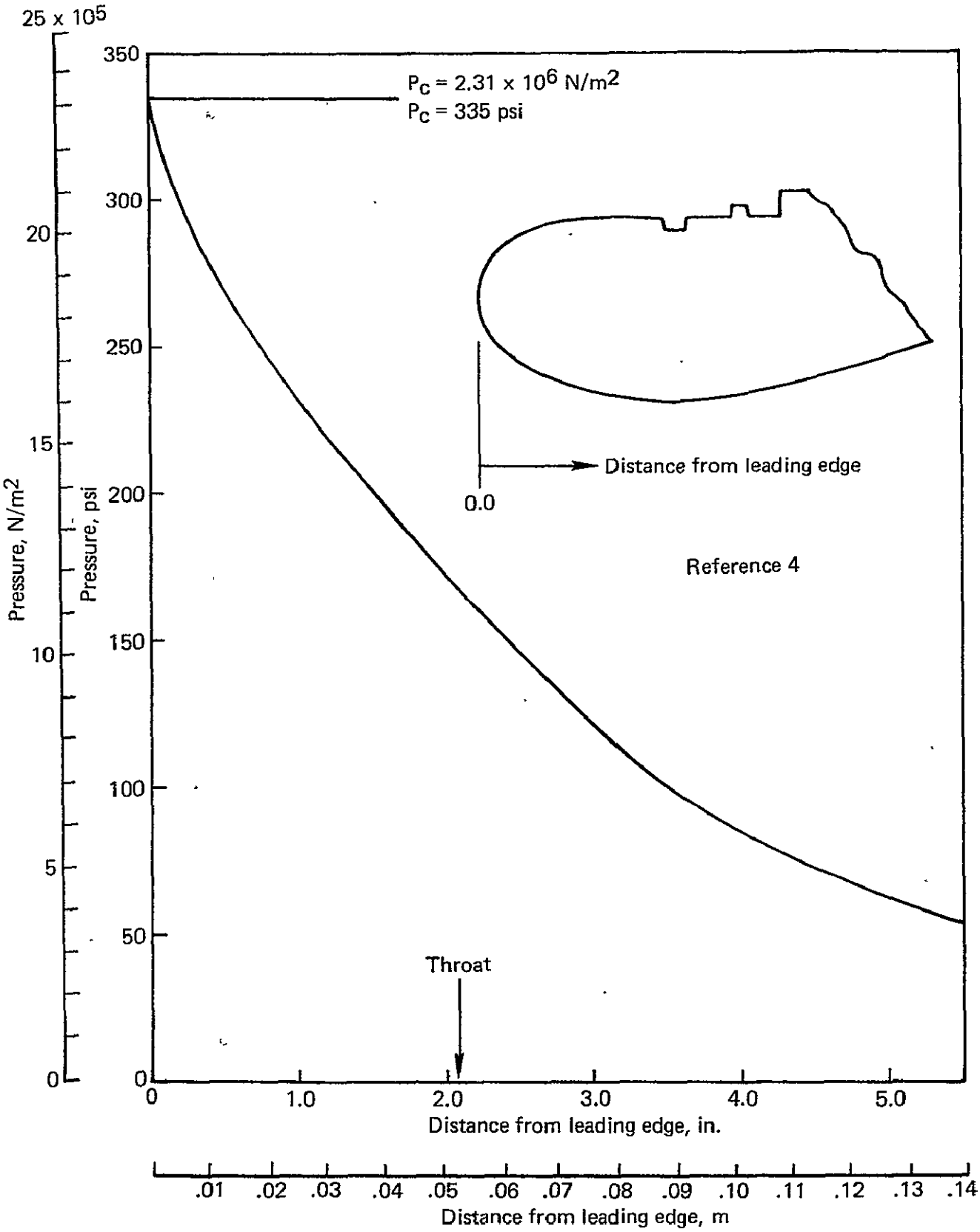

FIGURE 42. – PRESSURE DISTRIBUTION

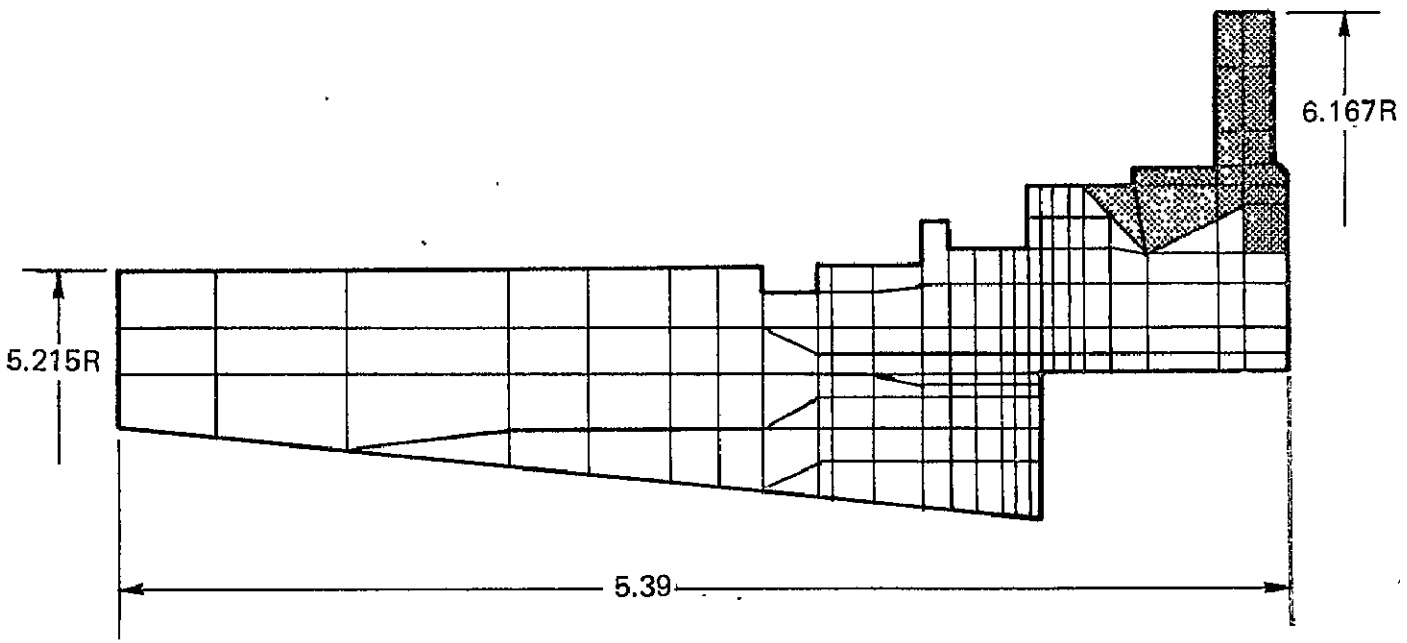

FIGURE 43. – RETAINER RING MODEL (INTERMEDIATE IN-PROCESS CONFIGURATION)

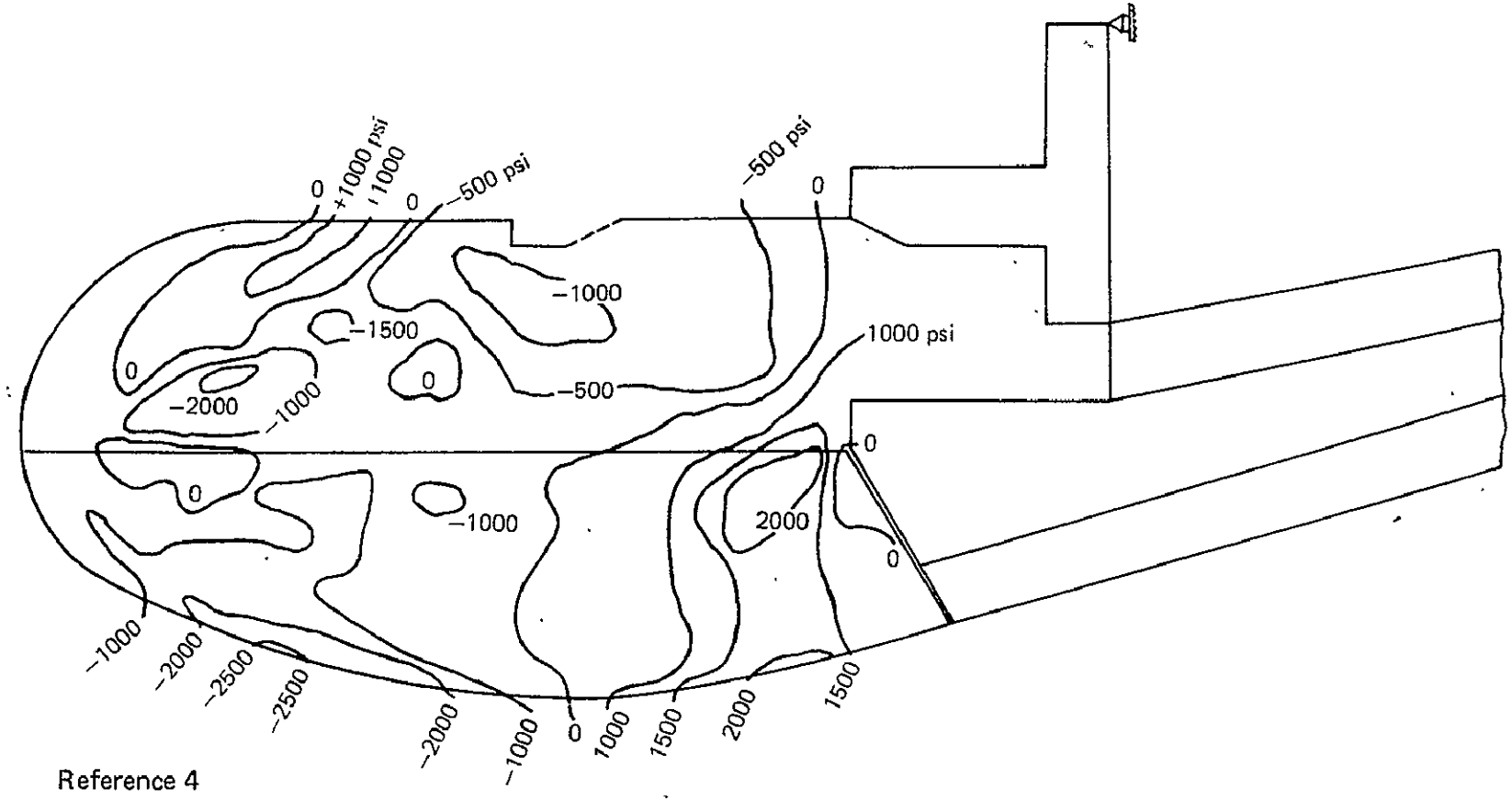

Reference 4

FIGURE 44. – AXIAL STRESSES AT 5 SECONDS

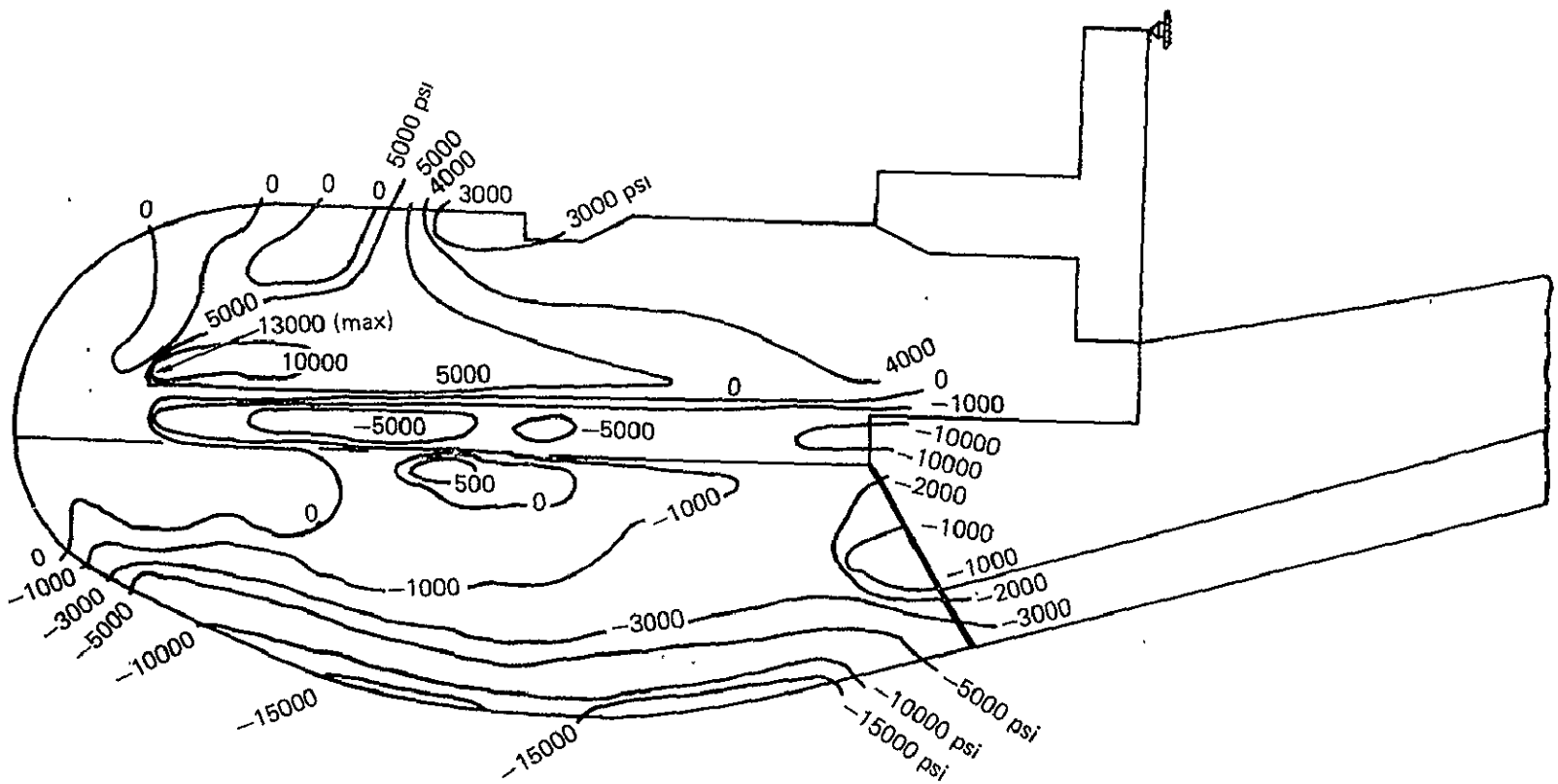

Reference 4

FIGURE 45. — HOOP STRESSES AT 5 SECONDS

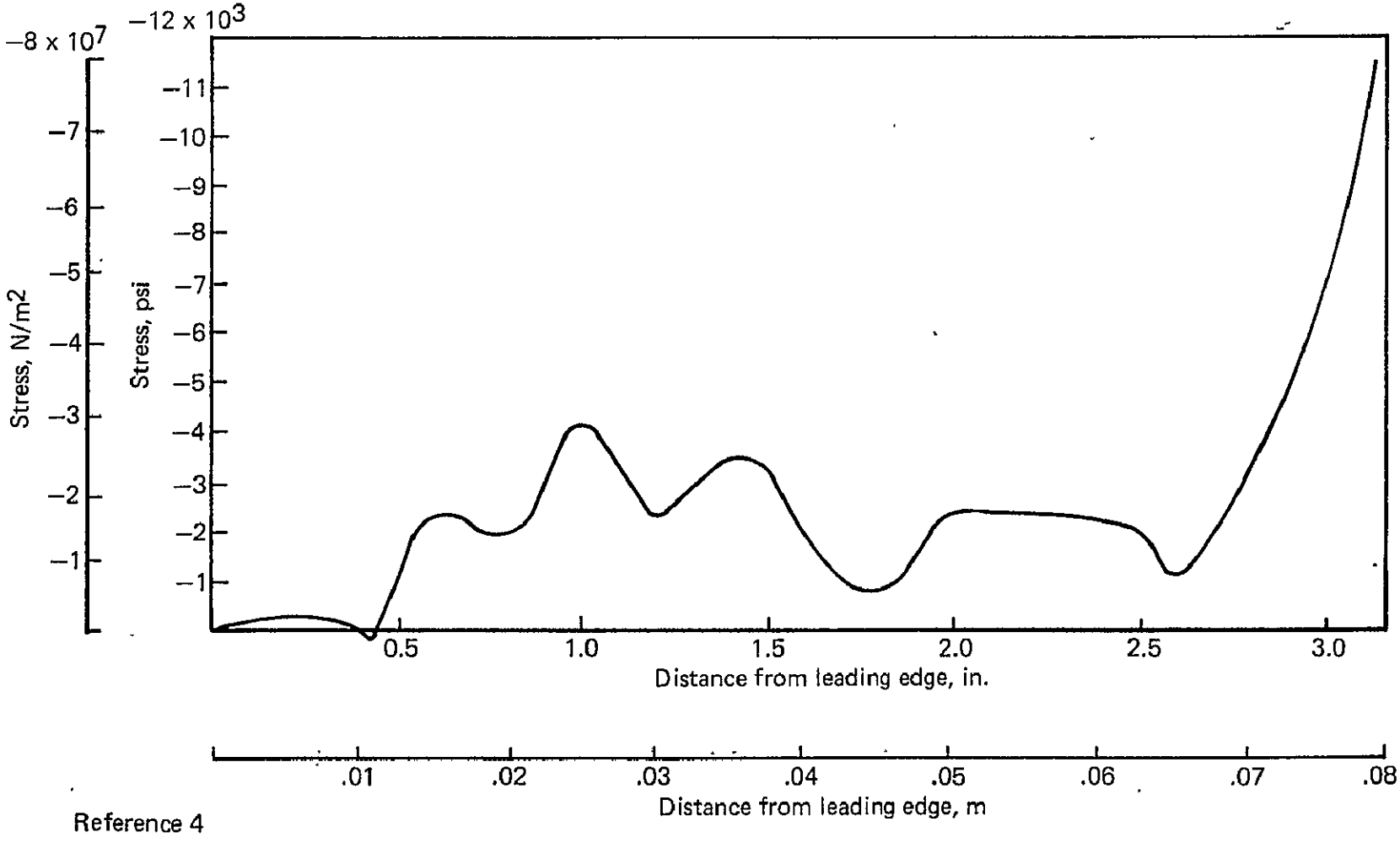

FIGURE 46. — BOND LINE (COMPRESSION) STRESSES AT 5 SECONDS

TABLE XIII. – ANTARES IIA NOZZLE MATERIALS

Component	Material	Vendor designation	Procurement specification
Retainer ring	Asbestos phenolic	RPD 150	HS-259-1-166
Attach ring	7075T6	Aluminum	QQ-A-367
Throat insert	Graphite	ATJ	HS-259-1-205
Fwd exit cone liner	Graphite phenolic	MX 2630A	HS-259-1-97
Aft exit cone liner	Silica phenolic	MX 2600 MX 2625	HS-259-1-195
Exit cone insulation	Asbestos phenolic	Tayleron PA-6	HS-259-1-111
Outer exit cone structure	Glass filament/ cloth/resin	ECG-140, 12 end with 801 sizing/ 181 glass cloth Epon 828 (resin)	HS-259-1-69 (Type I, Class I), HS-259-1-211, MIL-C-9084 (Type VIII)
Adhesive	Epoxy	Armstrong A–2 Epoxy/curing agent A	HS-259-1-186, Comp 4

TABLE XIV. – ANTARES IIA MOTOR CHARACTERISTICS

Propellant property	Type/Designation	Motor performance	
Propellant designation	CYI-75	Avg web thrust vacuum, N	95988 (21580 lb)
Propellant type	Composite modified double base	Total motor weight, kg	1278 ± 12 (2817 ± 25 lb)
Grain configuration	Cylindrical 4 pointed finocyl bore in aft end with a cylindrical bore in forward end.	Consumed weight, kg	1175 (2590 lb)
		Propellant weight, kg	1162 +11 −7 +25 (2562 −15 lb)
		Specific impulse vacuum (sec)	281.15
Propellant gas properties: (chamber)		Action time (sec)	33.7 ± 4.2 @ 75°F
		Web burn time (sec)	32.8
Specific heat ratio (γ)	1.15	Pressure, web time avg, N/m^2	$2.32 \pm .14 \times 10^6$ (337 ± 25 psi)
Cp, cal/gm-°K	0.425	MEOP, N/m^2	2.87×10^6 (416 psi)
Molecular weight	19.3		
C*, M/sec	1618 (5300 f/sec)	Proof pressure, N/m^2	3.27×10^6 (475 psi)
Flame temp, °K (at 337 psi)	3086 (6015°F)		

Reference 15.

TABLE XV. — ANTARES IIA NOZZLE MATERIAL PROPERTIES

Material: Asbestos phenolic (RPD-150)

Property	Temperature, °K (°F)				
	300°K (75)	811°K (1000)	1366°K (2000)	1782°K (2750)	3870°K (6500)
Modulus of elasticity $N/m^2 \times 10^9$ (psi x 10^6)	14.9 (2.17)	6.8 (0.98)	2.3 (0.34)	0.2 (0.025)	0.2 (0.025)
Shear modulus $N/m^2 \times 10^9$ (psi x 10^6)	6.0 (0.87)	2.6 (0.38)	0.9 (0.13)	0.07 (0.01)	0.07 (0.01)
Poisson's ratio	0.256	0.3	0.3	0.3	0.335
Coeff of expansion $m/m\text{-}^oK \times 10^{-6}$ ($in./in.\text{-}^oF \times 10^{-6}$)					
Hoop and axial	12.9 (7.2)	16.2 (9.0)	3.6 (2.0)	1.8 (1.0)	0.0 (0)
Radial	15.8 (8.8)	32.4 (18.0)	1.8 (1.0)	−.9 (−0.5)	−1.8 (−1.0)
Tensile strength $N/m^2 \times 10^6$ (ksi)	62.0 (9)	22.0 (3.2)	4.5 (0.66)	1.4 (0.21)	0.7 (0.10)
Shear strength $N/m^2 \times 10^6$ (ksi)	46.8 (6.8)	15.1 (2.2)	1.9 (0.28)	0.4 (0.06)	0.2 (0.03)
Thermal conductivity $cal/m\text{-}hr\text{-}^oK \times 10^3$ ($B\text{-}in./ft^2\text{-}hr\text{-}^oF$)	.55 (4.5)	.55 (4.5)	.55 (4.5)	.55 (4.5)	.55 (4.5)
Spcific heat ($cal/gm\text{-}^oK$)	.27	.27	.27	.27	.27

Reference 4

TABLE XV. – ANTARES IIA NOZZLE MATERIAL PROPERTIES – Continued

Material: ATJ graphite

		300°K R.T.	533°K (500°F)	811°K (1000°F)	1366°K (2000°F)	1922°K (3000°F)	2478°K (4000°F)
Thermal conductivity, cal/m-hr-°K X 10^4 (B-in./ft^2-hr-°F)	With lam.	9.4 (758)	7.05 (570)	5.4 (436)	3.52 (285)	2.44 (197)	2.05 (166)
	Against lam.						
Coeff of thermal exp M/M-°K x 10^{-6} (in./in.-°F x 10^{-6})	With lam.	1.4 (0.8)	1.8 (1.0)	2.1 (1.15)	2.9 (1.62)	3.5 (1.93)	4.0 (2.25)
	Against lam.	1.8 (1.0)	2.5 (1.4)	3.2 (1.8)	4.1 (2.3)	4.7 (2.6)	5.4 (3.0)
Modulus of elasticity N/m^2 x 10^9 (psi x 10^6)	With lam.	7.6 (1.1)	8.6 (1.25)	9.2 (1.34)	10.6 (1.54)	11.4 (1.66)	9.2 (1.33)
	Against lam.	5.2 (0.75)	5.8 (0.84)	6.1 (0.89)	6.4 (0.93)	6.5 (0.94)	6.1 (0.89)
Tensile ult strength N/m^2 x 10^6 (psi x 10^3)	With lam.	29.6 (4.3)	30.4 (4.4)	31.0 (4.5)	34.4 (5.0)	38.7 (5.6)	45.5 (6.6)
	Against lam.						
Interlaminar shear strength N/m^2 x 10^6 (psi x 10^3)							
Specific heat cal/gm-°K		0.14	0.32	0.39	0.46	0.49	0.51
Poisson's ratio, μ							

Reference 4

TABLE XV. – ANTARES IIA NOZZLE MATERIAL PROPERTIES – Continued

Material: Graphite phenolic (MX 2630A)

		300°K R.T.	533°K (500°F)	811°K (1000°F)	1366°K (2000°F)	1922°K (3000°F)	2478°K (4000°F)
Thermal conductivity, cal/m-hr-°K X 10^3 (B-in./ft^2-hr-°F)	With lam.	3.2 (26.4)	3.6 (28.8)	3.6 (28.8)	5.4 (43.2)	6.1 (49.1)	5.7 (46.3)
	Against lam.	1.1 (8.7)	1.2 (9.6)	1.2 (9.6)	1.8 (14.4)	2.1 (16.8)	2.4 (19.2)
Coeff of thermal exp M/M-°K x 10^{-6} (in./in.-°F x 10^{-6})	With lam.	14.4 (8.0)	(13.7)	12.6 (7.0)	1.8 (1.0)	0	0
	Against lam.	19.1 (10.6)	25.2 (14.0)	13.5 (7.5)	1.4 (0.8)	– .9 (–0.5)	– .9 (–0.5)
Modulus of elasticity N/m^2 x 10^9 (psi x 10^6)	With lam.	9.92 (1.44)	5.17 (0.75)	4.13 (0.6)	5.31 (0.77)	5.99 (0.87)	3.86 (0.56)
	Against lam.	7.99 (1.16)	2.76 (0.4)	2.20 (0.32)	3.45 (0.5)	3.03 (0.44)	2.00 (0.29)
Tensile ult strength N/m^{2}x 10^6 (psi x 10^3)	With lam.	164.0 (23.8)	117.8 (17.1)	49.61 (7.2)	53.74 (7.8)	58.57 (8.5)	72.35 (10.5)
	Against lam.	82.68 (12.0)	58.57 (8.5)	36.52 (5.3)	31.69 (4.6)	39.27 (5.7)	29.63 (4.3)
Interlaminar shear strength N/m^2 x 10^6 (psi x 10^3)		68.9 (10.0)	34.5 (5.0)	10.34 (1.5)	10.34 (1.5)	9.65 (1.4)	8.96 (1.3)
Specific heat cal/gm-°K		0.24	0.4	0.88	0.49	0.5	0.5
Poisson's ratio μ		0.16	0.14	0.13	0.11	0.16	0.21

Reference 4

TABLE XV. – ANTARES IIA NOZZLE MATERIAL PROPERTIES – Continued

Material: Silica phenolic (MX 2600)

		300°K R.T.	533°K (500°F)	811°K (1000°F)	1366°K (2000°F)	1922°K (3000°F)	2478°K (4000°F)
Thermal conductivity, cal/m-hr-°K X 10^3 (B-in./ft^2-hr-°F)	With lam.	.68 (5.5)	.66 (5.3)	.64 (5.2)	1.8 (14.6)	2.5 (20.0)	2.8 (23.0)
	Against lam.	.31 (2.5)	.3 (2.4)	.3 (2.4)	.85 (6.9)	1.1 (8.7)	1.3 (10.2)
Coeff of thermal exp M/M-°K x 10^{-6} (in./in.-°F X 10^{-6})	With lam.	12.6 (7.0)	15.1 (8.4)	16.2 (9.0)	5.0 (2.8)	1.8 (1.0)	0
	Against lam.	16.2 (9.0)	23.4 (13.0)	32.2 (17.9)	1.8 (1.0)	– .9 (–0.5)	– 1.8 (–1.0)
Modulus of elasticity N/m^2 x 10^9 (psi x 10^6)	With lam.	22.6 (3.28)	10.54 (1.53)	8.54 (1.24)	9.16 (1.33)	0.17 (0.025)	0.17 (0.025)
	Against lam.	5.86 (0.85)	3.10 (0.45)	2.96 (0.43)	3.38 (0.49)	0.62 (0.09)	0.62 (0.09)
Tensile ult strength N/m^2 x 10^6 (psi x 10^3)	With lam.	165.36 (24.0)	68.9 (10.0)	34.45 (5.0)	13.78 (2.0)	2.07 (0.3)	1.03 (0.15)
	Against lam.						
Interlaminar shear strength N/m^2 x 10^6 (psi x 10^3)							
Specific heat cal/gm-°K		0.2			0.4	0.49	0.49
Poisson's ratio, μ							

Reference 4

TABLE XV. – ANTARES IIA NOZZLE MATERIAL PROPERTIES – Continued

Material: Asbestos phenolic (PA–6)

		300°K R.T.	533°K (500°F)	811°K (1000°F)	1366°K (2000°F)	1922°K (3000°F)	2478°K (4000°F)
Thermal conductivity, cal/m-hr-°K X 10^3 (B-in./ft^2-hr-°F)	With lam.	.21 (1.7)	.22 (1.8)	.21 (1.7)	.65 (5.3)	1.2 (9.4)	1.25 (10.1)
	Against lam.	.28 (2.3)	.3 (2.4)	.27 (2.2)	.68 (5.5)	1.0 (8.4)	1.25 (10.1)
Coeff of thermal exp M/M-°K x 10^{-6} (in./in.-°F x 10^{-6}	With lam.	12.6 (7.0)	15.1 (8.4)	16.2 (9.0)	5.1 (2.8)		
	Against lam.	16.2 (9.0)	23.5 (13.0)	32.3 (17.9)	1.8 (1.0)		
Modulus of elasticity N/m^2 x 10^9 (psi x 10^6)	With lam.	22.6 (3.28)	10.54 (1.53)	8.54 (1.24)	9.23 (1.34)		
	Against lam.	5.86 (0.85)	3.10 (0.45)	2.96 (0.43)	3.38 (0.49)		
Tensile ult strength N/m^2 x 10^6 (psi x 10^3)	With lam.	108.17 (15.7)	102.66 (14.9)	50.99 (7.4)	17.91 (2.6)		
	Against lam.	12.75 (1.85)	6.34 (0.92)	1.03 (0.15)	1.03 (0.15)		
Interlaminar shear strength N/m^2 x 10^6 (psi x 10^3)		42.03 (6.1)	35.14 (5.1)	38.58 (5.6)	65.46 (9.5)		
Specific heat. cal/gm-°K		0.19			0.14	0.31	0.50
Poisson's ratio μ		0.018	0.029	0.031	0.063		

Reference 4

TABLE XV. – ANTARES IIA NOZZLE MATERIAL PROPERTIES – Concluded

Material: Fiberglass epoxy (ECG-140/181 Glass Cloth/Epon 828)

Property	Direction	Temperature	Value
Coeff of thermal exp $M/M-^{o}K \times 10^{-6}$ ($in./in.-^{o}F \times 10^{-6}$)	Warp	Room temperature	3.6 (2)
	Fill		9 (5)
	Across		18 (10)
Modulus of eleasticity $N/m^2 \times 10^9$ ($psi \times 10^6$)	Warp	Room temperature	48 (7)
	Fill		28 (4)
	Across		14 (2)
Tensile ult strength $N/m^2 \times 10^6$ ($psi \times 10^3$)	Warp	Room temperature	138 (20)
	Fill		69 (10)
	Across		14 (2)
Shear strength $N/m^2 \times 10^6$ ($psi \times 10^3$)	Warp – Fill	Room temperature	34 (5)
	Across		83 (12)
Poisson's ratio, μ	Warp – fill	Room temperature	0.10
	Warp - across		0.07
	Fill – across		0.10

Reference 4

TABLE XVI. — ANTARES IIA NOZZLE DRAWINGS AND SPECIFICATIONS

Drawing/specification	Title
83136D00002	Nozzle Closure
83136D00003	Exit cone, retainer ring and throat insert assembly
83136D00004	Nozzle exit cone retainer ring and throat insert assembly and machining
83136D00005	Nozzle Throat insert billet and preliminary machining
83136D00006	Nozzle exit cone and retainer ring assembly and machining
83136D00007	Nozzle altitude exit cone filament winding
83136D00008	Nozzle altitude exit cone liner machining
83136D00009	Nozzle altitude exit cone liner molding
83136D00010	Nozzle retainer ring machining
83136D00011	Nozzle retainer ring molding
83136D00012	Nozzle attachment ring
83136D00013	Nozzle attach ring forging
83136D00056	Nozzle filament wound exit cone maching
83136D00001	Nozzle closure assembly
83136A00001	Motor assembly 259-B3
Spec HD-259-1-801	Nozzle exit cone tape wrapping and molding
Spec HD-259-1-802	Nozzle exit cone filament winding
Spec HS-259-1-97	Fabric, graphite, impregnated resin and filler
Spec HS-259-1-111	Tape, asbestos paper impregnated with phenolic resin
Spec HS-259-1-186	Adhesive, thermosetting, epoxy resin base
Spec HS-259-2-166	Asbestos phenolic compound
Spec HS-259-1-205	Graphite molded for high temperature application
Spec HS-259-1-186	Adhesive, thermosetting, epoxy resin base
Spec HPC-259-08-0-2	Model specification
Spec MIL-A-22771	Attachment ring
Spec HS-259-2-159	Cloth, graphitized
Spec HS-259-1-195	Fabric, silica, phenolic
Spec HS-259-2-158	Fabric, woven, vitreous fiber, for plastic laminates
Spec HS-259-1-211	Roving, Glass, continuous filament, twelve end
Spec HS-259-1-69	Adhesive systems, epoxy resin base
Spec MIL-C-9084	181 Glass cloth
Spec HD-259-1-805	Nozzle hydrotest

ALTAIR IIIA

Background. - The SCOUT fourth stage motor was originally developed and qualified by Chemical Systems Division of United Technology Corporation and designated as FW-4. It was also used in the Delta, Burner I, Satar and Altus I programs. The original FW-4 had a free standing monolithic ATJ insert. In 1968 the nozzle design was modified and substituted the present Graphitite G90 insert and a carbon phenolic retainer ring for the ATJ insert. Since 1974, the motor (designated TEM-640) has been supplied by Thiokol, Elkton. Both the FW-4 and TEM-640 motors are established Altair IIIA fourth stage SCOUT motors. Nozzle geometry and materials are shown in Figures 47 and 48. Qualified materials are listed in Table XVII.

Performance Data. - The Altair IIIA motor has a maximum expected operating pressure of 5.92×10^6 N/m^2 (859 psi) and a flame temperature of 3220°K (5327°F). The CTPB composite propellant has 16% aluminum. Time dependent chamber pressure during firing is shown in Figure 49. This curve is averaged from two flights. Data from two subsequent flights compared favorably but has not yet been averaged into a new composite pressure curve. Motor performance parameters which affect the nozzle environment are summarized in Table XVIII.

Drawings and Specifications. - Table XIX lists Altair IIIA nozzle LTV/VSD drawings and material specifications.

Material Description. - Brief descriptions and temperature dependent physical and mechanical properties of each Altair IIIA nozzle material is included in this section. Material properties are listed in Table XX.

Graphitite G-90 (throat insert) is an extruded graphite which has been reimpregnated to obtain certain physical and mechanical properties that make it suitable for use in small, high performance rocket nozzle throats. It has a density of 1.9 gm/cm^3 and a maximum grain size of .033 inches. Its low modulus and low coefficient of thermal expansion makes it advantageous to use in thermal shock applications.

FM5072 (retainer ring) is a carbon fabric impregnated with a filled phenolic resin. The resin is a MIL-R-9299 phenolic and the carbon fabric is WCA cloth.

FM5014G (exit cone liner) is a graphite fabric impregnated with a filled MIL-R-9299 phenolic resin. The fabric reinforcement is Hitco G1550.

MX5707B (exit cone insulation) is a low density silica paper, impregnated with a high temperature phenolic resin. The paper reinforcement is Fiberite F904 and the resin is a MIL-R-9299, type II, phenolic.

HT 424 is a high temperature epoxy-phenolic film adhesive that meets the requirements of MIL-A-5090, Type III, structural adhesive. It is a gray film, moderately tacky with a glass fabric reinforcement. Assemblies may be bonded at pressures ranging from contact to 100 psi depending on the applications. The adhesive curing temperature is $330^{\circ}F \pm 10^{\circ}$ and cure time is 30 minutes at temperature.

EA 934 is a two-part epoxy adhesive consisting of a gray thisotropic epoxy paste (part A) and an amber liquid amine curing agent (part B). The adhesive is prepared by thoroughly mixing 100 parts of part A with 33 parts of part B. Cure is obtained after seven days at $75^{\circ}F$ or 1 hour at $200^{\circ}F$. Three-fourths full strength may be obtained after 24 hours at $75^{\circ}F$.

Vendor values of volatiles, resin content and specific gravity are tabulated below for each of the nozzle plastic laminate materials.

Material	Resin Solids, %		Volatiles %		Specific Gravity	
	Min.	Max.	Min.	Max.	Min.	Max.
FM 5072	30	36	--	8	1.40	---
FM 5014 G	30	37	--	5	1.38	1.50
MX5707 B	45	51	6	12	.80	.90

The nozzle thermal and physical properties were obtained from reference (8) and were used in that reference for the thermal and thermo-elastic stress analyses. Material properties were only reported for the graphite insert and carbon phenolic retainer ring in that analysis.

Fabrication and Process. - The fabrication and inspection procedures are summarized for each component of the Altair IIIA nozzle in Figure 50. That figure briefly summarizes the fabrication procedures and quality inspections for each nozzle component.

Thermal Data

Exit cone and attach ring temperature histories were obtained from a simulated altitude firing at AEDC. Char and erosion data were obtained by measurements of the sectioned nozzle from the test.

Char and Erosion. - Figure 51 presents a typical throat erosion profile after a 30 second firing duration (reference 9). Throat erosion values were averaged from five simulated altitude tests at AEDC. Typical char and erosion profiles are shown in Figure 52.

Figure 53 presents a typical ablation and charring profile in the nozzle extension section. Figure 54 is a graphical presentation of erosion and charring depths as measured in nozzle S/N 30210. It shows measurements for four other tests conducted at AEDC. Table XXI presents the same data in tabular form.

Temperature Distribution. - Figure 52 shows thermocouple locations on nozzle S/N 015. This nozzle was used on motor TE-M-640-1, E-11, which was test fired at the AEDC high altitude chamber on July 12, 1974.

Figure 55 presents the external nozzle surface temperature versus time histories to 450 seconds.

Figures 56 through 58 present analytically determined isotherms for the Graphitite G throat insert. These isotherms were for nominal pressure and a 200 rpm spin condition. Figure 56 presents isotherms at 7 seconds. At this time maximum thermal stress occurs in the Graphitite G insert. At 4 seconds Figure 57 shows isotherms when maximum thermal stress occurs in the carbon cloth phenolic back-up. Figure 58 represents maximum temperatures which the throat area experiences after a 30 seconds firing duration (reference 8).

Structural Analysis

The Altair IIIA nozzle was analyzed by Chemical Systems Division of United Technology Corporation (reference 8) to predict the structural reliability of the nozzle with a backed-up Graphitite G-90 insert. By combining expected rationale and test variances, results were determined in terms of probability values for component survival using a Coulomb-Mohr biaxial failure criteria. Uniaxial factors of safety were also used to evaluate insert reliability. The Coulomb-Mohr diagram criteria was used to construct a failure envelope for each element in the model at a given temperature based on maximum and minimum principal stresses combined with hoop stresses. These calculations are included in the UTC finite element program.

Loads. - Maximum chamber pressure at different times were obtained from Figure 49. The associated temperature distributions in the nozzle were also included for analyses at 2, 3, 4, 5, 6, 7, 8, 9, 20 and 25 seconds after ignition. Critical conditions for the insert occurred at 7 seconds; the carbon phenolic retainer ring stresses were critical at 4 seconds after ignition.

No proof test is required for the Altair IIIA nozzle. A 344000 N/m^2 (50 psi) leak test is used during nozzle fabrication.

Factors of Safety. - Uniaxial factors of safety were defined as:

$F.S. = F/f$

F = Ultimate strength for an element at temperature

f = Operating stress in the element

Biaxial factors of safety are calculated for each element as part of the analysis. These factors are based on a biaxial failure criteria shown in Figure 59.

Results of Analyses. - Results were calculated for three categories: (1) based on no cracking, (2) based on no failure in the event of graphite cracks, loss of bond between the insert and retainer ring, or cracking of the retainer ring; and (3) based on the biaxial failure criteria. For the SCOUT program only a no-crack criteria is considered acceptable. The calculated probability of no cracks was 0.977 for the insert.

Minimum factors of safety based on no cracks occurring were critical for hoop stresses. Hoop stress distributions at 4 and 7 seconds are shown in Figures 60 and 61.

Component	Time Sec.	Temperature ^{o}K (^{o}F)	F_{TU} $N/m^2 \times 10^6$ (psi)	f_{max} $N/m^2 \times 10^6$ (psi)	F.S.
Insert	7	1606 (2431)	25.98 (3770)	18.87 (2739)	1.38
Retainer	4	2551 (1242)	44.10 (6400)	28.94 (4200)	1.52

Several possible failure modes were assumed, such as cracks in insert or retainer ring and bond failures. The minimum factor of safety in the retainer ring (necessary to prevent insert ejection) was 1.24 when an initial crack in the insert was assumed at 4 seconds after ignition.

Initial results based on the Coulomb-Mohr failure criteria indicated factors of safety in the graphite insert less than 1.0 (i.e., .91) in an element where the temperature was $2439^{o}K$ ($3931^{o}F$) and at a compressive stress of 79.46×10^6 N/m^2 (11532 psi). For graphite materials

plastic relief may be expected when stress levels exceed 41.34×10^6 N/m^2 (6000 psi) and the temperature is higher than 1922°K (3000°F). When a reduced modulus was used, the iterated stresses were reported to be reduced to a non-critical level. They were as high or higher than corresponding factors of safety based on principal uniaxial stresses.

Parametric Variance Study. - An attempt was made in this analysis to define quantitatively the effect on calculated stresses of expected variations in material properties. These results are summarized in Tables XXII through XXIV.

This study also considered the beneficial effects of a rigid acceptance criteria for Graphitite G-90 as compared with commercially available material. Variances in resulting stress correction factors for insert and retainer ring were defined as follows:

Material	Standard Acceptance		Rigid Acceptance Criteria	
	1-Sigma %	3-Sigma %	1-Sigma %	3-Sigma %
Graphitite G-90	±2	±6	±1	±3
Carbon Phenolic	±2.3	±7	±1.15	±3.5

Estimated Accuracy of Altair IIIA Nozzle Analysis. - The analysis of this nozzle includes an evaluation of all significant factors which affect accuracy of the reported results (see Tables XXII, XXIII, and XXIV). These factors were combined in a rational manner to predict variances applied to assumed normal distributions of stress and strength. Standard probability methods (Reference 11) were used to predict nozzle success. Results of that analysis are summarized in Tables XXV and XXVI. Variances were related to two levels of acceptance criteria. Standard acceptance criteria was considered representative of normal quality control and acceptance procedures for the industry. Rigid acceptance criteria was not specifically defined in the analysis but was suggested as being related to the best obtainable quality of material and fabrication within practical cost

limitations. For such a criteria, variances were assumed to be reduced to 50% of normal levels.

This probability approach for defining material and methodology variations does not define the accuracy of the analysis in the literal sense, but is an alternate method for predicting design adequacy. If sufficient test samples are available, an additional confidence level can be determined. Like other analytical methods, the principal value of this probability method is in comparing one design to another.

Problem Areas. - There have not been any nozzle failures or serious problems attributed to the present nozzle of the Altair IIIA motor. Failures of the FW-4S monolithic ATJ throat insert during a test at AEDC and another during flight resulted in the present design which replaced the ATJ throat insert with a Graphitite G-90 insert backed up by a carbon phenolic overwrap. Due to its light weight, 5.45 Kg (12 lbs.), the steel encased exit cone is somewhat flexible and concentricity during final machining has on occasion caused minor concern. Evidence of a slight pitching of the nozzle during the ignition transient period was detected during a static firing test (S/N P-Q2) by observing the deformation of the aft polar boss with respect to the motor case. The misalignment was small, .044 degrees and was attributed to non-axisymmetric behavior of the aft dome. A procurement problem currently exists with regard to the silica phenolic exit cone insulation material. This material has no known usage besides SCOUT and its production has been discontinued. For future production, an alternate material, MXC-113, a carbon phenolic molding tape, will probably be used. This material has been test fired successfully on two high energy Altair IIIA motors. None of the above problems are considered to detract from the basic high reliability of the nozzle during service and no design changes were considered necessary.

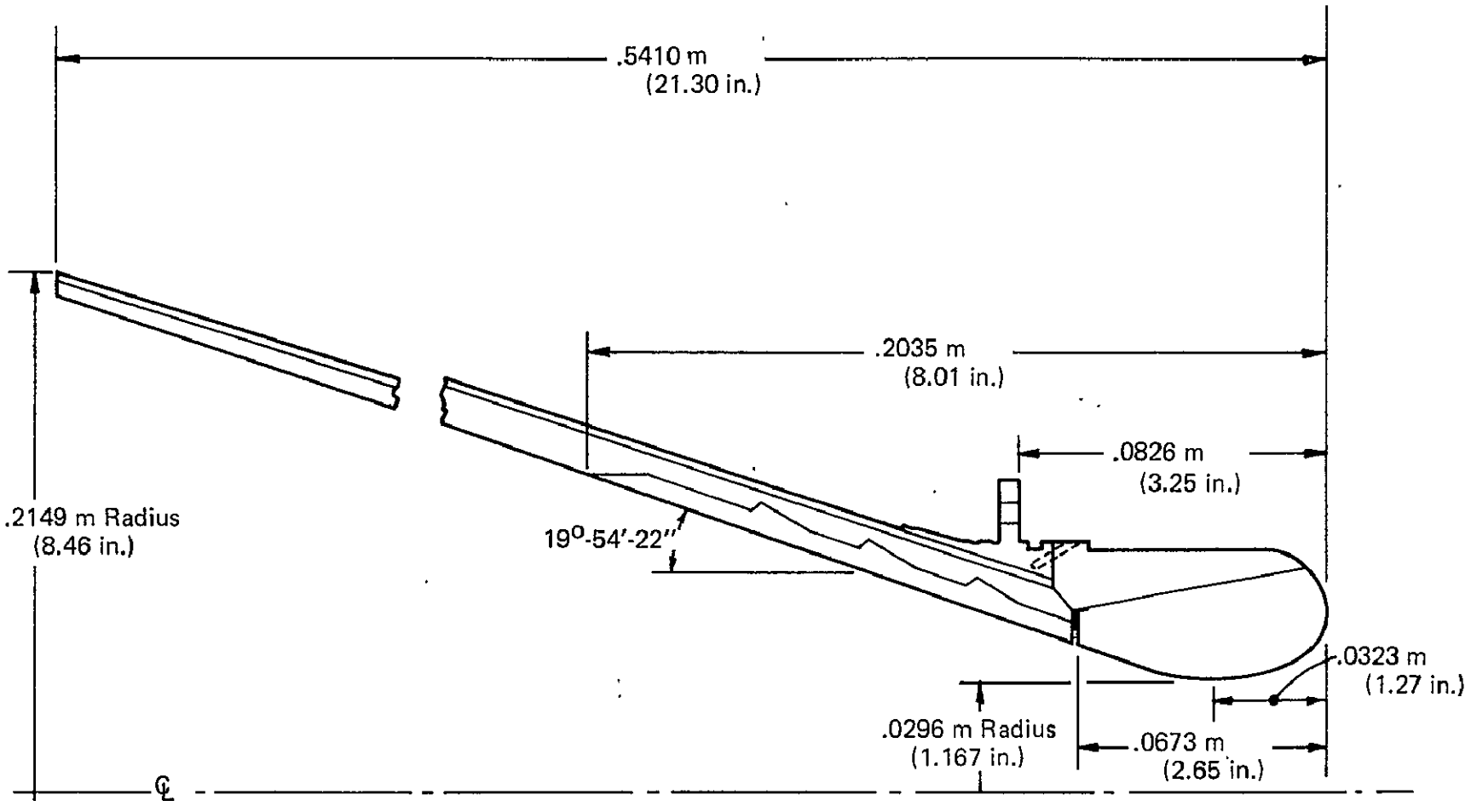

FIGURE 47. – ALTAIR IIIA NOZZLE GEOMETRY

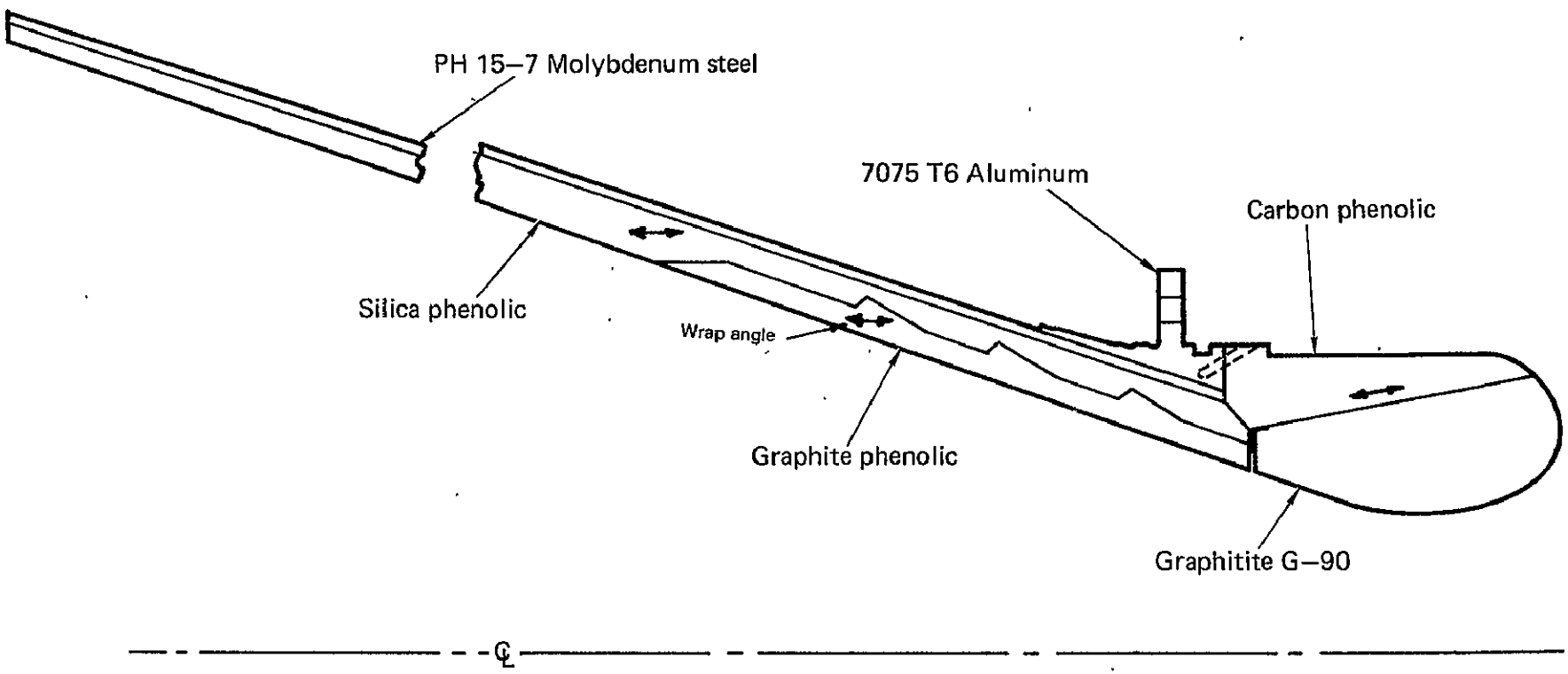

FIGURE 48. – ALTAIR IIIA NOZZLE MATERIALS

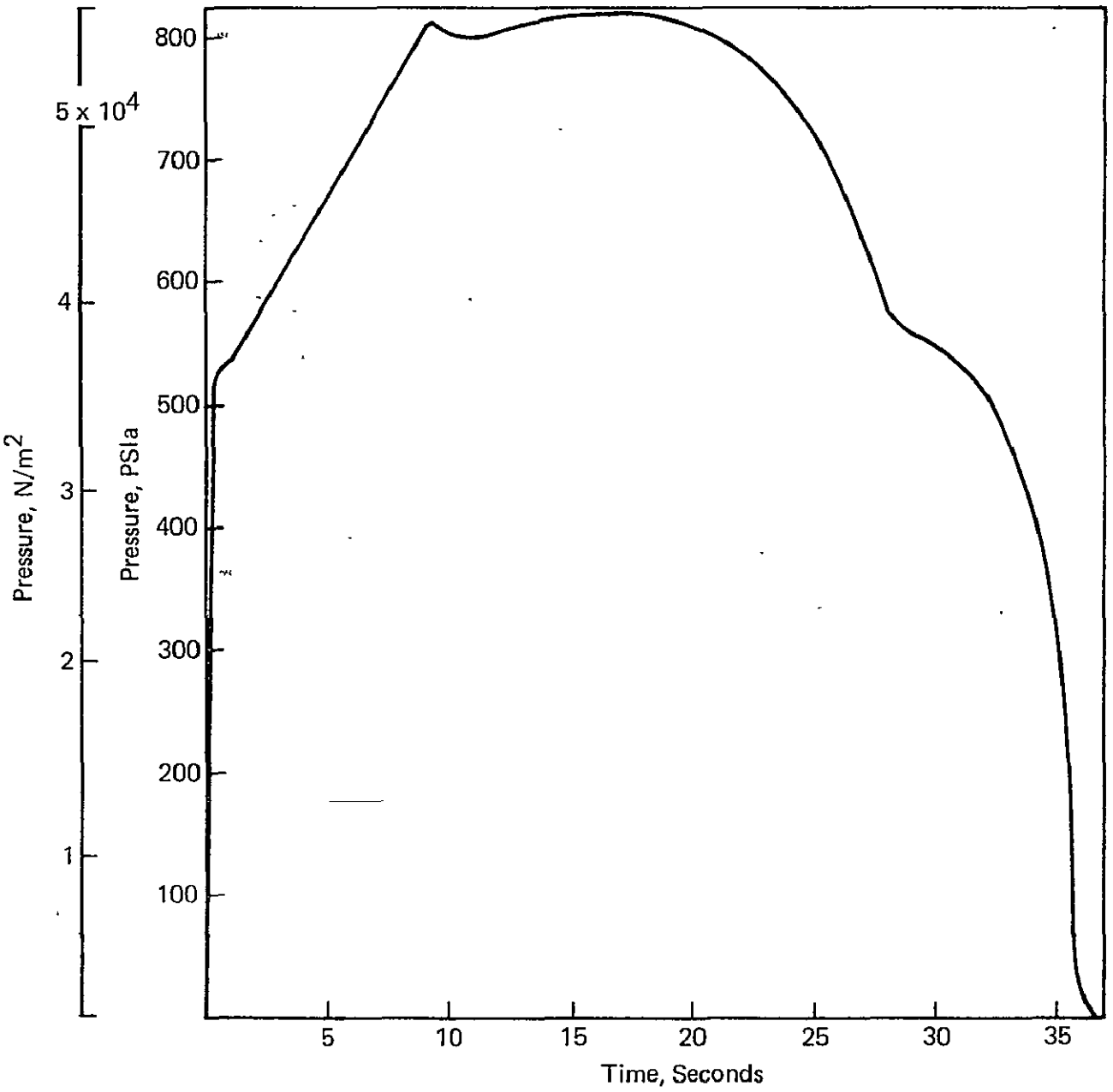

FIGURE 49. — ALTAIR III A PRESSURE vs TIME

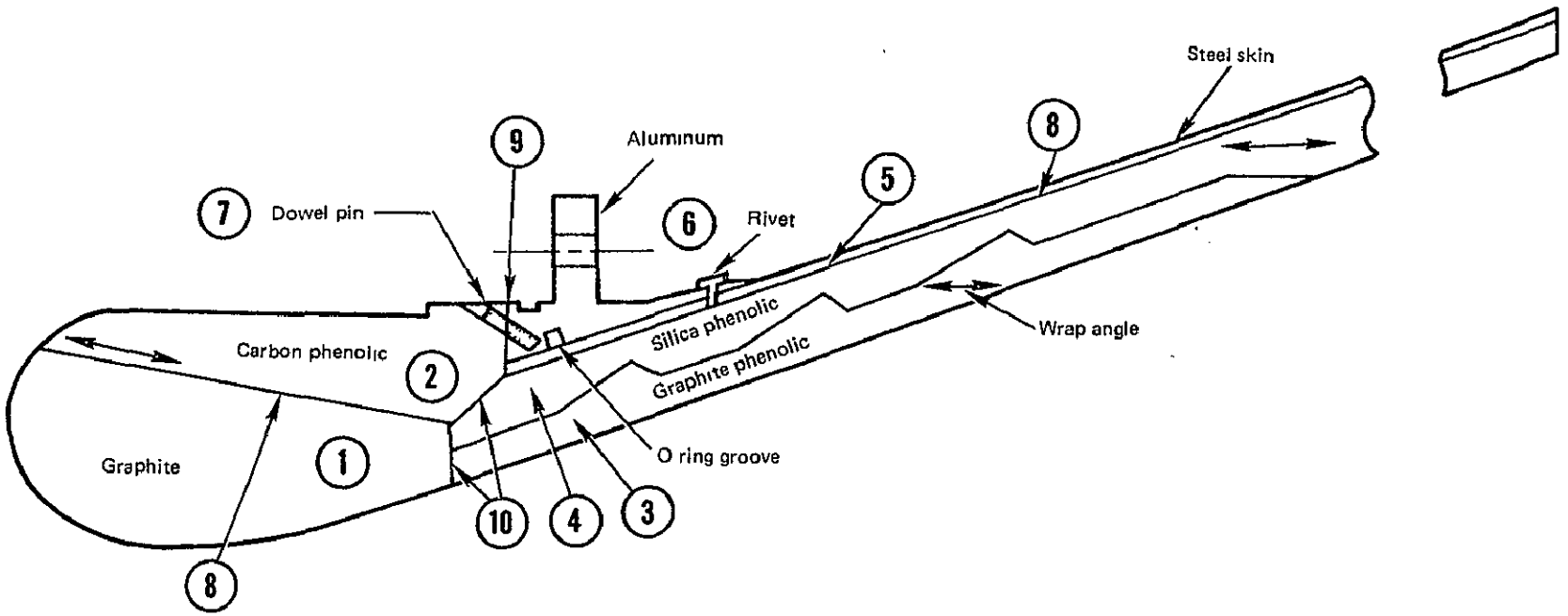

Item No.	Name	Material	Fabrication/inspection
1	Throat (Insert)	Graphite G 90 per LTV 307–13–4	The throat is machined from G–90 extruded graphite. The "with grain" direction or direction of extrusion is parallel to the nozzle centerline. After final assembly the throat is radiographically inspected and alcohol wipe inspected for internal and surface defects.
2	Throat insulator (Retainer ring)	FM 5072 carbon phenolic tape per LTV 307–7–19	The throat insulator is fabricated from (FM 5072) carbon phenolic bias tape which is wrapped on a steel mandrel at an 8^{o} angle to the nozzle centerline, debulked; bagged and hydroclave cured at 6.9×10^{6} N/m^2 (1000 psi). A test ring is cut off the cured part for verification tests to determine edgewise compression strength, density, degree of cure, residual volatiles and barcol hardness. The throat insulator machined billet is visually and radiographically inspected for cracks, voids and delaminations. An alcohol wipe inspection is also performed to determine the existence of external defects on the billet surface.

FIGURE 50. – ALTAIR IIIA FABRICATION AND INSPECTION

Item No.	Name	Material	Fabrication/Inspection
3	Exit cone liner	FM 5014 G graphite phenolic tape per LTV 307–7–21	The exit cone liner is made from two tape wrapped materials; graphite phenolic (FM 5014 G) in the forward end and low density silica phenolic (MX 5707 B) in the aft end. The FM 5014 G material is tape wrapped on a steel mandrel parrallel to the nozzle center line $\pm 20^{o}$ debulked, bagged and cured in a hydroclave a 1000 psi. The cured billet is machined to a preform configuration and overwrapped with MX 5707 B tape parallel to the nozzle centerline $\pm 2^{o}$, vacuum bagged and autoclave cured at 34.5×10^{3} to $69. \times 10^{3}$ N/m^2 (5 to 10 psi). "Tag end" test specimens are obtained from the forward and aft end of the silica and the forward end of the graphite liner for density degree of cure and residual volatile determinations. The exit cone liner/insulator assembly is bonded to the skin/flange assembly with HT 424 film adhesive. The bonding surfaces are MEK wiped, gritblasted with 220 aluminum oxide grit and wiped clean with MEK. The HT 424 adhesive is wrapped around the exit cone exterior and cut to provide a smooth butt joint. The skin/flange assembly is slipped on carefully so as not to disturb adhesive film, vacuum bagged and cured in an autoclave at $437–450^{o}$K ($325–350^{o}$F) for one hour at 75.7×10^{4} N/m^2 (110 psi). Lapshear test panels are prepared and cured with the assembly as a production control test of the bonding operation. The bond line between the skin and exit cone liner assembly is ultrasonically inspected for voids.
4	Exit cone insulator	MX 5707 B low density silica phenolic paper tape per LTV 307–7–20	
5	Exit cone outer shell	PH 15–7 Mo steel sheet per AMS 5520, cond A.	The exit cone skin is fabricated from $.25 \times 10^{-3}$ to $.3 \times 10^{-3}$ M (.010–.012 in) thick PH 15–7 Mo steel sheet which is cut to a cone development, rolled to a conical shape and tig welded per MIL–W–8611. The weld bead is trimmed flush within $.76 \times 10^{-4}$ M (.003 in) of the parent metal surface without undercuts. Radiographic inspection of the weld is performed to verify acceptability. The steel skin and aluminum flange is assembled by a combination of adhesive bonding and mechanical attachment. The bonding surfaces of both materials are MEK wiped, gritblasted with 220 aluminum oxide grit and rinsed with MEK. EC 1469 epoxy adhesive is applied to both bonding surfaces making sure that no adhesive is applied to O ring groove and surface forward of O ring groove. The two parts are placed in a bonding fixture, riveted, and cured at 437^{o} (325^{o}F) for three hours. Lapshear specimens using stainless steel adherends are bonded and cured with the assembly as a production control test of the bonding operation.
6	Nozzle Attach ring	7075–T651 aluminum per QQ–A–250/12	The nozzle flange ring is machined from 7075–T651 aluminum alloy plate. The machined ring is fluorescent penetrant inspected per MIL–I–6866, type I, method A or B. No cracks are permissable.
7	Dowel pin	Carbon steel per MS 16555	The steel dowel pins are installed to prevent the submerged throat assembly from falling into the motor after firing. EA 934 adhesive is used to bond the pins to the structure.

FIGURE 50. – ALTAIR III A FABRICATION AND INSPECTION – Continued

Item No.	Name	Material	Fabrication/Inspection
8	Adhesive	HT 424 epoxy phenolic film adhesive per LTV 307–8–2 type II	HT 424 film type adhesive is used to bond the G90 graphite throat insert to the FM 5072 carbon phenolic throat insulator. The bonding surface of each component is uniformly abraded with 120 grit paper, MEK wiped and air dried. A film of HT 424 is prefitted and cut to provide a smooth butt joint when wrapped around the throat. The insulator is placed over the throat and clamped to 100 psi minimum bonding pressure. The assembly is cured at 437 to 450°K (325°F to 350°F) for two and one half hours in an air oven. Lapshear specimens using stainless steel adherends are prepared and cured with the throat assembly as a production control test of the adhesive bond operation. The assembly is machined to final throat contour and alcohol wipe inspected for defects.
9	Adhesive	EA 934 epoxy	The EA 934 epoxy is used to bond the throat assembly to the exit cone. The aft end of the throat assembly is MEK wiped and the forward face of the aluminum flange is abraded with 120 grit emery cloth and rinsed with MEK prior to bonding. EA 934 is applied to forward face of aluminum and aft face of throat insulator using a glass scrim cloth spacer between the two bonding surfaces. Zinc chromate putty is applied to the taper portion of the exit cone and also the forward portion to provide a thermal expansion gap between the throat assembly and exit cone. The bond line thickness is controlled from $.2 \times 10^{-3}$ to $.3 \times 10^{-3}$ M (.010 to .012 in). Lapshear specimens are also prepared and cured with the nozzle assembly as a control for the EA 934 bonding operation. The parts are cured at 356°K (180°F) for one and one half hours.
10	Sealant	Zinc chromate putty	

FIGURE 50. – ALTAIR III A FABRICATION AND INSPECTION – Concluded

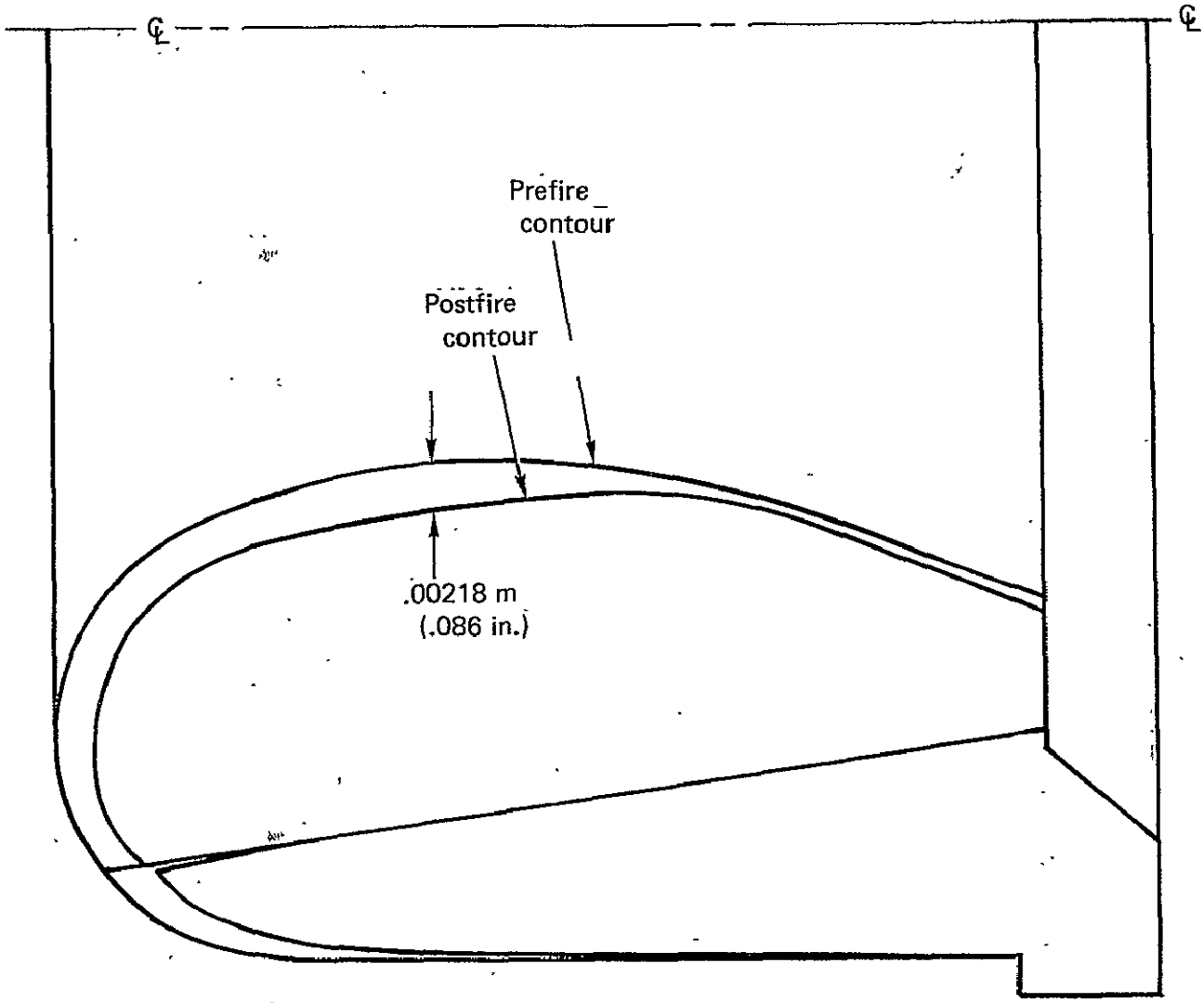

Reference 9

FIGURE 51. – AVERAGE NOZZLE EROSION PROFILE
(BASED ON FIVE STATIC FIRINGS)

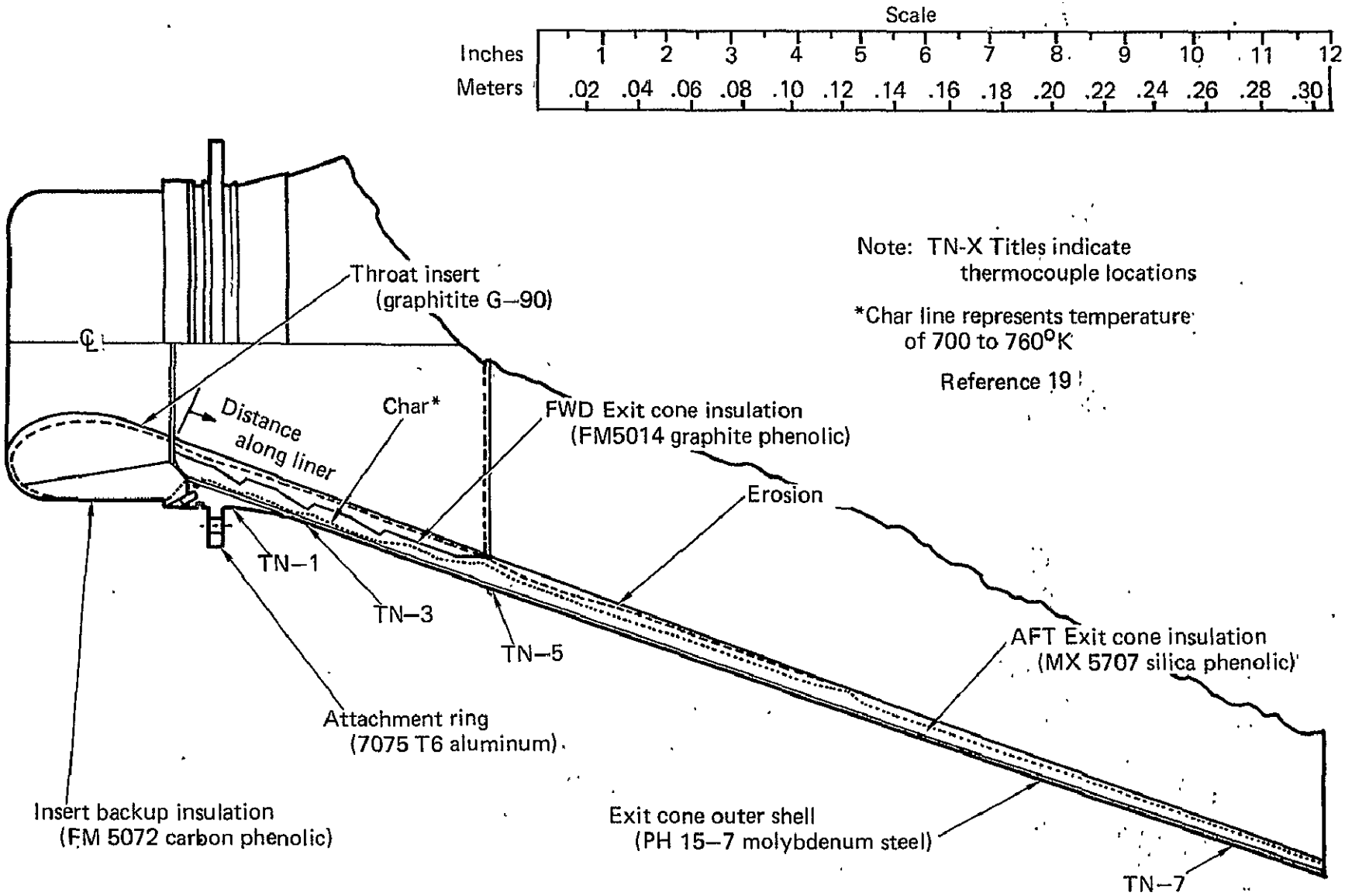

FIGURE 52. – CHAR AND EROSION PROFILES (NOZZLE S/N 015, MOTOR TE-M-640-1)

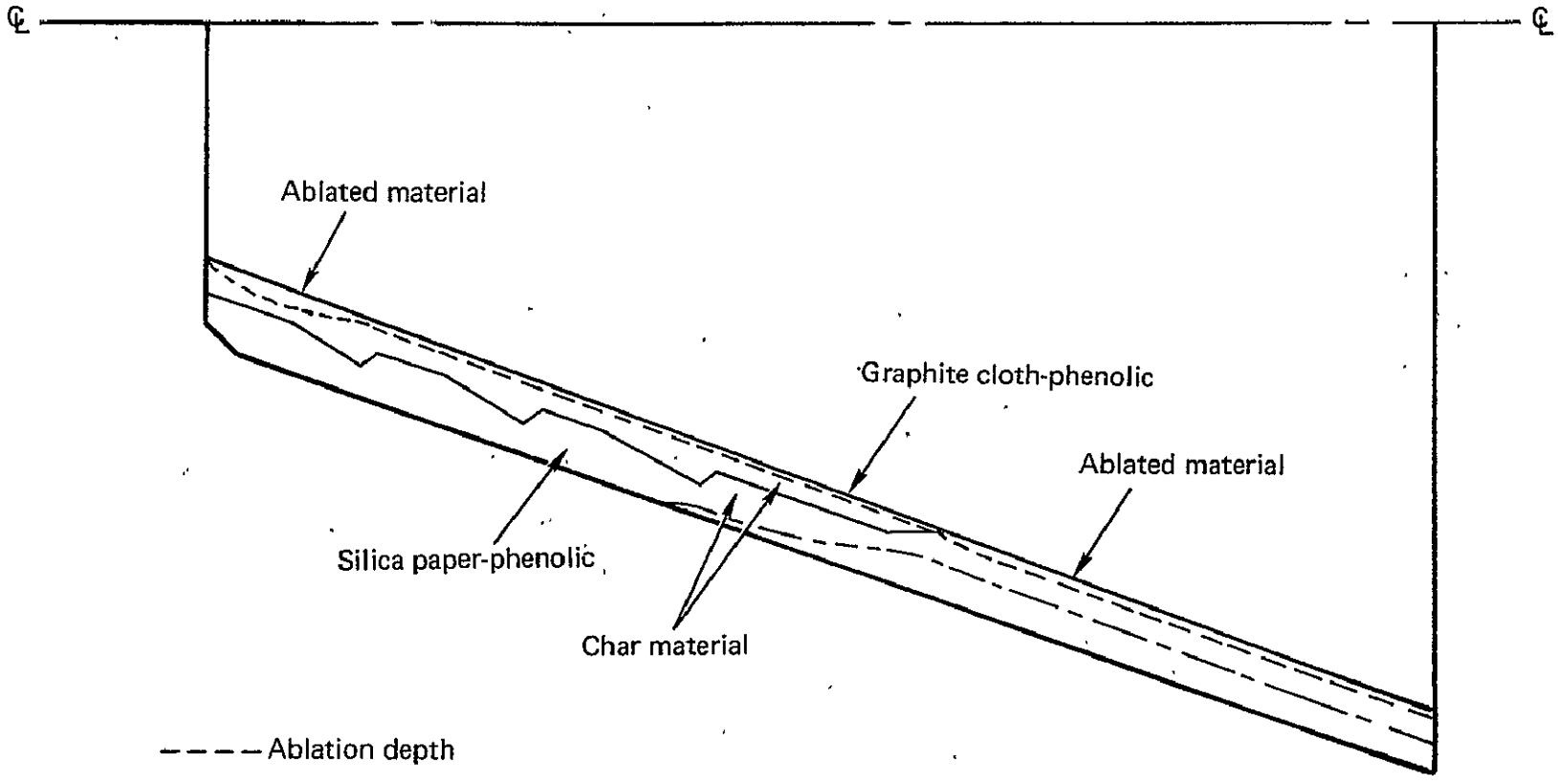

– – – – Ablation depth

— – — Char depth (indicates a temperature of 700°K to 755°K) (800°F to 900°F). Reference 19

FIGURE 53. – EXIT–CONE LINER ABLATION AND CHAR DEPTH PROFILE

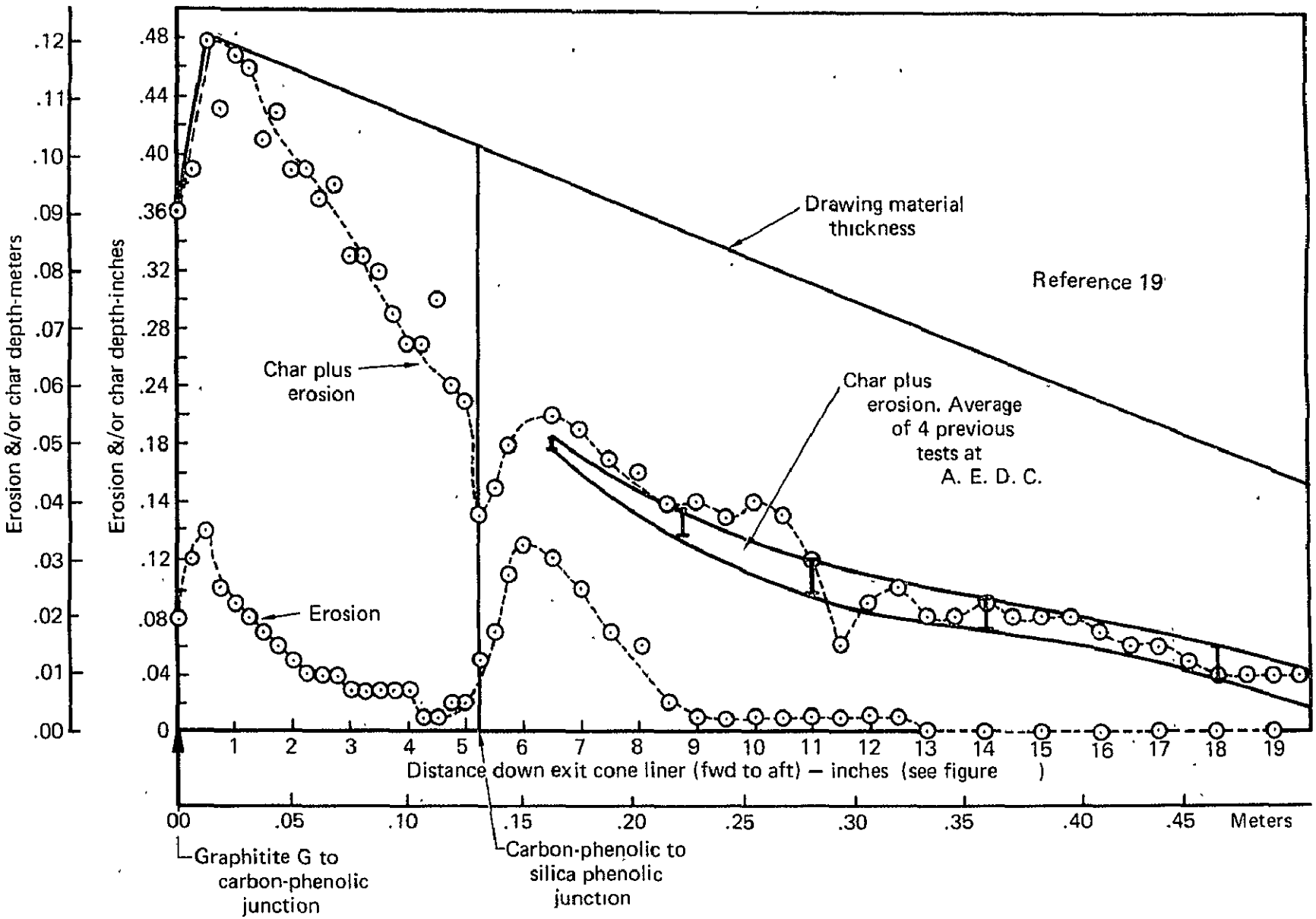

FIGURE 54. — PLOT OF CHAR AND EROSION DATA FOR NOZZLE S/N 30210

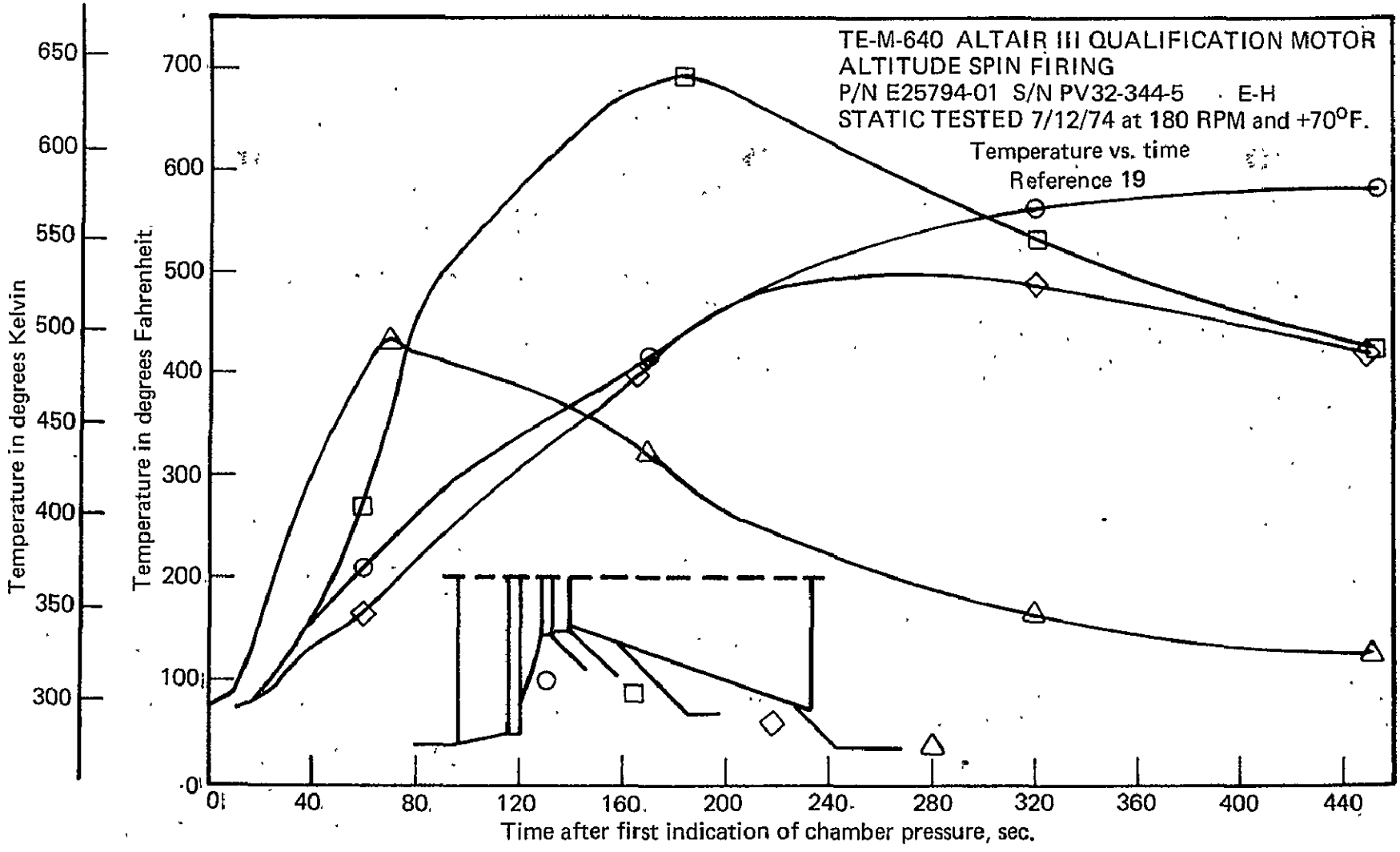

FIGURE 55. — TEMPERATURE PROFILE OF NOZZLE S/N PV32-344-5 E-11 TO 450 SEC.

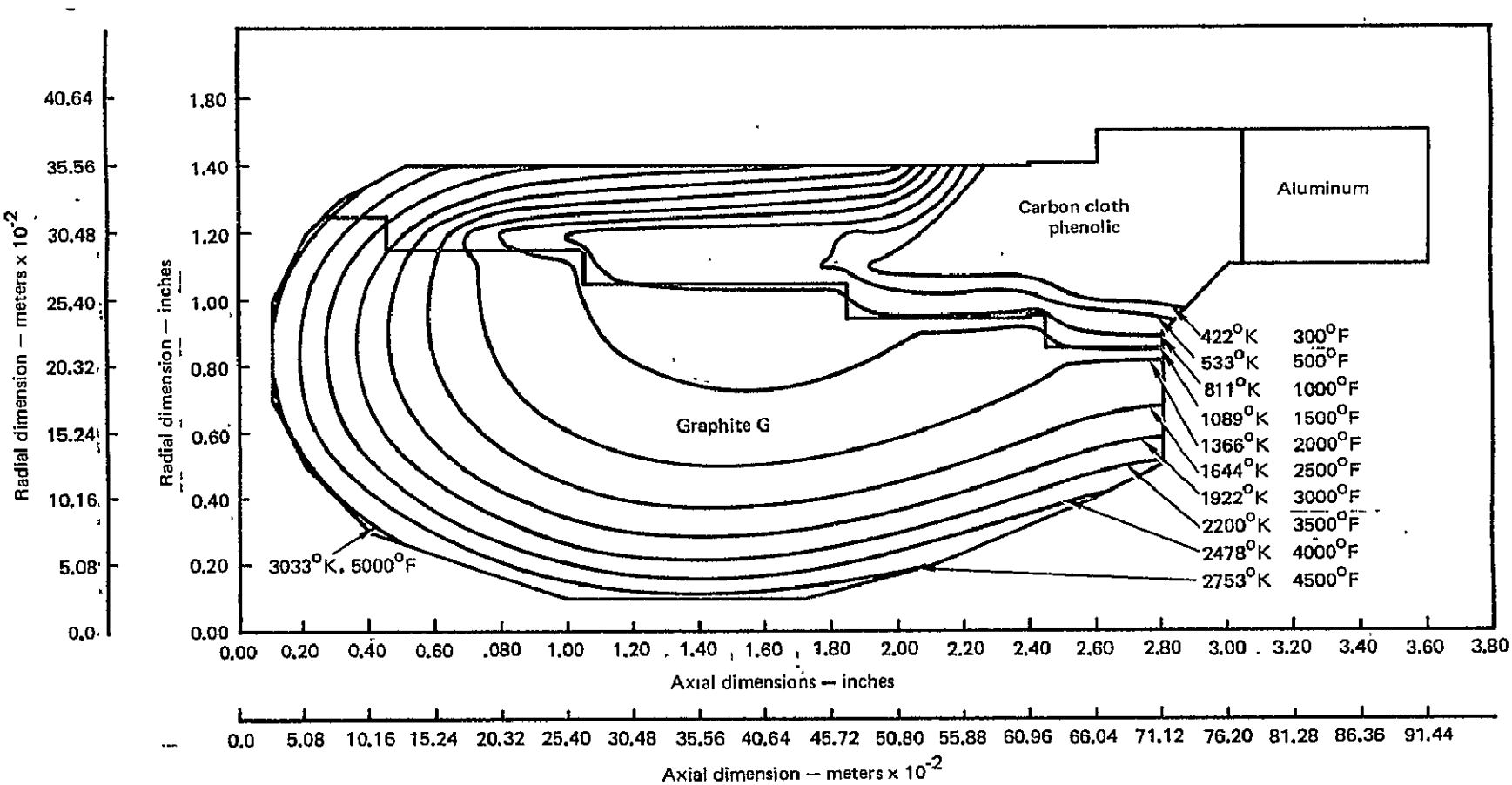

Reference 8

FIGURE 56. — TEMPERATURE DISTRIBUTION AT 7 SECONDS

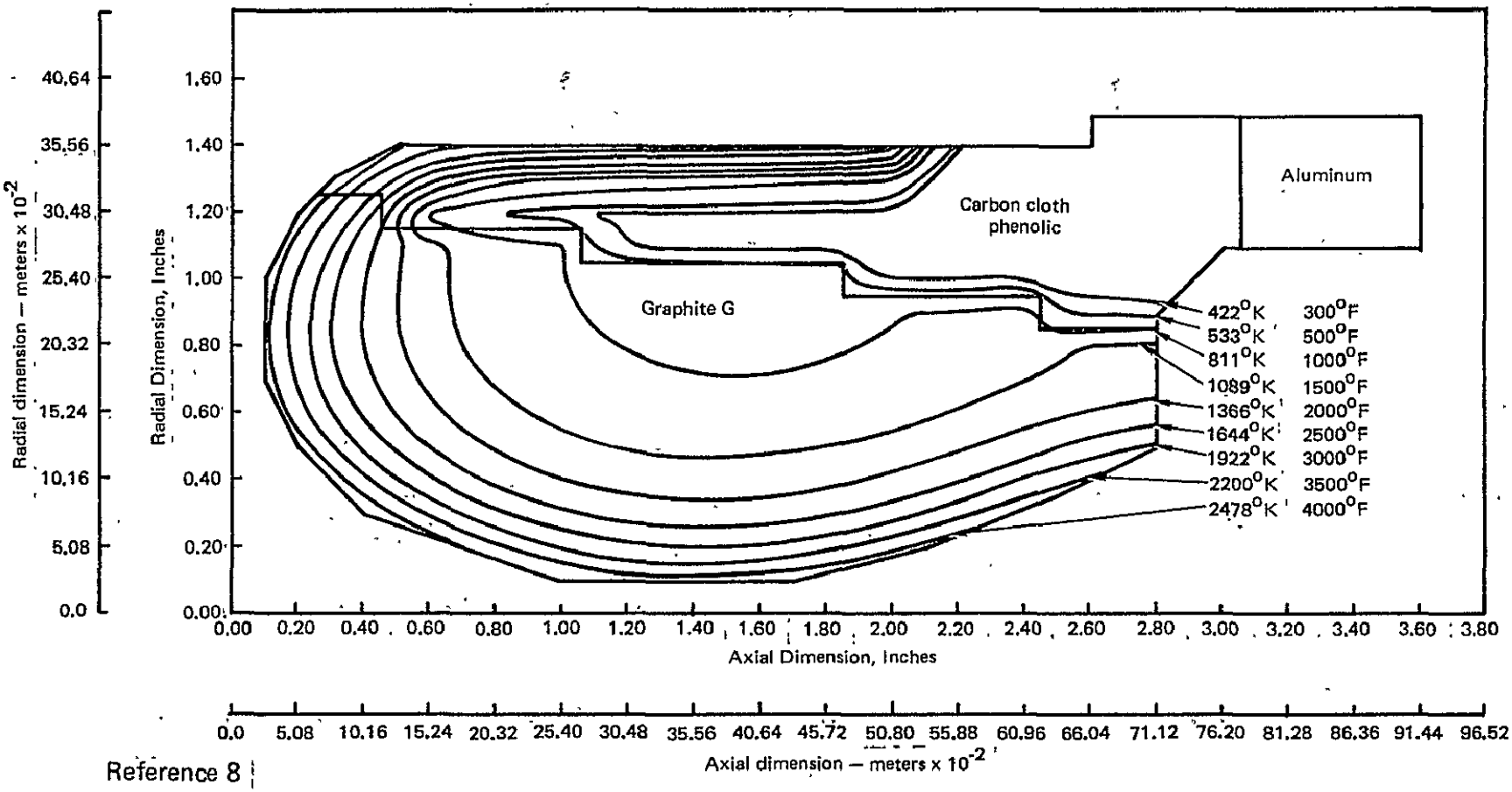

Reference 8

FIGURE 57. — TEMPERATURE DISTRIBUTION AT 4 SECONDS

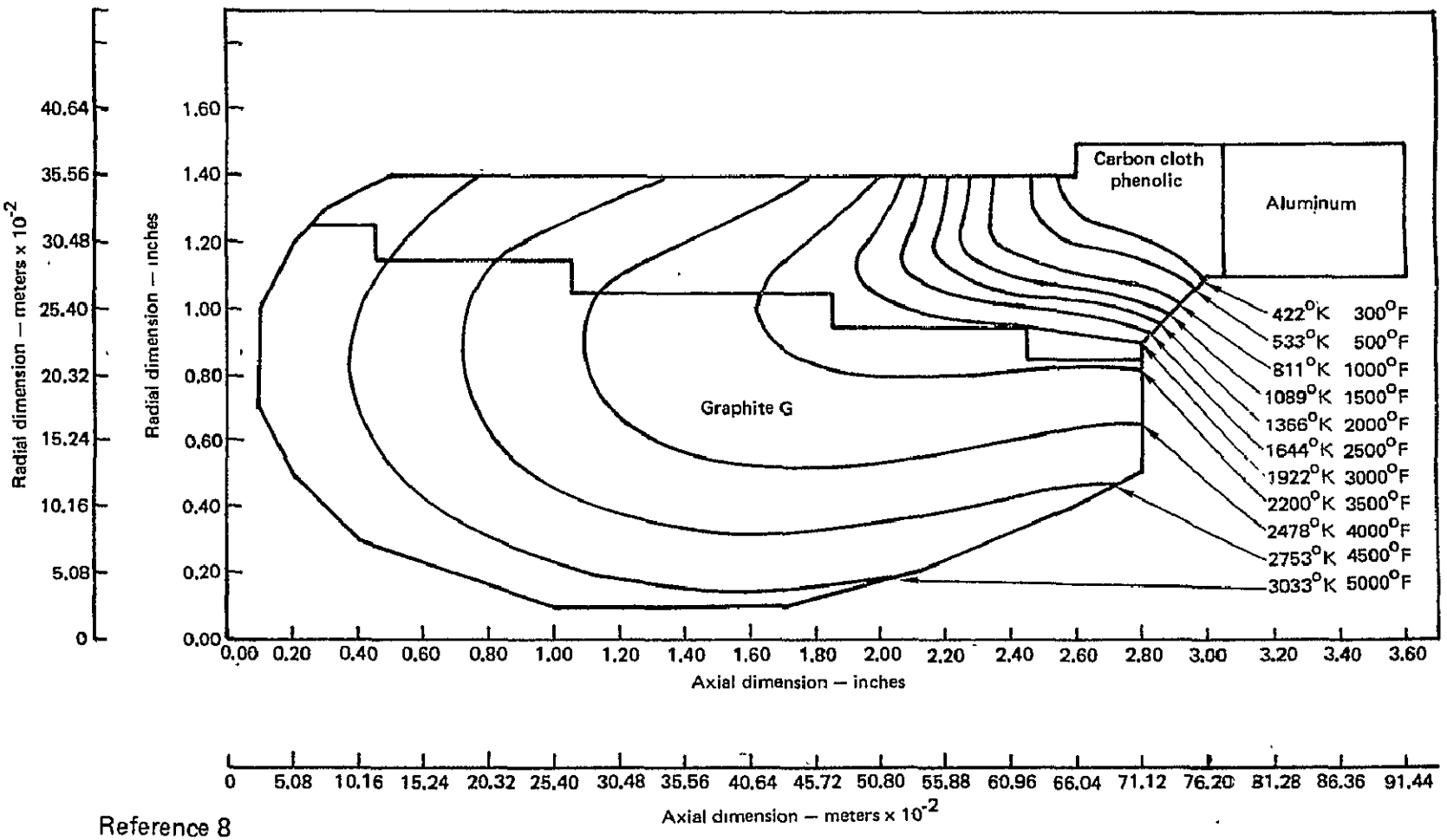

Reference 8

FIGURE 58. — TEMPERATURE DISTRIBUTION AT 30 SECONDS

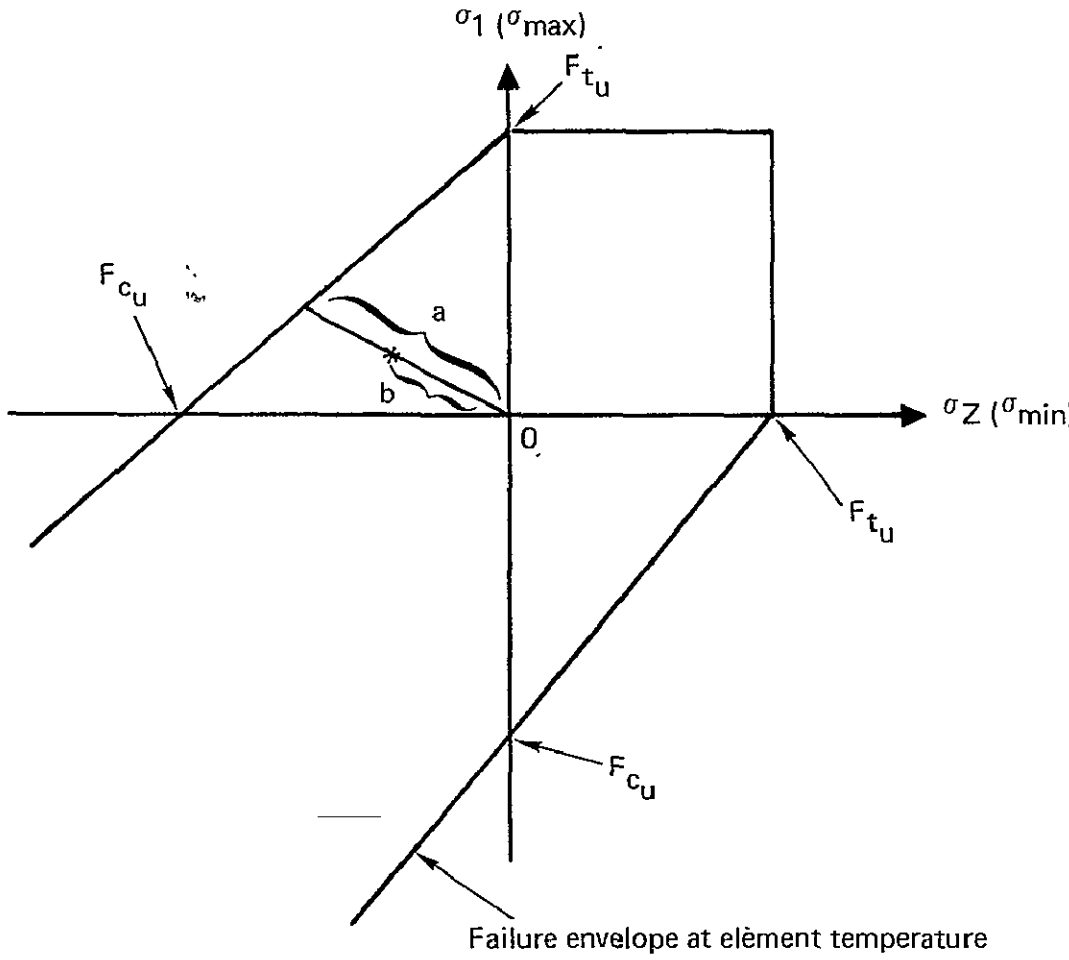

* = Element state of stress

Factor of safety, FS, $= \frac{a}{b}$

FIGURE 59. — COULOMB–MOHR DIAGRAM FOR AN ELEMENT

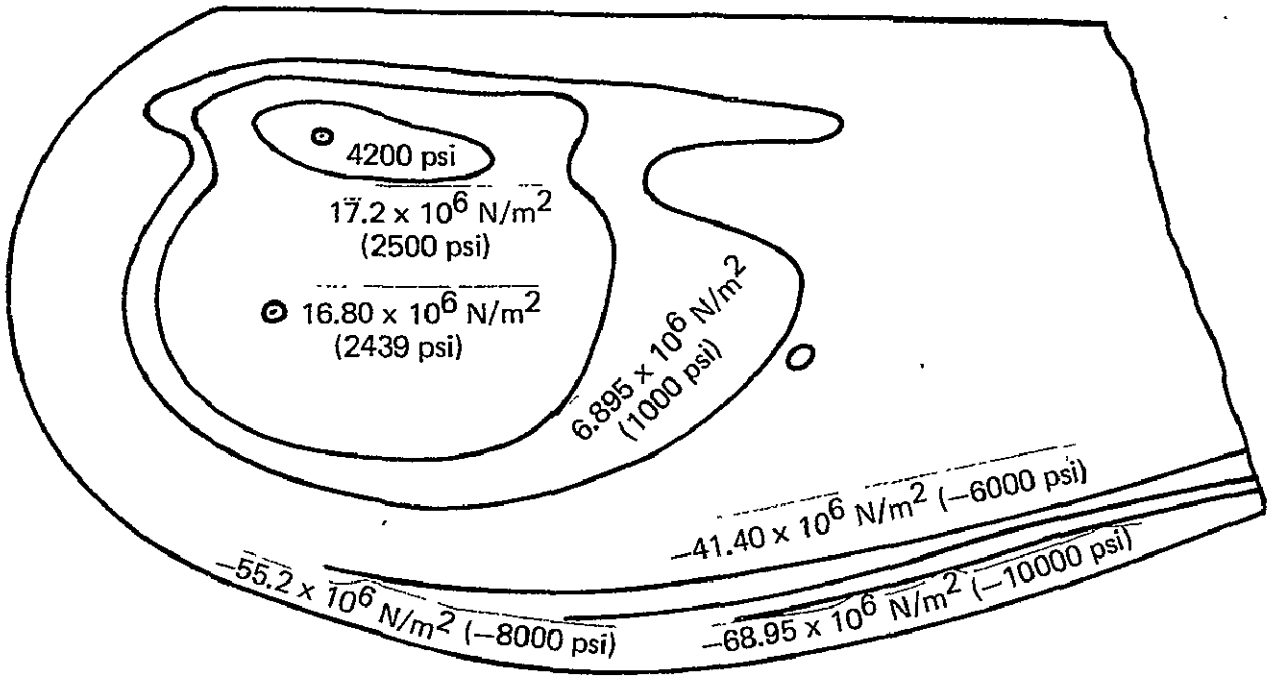

Reference 8

FIGURE 60. – HOOP STRESSES AT 4 SECONDS

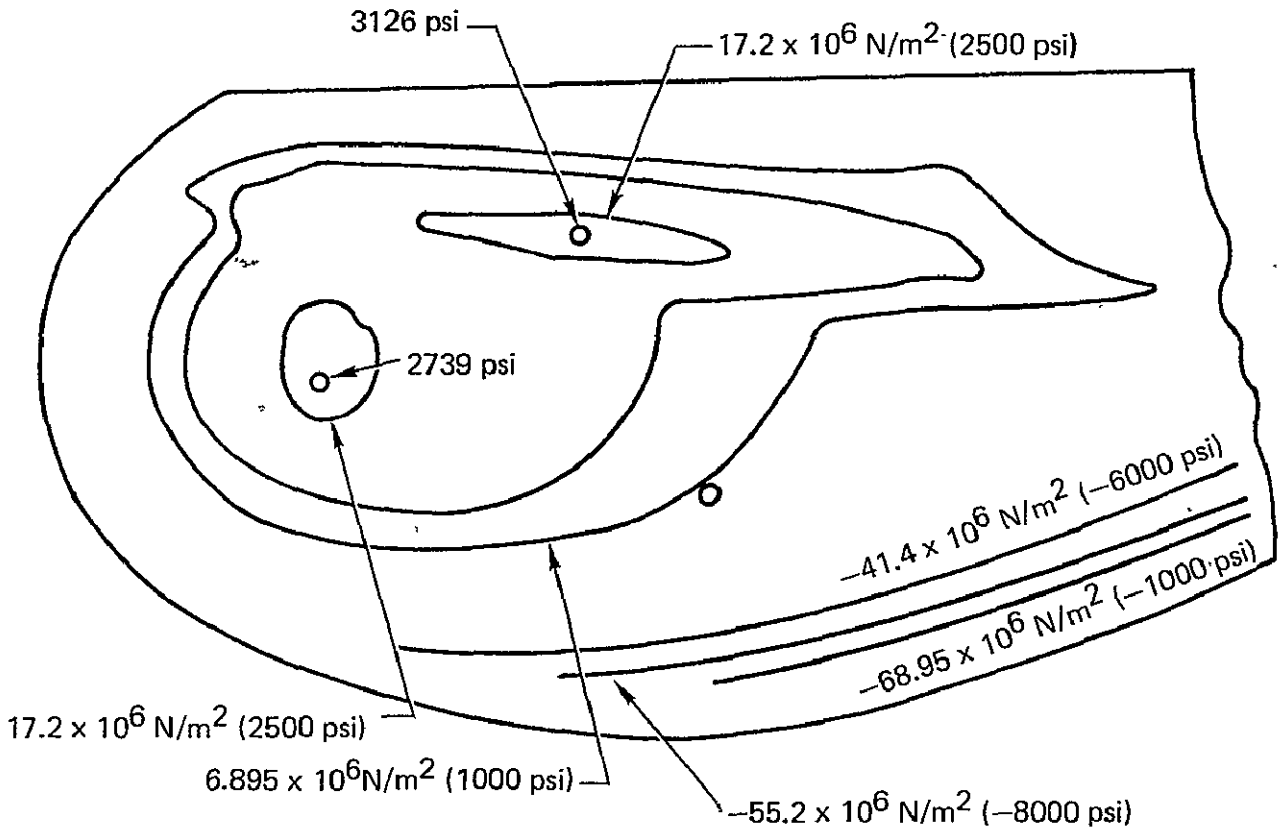

Reference 8

FIGURE 61. — HOOP STRESSES AT 7 SECONDS

TABLE XVII. – ALTAIR IIIA NOZZLE MATERIALS

Component	Material	Vendor designation	Procurement specification
Throat Insert	Graphite	Graphitite G-90	LTV 307-13-4
Retainer Ring	Carbon phenolic	FM 5072	LTV 307-7-19
Exit Cone Liner	Graphite phenolic	FM 5014G	LTV 307-7-21
Exit Cone Insulator	Silica paper phenolic, low density	MX 5707B	LTV 307-7-20
Exit Cone Outer Shell	Steel	PH 15-7 Molybdenum steel	AMS-5520 Cond. A
Nozzle Attach Ring	Aluminum	7075T6	QQ-A-367
Dowel Pin	Carbon steel	MS 16555	MS 16555
Adhesive	Epoxy phenolic	HT 424	LTV 307-8-2 (Type II)
Adhesive	Epoxy	EA 934	Commercial
Sealant	Zinc chromate putty	Zinc chromate putty	Mil-P-8116

TABLE XVIII. – ALTAIR III A MOTOR CHARACTERISTICS

Propellant property	Type/Designation	Motor performance	
Propellant Designation	TP-H-3062 M	Avg. Web Thrust Vacuum N	25900 @ 70°F (5817 lb)
Propellant Type	Aluminized Composite	Total Motor Weight, Kg	301 (664.4 lb)
Grain Configuration	Cylindrical bore with a forward circumferential slot.	Consumed Weight, Kg	275 (605.7 lb)
		Propellant Weight, Kg	273 (601 lb)
Propellant Gas Properties: (Chamber)		Specific Impulse Vacuum (Sec)	288.2
		Total Burn Time (Sec)	31
Specific Heat Ratio (γ)	1.16	Web Burn Time (Sec)	27.9
C_p, cal/gm-°K	.237	Pressure, Web Time Average, N/m^2	4.83 x 10⁶ @ 70°F (701 psi)
Molecular Weight	28.98	MEOP, N/m^2	5.92 x 10⁶ (859 psi)
C*, m/sec	1580 5176 f/sec	Proof Pressure, N/m^2	6.20 x 10⁶ (900 psi)
Flame Temp, °K	3320 (5327 °F)		
		Leak Test N/m^2	344,000 (50 psi)

Reference 17.

TABLE XIX. – ALTAIR III A NOZZLE DRAWINGS AND MATERIAL SPECIFICATIONS

Drawings and specifications	Title
Dwg 23-00427503	Nozzle Flange Ringe
Dwg 23-00427026	Nozzle Throat Assembly
Dwg 23-427025	Nozzle Exit Cone and Flange Assembly
Dwg 23-427002	Exhaust Nozzle Assembly
Spec 308-8-17	Adhesive Bonding
Spec 307-7-19	Tape, Carbon Cloth, Phenolic Resin Impregnated
Spec 207-13-4	Graphite, Extruded
Spec 307-7-20	Tape, Low Density Silica Paper Phenolic Resin Impregnated
Spec 307-7-21	Tape, Graphite Cloth, Phenolic Resin Impregnated
Spec 307-8-2	Epoxy Phenolic Adhesive

TABLE XX. – ALTAIR IIIA NOZZLE MATERIAL PROPERTIES

Material: G-90 Graphite

		300°K R. T.	395°K (250°F)	533°K (500°F)	811°K (1000°F)	1366°K (2000°F)	1922°K (3000°F)	2478°K (4000°F)
Thermal conductivity, cal/m-hr-°K x 10^4 (B-in/ft2-hr-°F)	With lam.	13.4 (1088)	12.9 (1050)	11.2 (906)	8.53 (689)	5.33 (430)	4.05 (327)	3.28 (265)
	Against lam.	11.7 (944)	11.3 (906)	9.5 (768)	6.95 (560)	4.25 (342)	3.15 (254)	2.56 (207)
Coeff. of thermal exp., M/M-°K x 10^{-6} (in/in-°F x 10^{-6}	With lam.	–	1.44 (.8)	1.8 (1.)	2.16 (1.2)	2.7 (1.5)	3.6 (2.0)	3.06 (1.7)
	Against lam.	–	2.16 (1.2)	2.52 (1.4)	3.06 (1.7)	3.78 (2.1)	4.3 (2.4)	4.85 (2.7)
Modulus of elasticity N/M^2 x 10^3 (psi x 10^6)	With lam.	8.82 (1.28)			8.96 (1.30)	10.1 (1.47)	10.3 (1.49)	10.5 (1.52)
	Against grain	5.5 (.80)			6.2 (.90)	7.0 (1.01)	8.6 (1.25)	8.1 (1.17)
Tensile ult. strength N/m^2 x 10^6 (psi x 10^3)	With grain	19.3 (2.8)			20.0 (2.9)	21.2 (3.08)	25.5 (3.7)	32.4 (4.7)
	Against grain	17.8 (2.58)			18.5 (2.68)	19.3 (2.80)	21.7 (3.15)	26.0 (3.77)
Specific heat cal/gm-°K		.17	.25	.32	.39	.46	.49	.51
Poisson's ratio, μ		.17	.17	.17	.17	.17	.17	.17

Reference 8

TABLE XX. — ALTAIR IIIA NOZZLE MATERIAL PROPERTIES — Concluded

Material: Carbon phenolic (FM 5072)

		300°K R. T.	395°K (250°F)	533°K (500°F)	811°K (1000°F)	1366°K (2000°F)	1922°K (3000°F)	2478°K (4000°F)
Thermal conductivity, cal/m-hr-°K x 10^3 (B-in/ft^2-hr-°F)	With lam.	1.15 (9.3)	1.21 (9.8)	1.35 (10.9)	1.73 (14)	3.34 (27)	6.1 (49.1)	9.4 (76)
	Against lam.	.77 (6.2)	.77 (6.2)	.77 (6.2)	.9 (7.25)	1.67 (13.5)	4.23 (34.2)	7.25 (62.6)
Coeff. of thermal exp. M/M-°K x 10^{-6} (in/in-°F x 10^{-6})	With lam.	—	5.1 (2.8)	7.2 (4.)	1.8 (1.0)	1.1 (.6)	2.2 (1.2)	3.8 (2.1)
	Against lam.	—	10.0 (5.6)	25.2 (14.)	3.6 (2.)	2.5 (1.4)	3.2 (1.8)	2.9 (1.6)
Modulus of elasticity N/m^2 x 10^3 (psi x 10^6)	With lam.	18.9 (2.75)	18.9 (2.75)	14.5 (2.1)	9.3 (1.35)	3.4 (.5)	3.0 (.44)	2.75 (.4)
	Against lam.	12.4 (1.8)	9.0 (1.3)	6.4 (.93)	4.1 (.6)	4.1 (.6)	4.1 (.6)	4.1 (.6)
Tensile Ult. strength N/m^2 x 10^6 (psi x 10^3)	With lam.	124. (18)	106. (15.4)	85. (12.4)	51. (7.4)	41. (6)	41. (6)	41. (6)
	Against lam.							
Interlaminar shear strength, N/m^2 x 10^6 (psi x 10^3)		18.9 (2.75)	13.1 (1.9)	9.6 (1.4)	2.75 (.4)	2.75 (.4)	2.75 (.4)	2.75 (.4)
Specific heat cal/gm-°K		.22	.37	.42	.47	.49	.495	.5
Poisson's ratio, μ		.2	.2	.2	.2	.2	.2	.2

Reference 8.

TABLE XXI. – CHAR AND EROSION DATA FOR NOZZLE S/N 30210

Distance down exit cone liner fwd aft (fig 68)		Erosion depth		Char depth		Char plus erosion depth	
M	Inches	M	Inches	M	Inches	M	Inches
0	0	.002032	.08	.005588	.22	.009144	.36
.0127	½	.003556	.14	.008636	.34	.012192	.48
.0254	1	.002286	.09	.009652	.38	.011938	.47
.0381	1½	.001778	.07	.008636	.34	.010414	.41
.0508	2	.001270	.05	.008636	.34	.009906	.39
.0635	2½	.001016	.04	.008382	.33	.009398	.37
.0762	3	.000762	.03	.007620	.30	.008382	.33
.0889	3½		.03	.007366	.29	.008128	.32
.1016	4		.03	.006096	.24	.006858	.27
.1143	4½	.000254	.01	.007366	.29	.007620	.30
.1270	5	.000508	.02	.005334	.21	.005842	.23
.1397	5½	.001778	.07	.002540	.10	.004318	.17
.1524	6	.003302	.13	.002032	.08	.005334	.21
.1651	6½	.003048	.12	.002540	.10	.005588	.22
.1778	7	.002540	.10	.002794	.11	.005334	.21
.1905	7½	.001778	.07	.003048	.12	.004826	.19
.2032	8	.001524	.06	.003048	.12	.004572	.18
.2159	8½	.000508	.02	.003556	.14	.004064	.16
.2286	9	.000254	.01	.003810	.15	.004064	.16
.2267	10½		.01	.003556	.14	.003810	.15
.2794	11		.01	.002794	.11	.003048	.12
.2921	11½		.01	.001270	.05	.001524	.06
.3048	12		.01	.002032	.08	.002286	.09
.3175	12½		.01	.002540	.10	.002794	.11
.3302	13	0	.00	.002032	.08	.002032	.08
.3683	14½		.00	.002032	.08	.002032	.08
.4064	16		.00	.001778	.07	.001778	.07
.4191	16½		.00	.001524	.06	.001524	.06
.4415	17½		.00	.001270	.05	.001270	.05
.4572	18		.00	.001016	.04	.001016	.04
.4953	19½		.00	.001016	.04	.001016	.04

Reference 19

TABLE XXII. — ESTIMATED ERRORS DUE TO HEAT TRANSFER METHODS AND ASSUMPTIONS

Case	Time, sec.	Material	Maximum hoop stress (σ), $N/m^2 \times 10^6$ (psi)	Temperature at maximum stress location, ^{o}K (^{o}F)	Material strength (σ u), $N/m^2 \times 10^6$ (psi)
1) Basic Finite Element Analysis	7	Graphite	18.87 (2739)	1606 (2431)	25.98 (3770)
2) Charring and Ablating Effects	7	Graphite	18.89 (2451)	1606 (2431)	25.98 (3770)
1) Basic Finite Element Analysis	4	Carbon Phenolic	28.94 (4200)	945 (1242)	44.10 (6400)
2) Charring and Ablating Effects	4	Carbon Phenolic	35.90 (5211)	714 (825)	58.57 (8500)

Mean Stress Correction Factor, $f_c = \frac{(\sigma)2}{(\sigma)1} \cdot \frac{(\sigma u)1}{(\sigma u)2}$

Graphite: $f_c = \frac{2451}{2739} \cdot \frac{3770}{3770} = 0.89$

Carbon Phenolic: $f_c = \frac{5211}{4200} \cdot \frac{6400}{8500} = 0.93$

Reference 8

TABLE XXIII. – ESTIMATED CORRECTION FACTORS DUE TO STRESS ANALYSIS METHODS AND ASSUMPTIONS

Source of error or variation	Estimated mean stress correction factor (fc) i	Estimated variation in stress (1 sigma), %	Estimated variation in stress (3 sigma), %
1. Linear Elastic, Secant Modulus Approach	0.975	0.87	2.6
2. Infinitesimal Strains	1.000	0.33	1.00
3. Nonsymmetric Loads	1.007	0.23	0.70
4. Nonsymmetric Geometry	1.020	0.33	1.00
5. Transient Loading	1.020	0.70	2.00
6. Element Size	1.060	0.94	2.83
7. Solution Accuracy	1.000	0.33	1.00
8. Boundary Fixity	0.970	1.37	4.10
9. Axisym. Geometry Variation	0.994	0.27	0.81
10. Insert Pressure Distribution	0.978	1.50	4.40
Composite Mean Correction Factor Due to Stress Analysis Methods and Assumptions = 1.02			
Composite Variation (1 sigma) Due to Stress Analysis Methods and Assumptions = 1.60			
Composite Variation (3 sigma) Due to Stress Analysis Methods and Assumptions = 7.80			

Reference 8

TABLE XXIV. – ERRORS IN PREDICTED STRESS DUE TO ANISOTROPIC EFFECTS

Material	Time, sec	Maximum hoop stress, $N/m^2 \times 10^6$ (psi)		Mean stress correction factor, fc
		Isotropic	Orthotropic	
Graphitite G–90	7	8.68 (1260)	8.31 (1206)	0.96
Carbon Phenolic	4	24.14 (3504)	22.77 (3305)	0.94

Reference 8

TABLE XXV. – PREDICTED PROBABILITY OF NONOCCURRENCE FOR GRAPHITITE G CRACKING AT 7 SECONDS

	Standard acceptance criteria	Rigid acceptance criteria
Finite element analysis stress	19.98×10^6 N/m^2 (2899 psi)	19.98×10^6 N/m^2
Temperature of critical element	1605 °K (2431°F)	1605 °K
Mean stress correction factor	0.87	0.87
Corrected mean predicted stress	17.4×10^6 N/m^2 (2522 psi)	17.4×10^6 N/m^2
Mean strength	25.9×10^6 N/m^2 (3760 psi)	25.9×10^6 N/m^2
Mean safety factor	1.49	1.49
Estimated 3 sigma variation in stress	82%	46%
Estimated 3 sigma variation in strength	19%	10%
Predicted probability of nonoccurrence, P	0.956	0.999

Assumed: (for this analysis) Cracked retainer ring; Retainer/insert bond partially destroyed

Reference 8

TABLE XXVI. – PREDICTED PROBABILITY OF NONOCCURRENCE FOR CARBON PHENOLIC CRACKING AT 25 SECONDS

	Standard acceptance criteria	Rigid acceptance criteria
Finite element analysis stress	6.44×10^6 N/m^2 (935 psi)	6.44×10^6 N/m^2
Temperature of critical element	1370°K (2003°F)	1370°K
Mean stress correction factor	0.91	0.91
Corrected mean predicted stress	6.14×10^6 N/m^2 (851 psi)	6.14×10^6 N/m^2
Mean strength	41.3×10^6 N/m^2 (6000 psi)	41.3×10^6 N/m^2
Mean safety factor	7.1	7.1
Estimated 3 sigma variation in stress	92%	51%
Estimated 3 sigma variation in strength	19%	10%
Predicted probability of nonoccurrence, P	1.000	1.000

Assumed: (for this analysis)
- Graphite cracked
- Bond failed completely
- Phenolic charred and temperature degraded
- Phenolic loads caused by graphite ejection force due to pressure

Reference 8

TRIDENT
NOZZLES DATA

INTRODUCTION

The current Trident program includes the most recent new nozzle development effort in the solid propellant motor industry. The development program investigated a large number of old and new nozzle materials in an effort to provide a reliable, minimum weight design for the solid propellant rocket nozzles system. Materials were evaluated, compared and screened for each component. Preliminary material selection was made based upon known behavior in similar nozzle environments and to a limited extent by use of numerical merit factors. Final screening was effected by subscale motor firing data and post test examinations of sectioned nozzles. Approximately twenty 0.762 m (30 in.) diameter motors will be fired to assist in the design optimization prior to final nozzle qualification.

Results of this program are applicable to current studies to improve performance and reliability of SCOUT motors. The materials used in the Trident program are considered in this report for their applicability to SCOUT nozzles.

The Trident vehicle propulsion system consists of three solid propellant rocket stages. Submerged nozzles were designed for each stage. A program objective was to obtain design similarity for the nozzles of all three motors, where practical. These nozzles utilize a flexible joint between the nozzle and support ring which permits thrust vector control. This feature has also been used successfully on Poseidon nozzles. All three stages use pyrolitic disc washers in the throat to minimize erosion. Fore and aft retainer rings are made of Carbitex 700 and other components are mainly graphite, carbon and silica phenolic composites with titanium, aluminum and graphite epoxy structures. The current configurations and material usage represent a preliminary design status. As more firing data is obtained during the nozzle development program, modifications may be made to the present design.

Data on these nozzles was obtained by review of Trident monthly reports, proposals and other available information.

Nozzle Environment. - The three Trident stages have the following characteristic parameters:

	First Stage	Second Stage	Third Stage
Chamber Temperature, ^{o}K (^{o}F)	3866 (6500)	3905 (6570)	3528 (6350)
MEOP, N/m^2(psi)	10.748×10^6 (1560)	9.302×10^6 (1350)	7.372×10^6 (1070)
Firing Time, Sec.	65	67	37
Throat Diameter, m (in)	0.267 (10.5)	0.185 (7.37)	0.122 (4.8)

In the throat area pyrolitic graphite (PG) washers achieve 90% of maximum surface temperatures in about 10 seconds. Typical throat temperature and erosion curves for the PG throat material, shown in Figure 62, are based on thermocouple data and post-test measurements of the eroded surfaces. Initial screening of materials and data acquisition was obtained from 30 inch development motor firings. This motor was quite similar in firing time and geometry to the Trident third stage motor. In later phases of the nozzle development program, firings of first, second and third stage motors provided supplementary data for final design. Chamber temperatures are based on gas analysis methods and resulting surface temperatures are measured for checks against the thermal computer analysis.

MATERIAL SELECTION

The following selection technique for each component was followed for the Trident motor nozzles. Component locations are shown in Figure 63.

Due to the design similarity of the first, second and third stage Trident motor nozzles, the following analysis for selection of nozzle component materials are applicable to all nozzles. Further refinements will be made based on development firings and final analyses.

Stationary Shell. - The critical load condition for this component occurs due to bending and buckling. The shell was designed using a factor of safety of 1.25. The shell is bending stress limited at the small diameter end, buckling limited in the conical thin shell section and bending stress limited at the large end. Bending loads are mainly induced by two thrust vector control (TVC) actuators which connect the nozzle stationary shell to the compliance ring at two azimuth locations 90^{o} apart. An aluminum or titanium end ring is pinned, bolted and/or bonded at the forward end of the graphite composite cone. Weight comparisons of four candidate materials were as follows for the (typical) third stage nozzle.

Material	Weight, kg (lb)
Aluminum	6.05 (13.3)
Titanium	6.85 (15.1)
Graphite Epoxy/Alum	5.31 (11.7)
Beryllium	3.76 (8.3)

Beryllium was not selected for the Trident program due to lead time procurement, special handling requirements, uncertain availability of forgings and higher cost. Aluminum forgings are used on first, second and third stage nozzles for the stationary shell. This material was selected as a compromise of modulus and favorable strength to weight ratio.

Stationary Shell Insulation.- Two elastometic materials, EPDM-CF and carbon fiber silicone rubber (DC 93-104), and silica cloth phenolic were compared for stationary shell insulation based on minimum weight.

Material	Thickness, CM (in)	Density, gm/cc (pci)	Weight, kg (lb)
Silica Cloth	2.03 (.80)	1.75 (.0632)	2.11 (4.65)
DC 93-104	1.78 (.70)	1.45 (.0523)	2.04 (4.51)
EPDM-CF	1.52 (.60)	1.05 (.0379)	1.15 (2.53)

The EPDM-CF material was selected based on weight advantage and demonstrated performance with XLDB propellant.

Exit Cone. - Carbon cloth phenolic was selected for the exit cone liner based on firing experience. In the forward section of the exit cone where the environment is more severe a higher (standard) density carbon cloth phenolic is used. Light-weight material employing carbon micro-balloons is used in the aft section. In the most forward transition area just aft of the throat, Carbitex 700, an edgewise oriented fiber carbon cloth phenolic, is utilized as a transition ring to reduce erosion and to provide additional structural support for the throat and forward area of the exit cone. The combination of exit cone liner and insulation was selected based on a minimum weight combination which limits the maximum outside temperature to 200°F at the end of motor action time. Carbon cloth and light-weight carbon cloth phenolic were selected in the forward and aft liner areas of the exit cone respectively for all three stage nozzles.

Liner	Insulation	Weight, kg (lb)
Carbon Cloth	Silica Cloth	21.8 (48.0)
Carbon Cloth	LW Silica Cloth	18.9 (41.7)
Carbon Cloth/ LW Carbon Cloth	Silica Cloth	19.1 (42.0)
Carbon Cloth/ LW Carbon Cloth	LW Silica Cloth	16.4 (36.0)

Exit Cone Compliance Ring. - This stiffener ring provides interface attachments for the TVC actuator and distributes actuator loads around the exit cone structure. The following materials were compared on the basis of weight required to provide equal stiffness. Graphite epoxy ring construction was selected based on minimum weight with low risk for second and third stage nozzles. Because weight had less impact on performance for the first stage, a steel compliance ring is used in that nozzle to reduce development cost. Beryllium was rejected for the reasons listed under the stationary shell section above.

Shell Material	Compliance Ring	Weight, kg (lb)
Aluminum	Steel	8.21 (18.1)
Aluminum	Titanium	6.39 (14.05)
Titanium	Titanium	6.39 (14.05)
Aluminum	Aluminum	5.93 (13.06)
Beryllium	Beryllium	1.41 (3.10)
Graphite Epoxy	Beryllium	1.83 (4.04)
Graphite Epoxy	Aluminum	4.22 (9.30)
Graphite Epoxy	Graphite Epoxy	3.90 (8.60)

Nozzle Inlet Insulation. - Nozzle inlet flow efficiency influences the delivered I_{SP} and has a more significant effect on range than does inert weight in that area. Inlet materials were selected based on their ability to maintain an efficient contour throughout motor action time. The XLDB environment requires a liner material with low erosion rate and good strength properties. Carbon cloth phenolic appeared best, based on strength and erosion resistance, but use of this material over the entire inlet section would result in a step in profile just forward of the pyrolitic graphite throat. Therefore, Carbitex 700 was employed as a transition material between nose cap and throat pack. Graphite cloth phenolic was used for the nose cap and carbon cloth for the submerged outside diameter (OD) liner of the inlet. This design was influenced by material evaluations and successful performance in the Polaris, Minuteman and Poseidon programs. In the OD area three combinations of liner and insulation were compared for minimum weight. The optimum combination of carbon cloth phenolic with backup insulation of silica cloth phenolic containing carbon microballoons was selected for the outer nozzle inlet components in the submerged area.

OD Liner	OD Insulation	Weight kg (lb)
Carbon Cloth	Carbon Cloth	2.86 (6.3)
Carbon Cloth	Silica Cloth	2.27 (5.0)
Carbon Cloth	LW Silica Cloth	1.82 (4.0)

Throat Insert. - Selection of insert material was dictated primarily by ballistic and thrust performance requirements. Minimum erosion was used as the selection criteria. Predicted erosion rates were as follows:

Material	Erosion Rate, cm/sec (mils/sec)
Graphite Cloth Phenolic	.0533 (21.1)
Carbitex 700	.0267 (10.5)
Monolithic Graphite	.0210 (8.3)
Pyrolitic Graphite Discs (PG)	.0084 (3.3)

All three stages currently use five .955 cm (.375 in) discs. To permit use of additional sources of material, a design change is currently being evaluated to utilize seven .636 cm (.25 in) discs. Teflon washers are used as spacers between PG discs to accommodate thermal growth at elevated temperature. The spacers are thermally degraded due to ablation early in firing and provide an expansion cavity for the pyrolitic graphite washers in the throat area.

30" Motor Materials Evaluation Matrix. - Preliminary assessment of material behavior under XLDB propellant environment was started early in the program. Some of the materials tested were eliminated prior to the analytical assessment and final candidate selections. At least seventeen 30 inch motor firings have been conducted or are scheduled at Hercules Incorporated, Magna, Utah. The material combinations for each motor nozzle scheduled for evaluation in XLDB propellant environment by use of 30 inch test motors is shown in Table XXVII.

Trident Nozzle Reliability. - At the present time there have been about seven firing tests using 30 inch test motor firings, one first stage, four second stage and eight third stage development motor firings.

Due to the large number of materials investigated, complete characterization of each material and complete thermal and thermoelastic analyses of each nozzle design would have entailed prohibitive cost and

schedule problems. Initial screening of materials was based upon known past performance and comparison of pertinent physical and mechanical properties. To provide a meaningful test environment, the test matrix shown in Table XXVII . used a 30 inch motor whose performance and environment closely simulated the Trident third stage motor. Other full size first, second and third stage development motors will supplement the initial test matrix. During early test firings a number of nozzle failures occured due to material and design inadequacies. The failed part was replaced or redesigned and verified by subsequent firings. These failures and the corrective actions are documented in the following three paragraphs.

During test of development motor 3SF-01 a Graphitite G-90 ring supporting the throat pack cracked and was ejected at 1.97 seconds after ignition. The throat was lost at 3.0 seconds. As a result of this test monolithic (G-90) material was replaced by Carbitex 700. This material substitution has given reliable performance in subsequent tests.

An exit cone was lost at 7.98 seconds on motor 3SF-03A as a result of shear failure of bolts connecting the exit cone adapter to the forward joint end ring. The joint was redesigned and additional shear pins added. No further problems were experienced in this area.

During a test at AEDC of motor SDE-11 the throat pack was lost at 36.89 seconds. The problem was attributed to gas flow into the nose cap bond area with subsequent loss of the carbon cloth segment and throat pack. The nose cap/OD liner interface was redesigned to provide a discontinuous bond line in this area. It is believed that the new design has corrected that problem area. Figure 64 shows this change.

Table XXVIII . lists the results of a third stage nozzle thermoelastic stress analysis. From this table it can be concluded that, due to low predicted margins of safety, occasional cracks in the PG insert washers might be experienced. Also, the area of minimum strength of structural components is just aft of the PG insert. The aluminum split ring in this area is a

redundant retention method and is capable of supporting the total ejection load. Redundancy is provided by metal screws which protrude into the throat support component. Further, the throat support has a jagged surface which prevents slippage of the adjacent liner material.

Since Teflon ablates at a temperature of about 644°K (700°F). the lateral support offered to the PG discs will be maintained until the pyrolitic washers expand and finally occupy the total space. This is a potential development problem but that material combination has worked satisfactorily to date. This type of expansion joint filler is also currently used with success in the Algol III SCOUT first stage nozzle aft of the insert.

MATERIAL PROPERTIES

First, second and third stage Trident nozzles are similar relative to material usage and component configuration. The current designs are shown in Figures 65, 66, and 67. Component material selection is summarized briefly in Table XXIX. The following table, Table XXX, tabulates the temperature dependent properties for each of these materials.

APPLICATION OF TRIDENT DESIGN RESULTS TO SCOUT MOTOR NOZZLE COMPONENTS

Introduction. - Design improvements for SCOUT motor nozzles are desired primarily to increase their structural reliability. New high energy propellants offer significant performance benefits, but impose a more severe thermal environment on the nozzles. In preparation for possible future use of these types of propellants in SCOUT motors, material usage in the Trident (C-4) program was surveyed to determine if they could be used in SCOUT nozzles. Factors which affect specific recommendations include evaluations of the accuracy of existing nozzle stress analyses and the severity of the expected environment. These factors are discussed in the following sections.

A number of improvements to the state-of-the-art for solid propellant motor nozzles have been accomplished in the Trident program. Some of these improvements may offer future potential benefits for SCOUT motor nozzles. These improvements include the following:

Use of graphite/graphite reimpregnated fibrous composite materials with minimum specific gravity of 1.5. These materials are compatible with XLDB high energy propellants and greatly reduce erosion in and around the throat areas. Current development efforts are investigating use of 3-D weave materials and materials with specific gravities as high as 2.0.

Use of carbon microballoons in low density silica and carbon phenolic laminates. These materials have good insulating, fair erosion and good strength characteristics in addition to their contribution toward minimizing nozzle weight.

Additional material characterization information has been generated and much test data obtained for the performance and erosion characteristics of nozzle materials exposed to high pressure, high temperature, XLDB motor environments.

Techniques have been developed to obtain very accurate nozzle finite element analyses. Analytical consideration is given to the time at which bond lines become thermally degraded and to the resulting strain redistributions of adjacent components. As a result of good analytical predictions, verified by strain gages during motor firings, some of the structural components are designed to permit yielding during bench or proof tests. Critical failure design criteria is based on strain rather than on stress. This results in a reliable and lightweight design. Some empirical data and adjustments must still be made to account for the plastic behavior of orthotropic materials under high stress and elevated temperature conditions. Analytical improvements in this area are currently under development.

Accuracy of Typical Solid Propellant Motor Nozzle Analyses. - In thermoelastic analyses accuracy of calculated stresses and deflections are dependent upon the methodology used and the material properties which are input data. The basic theory, equations and procedure for performing finite element computer analyses are described in Reference (12). The problems of anisotropic behavior and plastic characteristics of typical tape wrapped laminate materials at high stress levels and elevated temperatures are now amenable to solution as a result of current advances in methodology. Most aerospace corporations have finite element computer methods which provide acceptably accurate solutions. The variance study performed during the Altair IIIA analysis and included in this report concluded that a composite (1 sigma) mean correction factor due to stress analysis methods and assumptions was 1.02, or an error of 2% (percent). Similar errors due to anistropic effects were about 6% (percent). However, large errors in computed deflections and stresses may result from lack of accurate characterization of material properties. This implies that unless correct thermal and mechanical properties are available for the thermoelastic

analyses, significant errors can result. Current estimates of errors in resulting stresses and strains due to this data are as high as about 50% when currently available material properties are used. Little improvements in obtaining more reliable composite material properties at elevated temperatures have been reported in the literature in recent years. A nozzle failure investigation in 1971 during the Poseidon program concluded that there was a significant dependence of material thermal expansion data on the heating rate used to attain test temperatures. Nozzle materials in solid rocket motor firings are subjected to temperatures exceeding 2475°K (4000°F) in approximately 10 seconds. This results in a heating rate approaching 16900°K/min (30000°F/min). The highest heating rate under laboratory conditions for thermal expansion measurements is about 1367°K/min (2000°F/min). Attempts at extrapolating property values to higher heating rate levels have been unsatisfactory. To resolve the Poseidon material property problem, graphite phenolic and asbestos phenolic specimens were partially characterized at heating rates of 812°K/min (1000°F/min). The resulting values for secant coefficient of thermal expansion are listed in Table XXXI. Figures 68 and 69 show the differences in coefficients of thermal expansion values due to heating rates for graphite phenolic in the warp and fill directions. Differences were less pronounced for the asbestos phenolic specimens. Similar effects were published in 1972 in reference 10 for silica and cellulose phenolics tested at 300°K/min, and for a reimpregnated graphitized composite tested at heating rates to 1667°K/min (2000°F/min). Characterization results at high heating rates are applicable to nozzle analyses when the critical stress condition occurs shortly after ignition. When critical conditions exist late in firing, and for cooldown analyses, standard characterization methods appear adequate.

XLDB Environment. - Comparisons of the Antares IIA (CY1-75, a modified double-base propellant) motor environment with a similar motor using XLDB propellants show higher gas temperatures and possibly longer

burn times for that propellant. Longer burn times result in greater erosion and char depths but are not significant with regard to maximum stress conditions if critical time occurs shortly after ignition. In the SCOUT system only the Castor nozzle insert is stress critical toward the end of burn time (35 seconds after ignition). Due to the good insulating qualities of plastic laminates, convective heat transfer coefficients have little effect on calculated temperature distributions and maximum gradients in these low conductivity materials. This is due to the almost instantaneous surface response to the adjacent boundary layer temperature. Higher gas temperatures will tend to cause higher gradients and higher thermoelastic stresses. The following table compares gas temperatures of two XLDB propellants with the Antares IIB (CYI-75) propellant:

Propellant	CYI-75	VLZ(XLDB)	VOY(XLDB)
Gas Temperature, ^{o}K	3820	4068	4023
(^{o}F)	(6416)	(6863)	(6782)

From these comparisons the XLDB propellant appears to be slightly more severe for SCOUT nozzles components. The oxidation index appears to be the significant parameter.

Recommendations for Future Improvements. - A number of possible areas for improvement in SCOUT nozzle components are listed in Table XXXII. Some of the component materials used in the Trident (C-4) program provide the necessary qualifications for improvement. Each nozzle area was reviewed and the following recommendations are made to improve SCOUT nozzle reliability in a more severe thermal environment than currently exists. Although present SCOUT nozzle reliabilities are acceptably high, some design improvements are desirable, particularly in the exit cone areas aft of the insert. The possibility of longer burn times may also require some redesign.

(a) Inserts. - The requirement for maximum performance in the Trident system demands minimum throat erosion. This requirement

becomes secondary to structural reliability in the SCOUT system. Trident nozzle inserts use pyrolitic graphite washers in the throat. This "throat pack" is supported at the front and rear by Carbitex 700 graphitized composite rings. This material has good erosion resistance and has demonstrated good reliability since there have been no support ring failures in the Trident demonstration firings. The area just forward of the throat in Trident nozzles experiences a less severe environment than exists at the throat. This may be considered roughly equivalent to the throat area in SCOUT nozzles due to the lower pressures used in SCOUT motors. If low erosion rates become desirable for SCOUT nozzles, then Carbitex 700 would provide a suitable insert material for the Algol III or Antares II motors. However, since total thrust is affected only slightly by moderate throat erosion, the better insulating qualities of graphite phenolic laminates offer more advantages to the SCOUT nozzles at the present time, particularly in the small insert of the Antares motor. For projected future consideration, another promising developmental material appears to be reimpregnated 3-D weave graphite composites with a specific gravity of about 2.0 and more readily available carbon-carbon materials having densities approaching 2.0. These materials may provide increased performance without loss of structural integrity. Current costs of the 3-D material appear excessive, but a successful development program could result in wide usage and reduced cost.

(b) Retainer Rings. - RPD-150 molded asbestos phenolic materials have experienced considerable processing difficulties in the Antares IIA and IIB designs. A current change to graphite phenolic is under consideration for the Antares nozzle. For the more erosion resistant materials, such as Carbitex 700, detailed thermal analyses are required to determine the increased heating effects in the attach ring area due to higher thermal conductivity. Approximate one-dimensional analyses indicate feasibility for the Antares nozzle, but excessive temperatures in the attach ring for the smaller Altair IIIA design.

(c) Exit Cone Liner. - The third stage Trident nozzle is most similar in size and firing times to SCOUT motors. The Algol III has a firing time about 15 seconds longer than the Trident first and second stage motors, but has the lowest average pressure and gas temperature of the SCOUT motors. Therefore, the third stage Trident nozzle exit cone design is roughly comparable to all SCOUT nozzles. The Trident third stage exit cone design that was selected for development firings is shown below.

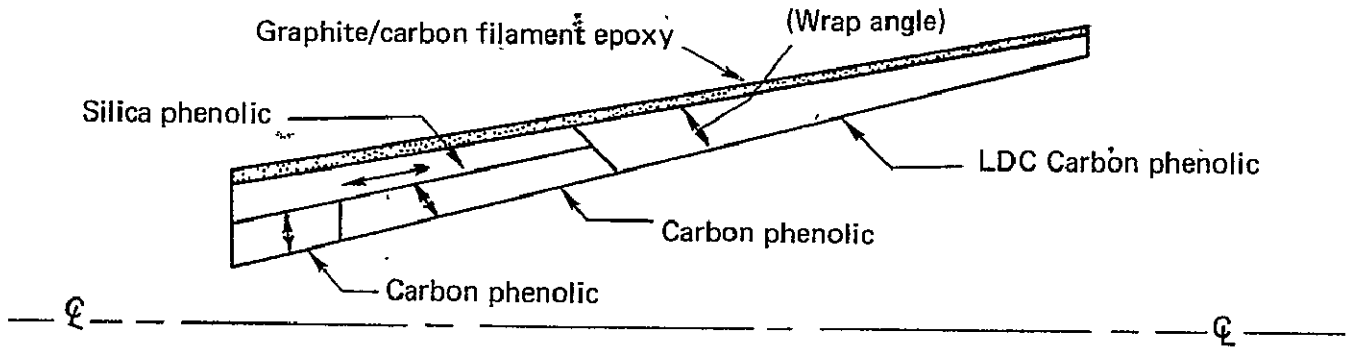

TRIDENT 3RD STAGE EXIT CONE PRELIMINARY DESIGN

During the development phase cracks and delaminations were found in and between the silica phenolic insulator and carbon phenolic liner prior to firing. The extent of these process related deficiencies were sufficient to result in exit cone failure during firing. This problem was attributed to high residual stresses after processing. A test item, shown below, was instrumented with strain gages and strains were measured at individual steps in the fabrication and processing cycle.

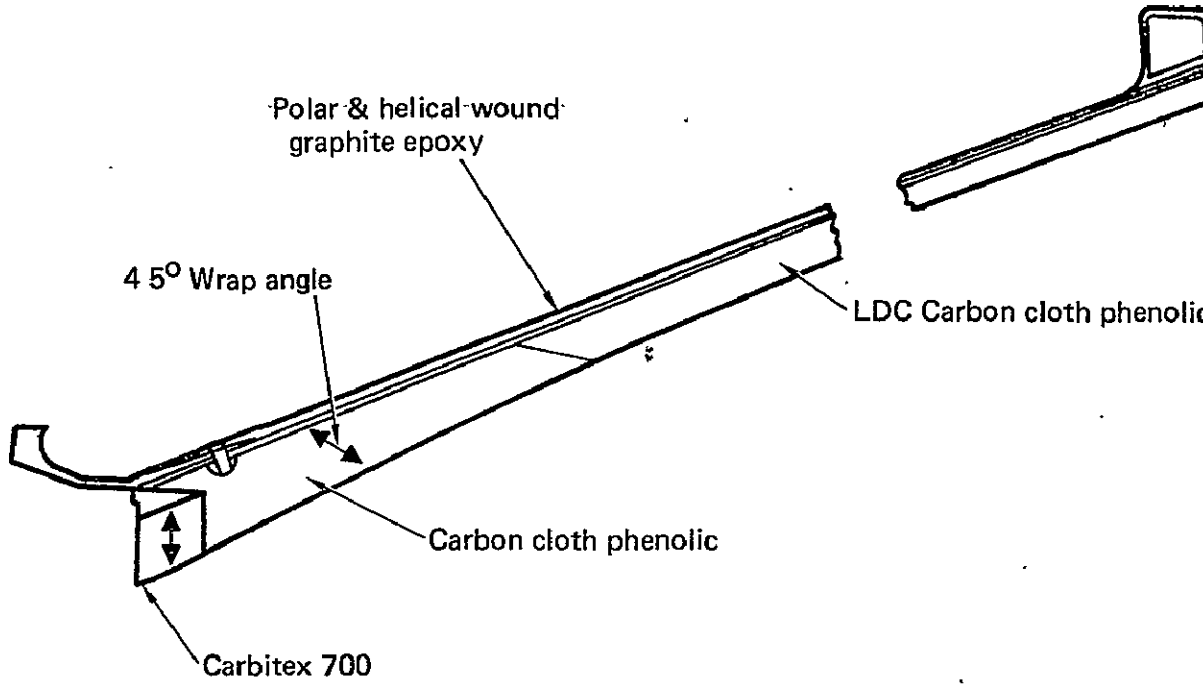

TRIDENT 3RD STAGE EXIT CONE INTERIM CONFIGURATION

The use of graphite/carbon filament epoxy and the low density carbon phenolic liner are related to weight optimization. A similar, but slightly heavier, configuration suitable for SCOUT nozzles would be as follows:

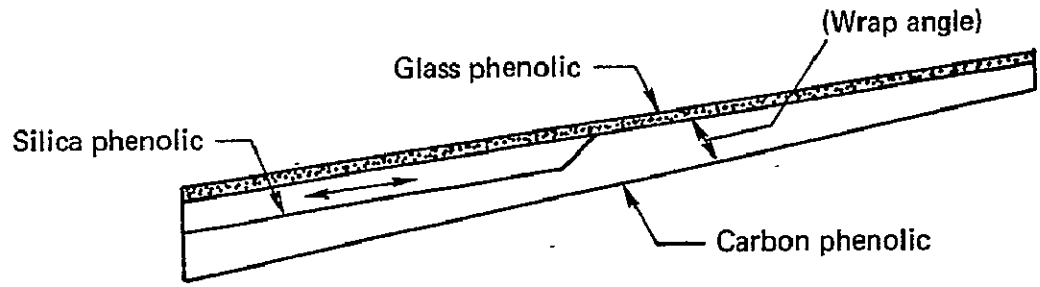

SUGGESTED SCOUT EXIT CONE

Two design features which are used in Antares and Altair SCOUT motor exit cones that are considered undesirable are the use of asbestos phenolic insulating layers and wrap angles parallel to centerline. If the asbestos and interface boundary remain below about 533°K (500°F) throughout firing, then the material is adequate. If, however, significant heating occurs this material contains water of hydration, outgasses excessively above 533°K and there is a possibility of interlaminar pressure buildup with resulting delamination and spalling in that area. In order to eliminate this problem, holes must be drilled through the liner to provide pressure relief. This is also a significant cost item which might be eliminated by substitution of silica phenolic for asbestos phenolic. This logic was the basis for insulator selection in the Trident exit cones.

If exit cone liner wrap angles are parallel to centerline they provide gas passages for combustion products during charring; however, this construction also results in undesirable weak shear planes where an entire ring of material may be lost in the critical region just aft of the insert. This occurrence is possible due to a combination of delamination due to thermal and interlaminar shear effects and gas pressure or physical loading due to thermal expansion of the insert at the forward edge of the ring. The displaced ring of liner material may then be ejected with resulting exposure of the outer insulating material to thermal damage. A different wrap angle, similar to that shown in the above sketch, may be used which permits suitable gas passages and also provides better retention if delamination occurs. The ring would be mechanically locked in place and would require extensive across-laminate shear failure of adjacent liner material before ejection were possible.

A low density carbon phenolic laminate, MXC-113 in the exit cone, has been used successfully on two Altair IIIA demonstration firings using high energy propellants. This material is planned for use on future production motors.

Where minimum weight of the exit cone is necessary as in the Trident program, graphite/carbon filament construction is optimum. Since the weight penalty is small for SCOUT non-load-carrying exit cones, a glass cloth laminate provides adequate strength at reduced cost.

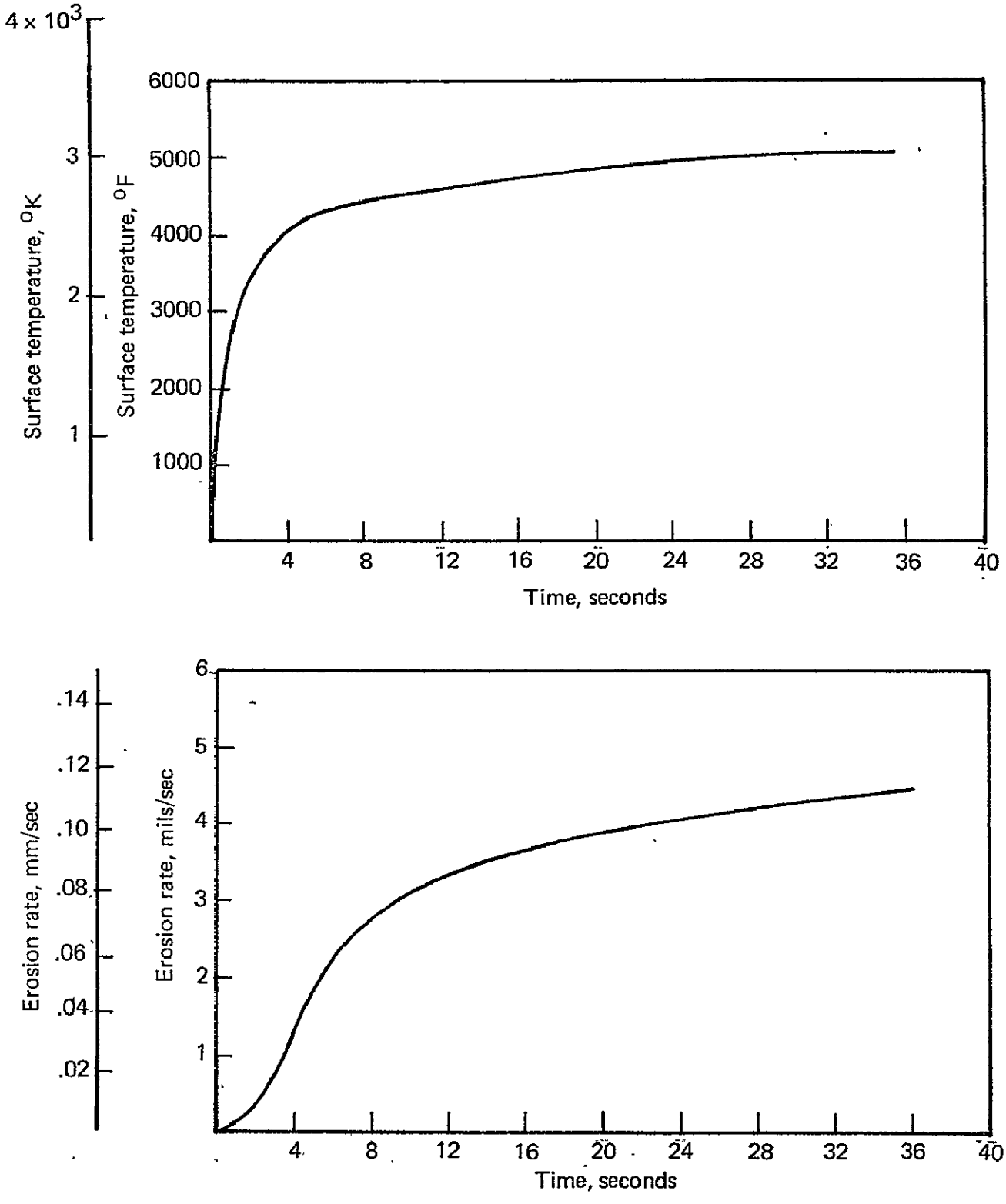

FIGURE 62. – TYPICAL THROAT TEMPERATURE AND EROSION FOR TRIDENT NOZZLES

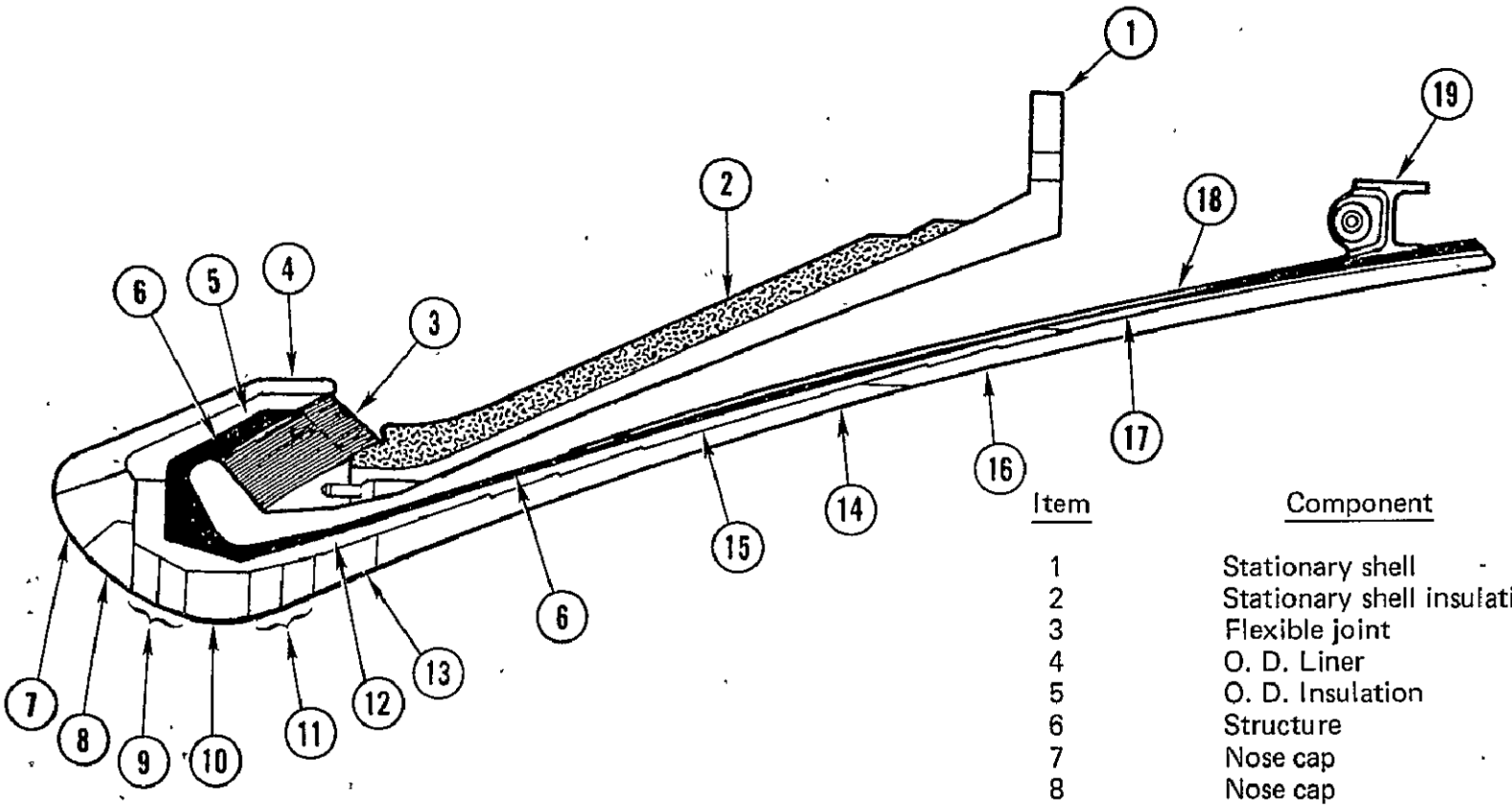

Item	Component
1	Stationary shell
2	Stationary shell insulation
3	Flexible joint
4	O. D. Liner
5	O. D. Insulation
6	Structure
7	Nose cap
8	Nose cap
9	Throat inlet rings
10	Throat pack
11	Fwd exit rings
12	Throat support
13	Aft exit ring
14	Fwd exit liner
15	Fwd exit insulation
16	Aft exit liner
17	Aft exit insulation
18	External insulation
19	Compliance ring

FIGURE 63. – NOZZLE COMPONENTS

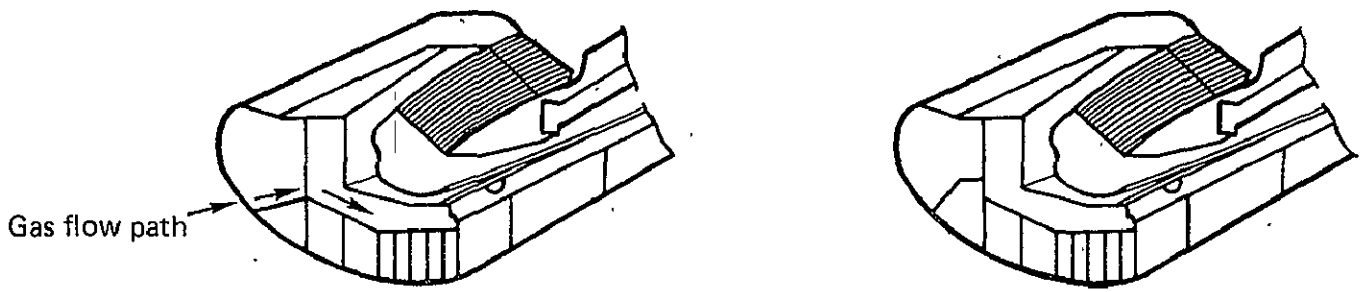

Motor SDE-05

Nose cap redesign

FIGURE 64. – DEVELOPMENT NOSE CAP REDESIGN

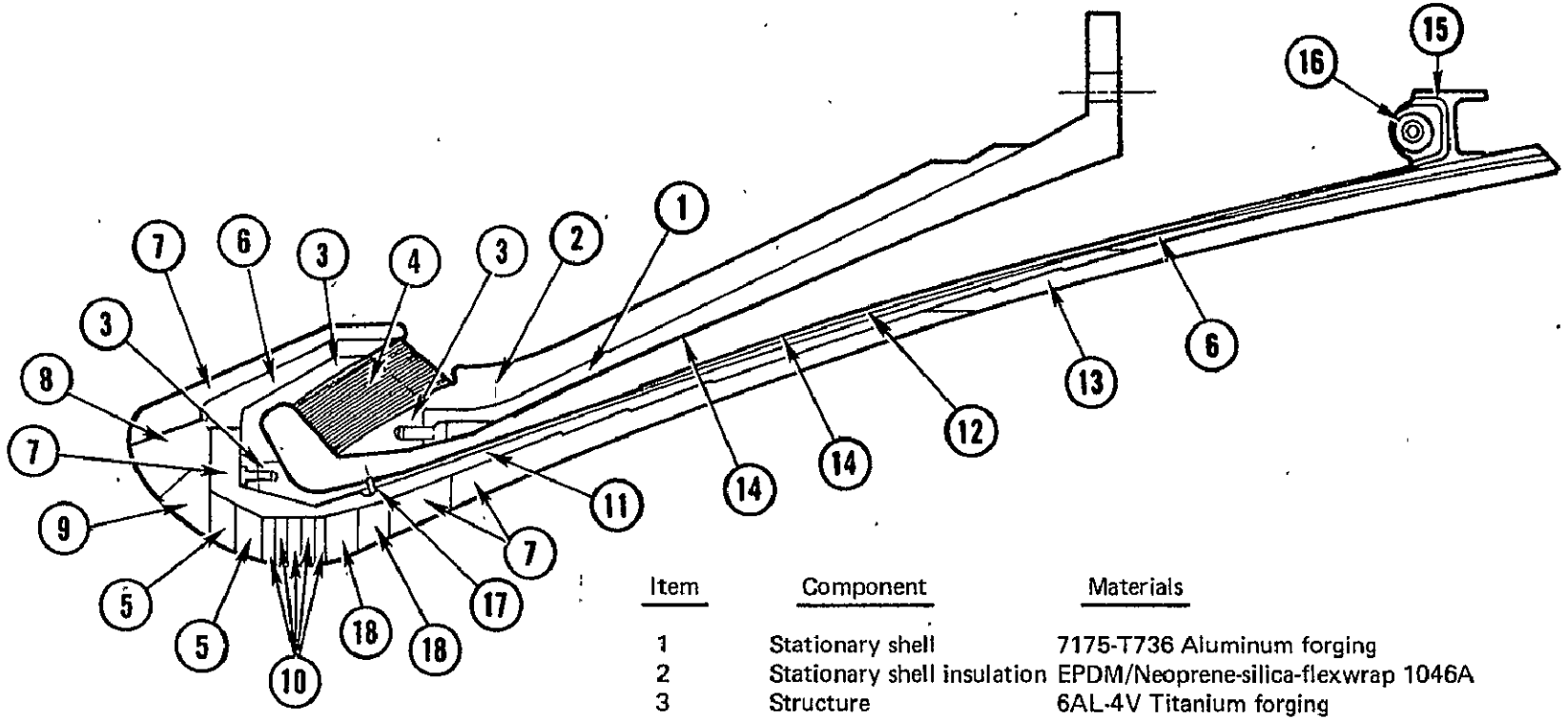

Item	Component	Materials
1	Stationary shell	7175-T736 Aluminum forging
2	Stationary shell insulation	EPDM/Neoprene-silica-flexwrap 1046A
3	Structure	6AL-4V Titanium forging
4	Flex-joint	Flex-joint, glass carbon cloth reinforcement, natural rubber elastomer
5	Throat inlet rings	Carbitex 700
6	O. D. Insulation	L. D. silica cloth phenolic
7	O. D. Liner	Carbon cloth phenolic
8	Nose cap	Graphite cloth phenolic
9	Nose cap	Carbitex 700
10	Throat pack	Edge grain pyrolytic graphite washers
11	Fwd exit insulation	Silica cloth phenolic
12	External insulation	Carbon epoxy
13	Aft exit liner	L. D. carbon cloth phenolic
14	Insulation	Cork phenolic
15	Compliance ring	316 Cres ring forging
16	Actuator attachment	316 Cres plate
17	Retention pin	6061-T6 Aluminum
18	Fwd exit rings	Carbitex 700

FIGURE 65. — FIRST STAGE FLIGHT DESIGN NOZZLE

Item	Component	Materials
2.	Flex-joint	Flex joints, glass carbon cloth reinforcement—natural rubber elastomer
3.	Structure	6Al-4V Titanium
4.	O. D. Insulation	L. D. Silica cloth phenolic tape-wrapped parallel to centerline
5.	O. D. Liner	Carbon cloth phenolic, tape-wrapped 15 deg to centerline

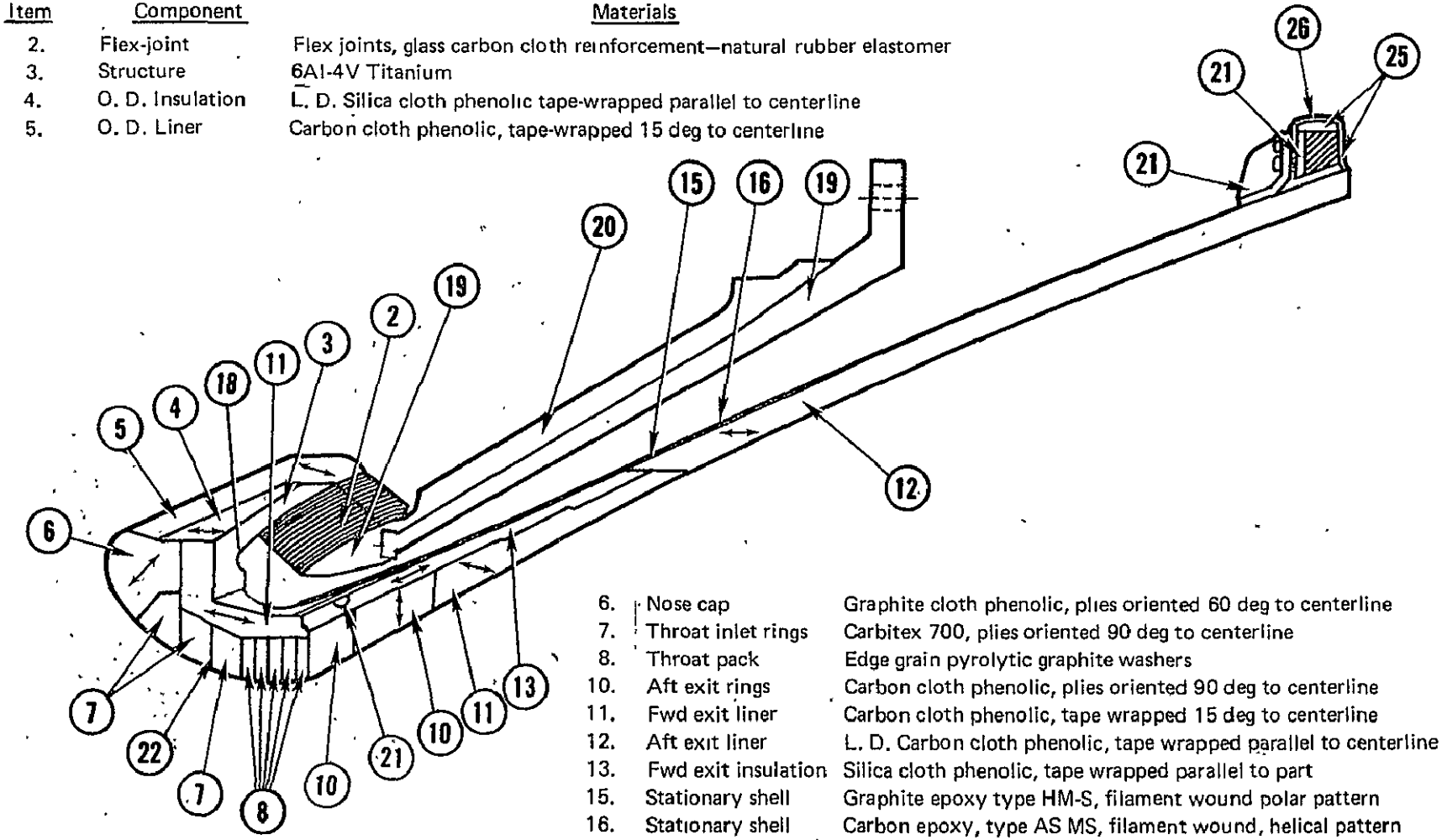

6.	Nose cap	Graphite cloth phenolic, plies oriented 60 deg to centerline
7.	Throat inlet rings	Carbitex 700, plies oriented 90 deg to centerline
8.	Throat pack	Edge grain pyrolytic graphite washers
10.	Aft exit rings	Carbon cloth phenolic, plies oriented 90 deg to centerline
11.	Fwd exit liner	Carbon cloth phenolic, tape wrapped 15 deg to centerline
12.	Aft exit liner	L. D. Carbon cloth phenolic, tape wrapped parallel to centerline
13.	Fwd exit insulation	Silica cloth phenolic, tape wrapped parallel to part
15.	Stationary shell	Graphite epoxy type HM-S, filament wound polar pattern
16.	Stationary shell	Carbon epoxy, type AS MS, filament wound, helical pattern
18.	Structure	6AL-4V Titanium
19.	Structure	7175-T736 Aluminum
20.	Stationary shell insulation	EPDM/Neoprene-silica, layed-up and cured in place
21.	Compliance ring	7075-T73 Aluminum
22.	Spacer	Teflon sheet stock, 7 places
25.	Compliance ring	Graphite epoxy, type HM-S
26.	Compliance ring	Phenolic microballoon-epoxy resin room

FIGURE 66. — SECOND STAGE FLIGHT DESIGN NOZZLE

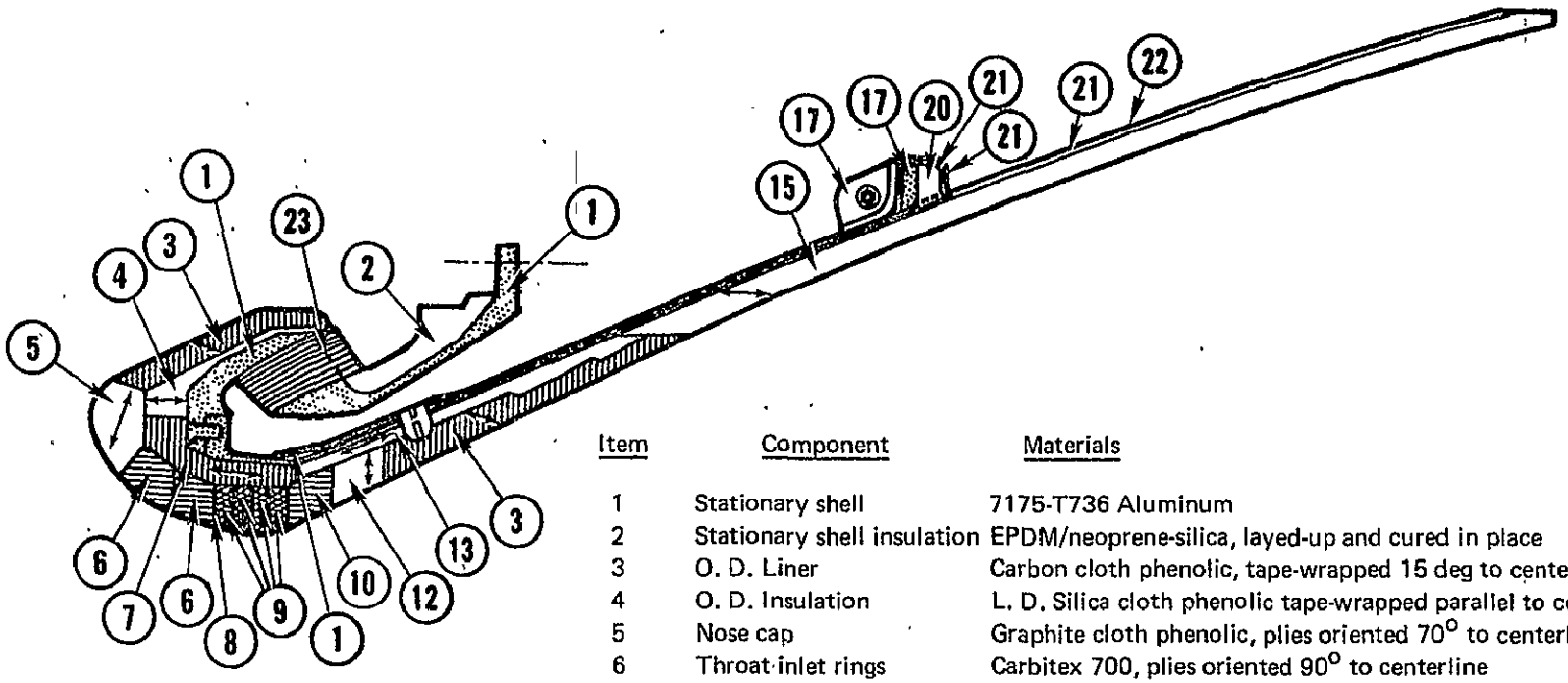

Item	Component	Materials
1	Stationary shell	7175-T736 Aluminum
2	Stationary shell insulation	EPDM/neoprene-silica, layed-up and cured in place
3	O. D. Liner	Carbon cloth phenolic, tape-wrapped 15 deg to centerline
4	O. D. Insulation	L. D. Silica cloth phenolic tape-wrapped parallel to centerline
5	Nose cap	Graphite cloth phenolic, plies oriented 70° to centerline
6	Throat inlet rings	Carbitex 700, plies oriented 90° to centerline
7	Throat support	Carbon cloth phenolic, tape-wrapped 5 deg to centerline
8	Spacer	Teflon sheet stock, 5 places
9	Throat pack	Edge grain pyrolytic graphite washers
10	Fwd exit ring	Carbitex 700
12	Fwd exit ring	Carbon cloth phenolic—plies oriented 90° to centerline
13	Fwd exit insulation	Silica cloth phenolic—plies oriented parallel to part
15	Aft exit liner	LDC Carbon cloth phenolic tape wrapped parallel to centerline
17	Compliance ring	7075-T73 Aluminum
20	Compliance ring	Phenolic microballoon—epoxy resin foam
21	Structure	Graphite epoxy type HM-S filament wound
22	Structure	Carbon epoxy type AS MS filament wound, helical pattern
23	Flex-joint	Flex joints, glass cloth reinforcement—natural rubber elastomer

FIGURE 67. — THIRD STAGE FLIGHT DESIGN NOZZLE

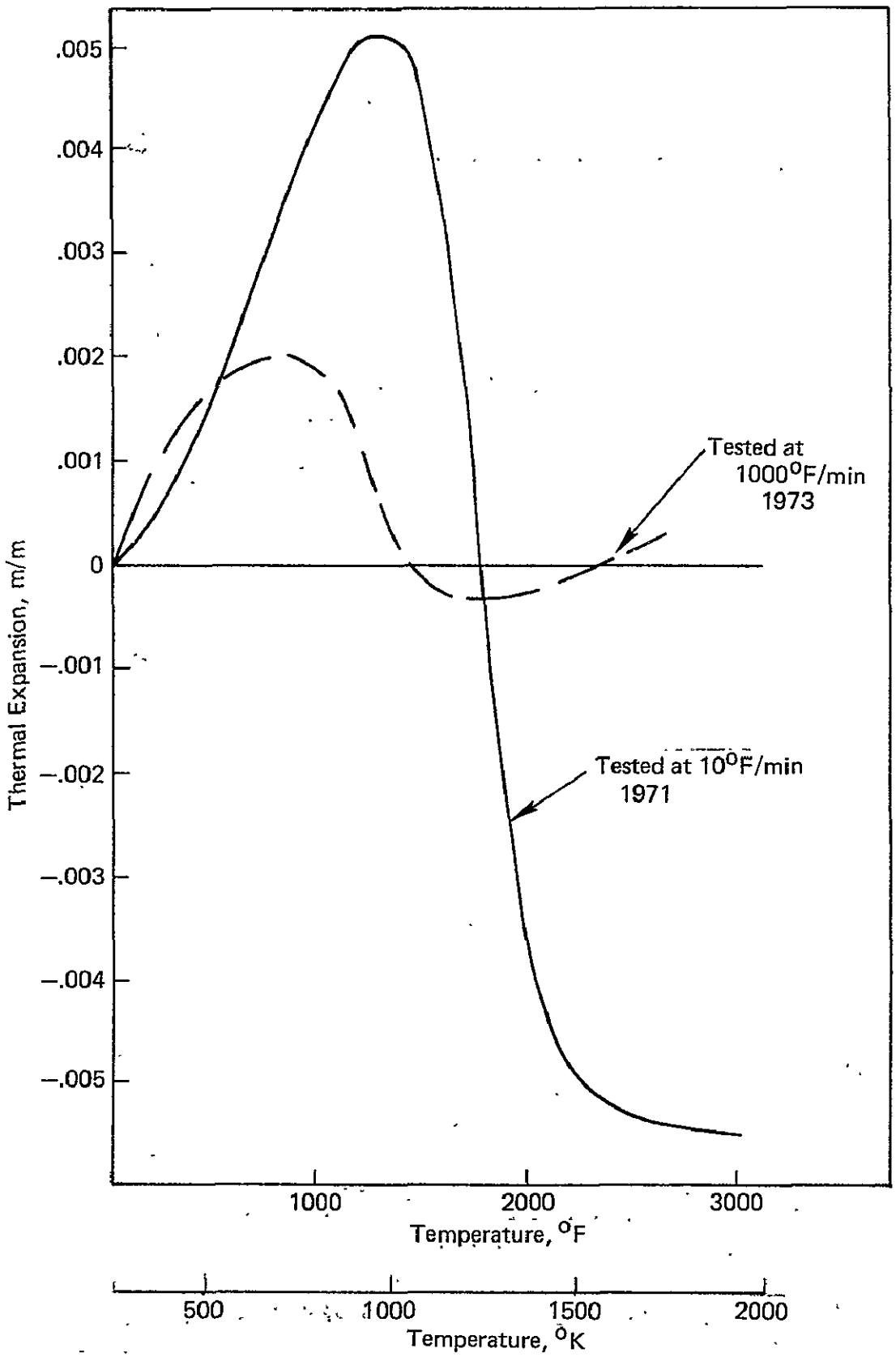

FIGURE 68. — THERMAL EXPANSION OF GRAPHITE PHENOLIC, FILL DIRECTION

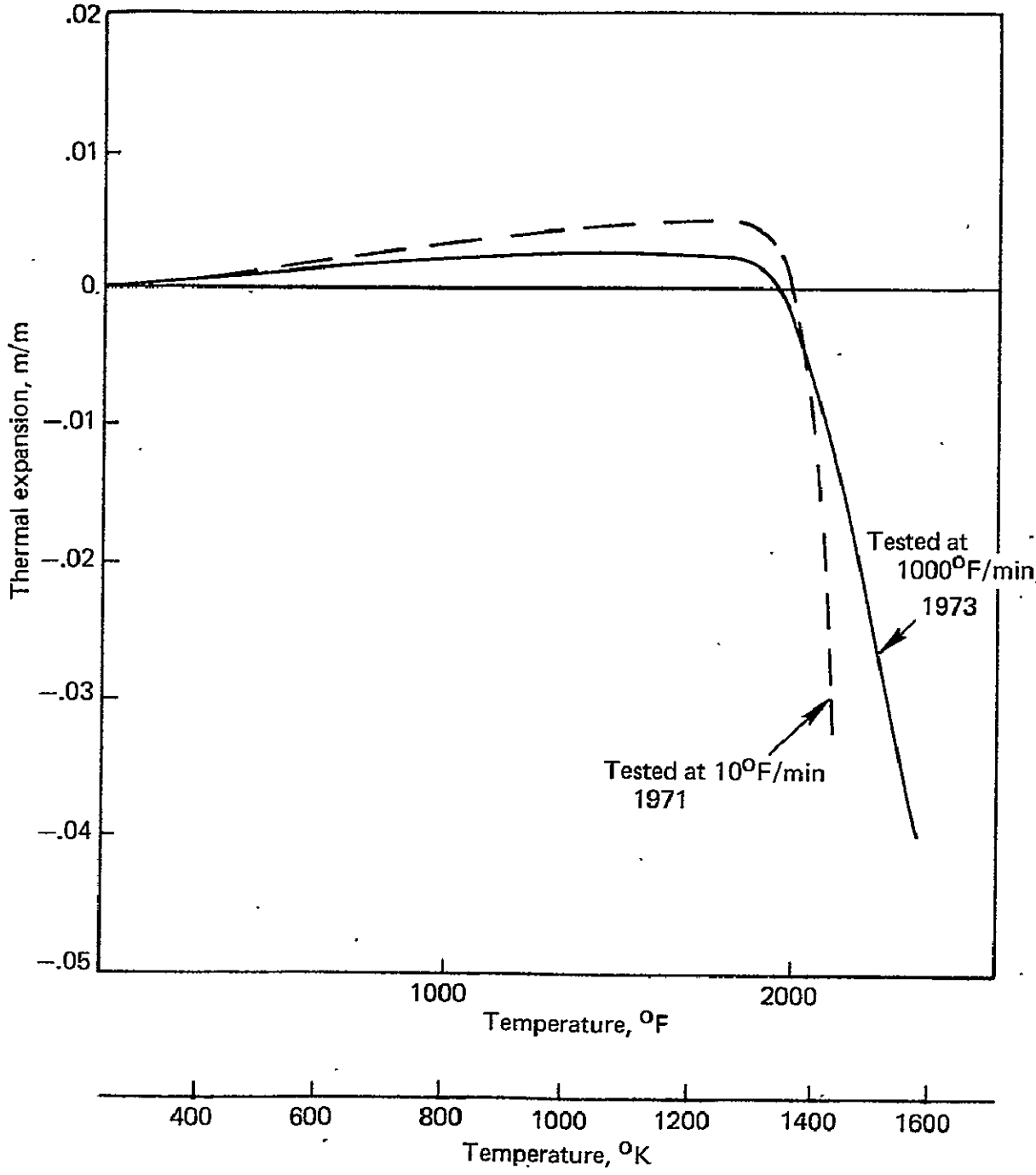

FIGURE 69. — THERMAL EXPANSION OF GRAPHITE PHENOLIC, WARP DIRECTION

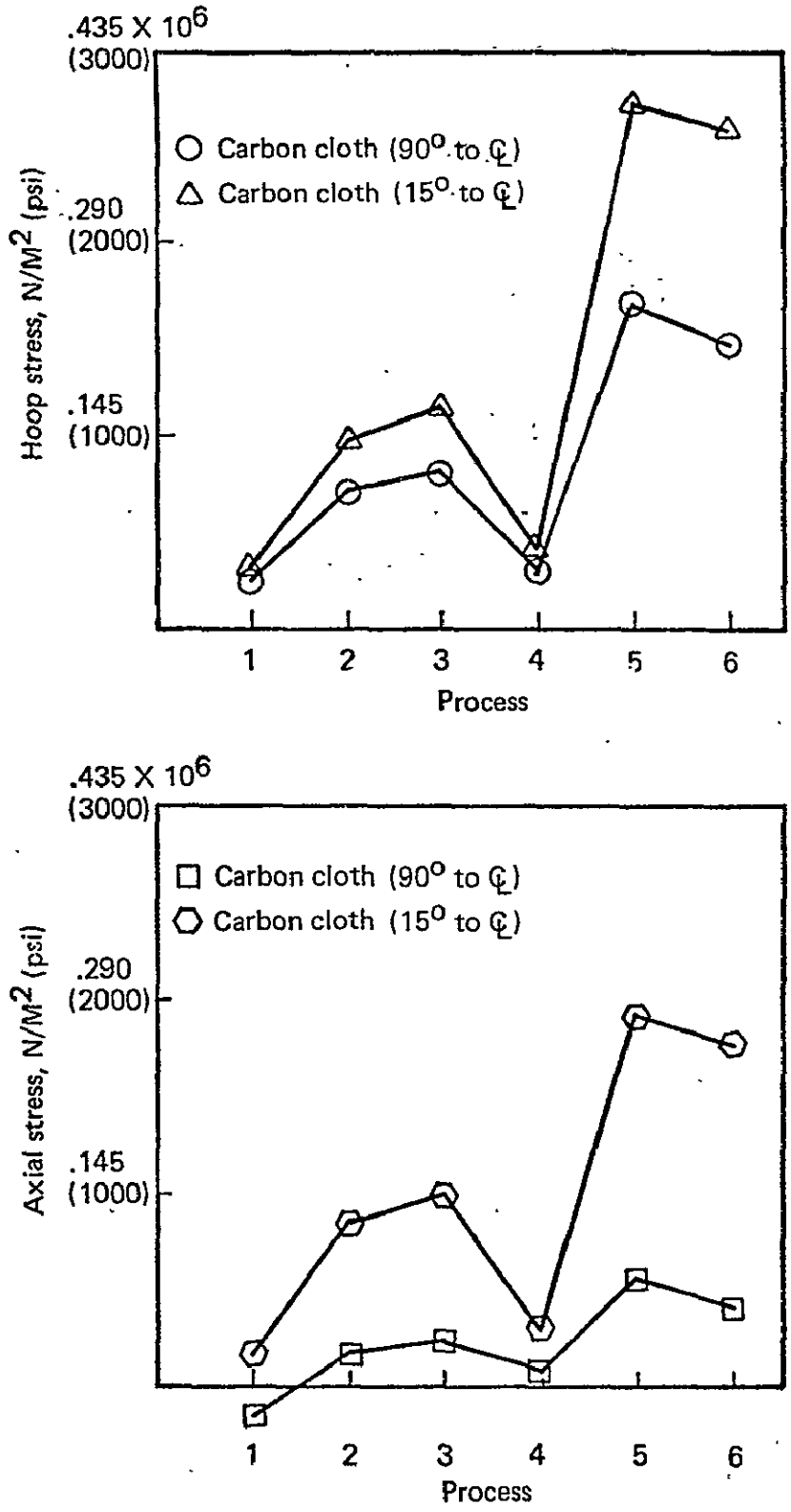

Process

1. After primer coat
2. After polar windings
3. After 16-hour delay
4. After helical winding
5. After oven cure
6. After exit cone was trimmed

FIGURE 70. – MEASURED RESIDUAL STRESSES IN TRIDENT DEVELOPMENT EXIT CONE

TABLE XXVII. — 30 IN. MOTOR MATERIALS EVALUATION MATRIX

Hercules Part no.	Sta. shell insul.	Submerged Nose			Throat		
		OD insul.	OD liner	Nose cap	Throat support	Inlet*	Throat
D00539	CA2230	CA2230	MX4926	MXG175	FM5055	C-700	Pfizer/UCC
D00413	1045-A6	4S4107	*FM5055	MXC313P	FM5072	C-700/PTE	Union Carbide
D00248	EPDM Neo/ Silica 7180-053	FM5504 LDC	ACXC86C	MXC313P	CA8203	Pyrocarb 901/ PTE	Pfizer
D00435	7180-053	CA2230	MX4926	ACX-G79	4C1008	Fibergraph GG (L-400)	Super-Temp
D00224	7180-053	MXS175	FM5055	FM5014	MX4926	C700/C700	Pfizer
D00253	7180-053	FM5020	FM5055	FM5014 WG	Pyrocarb 502	HRX 5125/ C706AE	Super-Temp
D00509	7180-053	CA2230	MX4926	HRX2125	4C1246	Pryocarb 901	Pfizer
D00239-01	EPDM 1045-A6	MX2600	MX4926	MXG175	MX4926	PTD282	Union Carbide
D00256	MX4926/ MX2600	N/A	MX4926	MXG1033F	4C1686	Fibergraph G/G C706AE	Pfizer
D00239-03	1040A	FM5504 LDC	4C1246	4G3008	FM5055	HRX-5120	Union Carbide
D00239-04	7180-053	4S4107	FM5072	HRX2125	MX4926	6709AE	Union Carbide
D00239-05	7180-053	4S4107	ACX-C86	FM5782 MC	ACX-C86	Pycobond 410	Union Carbide
D00250	1040A	MXS175	CA8203	MSG175	Pyrocarb 502	PTD282	Pfizer/UCC
D00431	7180-053	CA6315	4C1246	MXC-313P	4C1246	KGG/HRX 5120	Super-Temp
D00246	7180-053	CA2230	MX4926	FM5724	Karbon 408E	Pycobond 407/ 3D Composite	Union Carbide
D00239-02	DC93-104	MXS-175	4C 1008	FM 5014	MX4933	C-700	Union Carbide
D00497	7180-053	MXS175	LDC MX4926	ACX-G79	MX4933	901 Pyrocarb/ G-90	Super-Temp

*XXX/XXX = Fwd/aft inlet ring
Single entry indicates both inlet rings or that the design includes only one inlet ring.

TABLE XXVII. — 30 IN. MOTOR MATERIALS EVALUATION MATRIX — Concluded

Hercules part no.	Exit cone						
	Fwd exit ring	Aft exit ring	Upper exit liner	Lower exit liner	Upper exit insul.	Lower exit insul.	Structure
D00539	C700	FM5055	FM5055	FM5055 LDC	CA2230	None	ASMS
D00413	C700	FM5072	MX4926	MX4926 LDC	4S4107	MX2600 LD	ASMS
D00248	C700	ACXC86	4C1246	MX4926 LDC	CA2230	FM5504 LDC	Thornel 400
D00435	C700	FM5055	MX4926	MX4926 LDC	MXS-175	N/A	ASMS
D00224	C700	FM5055	FM5055	FM5055 LDC	FM5020	None	ASMS
D00253	Part of throat support	Vendor fab	Pyrocarb 409-45		MXS175	Graphite felt	N/A
D00509	C700	MX4926	MX4926	N/A	MXS175	N/A	ASMS
D00239-01	C700	MX4926	4C1008	4C2110	4S4107	None	HMS-MS/ASMS
D00256	C700	4C1008	4C1008	4C2110	4S4107	None	ASMS
D00239-03	C700	4C1008	4C1246	FM5055 LDC — AMB	4S4107	None	ASMS
D00239-04	C700	4C1246	CA8203	CA8214	MXS175	None	HMS-MS/ASMS
D00239-05	C700	4C1686	ACXC86	CA8214	MXS175	None	Thornel 400
D00250	Part of throat support	Vendor fab	Pyrocarb 409-45		FM5020	Graphite felt	N/A
D00431	C700	FM5055	MX4926	MX4926 LDC	MXS175	N/A	ASMS
D00246	Part of throat support	TCC fab	Karbon 408E		MXS175	Graphite felt	N/A
D00239-02	C700	CA8203	ACX-C86	4C2110	4S4107	None	Thornel50/ ASMS
D00497	C700	MX4926	MX4926	N/A	MXS175	N/A	ASMS

TABLE XXVIII. – MARGINS OF SAFETY IN 3RD STAGE TRIDENT NOZZLE

Component	Material	M. S.	Remarks
Nose Cap	FM5014 MXG 175	2.8	Hoop stress
O. D. Liner	FM5055 MXG 4926	0.12	Hoop, Plastic Anal.
O. D. Insulator	FM5072LD MX 4926 LDC	0.95	Shear stress
Exit Cone Adapter	7175-T736 Al.	0.64	
Fwd End Ring	7175-T736 Al.	0.12	Hoop, Plastic Anal.
Throat Supt. Insul.	FM5055 MX 4926	0.50	Hoop @ 37.5 sec
Insert Approach (fwd)	Carbitex 700	0.2	
Insert Approach (aft)	Carbitex 700	0.4	
Throat Ring	PG	0.05	
Fwd Exit Ring	Carbitex 700	0.09	Hoop @ 37.5 sec
Aft Exit Ring	FM5055 MX 4926	1.5	Shear stress
Split Ring	Steel HY-E 1334 C	1.82	Shear stress
Exit Cone Shell	Graphite Epoxy Fil. HY-E 1334 C	1.9	Hoop stress
Compliance Ring	Graphite Epoxy Fil.	0.37	Shear stress

TABLE XXIX. – NOZZLE MATERIAL TRADEOFF SUMMARY

Component	Candidate materials	Basis for selection	Selected material
Nose cap	Graphite cloth phenolic Carbon cloth phenolic	Erosion resistance High temp stability	Graphite cloth phenolic, FM5014
Throat approach	Graphite cloth phenolic Carbitex 700 Billet graphite	Erosion resistance Structural properties	Carbitex 700, plies normal to ℄
Throat insert	Billet graphite Carbitex 700 Pyrolytic graphite	Minimum erosion Structural properties	Pyrolytic graphite washers
Exit cone liner	Carbon cloth phenolic	Erosion resistance	Carbon cloth phenolic at expansion ratios < 7.0 to 1, FM5055
Liner	Silica cloth phenolic	Weight/thermal diffusivity	LD carbon cloth phenolic at expansion ratios > 7.0 to 1, FM 5055 LD
Insulation	Silica cloth phenolic LD silica cloth phenolic Asbestos cloth phenolic	Weight/thermal diffusivity Structural properties	Silica cloth phenolic at low expansion ratios, FM 5020 LD silica cloth phenolic at high expansion ratios, CA 2230
Exit cone structure and compliance ring	Aluminum Titanium Graphite epoxy Beryllium	Stiffness/weight Ease of fabrication	Graphite/epoxy filament

TABLE XXX. – MATERIAL PROPERTIES

Material: Graphite cloth phenolic (FM 5014)

Directions
1 = With ply
3 = Across ply

		300°K R. T.	533°K (500°F)	811°K (1000°F)	1366°K (2000°F)	1922°K (3000°F)	2478°K (4000°F)
Thermal conductivity, cal/m-hr-°K x 10^3 (B-in/ft^2-hr-°F)	With lam	3.3 (26.40)	3.5 (28.2)				
	Against lam	1.1 (8.76)	1.5 (12.12)				
Coeff of thermal exp M/M-°K x 10^{-6} (in/in-°F x 10^{-6})	With lam	9.2 (5.14)	6.1 (3.41)	3.7 (2.06)	1.2 (0.69)	0.0	
	Against lam	4.6 (2.57)	7.4 (4.12)	34. (18.8)	– 1.9 (–1.04)	– 10.0 (–5.6)	
Modulus of elasticity N/m^2 x 10^9 (psi x 10^6)	With lam	10.13 (1.47)	8.27 (1.20)	6.89 (1.0)	3.79 (0.55)	3.72 (0.54)	
	Against lam	5.17 (0.75)	2.14 (0.31)	0.689 (0.10)	0.34 (0.05)		
Tensile ult strength N/m^2 x 10^6 (psi x 10^3)	With lam	164.0 (23.8)	135.7 (19.7)	99.91 (14.5)	62.01 (9.0)	57.19 (8.3)	
	Against lam	6.96 (1.01)	4.48 (0.65)	2.07 (0.30)	1.38 (0.20)	1.86 (0.27)	
Interlaminar shear strength N/m^2 x 10^6 (psi x 10^3)	With lam	43.75 (6.35)	22.74 (3.30)	13.09 (1.9)	14.47 (2.1)	25.49 (3.7)	
	Against lam	44.79 (6.50)	27.22 (3.95)	11.71 (1.7)	9.99 (1.45)	8.96 (1.3)	
Specific heat cal/gm-°K		0.25	0.37	0.45	0.48	0.50	
Poisson's ratio, μ_{13}		0.24	0.25	0.16	0.04	0.064	
μ_{31}		0.23	0.10	0.04	0.03	0.53	

TABLE XXX. – MATERIALS PROPERTIES – Continued

Material: Carbitex 700

		300°K R.T.	533°K (500° F)	811°K (1000° F)	1366°K (2000° F)	1922°K (3000° F)	2478°K (4000° F)
Thermal conductivity, cal/m-hr-°K X 10^3 (B-in./ft^2-hr-° F)	With lam.	82 (663)	62 (498)	50 (399.6)	35 (279.6)	25 (201.6)	18 (146.4)
	Against lam.	32 (258)	25 (202.8)	21 (169.2)	16 (126)	12 (98.4)	10 (76.8)
Coeff. of thermal exp. M/M ° K x 10^{-6} (in./in-° F x 10^{-6}	With lam.	.94 (0.52)		1.37 (0.76)	2.16 (1.2)	2.7 (1.5)	3.06 (1.7)
	Against lam.	2.53 (1.4)		3.25 (1.8)	3.95 (2.2)	4.5 (2.5)	5.0 (2.8)
Modulus of elasticity N/m2 x 109 (psi x 106)	With lam.	11.02 (1.60)	10.2 (1.48)	9.58 (1.39)	8.27 (1.2)	6.06 (0.88)	5.31 (0.77)
	Against lam.	2.62 (0.38)		2.96 (0.43)		3.31 (0.48)	
Tensile ult. strength N/m2 x 106 (psi x 103)	With lam.	37.48 (5.44)	39.96 (5.80)	41.62 (6.04)	44.03 (6.39)	45.89 (6.66)	47.54 (6.90)
	Against lam.	1.52 (0.22)		3.10 (0.45)		3.93 (0.57)	
Interlaminar shear strength N/m2 x 106 (psi x 103)		9.65 (1.4)					
		37.21 (5.4)					
Specific heat cal/gm-°K		0.169	0.306	0.377	0.449	0.480	0.491
Poisson's ratio, $\mu 13$		0.30		0.39	0.38	.09	.26
$\mu 31$		0.033		0.066		.083	

Directions

1 = With ply
3 = Across ply

TABLE XXX. – MATERIAL PROPERTIES – Continued

Material: Pyrolytic graphite

Directions
R = Radial
Z = Axial
θ = Hoop

		300°K R.T.	533°K (500°F)	811°K (1000°F)	1366°K (2000° F)	1922°K (3000°F)	2478°K (4000°F)
Thermal conductivity cal/m-hr-°K x 10^3 (B-in./ft^2-hr-°F)	With lam.	333 (2688)	257 (2076)	169 (1368)	96 (780)	82 (660)	76 (612)
	Against lam.	1.92 (15.6)	1.48 (12.0)	1.13 (9.12)	.93 (7.56)	.81 (6.52)	1.21 (9.84)
Coeff of thermal exp. M/M-°K x 10^{-6} (in./in.-°F x 10^{-6}	With lam.	0.0	−.2 −(0.1)	.68 (0.38)	1.06 (0.59)	1.24 (0.69)	1.48 (0.82)
	Against lam.	0.0	19.8 (11.0)	23.2 (12.9)	24.8 (13.8)	23.4 (13.0)	23.4 (13.0)
Modulus of elasticity N/m^2 x 10^9 (psi x 10^6)	With lam.	31.0 (4.5)		28.39 (4.12)	25.84 (3.75)	23.22 (3.37)	20.67 (3.0)
	Against lam.	10.34 (1.5)		9.44 (1.37)	8.54 (1.24)	7.85 (1.14)	6.89 (1.0)
Tensile ult. strength N/m^2 10^6 (psi x 10^3	With lam.	5.51 (0.8)					
	Against lam.	145. (22.0)		145. (22.0)	145. (22.0)	186. (27.0)	248. (36.0)
Interlaminar shear strength N/m^2 x 10^6 (psi x 10^3		47.54 (6.9)		47.54 (6.9)	53.74 (7.8)	68.90 (10.0)	93.02 (13.5)
Specific heat cal/gm-°K		0.25		0.375	0.475	0.54	0.575
Poisson's ratio μ RZ		0.9					
$\mu \theta$Z		0.9					
μ R θ		−0.16					

TABLE XXX. – MATERIAL PROPERTIES–Continued

Material: Carbon cloth phenolic (FM 5055 or MX 4926)

Directions
1 = With ply
3 = Across ply

		300°K R. T.	533°K (500°F)	811°K (1000°F)	1366°K (2000°F)	1922°K (3000°F)	2478°K (4000°F)
Thermal conductivity, cal/m-hr-°K x 10^3 (B-in/ft^2-hr-°F)	With lam	1.1 (9.0)	1.5 (12.36)	1.2 (9.6)	2.5 (20.04)		3.7 (29.28)
	Against lam	.4 (3.0)	.5 (3.96)	.6 (4.8)	1.1 (9.0)		1.7 (13.44)
Coeff of thermal exp. M/M-°K x 10^{-6} (in/in-°F x 10^{-6})	With lam	0	4.1 (2.3)	7.4 (4.1)	4.5 (2.5)		
	Against lam	0	10.8 (6.0)	127 (70.7)	19.1 (10.6)		
Modulus of elasticity N/m^2 x 10^9 (psi x 10^6)	With lam	21.15 (3.07)			11.71 (1.70)	10.47 (1.52)	1.72 (0.25)
	Against lam	18.81 (2.73)					
Tensile ult strength N/m^2 x 10^6 (psi x 10^3)	With lam	140.5 (20.4)			73.03 (10.6)	33.07 (4.8)	51.68 (7.5)
	Against lam	14.95 (2.17)					
Interlaminar shear strength N/m^2 x 10^6 (psi x 10^3)	With lam	97.15 (14.1)			12.2 (1.77)		
	Againt lam	58.57 (8.50)			7.92 (1.15)		7.85 (1.14)
Specific heat cal/gm-°K		0.23	0.38		0.46		0.49
Poisson's ratio, μ_{13}		0.16				0.21	
μ_{31}		0.195					

TABLE XX.X. – MATERIAL PROPERTIES – Continued

Material: LD Carbon cloth phenolic (FM 5055 LDC)

		300°K R. T.	533°K (500°F)	811°K (1000°F)	1366°K (2000°F)	1922°K (3000°F)
Thermal conductivity, cal/m-hr-°K x 10^3 (B-in/ft^2-hr-°F)	With lam	.16 (1.30)				
	Against lam	.37 (3.0)	.49 (3.96)			
Coeff of thermal exp M/M-°K x 10^{-6} (in/in-°F x 10^{-6})	With lam		7.7 (4.3)			
	Against lam					
Modulus of elasticity N/m^2 x 10^9 (psi x 10^6)	With lam	6.5 (0.95)		1.2 (0.175)		0.76 (0.11)
	Against lam					
Tensile ult strength N/m^2 x 10^6 (psi x 10^3)	With lam	36.5 (5.300)		11.5 (1.665)		12.5 (1.815)
	Against lam					
Interlaminar shear strength N/m^2 x 10^6 (psi x 10^3)	With lam	13.09 (1.9)				
	Against lam					
Specific heat cal/gm-°K	char	0.27 0.21	0.33 0.34	0.35		
Poisson's ratio, μ		0.20		0.21		

TABLE XXX . — MATERIAL PROPERTIES — Continued

Material: LD Silica cloth phenolic (CA 2230), Silica cloth phenolic (MX 2600 and FM 5020)

Directions
R = Radial
Z = Axial
θ = Hoop

		300°K R. T.	533°K (500°F)	811°K (1000°F)	1366°K (2000°F)	1922°K (3000°F)	2478°K (4000°F)
Thermal conductivity, cal/m-hr-°K X 10^3 (B-in/ft^2-hr-°F)	With lam	.68 (5.52)		.82 (6.60)	.86 (6.90)	1.08 (8.76)	1.26 (10.2)
	Against lam	.31 (2.52)		.39 (3.12)	1.82 (14.64)	2.33 (18.84)	2.8 (22.56)
Coeff of thermal exp M/M-°K x 10^{-6} (in/in-°F x 10^{-6})	With lam	5.4 (3.0)	7.2 (4.0)	7.7 (4.3)	9.0 (5.0)		3.6 (2.0)
	Against lam	16.2 (9.0)	20.5 (11.4)		21.3 (11.8)		— 1.8 (—1.0)
Modulus of elasticity N/m^2 x 10^9 (psi x 10^6)	With lam	16.19 (2.35)	12.06 (1.75)	7.58 (1.10)	1.72 (0.25)	0.17 (0.025)	
	Against lam	8.61 (1.25)	3.45 (0.50)	1.72 (0.25)	2.07 (0.30)		
Tensile ult strength N/m^2 x 10^6 (psi x 10^3)	With lam	165.4 (24.0)	68.9 (10.0)	34.45 (5.0)	1.38 (2.0)	1.38 (0.2)	0.07 (0.011)
	Against lam	7.58 (1.1)		2.41 (0.35)	1.17 (0.17)	1.86 (0.27)	
Shear strength N/m^2 x 10^6 (psi x 10^3)	With lam						
	Against lam	189.5 (27.5)	77.86 (11.3)	51.68 (7.5)	13.78 (2.0)	0.69 (0.1)	
Specific heat cal/gm-°K		0.20	0.30	0.35	0.40	0.49	0.49
Poisson's ratio, μ_{RZ}		0.22					
$\mu_{\theta Z}$		0.37					
$\mu_{R\theta}$		0.33					

TABLE XXX. – MATERIAL PROPERTIES – Continued

Material: EPDM-CF flex wrap 1040A

		300°F R. T.	533°F (500°F)
Thermal conductivity, cal/m-hr-°K x 10^3 (B-in/ft^2-hr-°F)	With lam	.193 (1.56)	.267 (2.16)
	Against lam		
Coeff of thermal exp M/M-°K x 10^{-6} (in/in-°F x 10^{-6})	With lam		
	Against lam		
Modulus of elasticity N/m^2 x 10^6 (psi x 10^3)	With lam	0.172(1) (25.0)	
	Against lam		
Tensile ult strength N/m^2 x 10^6 (psi)	With lam	3.514(2) (510)	
	Against lam		
Interlaminar shear strength N/m^2 x 10^6 (psi x 10^3)			
Specific heat cal/gm-°K		0.403	0.552
Poisson's ratio, μ			

(1) Modulus at 1.7% strain
(2) At 2% strain, Maximum strain ≅ 11%

TABLE XXX. — MATERIAL PROPERTIES — Concluded

Material: Graphite epoxy filament wrap composite

		300°K R. T.	395°K (250°F)	533°K (500°F)
Thermal conductivity, cal/m-hr-°K x 10^3 (B-in/ft^2-hr-°F)	With lam			
	Against lam	.49 (3.96)	.56 (4.56)	.7 (5.64)
Coeff of thermal exp M/M-°K x 10^{-6} (in/in-°F x 10^{-6})	With lam		−.36 (−0.2)	
	Against lam		27 (15.0)	
Modulus of elasticity N/m^2 x 10^9 (psi x 10^6)	With lam	136.1 (19.75)		
	Against lam	9.65 (1.4)		
Tensile ult strength N/m^2 x 10^6 (psi x 10^3)	With lam	20.67 (3.0)		
	Against lam	110.24 (16.0)		
Interlaminar shear strength N/m^2 x 10^6 (psi x 10^3)		12.82 (1.86)		
Specific heat cal/gm-°K		(0.23)	(0.294)	(0.395)
Poisson's ratio, μ_{RZ}		0.30		
$\mu_{\theta Z}$		0.03		
$\mu_{R\theta}$		0.30		

Direction
R = Radial
Z = Axial
θ = Hoop

TABLE XXXI. – SECANT COEFFICIENT OF THERMAL EXPANSION, HEATING RATE = 811°K/MINUTE (1000°F/MINUTE)
$\Delta L/L\ (T - 297^{\circ}K) \times 10^{-6}$ IN/IN –°K

Temperature Range °K	Temperature Range °F	Graphite Phenolic			Asbestos Phenolic		
		Warp	Fill	Across	Warp	Fill	Across
297 – 394	75-250	2.86	3.65	1.43	.19	2.86	.32
297 – 533	75-500	1.90	2.29	2.29	1.31	3.27	2.48
297 – 672	75-750	1.42	1.66	3.96	1.15	3.50	4.33
297 – 811	75-1000	1.15	1.12	7.65	1.20	3.24	4.08
297 – 950	75-1250	.91	.39	11.58	1.04	2.64	9.45
297 – 1089	75-1500	.71	–.07	15.35	.94	1.33	3.22
297 – 1228	75-1750	.54	–.12	.83	–.50	–.38	–7.64
297 – 1366	75-2000	.39	–.07	.58	–7.52	–2.60	–26.00
297 – 1506	75-2250	.26	–.02	2.18	–	5.05	–
297 – 1644	75-2500	.15	.03	3.10	–	–6.88	–
297 – 1783	75-2750	.07	–	–	–	–	–
297 – 1922	75-3000	0	–	–	–	–	–

TABLE XXXII. – SUMMARY OF POSSIBLE AREAS FOR IMPROVEMENT

Motor	Component	Material	Reason
Algol IIIA	FWD Insulator	Silica Phenolic	Possible Excessive Erosion
Castor IIA	Throat Insert Insulation Throat Insert (1) Insert FWD Insulators	Asbestos Phenolic ATJ Glass Phenolic	Possible outgassing Possible cracking Excessive erosion
Antares IIA	Retainer	Asbestos Phenolic	Fabrication problems
Antares IIB	Retainer Exit Cone Insulation Exit Cone FWD Liner Throat Insert	Asbestos Phenolic Asbestos Phenolic Graphite Phenolic Graphite Phenolic	Fabrication problems Outgassing Wrap angle and locally high erosion High erosion rate
Altair IIIA	Throat Insert Exit Cone Insulation	Graphite (G-90) Silica Phenolic	Marginal F. S. with more severe environment (based on C–4 experience) Procurement problem

(1) Insert reliability of the Castor II insert is believed to be high based on existing stress analysis and past performance. However, if this nozzle were to be redesigned to reduce weight, the graphite insert would experience higher tensile stresses and might then be susceptible to cracking.

REFERENCES

1. Thermal Analysis of the Insulated Case, Nozzle and Igniter Assembly, Algol III Program, UTC Report 5500-DR-004, 16 October 1969.
2. Structural Analysis of the Nozzle, Algol III Program, UTC Report 5500-DR-003, Rev. 1, 29 January 1971.
3. Analysis and Data Summary, TX354-3 (Castor II) Nozzle, Thiokol Corporation Report U-74-4510 (1974).
4. Final Report FW-4S Nozzle Insert Design Analysis, UTC Report 2228-FR, 2 September 1966.
5. Thermal and Structural Analysis of a Modified Nozzle for the High Pressure X-259 Motor, H.I. Report X-259/6/3525, March 1973.
6. Final Report on the Manufacture and Static Firing of X-259-E6 Rocket Motor Serial Number XJ04/0001, NASA CR-132557, 1974.
7. FW-4S Nozzle Examination, LTV Report 23.404, May 1969.
8. Final Report, FW-4S Motor Nozzle Throat Insert Redesign, Thermal and Structural Analysis, UTC Report 2268-FR2, Volume VI, Structural Analysis of the Backed-Up Graphitite "G" Configuration, May 1967.
9. FW-4S Motor Design Review, LTV Report 23.360, 26 September 1968.
10. Thermophysical Characterization of Composite Materials Under Transient Heating Conditions, NASA CR-112082.
11. Engineering Statistics, Prentice Hall Inc., 1959.
12. Handbook for the Engineering Structural Analysis of Solid Propellants, CPIA Publication 214, Appendix A, May 1971.
13. Rocket Motor Algol III, UTC Model Specification SEO385, 12 February 1975.
14. Motor, Rocket, Solid Propellant, Model TX354-3, Thiokol, Huntsville Model Specification SP561C, 13 December 1971.
15. Rocket Motor, Solid Propellant, Model 259-B3, Hercules, Magna Model Specification HPC259-08-0-2C, 16 November 1970.
16. Effect of Material Property Variations on the Thermal-Structural Analyses of the X-259-B4 Antares IIB Nozzle, Hercules, Magna, Report X259/6/30-2597, May 1976

APPENDIX A

SUMMARY OF PHASE I STUDY

LTV Report 23.412, Phase I Report
Study of Improved Materials for Use on SCOUT
Solid Rocket Motor Nozzles
6 September 1969

APPENDIX A

SUMMARY OF PHASE I STUDY

LTV Report 23,412, Phase I Report
Study of Improved Materials for Use on SCOUT
Solid Rocket Motor Nozzles
6 September 1969

SUMMARY

This study summarized material usage, performance and nozzle configurations in six Scout motors. It investigated the current status of nozzle component materials development in the industry and selected the best candidate materials for possible future use in Scout nozzles. An extensive review of available test data was made to provide temperature dependent material properties of Scout nozzle components. These properties were then compared with those of promising new materials. A selection criteria was based on use of merit factors for each component. These factors were defined during the study and attempted to relate the design use and failure mechanism of a material to its environment. The resulting merit factors yielded quantitative ratings based solely on material properties. The selected material candidates are listed in Table I. Material usage in current motors is shown in Table II, III, and IV.

Review of Scout Motor Nozzles. - A review of Scout motor reports and documents was made to accumulate pertinent engineering information. Tables V and VI list specification and drawing numbers for the motors. Throat and insulation erosion data are listed in Tables VII and VIII.

Nozzle Configurations. - Nozzles of the six Scout motors are shown in Figures 1 through 6. All of these nozzles except Algol and Castor are submerged designs; all use graphite throats. Table IX lists dimensions, weights and expansion ratios for each nozzle. Propellant characteristics and performance data are summarized in Tables X and XI.

Material Properties. - All of the Scout nozzle materials have not been fully characterized through their expected temperature environment. Some of the data is limited to vendor catalog values. Available physical and mechanical properties are included in this appendix.

Review of Candidate Materials. - Four major classes of materials were investigated: ceramic materials, graphite materials, refractory materials, and ablative materials.

Based upon the most desirable characteristics of each class of materials and the results of tests and comparisons in the literature, the best potential candidates were selected in each group. This approach avoided deletion of one or more classes of materials too early in the screening process. All possible candidates were then compared analytically based upon component requirements which were reflected in the selection criteria.

Preliminary candidate materials for SCOUT nozzle use were identified from five sources:

Review of the literature to determine materials used in operational systems.

Selection of best performing materials from the NOMAD program.

Selection of materials tested during subscale and R&D motor tests.

Best performing materials tested in other low area ratio regions of solid rocket nozzles.

Contacts with vendors, propulsion and government agencies and nozzle manufacturers.

Some material compositions which were evaluated prior to 1964 were eliminated because the materials have been replaced by equivalent or better materials. The materials have been segregated into different groups which exhibited best performance for the particular component in a solid propellant environment.

The resin systems most used by industry are 91-LD, SC-1008 and USP-39. The use of napthalene diol, phenylphenol phenol formaldehyde and X-8 furane offers potential performance increases but requires further evaluation to determine their availability and characterization status and they should be considered only as future candidates. The epoxy novolac resin systems were not recommended as preliminary candidates, even though they performed well in material screening motors, due to inferior performance during NOMAD evaluation tests. These latter tests were more representative of SCOUT motors.

Selection of Candidate Materials. - Several attempts have been reported (References 13 and 14) to define rational, quantitative factors which might provide reliable methods for comparing and selecting nozzle materials. These factors were made up of various combinations of physical and mechanical properties. The use of one combination in preference to another has not usually been explained or justified. An attempt has been made in the present study to relate the design use and failure mechanism of a material to its environment. In the present study nozzle materials have been divided into two basic functional groups:

Those materials whose reliability depends primarily upon strength. (These are usually brittle materials which often fail catastrophically when local stresses exceed strength.)

Those materials whose reliability depends primarily upon their insulative and erosion characteristics. (Molded and tape wrapped composites comprise the greatest number of these materials. Low moduli and large strains under tensile loads generally preclude failure due to thermoelastic stresses for these materials.)

Different criteria have been formulated for each of these two groups for use in selecting candidate nozzle materials. Since one of the basic guidelines followed in this study is that any candidate material should be at least as good as those used in existing SCOUT nozzles, the resulting merit factors have been non-dimensionalized with respect to a typical existing SCOUT nozzle material. For inserts ATJ graphite was used as the norm while silica phenolic was used as the norm for insulative materials. 4130 steel was used as a baseline for metal housings and exit cone shells.

Metal rings and housings are generally designed to maximize their strength to weight characteristics, but the net stresses in the insert and insulators may be significantly affected by the stiffness of the structural support. These metal structures generally receive minimum conducted

heat from the throat area and experience little if any temperature rise during motor firing. For this reason a separate selection criteria was devised for the housings which included strength, stiffness and weight.

Merit Factors

Components fabricated from brittle materials must be carefully designed to assure structural reliability. The selection criteria formulated for this class of material emphasizes this requirement. Each of the other components were considered in a similar manner. Merit factors for each component are listed in Table XII.

TABLE XII - COMPONENT MERIT FACTORS

Component	Merit Factor
Brittle Materials	$\frac{F_{TU}}{E \alpha T} \left\{ \frac{k}{\rho C_p} \right\}^{1/3}$
Ablative Inserts	$1/\dot{x}$
Forward Insulators	$1/(\dot{x} + \dot{d})$
Backface Insulators	$\rho C_p / k$
Exit Cone Insulators	$(k \rho / C_p)^{1/2}$
Structural Housings	$F_{TU} E / \rho$
Exit Cone Structures	F_{TU} / ρ

In Table XII, the following terms are used:

F_{TU} = Tensile Ultimate Strength

E = Tensile Modulus of Elasticity

α = Coefficient of Thermal Expansion

T = Temperature Change

k = Thermal Conductivity

ρ = Density

C_p = Specific Heat

$\dot{x}$ = Erosion Rate

$\dot{d}$ = Char Rate

Comparison of Materials

All of the preliminary materials for each component were evaluated by their respective merit factors, normalized and listed preferentially. The ratings of each component are shown in Tables XIII through XX.

TABLE XIII - NORMALIZED MERIT FACTORS FOR BRITTLE MATERIALS

$$\text{Merit Factor} = \frac{F_{TU}}{E\ \alpha\ T} \left\{ \frac{k}{\rho\ C_p} \right\}^{.33}$$

Material	Normalized Merit Factor	
	With Grain	Against Grain
PG	3.62	0.037
8882	1.32	.82
Graphitite G	1.14	.98
ATJS	1.14	1.37
9326	1.06	.94
HS-82	1.01	.99
ATJ (Norm.)	1.00	0.81
AXF-5Q	.67	
AXF-9Q	.59	
Wire Wound W	.32	N/A
W	.27	
Ta-Hf-C	.071	
Nb C	.046	0.051
Zr C	.045	
Hf C	.027	
Ta C	.022	N/A

Selected Candidate Materials

After initial screening, a number of preliminary candidate materials for each nozzle component were evaluated. The major problem in comparing these materials has been the lack of uniformity of test environments between the different test and evaluation programs. For this reason the number of ablative materials selected for further tests, analyses and evaluation during Phase II is larger than desired, but is deemed necessary to determine the optimum material for each application. Candidate materials were selected based upon:

Their preferential merit factor ratings.

Unique desirable characteristics such as zero erosion rate.

Demonstrated reliability in operational systems including SCOUT, Poseidon and Minuteman.

The materials selected for further characterization and analysis during Phase II are summarized in Table XXI.

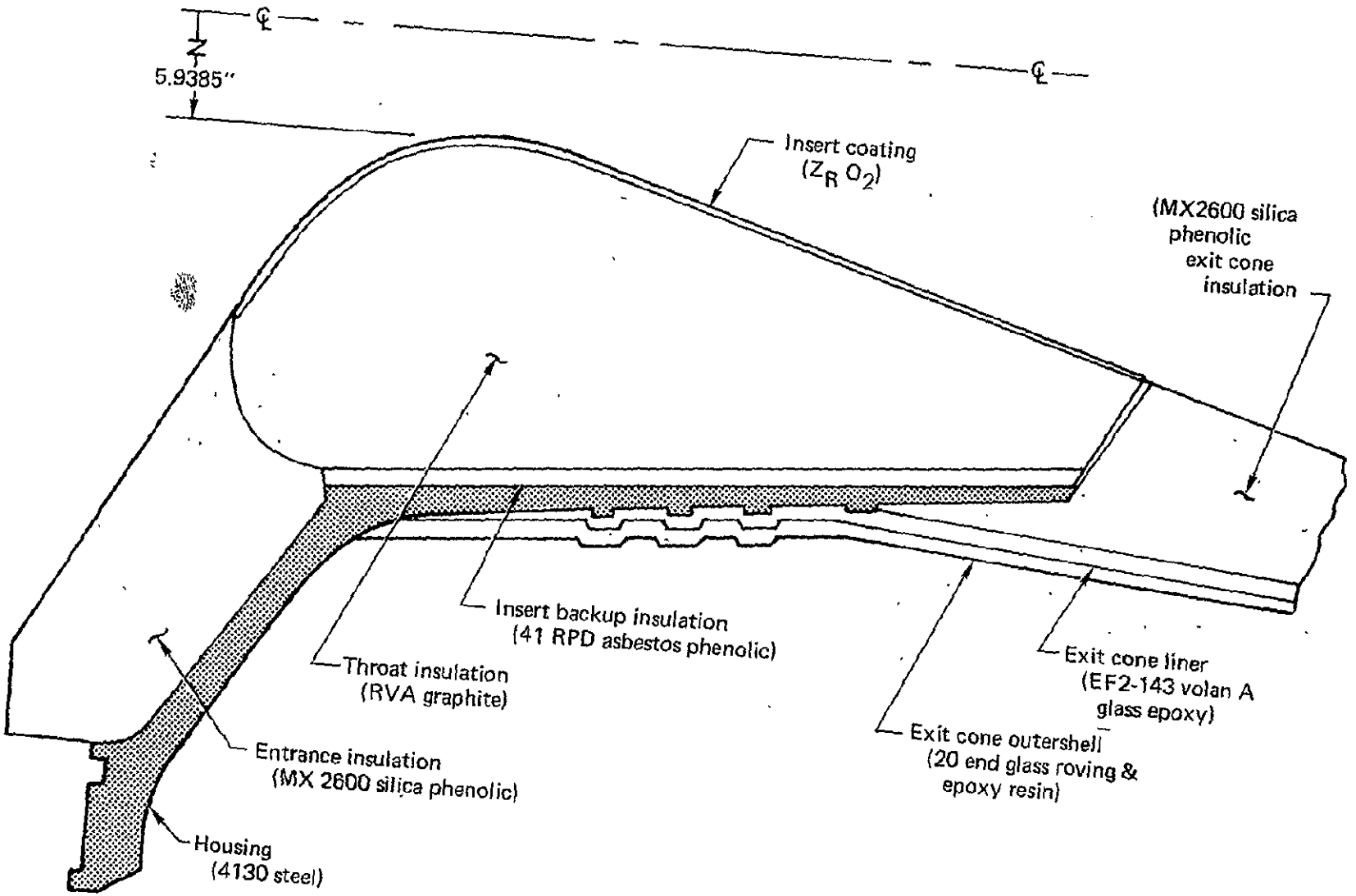

FIGURE 1. — ALGOL IIB

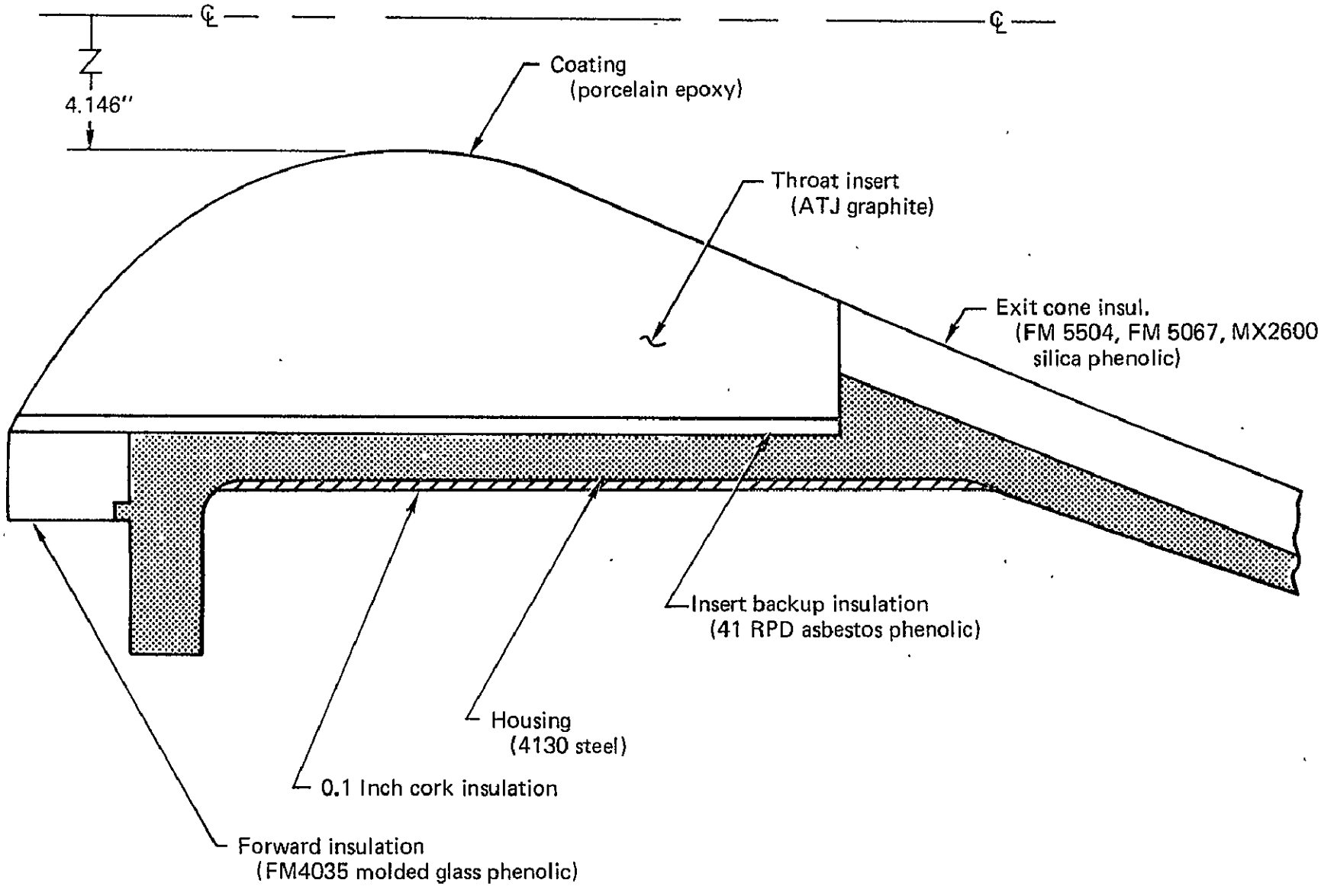

FIGURE 2. — CASTOR IIA

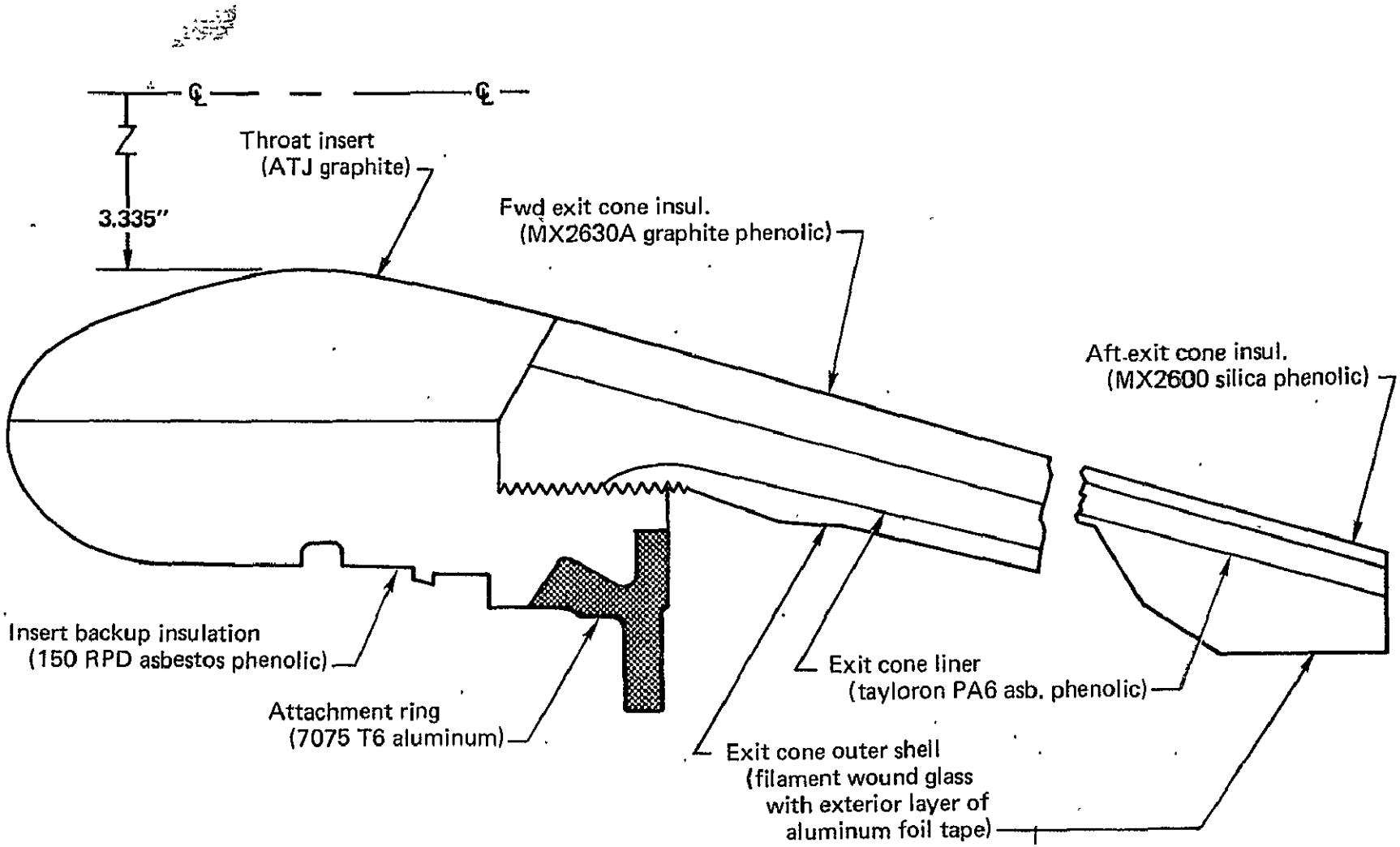

FIGURE 3. – ANTARES IIA, X-259 – B3

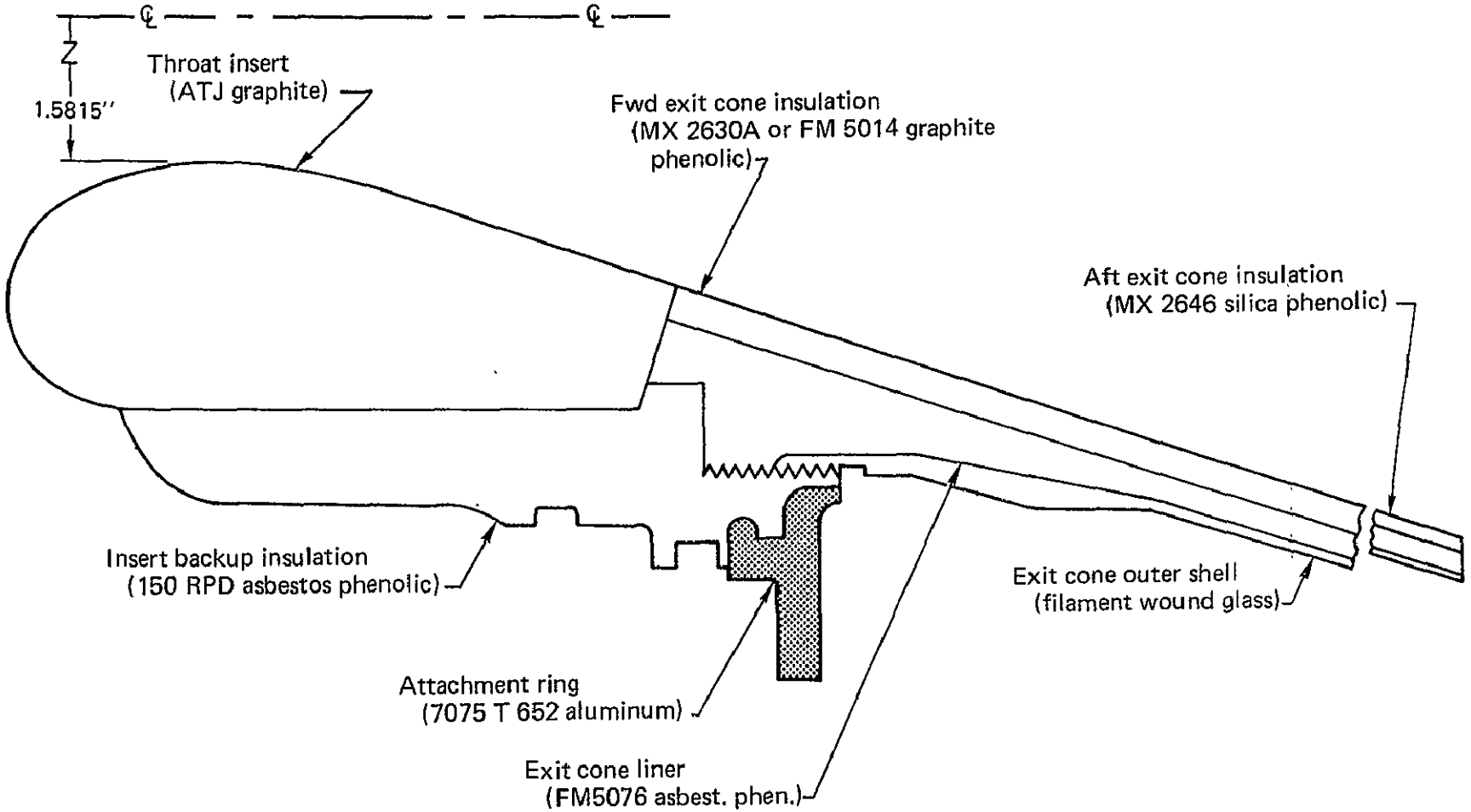

FIGURE 4. – ALTAIR IIA, X-258

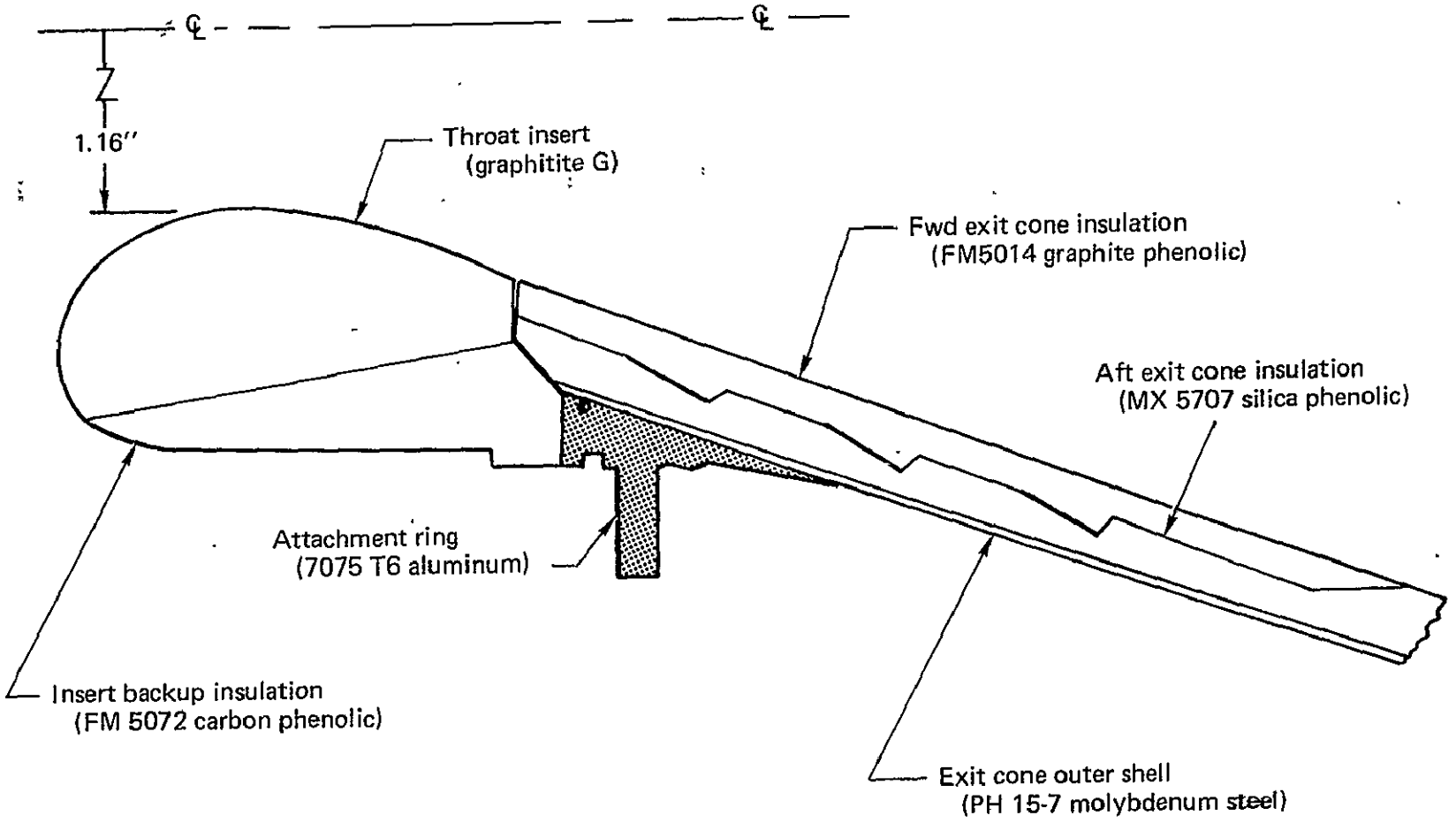

FIGURE 5. – ALTAIR IIIA, FW4S

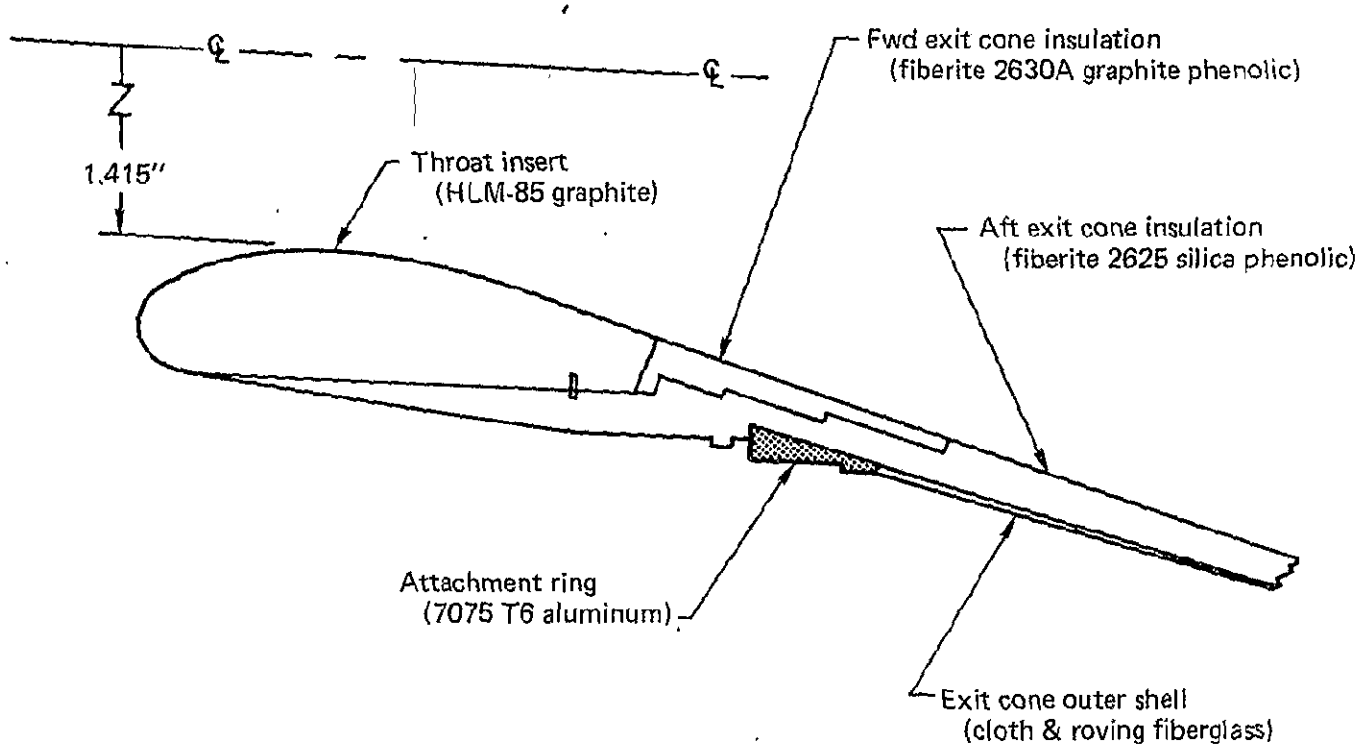

FIGURE 6. – ALCYONE IA, BE3-A9

TABLE I. – SELECTED CANDIDATE MATERIALS

Component	Material	Type
Insert	FM-5014 Carbitex 700 Pyrolarex 400 HD RPG-17300 PG Discs	Graphite Phenolic Graphite Fiber Carbonized Fiber Carbonized Fiber Graphite
Forward Insulator	FM-5272 MXCE-280	Kraft Paper Carbon Phenolic
Backface Insulator	Tayleron PA6 FM-5272	Asbestos Phenolic Kraft Paper
Exit Cone Insulators ($A/A^* \geqslant 4.0$)	FM-5272 FM-5525	Kraft Paper Asbestos Phenolic
Exit Cone Insulators ($A/A^* \leqslant 5.0$)	FM-5072 LD MXCE-280	Carbon Phenolic Carbon Phenolic
Structural Housings	B/Al (300) Maraging Steel 4340 Steel 4130 Steel	Metal Composite Steel Steel Steel
Exit Cone Structure	S-Glass Filament	Composite

TABLE II. – COMPARISON OF MATERIAL USAGE IN SCOUT NOZZLES

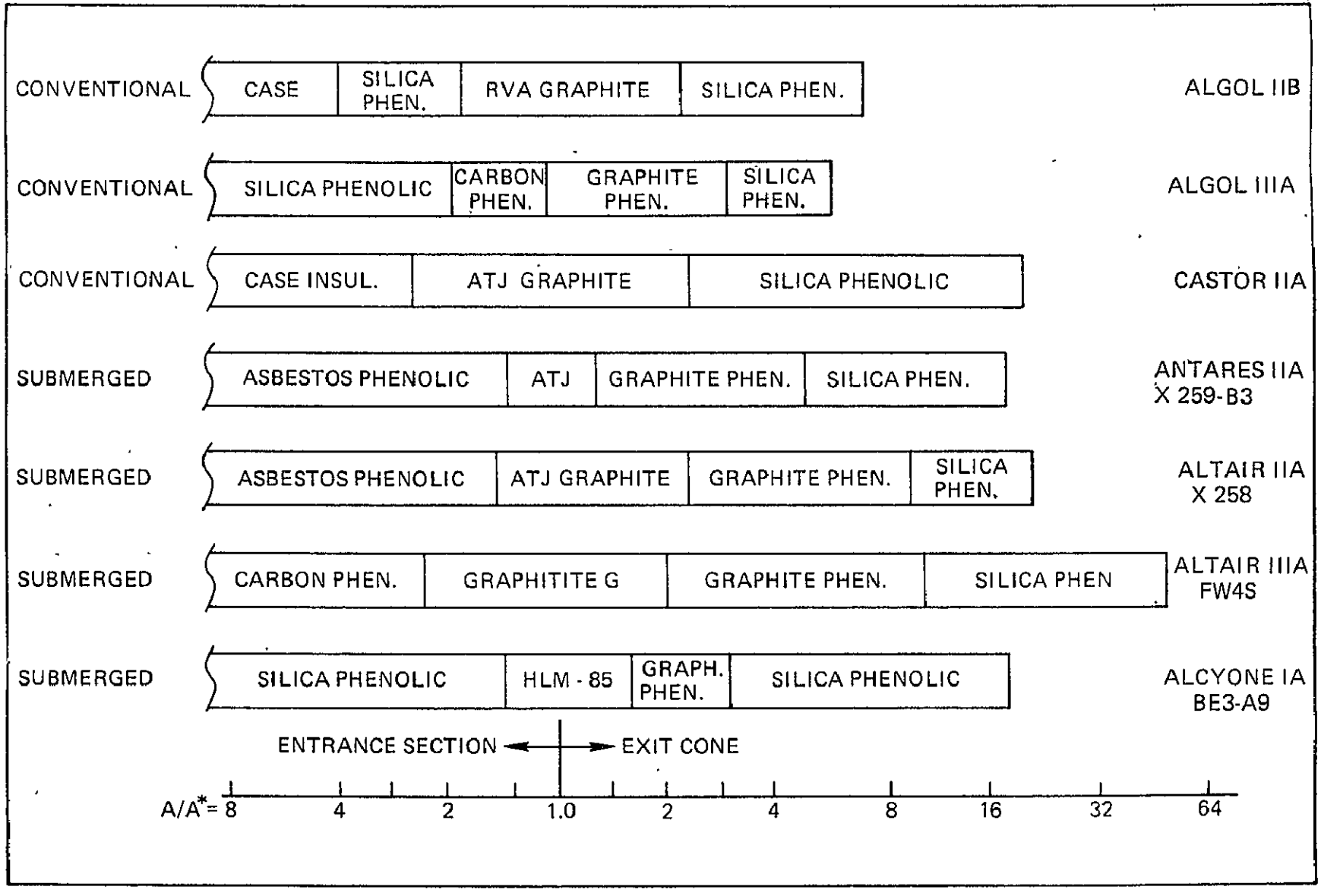

TABLE III. – SCOUT NOZZLE MATERIALS

NOZZLE COMPONENT		ALGOL IIB	CASTOR IIA	ANTARES IIA X259	ALTAIR IIA X258	ALTAIR IIIA FW4S	ALCYONE IA BE3-A9
ENTRANCE INSULATION		HIGH SILICA FABRIC PHENOLIC MX 2600 PREIMPREGNATED (SILICA FLOUR FILLED)	← N/A →				
INSULATION FORWARD		N/A	GLASS FIBER PLASTIC, HIGH PRESSURE, FIBERITE 4035	← N/A →			
THROAT INSERT		RVA GRAPHITE	ATJ GRAPHITE	ATJ GRAPHITE	ATJ GRAPHITE	GRAPHITITE G	GRAPHITIZED HLM-85
INSERT BACKUP INSULATION		FELT ASBESTOS, PHENOLIC PRE-IMPREGNATED 41 RPD	RESIN IMPREGNATED ASBESTOS FELT 41 RPD	150 RPD ASBESTOS PHENOLIC	150 RPD ASBESTOS PHENOLIC	FM 5072 CARBON PHENOLIC TAPE	INTEGRAL WITH AFT EXIT CONE INSULATION
INSERT COATING		ZIRCONIUM OXIDE TYPE I WITH MOLYBDENUM UNDERCOAT	PORCELAIN EPOXY 225A & 225B	← N/A →			
EXIT CONE INSULATION	FWD	HIGH SILICA FABRIC PHENOLIC MX2600 OVERWRAPPED WITH	RESIN IMPREGNATED HIGH SILICA FABRIC TAPE FM 5504, 5067, & MX 2600 OVERWRAPPED WITH TAPE FM 5504, 5067, & MX 2600	GRAPHITE PHENOLIC MX 2630A	GRAPHITE PHENOLIC TAPE MX 2630A OR FM 5014	GRAPHITE PHENOLIC TAPE FM 5014	MOLDED GRAPHITE FABRIC REINFORCED FIBERITE 2630A
	AFT	PREIMPREGNATED SILICA FLOUR FILLED		SILICA PHENOLIC TAPE MX 2600	SILICA PHENOLIC TAPE MX 2646	SILICA PHENOLIC LOW DENSITY MX 5707	MOLDED SILICA FABRIC REINFORCED FIBERITE MX 2625
EXIT CONE LINER		GLASS CLOTH, EPOXY RESIN, IMPREGNATED EF-Z-143 VOLAN A	N/A	ASBESTOS PHENOLIC TAPE TAYLORON PA6	ASBESTOS PHENOLIC TAPE FM 5076	N/A	N/A
EXIT CONE OUTER SHELL		GLASS ROVING, 20 END, EPOXY RESIN MOBALOY 20EF-2-59 IMPREGNATED	4130 STEEL COND D	FILAMENT WOUND GLASS ROVINGS HS259-1-211 ECG140-801 FINISH	FILAMENT WOUND GLASS ROVINGS HYS-1-211 1-3 1-15 ECG-140 5994 E GLASS HTS	PH 15-7 MO STEEL COND. A	ONE LAYER =181 FIBERGLASS CLOTH ½ LAYER GLASS ROVING 144 ENDS/ INCH
ATTACHMENT RING		4130 STEEL COND D-3	4130 STEEL COND D	7075-T6 ALUMINUM	7075-T652 ALUMINUM	7075-T6 ALUMINUM	7075-T6 ALUMINUM

N/A = NOT APPLICABLE

TABLE IV. – SCOUT NOZZLE ADHESIVES

	ALGOL IIB	CASTOR IIA	ANTARES IIA X259	ALTAIR IIA X258	ALTAIR IIIA FW4S	ALCYONE IA BE3-A9
THROAT INSERT TO BACKUP INSULATION	RESIN PHENOLIC TYPE II, CLASS 2 (MIL R 9299)	TA-L703	EPOXY, RESIN BASE	EPOXY RESIN WITH CURING AGENT	HT 424 TYPE III	N/A
ENTRANCE INSULATION TO HOUSING	EPON 919 (WS 1065)	← N/A →				
FORWARD INSULATION TO HOUSING AND INSERT BACK-UP INSULATION	N/A	TA-L721	← N/A →			
INSERT BACKUP INSULATION TO HOUSING	EPON 919 (WS 1065)	TA-L721	← N/A →			
HOUSING TO EXIT CONE	EPON 919 (WS 1065)	RTV SILICONE RTV-88 & SS-4004 PRIMER OR SEALANT NO 90-006 & PRIMER NO 1200	← N/A →			
EXIT CONE OUTER SHELL TO EXIT CONE LINER	E 787 OR EQUIV	← N/A →				
INSERT BACKUP INSULATION TO EXIT CONE LINER	N/A	N/A	EPOXY, RESIN BASE (ARMSTRONG A2 RESIN)	EPOXY RESIN WITH CURING AGENT	N/A	N/A
INSERT TO EXIT CONE	N/A	N/A	EPOXY, RESIN BASE (ARMSTRONG A-2 WITH A)	EPOXY RESIN WITH CURING AGENT	N/A	SHELL EPON 913,1
EXIT CONE OUTER SHELL TO EXIT CONE INSULATION	← N/A →				HT 424	SHELL EPON 828/CL
INSERT BACKUP INSULATION TO ATTACHMENT RING	N/A	N/A	MOLDED WITH 150 RPD	MOLDED WITH 150 RPD	EPON 934	N/A
EXIT CONE INSULATION TO ATTACHMENT	← N/A →					SHELL EPON 828/CL

TABLE V. – SCOUT NOZZLE COMPONENTS DRAWING AND SPECIFICATION NUMBERS

NOZZLE COMPONENT		ALGOL IIB		CASTOR IIA		ANTARES IIA X259		ALTAIR IIA X258		ALTAIR IIIA FW4–S		ALCYONE IA BE3–A9	
		DWG. NO.	SPEC. NO.	DWG. NO.	SPEC. NO.	DWG. NO.	SPEC. NO.	DWG. NO.	SPEC. NO.	DWG. NO.	SPEC. NO.	DWG. NO.	SPEC. NO.
ENTRANCE INSULATION		382378	AGC-10803	← N/A →									
INSULATION FORWARD		N/A	N/A	CR40441	TCC SP-262	← N/A →							
THROAT INSERT		382385	AGC-34314	R42148	TCC SP-531 SP-537	83136D-00003	HS-259-1-205	258 B2-6-03 0003	HXS 1-205	B03533	UTC SEO 238	10A00005	HPC-253 -02-3-2 TYPE I
INSERT BACKUP INSULATION		382380 382385	AGC-10790	R42148	TCC SP-319 TYPE II CLASS 2	83163D-00011	HS-259-2-166	25882-1-03-0007	HXS-1-203	BE3533	UTC SEO 230 TYPE 2	–	–
INSERT COATING		382385	AGC-34116	R42148 NOTE 20	PROTEX-A- COTE CO. 225-A 225-B	← N/A →							
EXIT CONE INSULATION	FWD	382381	AGC-10803	R41993	TCC SP-521 TYPE II CLASS A	83136D-00009	HS-259-1-97	258 B2-6-03-0013	HXS 1-97 TYPE II HXS 1-13 TYPE I	5M0004 ITEM 1	5MCS0003	10A00007	HPC-253-02-3-3
	AFT	382381	AGC-10803	R41993 R42148	TCC SP-521, II, CLASS A	83136D-00009	HS-259-1-195	258 B2 6-03-0013	HXS 1-260	5M0004 ITEM 2	5MCS0001	10A00008	HPC-253-02-3-3 TYPE II
EXIT CONE LINER		382383	AGC-10848	N/A	N/A	83136D-00008	HS-259-1-111	258 B2-6-03 0013	HXS 1-14 TYPE I	← N/A →			
EXIT CONE OUTER SHELL		382383	WS 1028A	FR40749	MIL-S-6758	83136D-00007	**	258 B2-6-03 0012	HXS 1-211 HXS 1-3 HXS 1-15	5M0007 ITEM 6	AMS-5520 COND. A	10A00009	HPC-253 02-2-3 HPC-253 02-2-2
ATTACHMENT RING		383777	MIL-S-6758	FR40749	MIL-S-6758	83136D-00012	MIL-A-22771	258 B2-6-03-0009	MIL-A-22771	5M0005	MIL-A-22771	10A00010	QQ-A-250/12 QQ-A-250/11 MIL-A-22771

MMM = 3M CO.
WS = NAV. WEPS. – WEAPONS SYSTEMS SPEC NO.
AGC = AEROJET GENERAL SPEC. NO.
HS, HXS, HD = HERCULES SPEC NO.
SEO = UTC SPEC NO.
TCC = THIOKOL SPEC NO.
HPC = HERCULES SPEC. NO.

**MIL-C-9084, VIII
HS-259-1-211
HS-259-1-69

TABLE VI. – SCOUT NOZZLE ADHESIVES DRAWING AND SPECIFICATION NUMBERS

	ALGOL IIB		CASTOR IIA		ANTARES IIA X259		ALTAIR IIA X258		ALTAIR IIIA FW4S		ALCYONE IA BE3-A9	
	DWG. NO	SPEC NO.	DWG. NO.	SPEC. NO.	DWG NO	SPEC. NO	DWG. NO.	SPEC. NO.	DWG. NO.	SPEC. NO.	DWG NO.	SPEC. NO
THROAT INSERT TO INSERT BACKUP INSULATION	382385	MIL R-9299, II, CLASS 12	DR40465	TCC SP 408	83136D-00004	HS 259 1-186 COMP. 4	258 B2 06-03 0004	HXS 1 186 TYPE I	8O3533 ITEM 4	MMM–A–132 TYPE III	N/A	N/A
ENTRANCE INSULATION TO HOUSING	382385	WS1065	← N/A →									
FORWARD INSULATION TO HOUSING AND INSERT BACK-UP INSULATION	N/A	N/A	R42148	TCC SP-17	← N/A →							
INSERT BACKUP INSULATION TO HOUSING	382385	WS1065	R42148	TCC SP 17	← N/A →							
HOUSING TO EXIT CONE	382385	WS1065	← N/A →									
EXIT CONE OUTER SHELL TO EXIT CONE LINER	382383	EPON 787	← N/A →									
INSERT BACKUP INSULATION TO EXIT CONE LINER	← N/A →				83136D-00006	HS 259 1 1 86 COMP 4	258 B2 6 03 0006	HXS 1 186 TYPE 1	← N/A →			
INSERT TO EXIT CONE	← N/A →				83136D 00004	HS 259 1 186 COMP 4	258 B2-6 03 0004	HXS 1 186 TYPE I	N/A	N/A	10A00009	HPC-253 02 5-1 COMP 1
EXIT CONE OUTER SHELL TO EXIT CONE INSULATION	–	–	R42148	TCC SP 525	← N/A →				5M0007	MMM–A-132 TYPE III	10A00009	HPC-253 -02-2-4
INSERT BACKUP INSULATION TO ATTACHMENT RING	← N/A →				83136D 00011	HD259 2 168 PRIME RING WITH RPD 150	258 B2 6 03 0007	HXD 1 2149 PRIME RING WITH RPD 150	5M0008 ITEM 6	EPON 934	–	–
EXIT CONE INSULATION TO ATTACHMENT RING	← N/A →										10A00009	HPC 253 02-2 4 TYPE I CLASS I

TABLE VII. – THROAT INSERT EROSION DATA

Motor	Graphite Type	Avg. Erosion Rate, m/sec	± Range, m	No. of Firings	Avg. Percent Area Increase
Algol IIB	RVA	**.914 x 10^{-4} (3.6 mils/sec)	.014 (.55 in)	4	5.7
Castor IIA	ATJ	**787 (3.1)	.0051 (.2)	6	2.8
Antares IIA X259	ATJ	*.584 (2.3)	.0127 (.5)	10	4.9
Altair IIA X258	ATJ	*.686 (2.7)	.0152 (.6)	8	7.5
Altair IIIA FW4S	G-90	**.635 (2.5)	—	1	12.7
Alcyone IA	ATJ	**1.092 (4.3)(b)	.0152 (.6)	6	26.0
BE3-A9(a)	HLM-85	*1.321 (5.2)	.0445 (1.75)	13	13.8

* Erosion rate based on motor action time.
** Erosion rate based on motor web time.
(a) Data from BE3-A9 motors which have same propellant and nozzle included.
(b) Ref. 220 contains erosion data of 4.14 mils/sec average for 6 firings based on action time.

TABLE VIII. – INSULATION EROSION DATA

Motor	Material	Location	Erosion and Char, m
Algol IIB	Silica Phenolic	Selected exit cone throat locations	.0095 (0.375*) .0071 (0.280*) .0046 (0.180*) .0025 (0.100*)
Castor IIA	Silica Phenolic	Downstream of throat insert	.0165 (0.65 in)
	Silica Phenolic	Expansion Ratio 4.8	.0084 (0.33)
	Silica Phenolic	Expansion Ratio 11.6	.0051 (0.20)
	Silica Phenolic	Expansion Ratio 18	.0053 (0.21)
Altair IIA X-258	Graphite Phenolic	Downstream of throat insert	.0032 (0.127)
	Silica Phenolic	Graphite/silica junction	.0021 (0.082)
	Silica Phenolic	Nozzle exit	.0010 (0.040)
Altair IIIA FW4S	Graphite Phenolic	Throat extension	.0122 (0.48)
	Graphite Phenolic	Upstream of graphite/silica junction	.0061 (0.24)
	Silica Phenolic	Graphite/silica junction	.0051 (0.20)
	Silica Phenolic	Nozzle exit	.0015 (0.06)

*Erosion only. Char varies from 0.20 inch downstream of throat/exit cone junction to 0.38 inch at exit plane.

TABLE IX. – SCOUT NOZZLE GEOMETRY

Description	Algol IIB	Castor IIA	Antares IIA X 259 B3	Altair IIA X 258	Altair IIIA FW4S	Alcyone IA BE 3 A9
Initial Expansion Ratio	7.25	21.212	17.91	25.0	50.37	18.6
Exit Area, m^2	.527 (5.67 ft^2)	.739 (7.95 ft^2)	.404 (4.35 ft^2)	.127 (1.36 ft^2)	.139 (1.50 ft^2)	.077 (0.833 ft^2)
Throat Area, m^2	.073 (0.78 ft^2)	.035 (0.38 ft^2)	.023 (0.24 ft^2)	.005 (0.055 ft^2)	.003 (0.357 f ^{2})	.004 (0.052 ft^2)
Throat Diameter, m	.304 (0.998 ft)	.211 (0.691 ft)	.169 (0.556 ft)	.080 (0.264 ft)	.059 (0.1945 ft)	.072 (0.236 ft)
Exit Cone O. D., m	.855 (33.66 in)	1.016 (40.00 in)	.743 (29.24 in)	.414 (16.28 in)	.430 (16.91 in)	.307 (12.08 in)
Exit Cone I. D., m	.819 (2.687 ft)	.969 (3.18 ft)	.717 (2.354 ft)	.402 (1.319 ft)	.421 (1.38 ft)	.310 (1.017 ft)
Mismatch, Throat to Exit Cone, m	.000254 (0.010 in)	.00254 (0.010 in)	NO REQ'T.	NO REQ'T.	.000965 (0.038 in)	.000051 (0.002 in)
Throat Closure Plug-Material & Function	Plastic Seal. Prevent Contamination	Plastic Foam. Assure Pressurization	High Density Styrofoam. Assure Pressurization	High Density Styrofoam. Assure Pressurization	Ethafoam. Prevent Contamination	High Density Styrofoam. Prevent Contamination
Expansion Cone Half Angle	17°	22°34′	18°	18°	20°	16°
Nozzle Wt., N	2562 (576 lbs)	2397 (539 lbs)	338 (76 lbs)	107 (24 lbs)	53 (12 lbs)	32 (7.2 lbs)

TABLE X. – SCOUT MOTOR PROPELLANT CHARACTERISTICS

Description	Algol IIB	Castor IIA	Antares IIA X259	Altair IIA X258	Altair IIIA FW4S	Alcyone IA BE3A9
Propellant Designation	ANP-2872 JM Mod 1	TP-H 7025	CYI-75	CYI-75	UTP-3096 A	DDP-80
Propellant Type	Aluminized Composite	Aluminized Composite	Composite Modified-Double Base	Composite Modified-Double Base	Aluminized Composite	Composite Modified Double Base
Flame Temp (^{o}F)	5480	6080	6384	6384	5600	6562
Propellant Gas Properties (Chamber)						
Specific Heat Ratio (γ)	1.17	1.16	1.15	1.13	1.18	1.17
C_p (cal/gm-^{o}K)	0.59	.421*	.425	.425	0.439	0.372
Molecular Weight	22.6	30.9	19.3	19.3	20.11	20.2
C* (ft/sec)	5660	5210	5300	5300	5035	4981
Grain Configuration	Cylindrical 4 pointed Star	Cylindrical bore with 2 circumferential slots.	Cylindrical 4 pointed gear bore in aft end with a cylindrical bore in forward end.	Cylindrical gear bore with 4 deep and 6 shallow rays in aft end with a cylindrical bore in forward end.	Cylindrical bore with a forward circumferential slot.	Cylindrical bore with 6 slots in aft end.

* Exhaust properties calculated at 1000 psi chamber pressure and 1 atm exhaust pressure.

TABLE XI. – SCOUT MOTOR PERFORMANCE

Description	Algol IIB	Castor IIA	Antares IIA X259	Altair IIA X258	Altair IIIA FW4S	Alcyone IA BE3-A9
Avg. Web Thrust, Vacuum (lbs)	98,150	61,840	20,930	6,540	5,860	5,900
Total Motor Weight (lbs)	23,800	9,760	2,813	577	664	214
Consumed Weight (lbs)	21,390	8,267	2,600	510	611	194
Propellant Weight (lbs)	21,180	8,210	2,575	505	606	191
Specific Impulse Vacuum (sec)	258.9	281.9	281.4	279.0	284.1	276.0
Total Burn Time (sec)	76.1	39.0	35.9	22.2	31.5	9.1
Web Burn Time (sec)	47.1	36.9	32.0	21.2	28.9	8.75
Pressure, Web Time Avg. (psia)	530	700	337	450	670	500
MEOP (psia)	675	799	416	485	859	550
Proof Pressure (psig)	750	910	475	505	900	727

TABLE XIV. – NORMALIZED MERIT FACTORS FOR ABLATIVE INSERTS

(MERIT FACTOR = $1/\dot{x}$)

Material	Type	Test	$\dot{x}$	Normalized Merit Factor
MX 4551	Graphite Phenolic	Screening motor	5.5/3.3[a]	1.36 to 1.45
FM-5072	Carbon Phenolic	Screening motor	5.6 to 3.3	1.34 to 1.45
FM-5063	Carbon Phenolic	Screening motor	5.75 to 4.8	1.30 to 1.00
MX-4926	Carbon Phenolic	Screening motor	7.0 to 4.6	1.07 to 1.04
MX-4926	Carbon Phenolic	NOMAD MM	6.2	.83
MX-4926	Carbon Phenolic	Aerojet 120"	4.4 to 7.5	1.17 to .69
MX-4926	Carbon Phenolic	Aerojet 260"	2.96 to 5.7	1.74 to .90
FM-5014	Graphite Phenolic	Screening motor	7.5 to 4.8	1.0
		UTC 120"	5.15	1.0
FM-5014	Graphite Phenolic	Titan IIIC	4.5 ± 0.5 [b]	1.14
MXG-175	Graphite Phenolic	Titan IIIM	4.5 [b]	1.14
MXC-175	Carbon Phenolic	Titan III	-------(c)	------
WB-8712	Carbon Phenolic	NOMAD MM	6.4	.80
N 4034	Carbon Phenolic	Screening motor	12.8 to 4.5	.59 to 1.07
N-4034	Carbon Phenolic	NOMAD MM	6.2	.83
MX-2630A	Graphite Phenolic	Poseidon & MM IV	--------(c)	---------
FM-5441	Graphite Phenolic	Subscale	--------	--------

NOTE: (a) A/B = A value at 600 psi, B value at 400 psi.
(b) Obtained from Titan III Program Office.
(c) Operational materials but no data available.

TABLE XV. – NORMALIZED MERIT FACTORS FOR FORWARD INSULATORS

(MERIT FACTOR = $1/(\dot{x} + \dot{d})$

Material		$\dot{x}$	$\dot{d}$	Normalized Merit Factor
Type	Designation			
Kraft Paper	FM-5272	2.6	5.1	1.52
Asbestos	WB-2212-BAP	3.7	5.6	1.26
Canvas Duck	KF-418	3.5	7.6	1.05
Silica	ACFX-R 84	3.5	7.9	1.03
Asbestos	MXA-6012	4.8	6.9	1.0
Silica	SP-8030-96	5.3	8.8	0.83

Type	Designation	Remarks
Carbon	FM-5072 LD	NOMAD and Minuteman
Carbon	FM-5072	Used on Scout
Carbon	MX-4926	Used on Poseidon
Carbon	MXCE-280	Used on Algol III

TABLE XVI . -- NORMALIZED MERIT FACTORS FOR BACKFACE INSULATORS

(MERIT FACTOR = $\rho C_p/K$)

Material Type	Material Designation	Angle	Diffusivity	Normalized Merit Factor
Asbestos	Tayleron PA6	90°	.0025	4.04
Kraft Paper	FM-5272	90°	.0031	3.26
Asbestos	MXA-198	75°	.00465	2.17
Asbestos	FM-5525	75°	.0050	2.02
Silica	ACFX-R 84	75°	.00582	1.74
Canvas Duck	KF-418	90°	.0062	1.63
Silica	MXS-112	--	.00625	1.62
Silica	MXS-56	--	.00722	1.40
Silica	FM-5131	--	.00816	1.24
Asbestos	41 RPD	75°	.0101	1.00

TABLE XVII . — ABLATIVE PERFORMANCE OF EXIT CONE INSULATORS

Material Type	Material Designation	Erosion/char Rates		
		A/A* = 2	A/A* = 4	A/A* = 8
Kraft Paper	FM-5272	19.9/21.5	3.3/4.6	1.3/2.6
Canvas Duck	KF-418	11.5/13.3	3.5/6.2	1.7/5.2
Asbestos	FM-5525	——	6.6/8.0	1.4/2.4
Asbestos	WB-7211	——	4.2/5.7	0.8/3.3
Carbon	FM-5072 LD	1.9/7.7	(Est. 6.5 Erosion + Char)	——

A* = Throat Area

TABLE XVIII. — NORMALIZED MERIT FACTORS FOR EXIT CONE INSULATORS
(MERIT FACTOR = $(k \rho / C_p)^{-1/2}$)

Material		Diffusivity	Density	Normalized Merit Factor
Type	Designation			
Kraft Paper	FM-5272	.0031	83.	2.43
Canvas Duck	KF-418	.0062	84.3	1.69
Asbestos	FM-5525	.0050	105.	1.51
Asbestos	WB-7211	.0062	98.4	1.45
Carbon	FM-5072 LD	.0097	82.4	1.38
Silica	MX-2646	.0058	118.3	1.24
Carbon/Silica	WB-8251	.0097	94.	1.21
Silica	FM-5131	.0082	108.2	1.15
Silica	WB-2233-96	.0093	107.9	1.08
Silica	MX-2600	.0107	108.6	1.0
Carbon	MX-4926	.0205	89.4	0.88

TABLE XIX. – NORMALIZED MERIT FACTORS FOR STRUCTURAL HOUSINGS

(MERIT FACTOR = $F_{TU}E/\rho$)

Material	F_{TU}, N/m^2	Normalized Merit Factor
B/Al Composite	1102×10^6 (160,000 psi)	2.78
(300) Maraging Steel	2067 (300,000)	1.800
4340 Steel	1791 (260,000)	1.444
PH 15-7 M_o Steel	1240 (180,000)	1.027
4130 Steel	1240×10^6 (180,000 psi)	1.0 (Baseline)
Rene' 41	1171×10^6 (170,000 psi)	.981
Lockalloy	317 (46,000)	.936
Inconel X-750	1102 (160,000)	.901
17-4-PH Steel	1034 (150,000)	.835
HY-140 Steel	1013 (147,000)	.830
S-Glass Filament	1723 (250,000)	.723
Titanium	551 (80,000)	.415
7075-T6 Aluminum	489 (71,000)	.398
AZ 61 A Magnesium	276 (40,000)	.212
181 Glass Laminate	241 (35,000)	.098

TABLE XX. – NORMALIZED MERIT FACTORS FOR EXIT CONE STRUCTURES

(MERIT FACTOR = F_{TU}/ρ)

Material	F_{TU}, N/m^2	Normalized Merit Factor
S-Glass Filament	1723×10^6 (250,000 psi)	5.246
Thornel 50 Laminate	717 (104,000)	2.730
B/Al Composite	1102 (160,000)	2.52
(300) Maraging Steel	2067 (300,000)	1.800
4340 Steel	1791 (260,000)	1.444
HY-140 Steel	1013 (147,000)	1.225
7075-T6 Aluminum	489 (71,000)	1.119
Rene' 41	1171 (170,000)	1.111
PH 15-7 M_o Steel	1240 (180,000)	1.027
4130 Steel	1240×10^6 (180,000 psi)	1.0 (Baseline)
AZ 61A Magnesium	276×10^6 (40,000 psi)	.974
Lockalloy	317 (46,000)	.969
Inconel X-750	1102 (160,000)	.843
301 Stainless Steel (1/2 H)	1034 (150,000)	.828
181 Glass Laminate	241 (35,000)	.816
Titanium	551 (80,000)	.777

TABLE XXI. – SELECTED CANDIDATE MATERIALS

Component	Material	Type
Insert	FM 5014 Carbitex 700 Pyrolarex 400 HD RPG 17300 PG discs	Graphite Phenolic Graphite fiber Carbonized fiber Carbonized fiber Graphite
Forward Insulator	FM-5272 MXCE-280	Kraft Paper Carbon Phenolic
Backface Insulator	Tayleron PAG FM-5272	Asbestos Phenolic Kraft Paper
Exit Cone Insulators ($A/A^* \geq 4.0$)	FM-5272 FM-5525	Kraft Paper Asbestos Phenolic
Exit Cone Insulators ($A/A^* \leq 4.0$)	FM-5072 LD MXCE-280	Carbon Phenolic Carbon Phenolic
Structural Housings	B/Al (300) Maraging Steel 4340 Steel 4130 Steel	Metal Composite Steel Steel Steel
Exit Cone Structure	S-Glass Filament	Composite

PROPERTIES OF MATERIALS USED IN SCOUT NOZZLES

Physical and mechanical properties were collected for all of the materials used in present Scout nozzles. Where temperature dependent information was available, a curve is presented and on each figure the report is referenced from which the information was obtained. If only room temperature properties were found, this information is presented in tabular form at the end of this appendix. To facilitate information retrieval the following list shows the figure number for each material property presented.

Figure no.	Materials	Property
A–1.1	Carbon phenolic (FM 5072)	Double shear strength
A–1.2		Flexural strength
A–1.3		Tensile strength
A–1.4		Tensile modulus of elasticity
A–1.5		Interlaminar shear
A–1.6		Compressive strength
A–1.7		Thermal expansion
A–1.8		Specific heat
A–1.9		Thermal conductivity
A–2.1	Silica phenolic (FM 5504) & carbon phenolic (FM 5072)	Flexural modulus of elasticity
A–3.1	Silica phenolic (FM 5504) (FM 5067) (FM 2646)	Thermal expansion (11)
A–3.2		Specific heat
A–3.3		Thermal diffusivity
A–3.4		Thermal conductivity ( )
A–3.5		Tensile strength
A–3.6		Double shear strength
A–3.7		Tensile modulus of elasticity
A–3.8		Flexural strength
A–3.9		Compressive strength

Figure no.	Materials	Property
A–3.10	↑	Interlaminar shear strength
A–3.11	Silica phenolic	Compressive modulus of elasticity
A–4.1	H T – 424 adhesive	Shear strength
A–5.1	↑	Thermal conductivity ( )
A–5.2		Thermal conductivity (11)
A–5.3		Tensile strength ( )
A–5.4	ATJ graphite	Tensile strength (11)
A–5.5		Specific heat
A–5.6		Thermal expansion ( )
A–5.7		Thermal expansion (11)
A–5.8		Elastic modulus of elasticity ( )
A–5.9	↓	Elastic modulus of elasticity (11)
A–6.1	↑	Tensile strength ( )
A–6.2		Tensile strength (11)
A–6.3	Graphitite-G	Elastic modulus of elasticity ( )
A–6.4		Elastic modulus of elasticity (11)
A–6.5		Thermal expansion ( )
A–6.6		Thermal expansion (11)
A–6.7		Thermal expansion ( )
A–6.8		Thermal conductivity (11)
A–6.9	↓	Specific heat

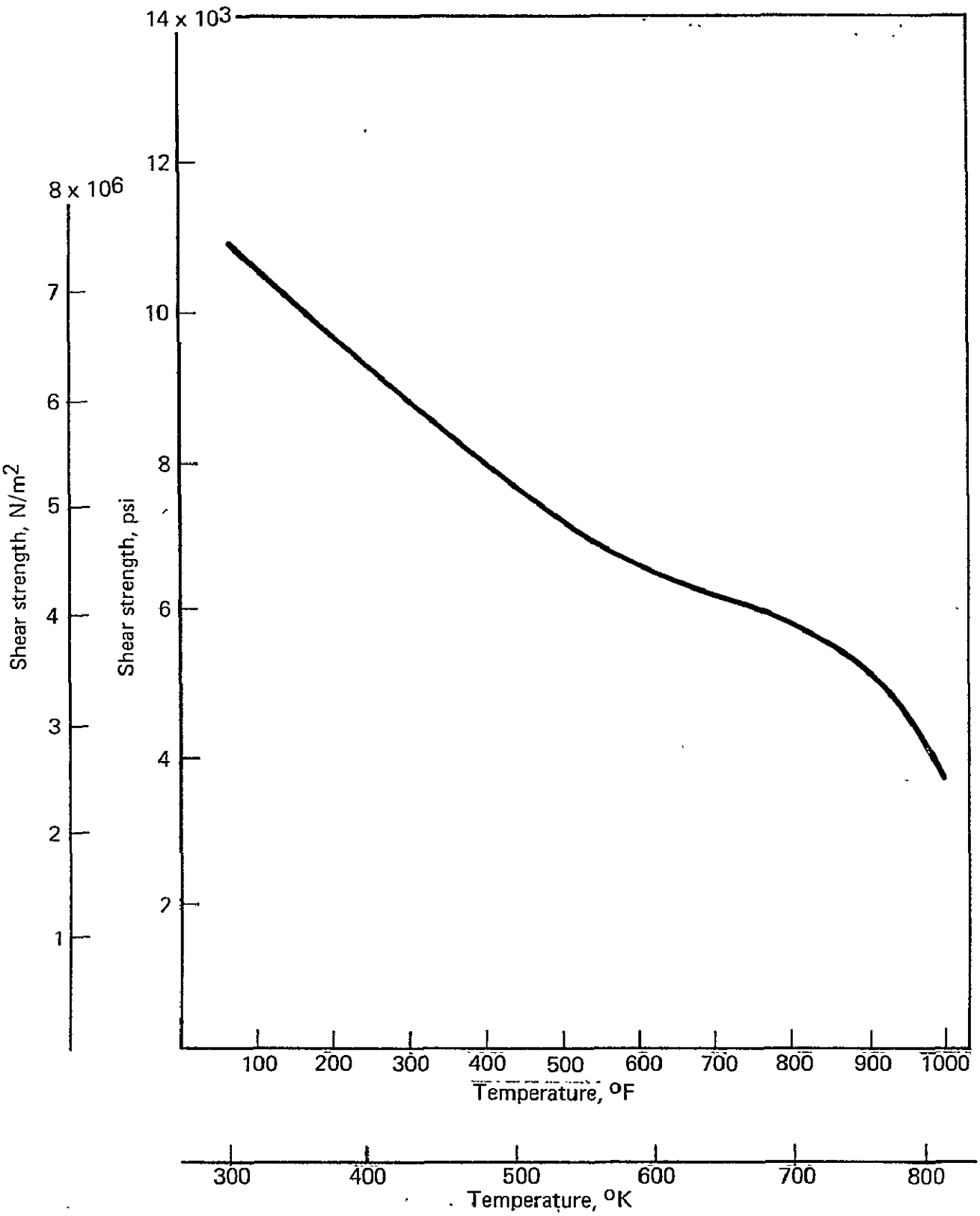

FIGURE A–1.1 SHEAR STRENGTH VERSUS TEMPERATURE OF FM 5072 CARBON PHENOLIC, ACROSS GRAIN

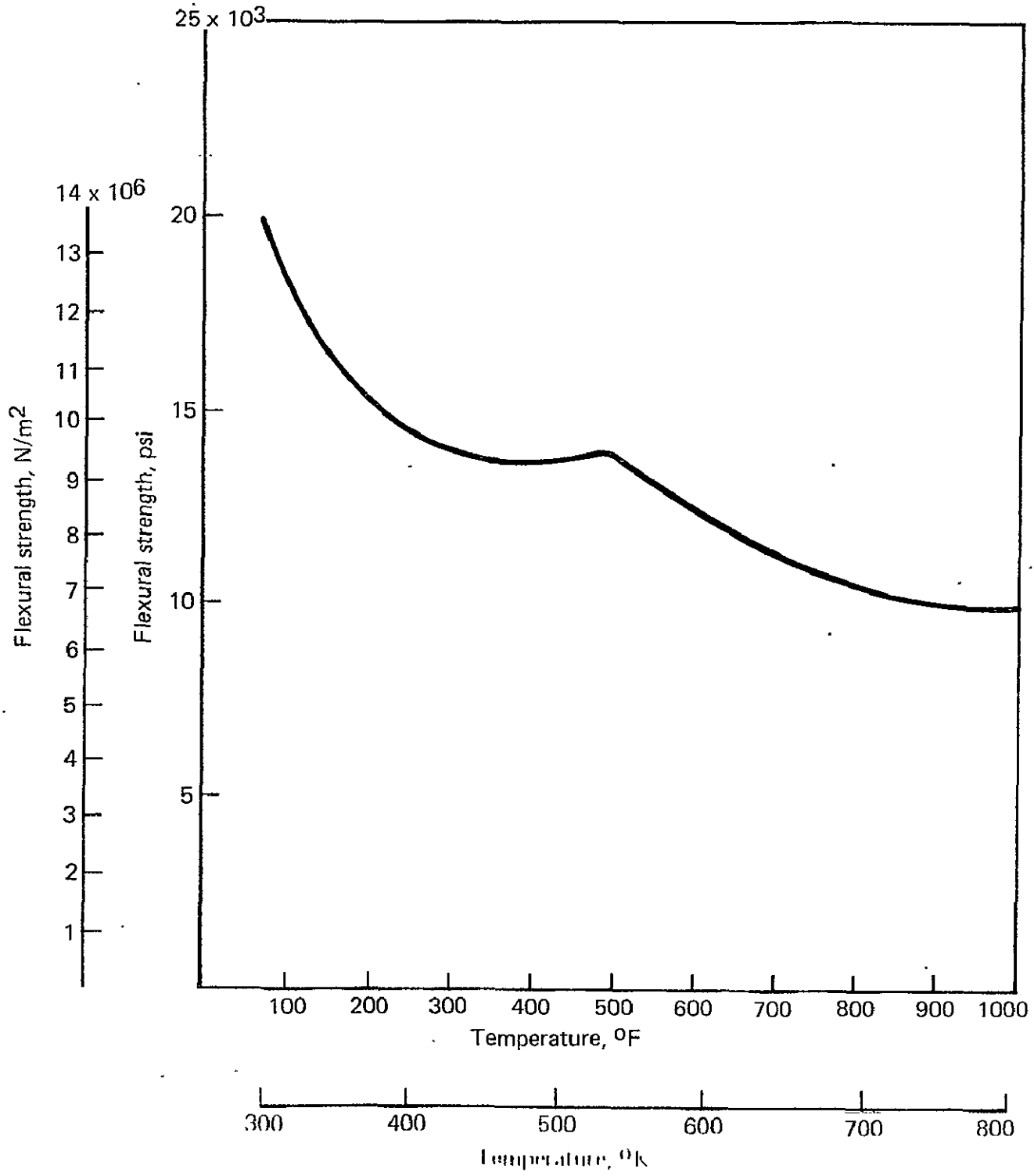

FIGURE A–1.2 FLEXURAL STRENGTH VERSUS TEMPERATURE OF FM 5072

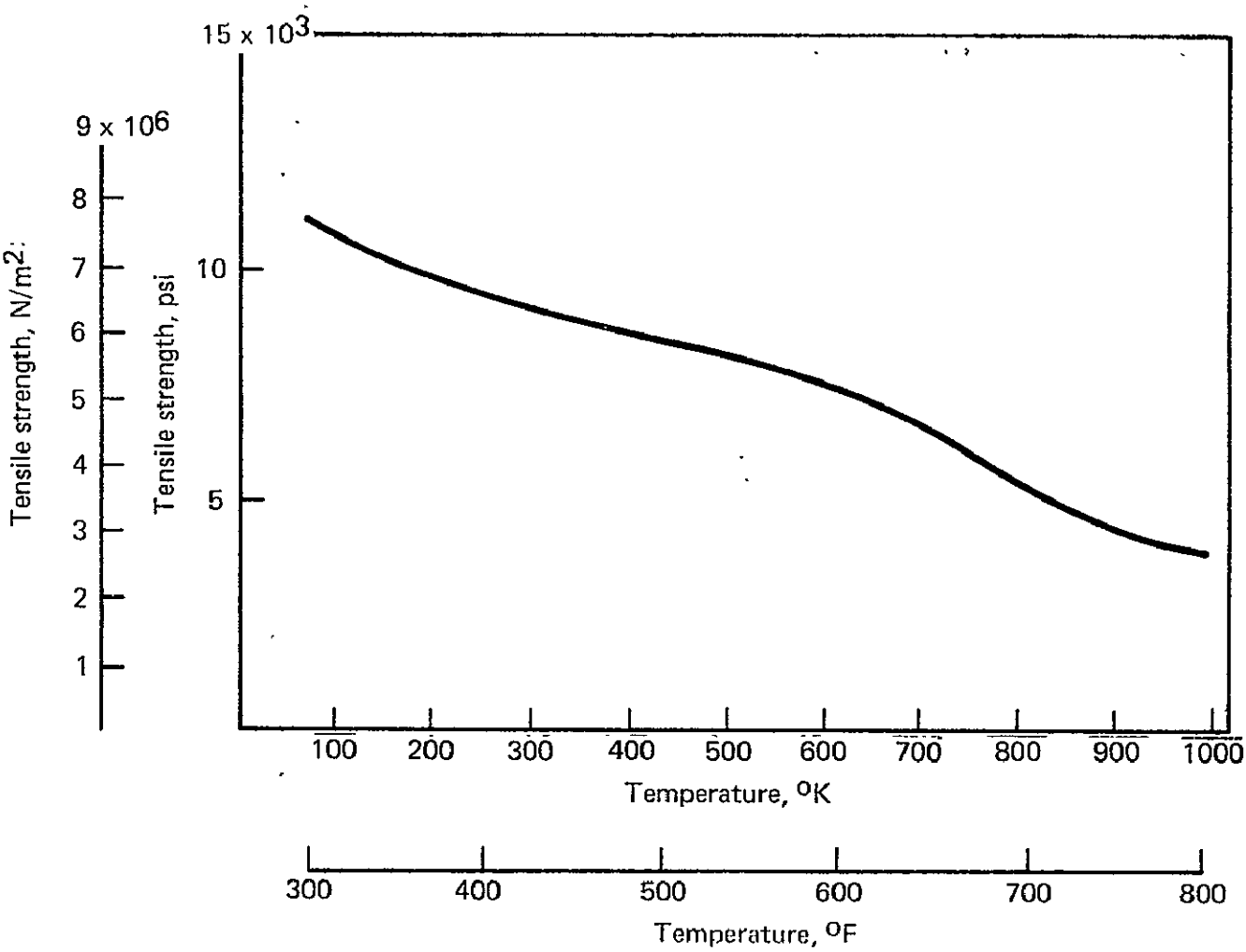

FIGURE A–1.3 TENSILE STRENGTH VERSUS TEMPERATURE OF FM 5072

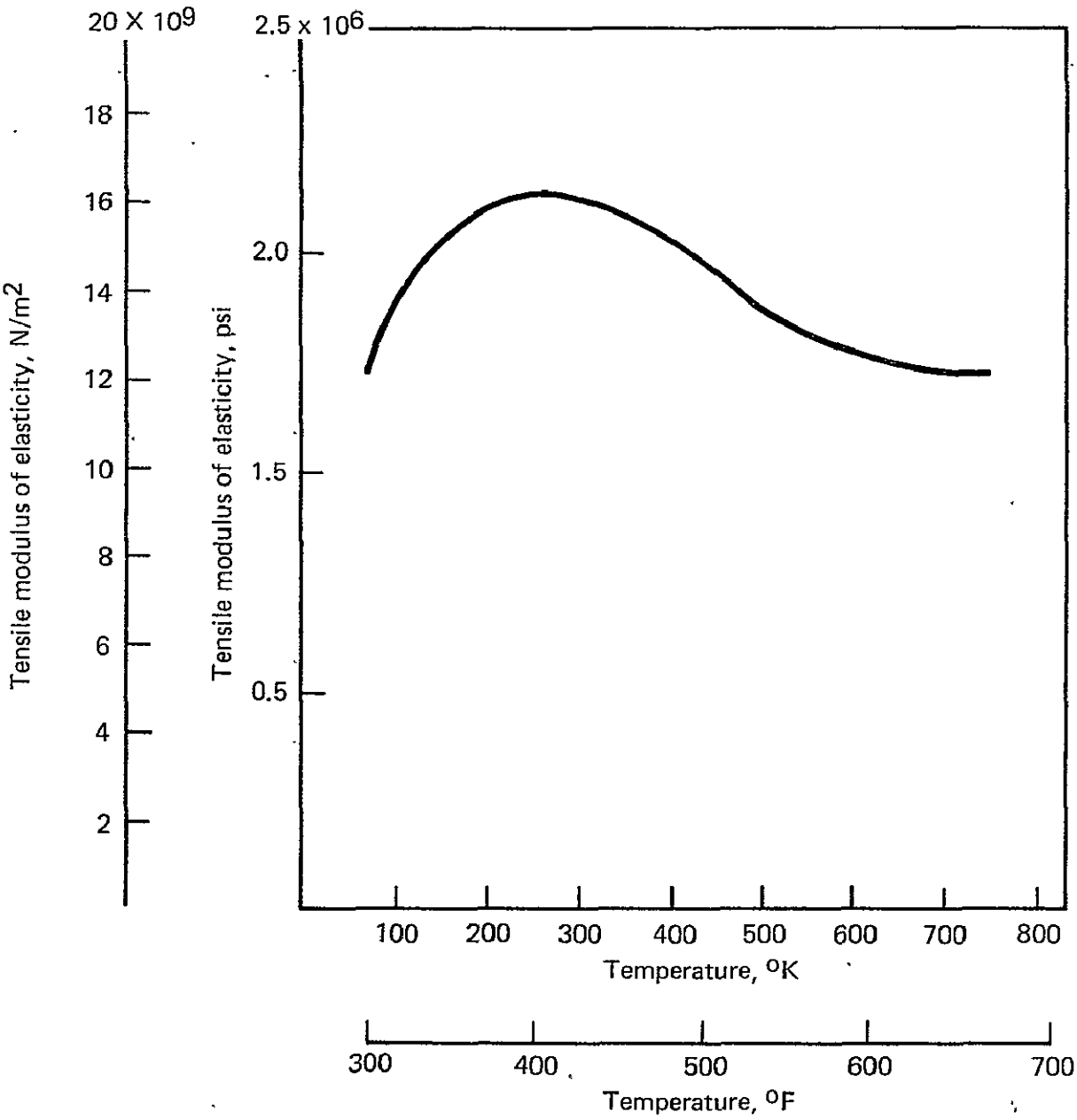

FIGURE A–1.4 TENSILE MODULUS OF ELASTICITY VERSUS TEMPERATURE OF FM 5072 (REFERENCE 1)

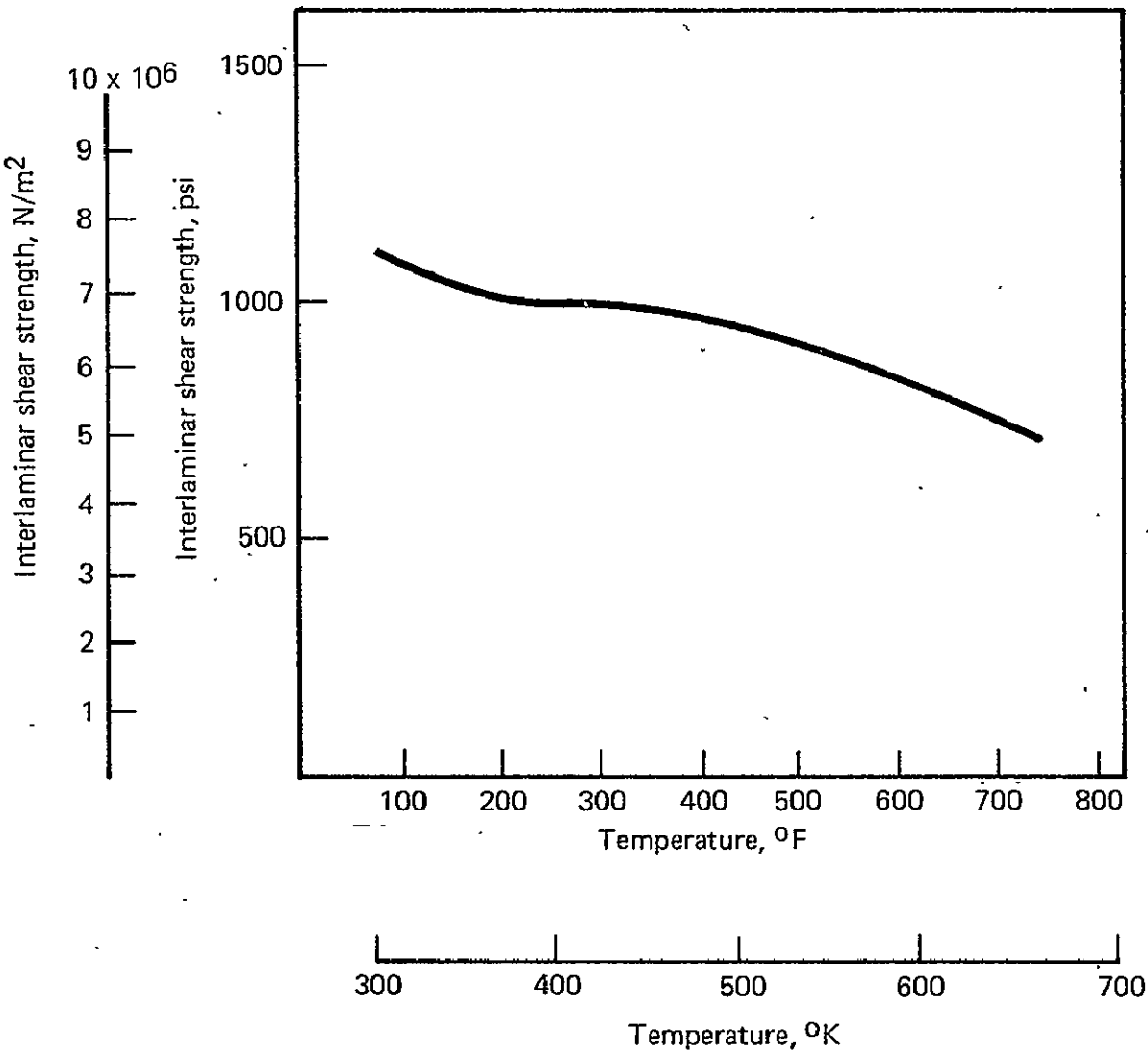

FIGURE A–1.5 INTERLAMINAR SHEAR STRENGTH VERSUS TEMPERATURE OF FM 5072

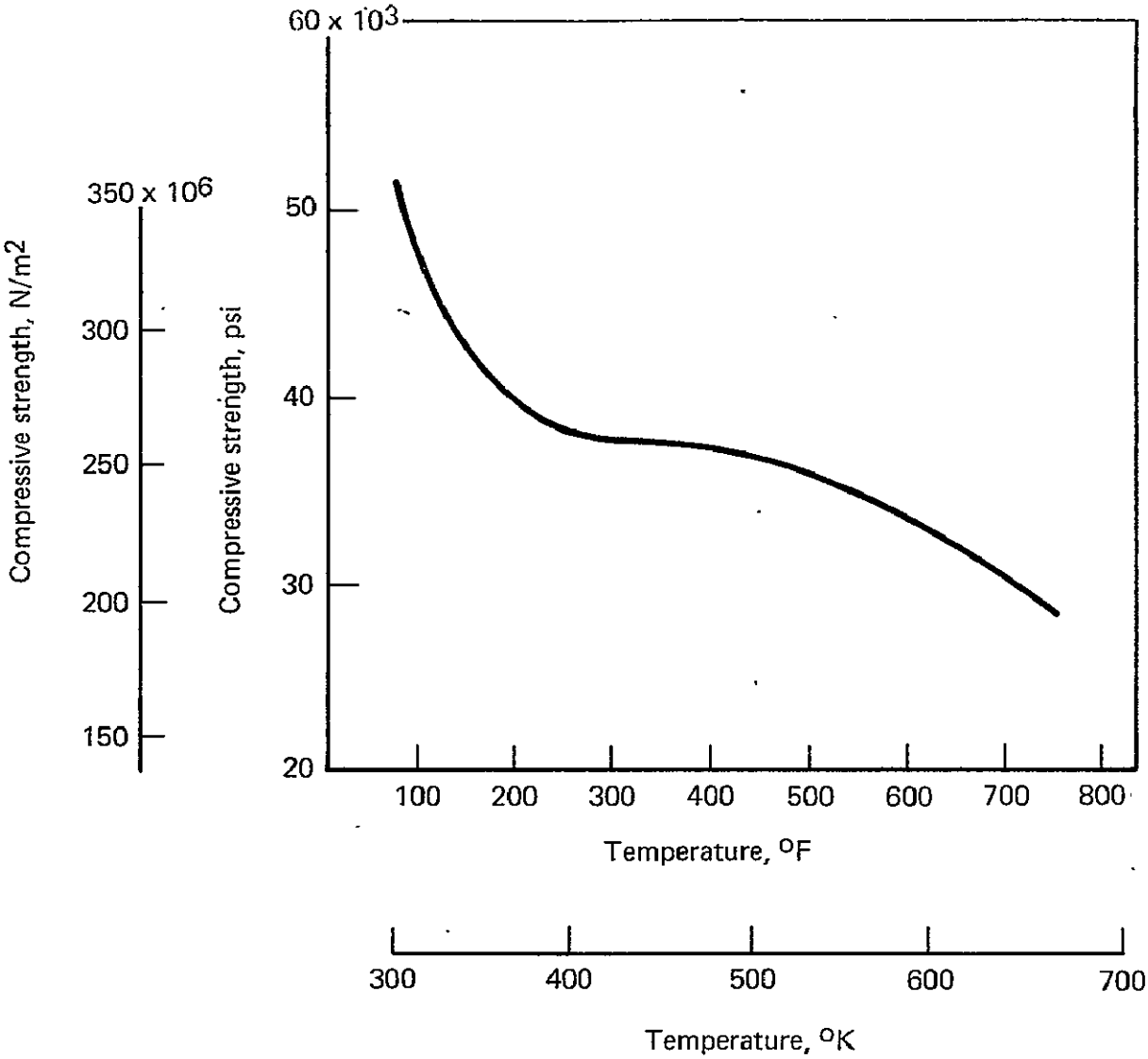

FIGURE A–1.6 COMPRESSIVE STRENGTH VERSUS TEMPERATURE OF FM 5072

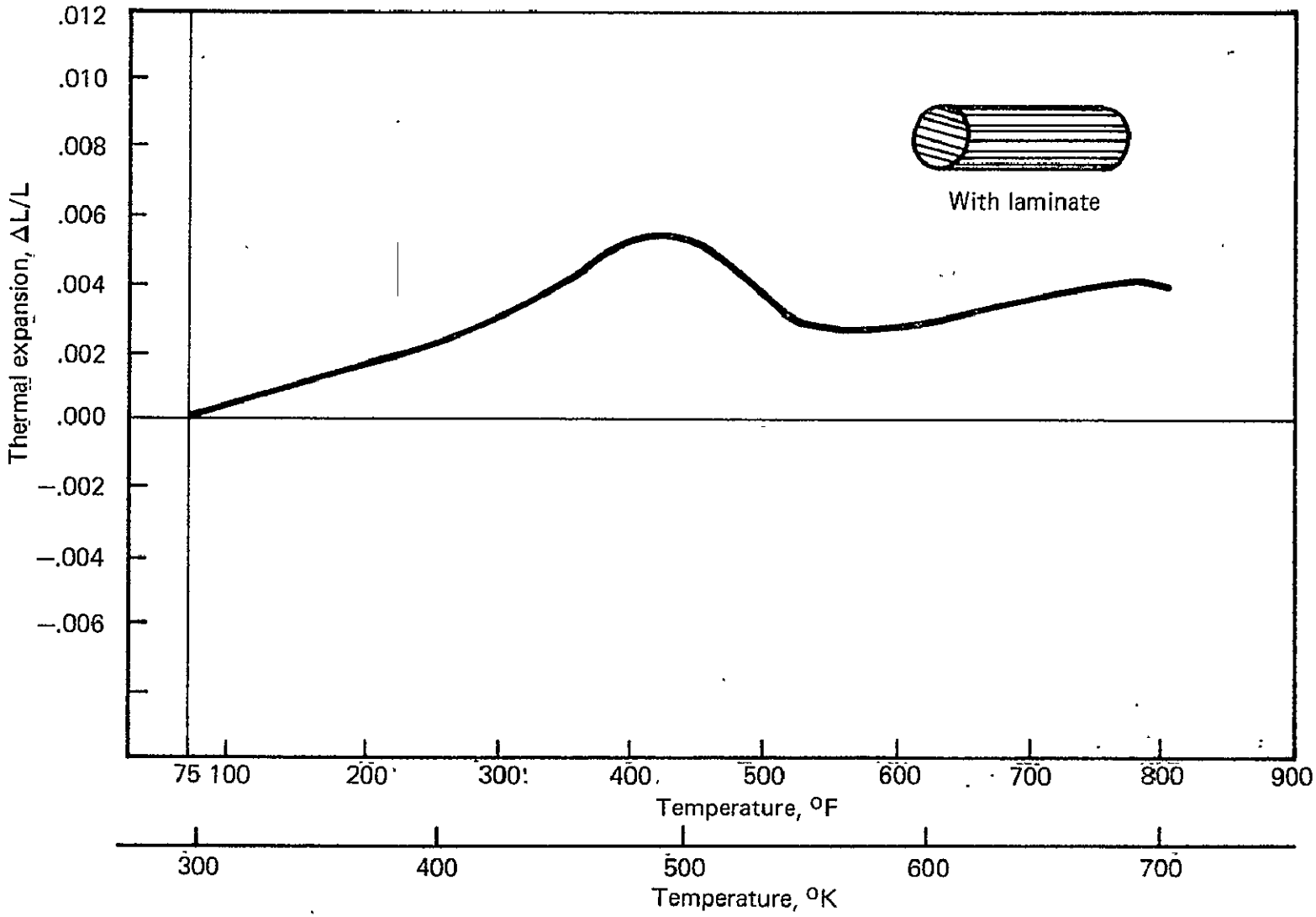

FIGURE A–1.7 THERMAL EXPANSION VERSUS TEMPERATURE OF FM 5072

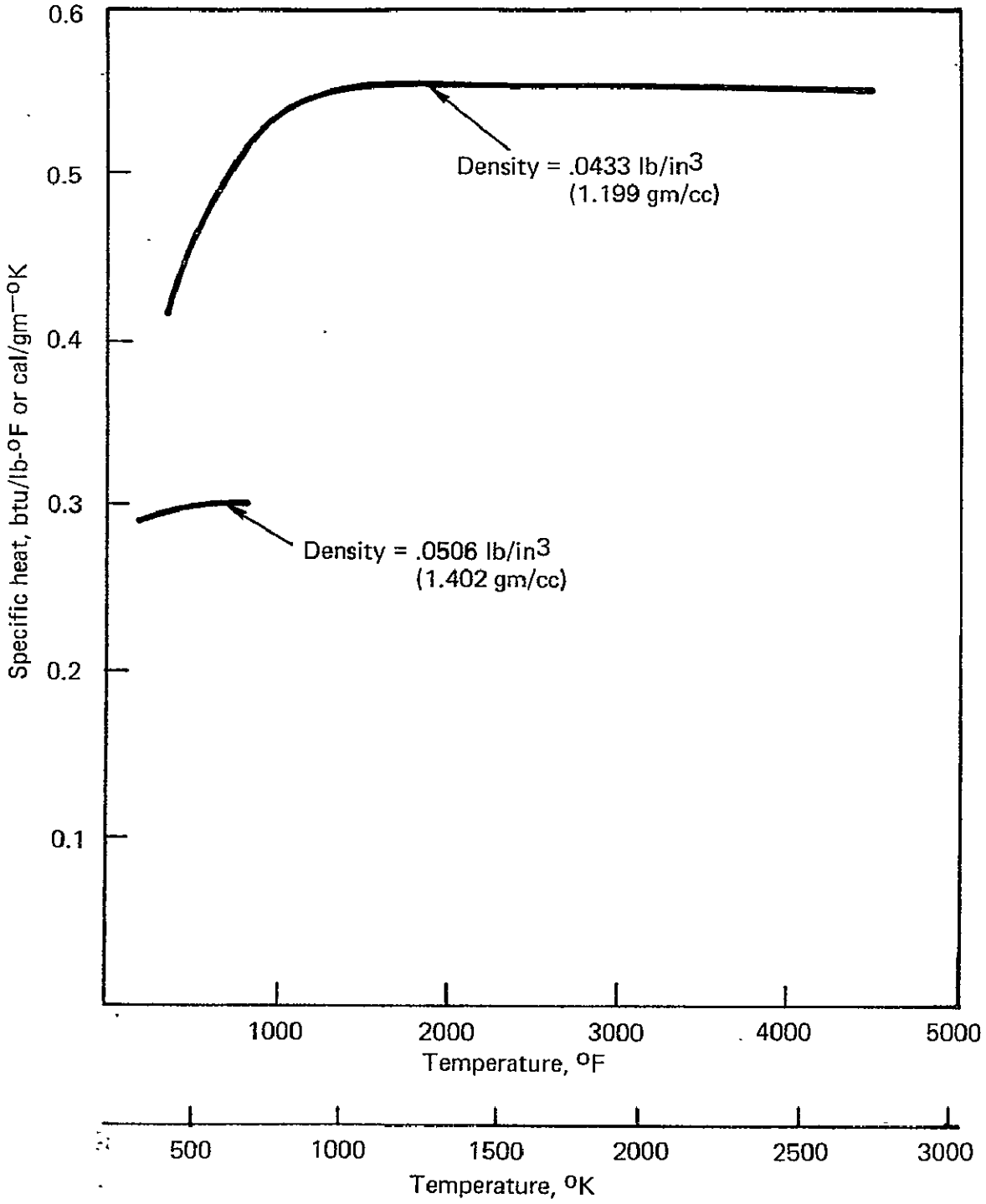

FIGURE A–1.8 SPECIFIC HEAT VS TEMPERATURE OF CARBON PHENOLIC FM 5072

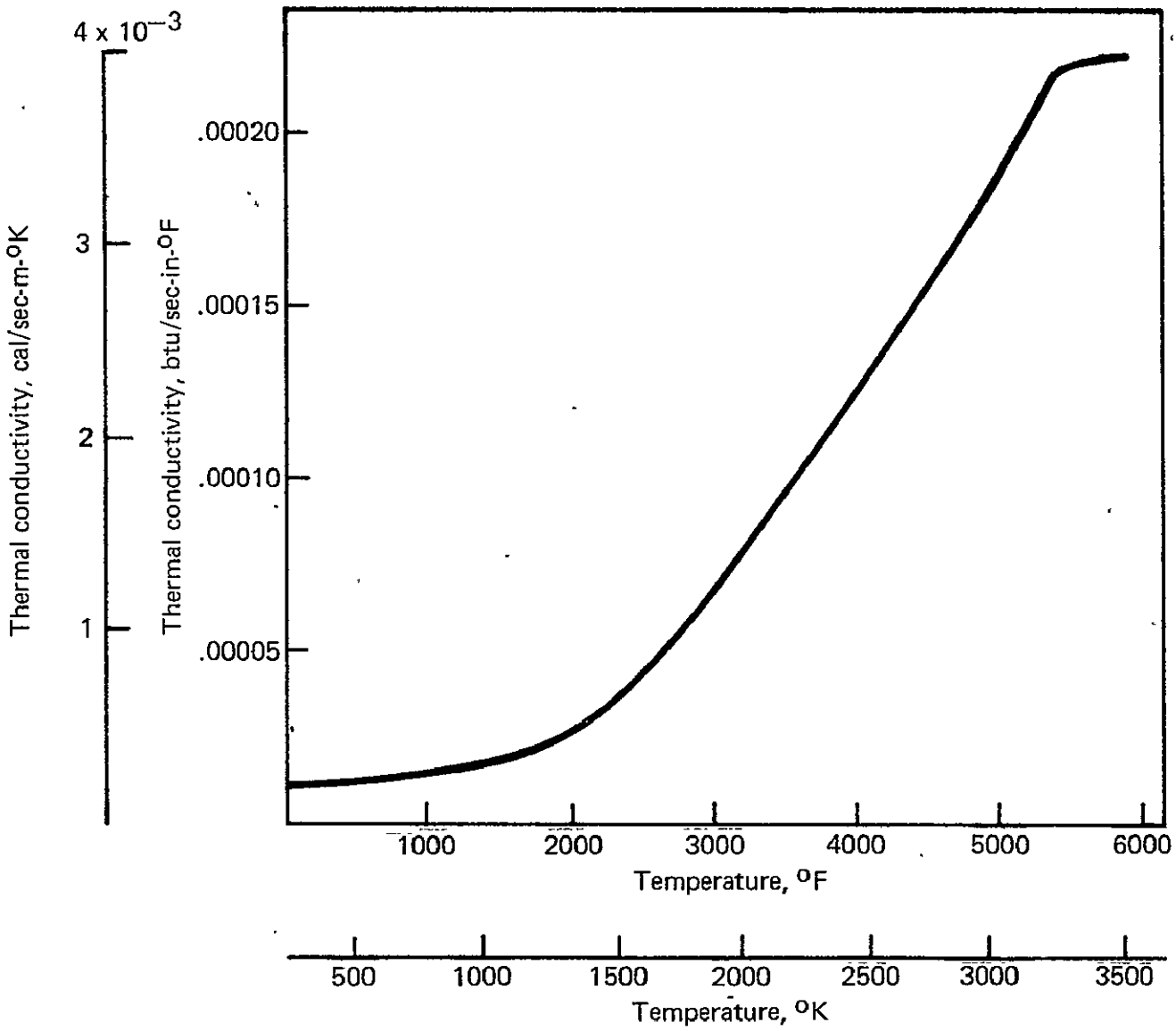

FIGURE A–1.9 THERMAL CONDUCTIVITY VERSUS TEMPERATURE OF CARBON PHENOLIC (FM 5072)

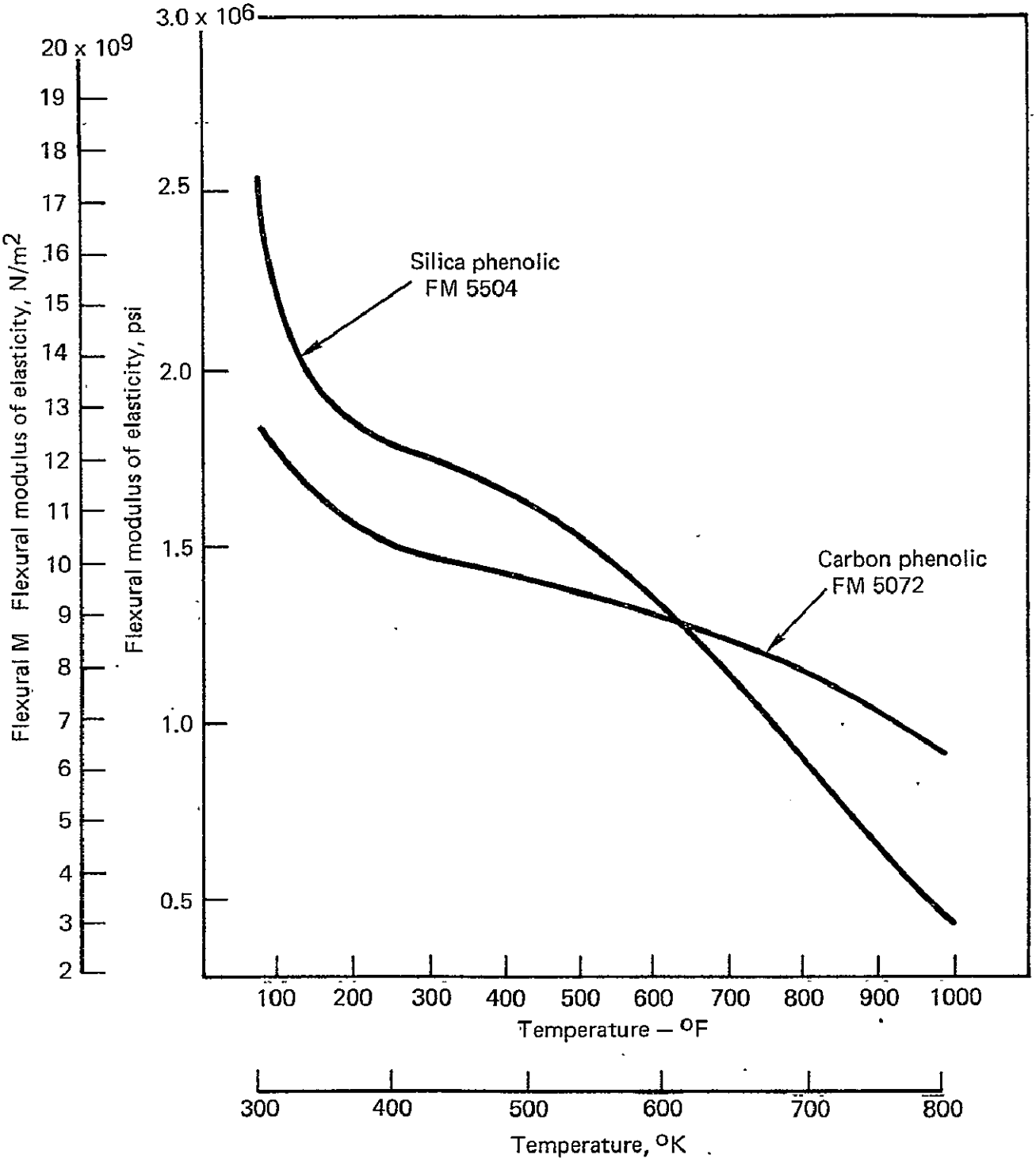

FIGURE A–2.1 FLEXURAL MODULUS OF ELASTICITY VERSUS TEMPERATURE OF FABRIC REINFORCED COMPOSITES

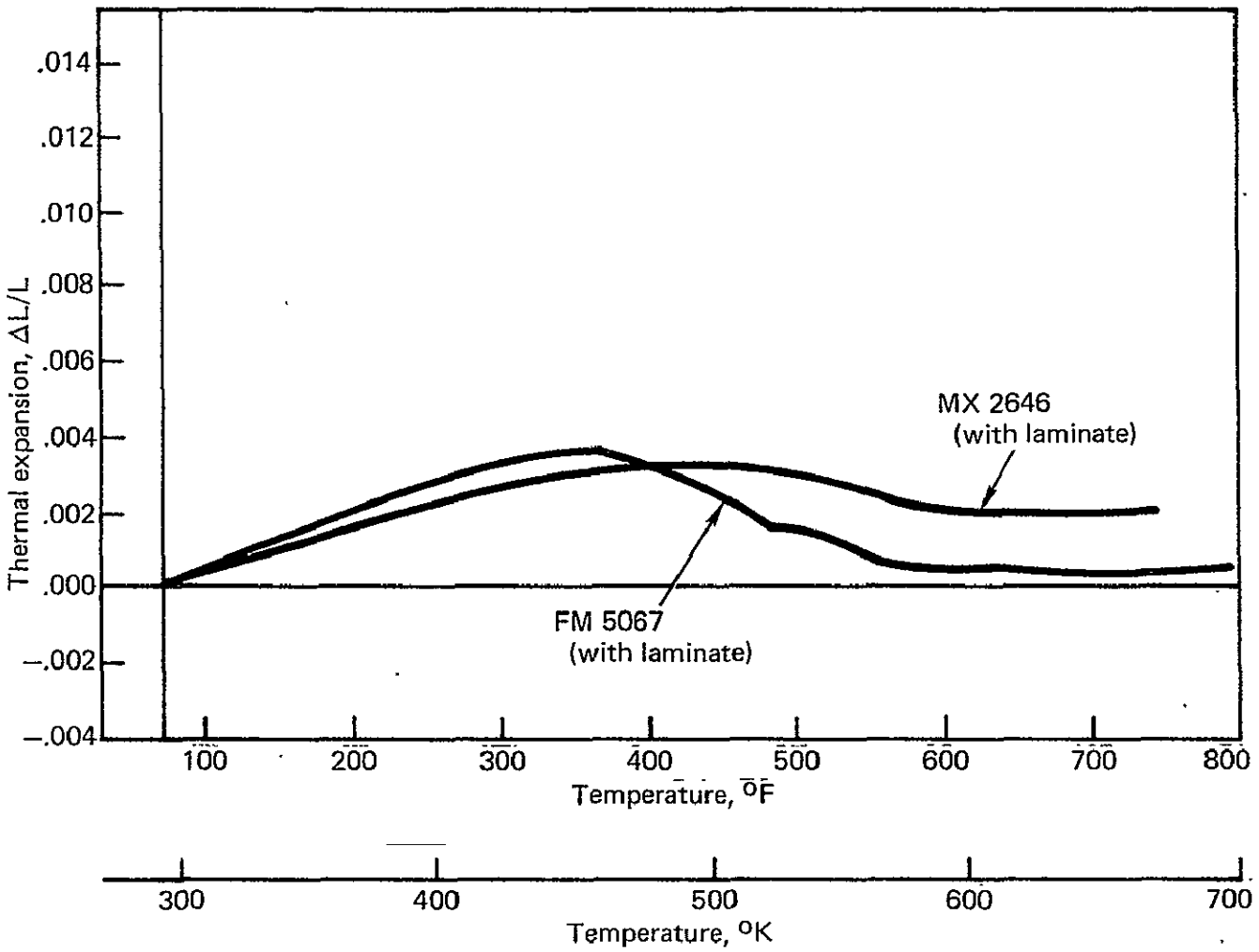

FIGURE A–3.1 THERMAL EXPANSION VERSUS TEMPERATURE OF SILICA REINFORCED PHENOLICS

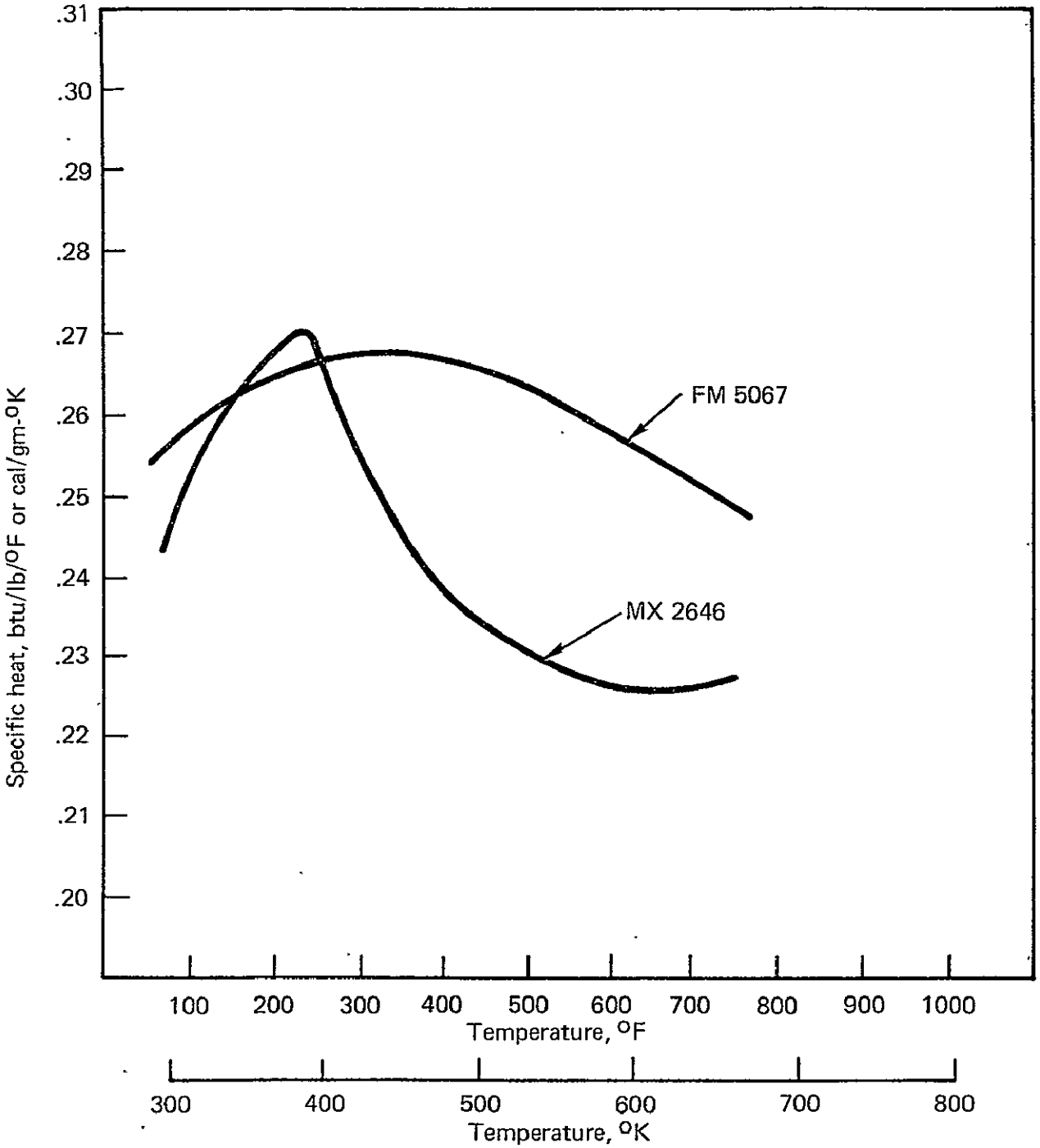

FIGURE A–3.2 SPECIFIC HEAT VERSUS TEMPERATURE OF SILICA REINFORCED COMPOSITES

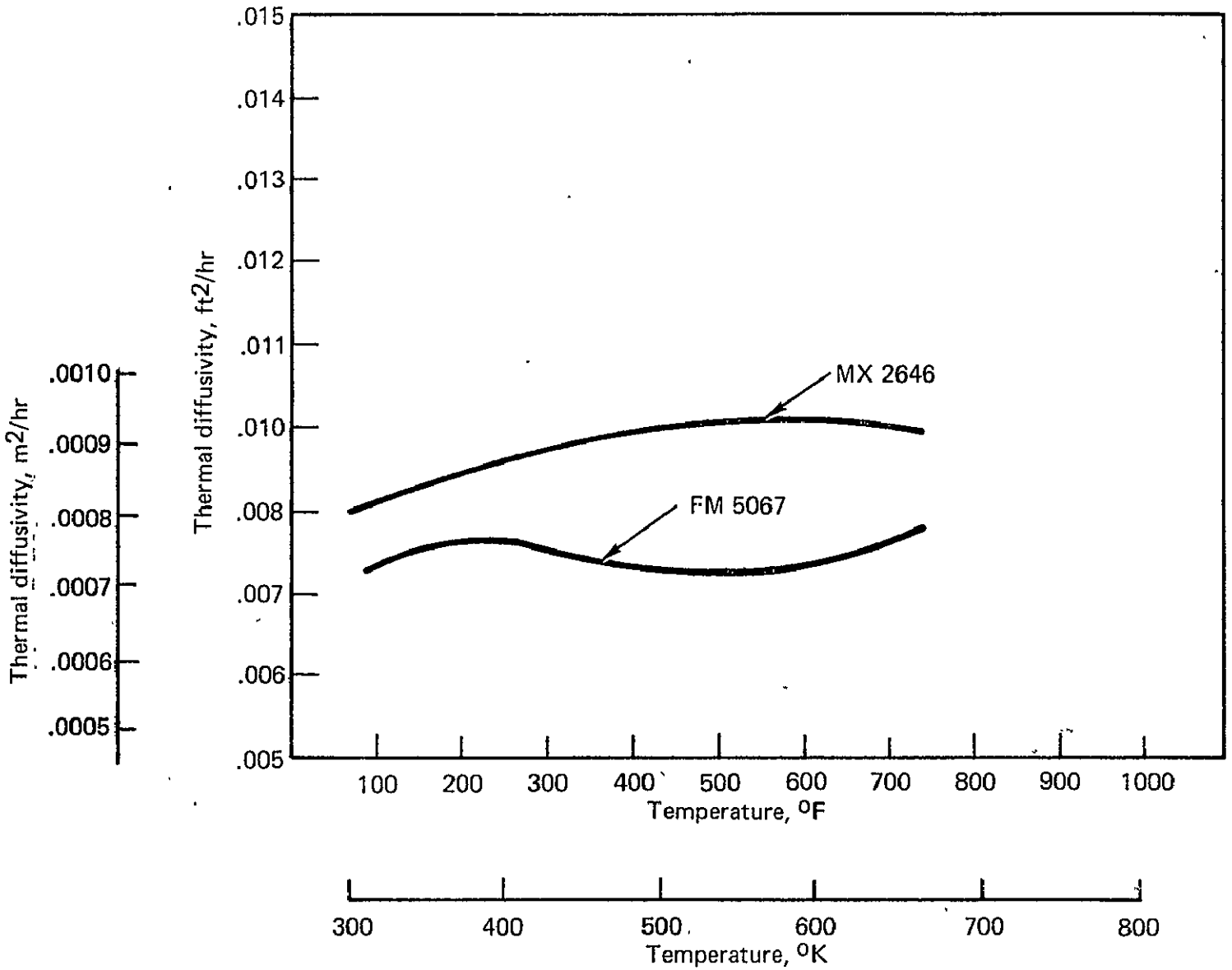

FIGURE A–3.3 THERMAL DIFFUSIVITY VERSUS TEMPERATURE OF SILICA REINFORCED COMPOSITES

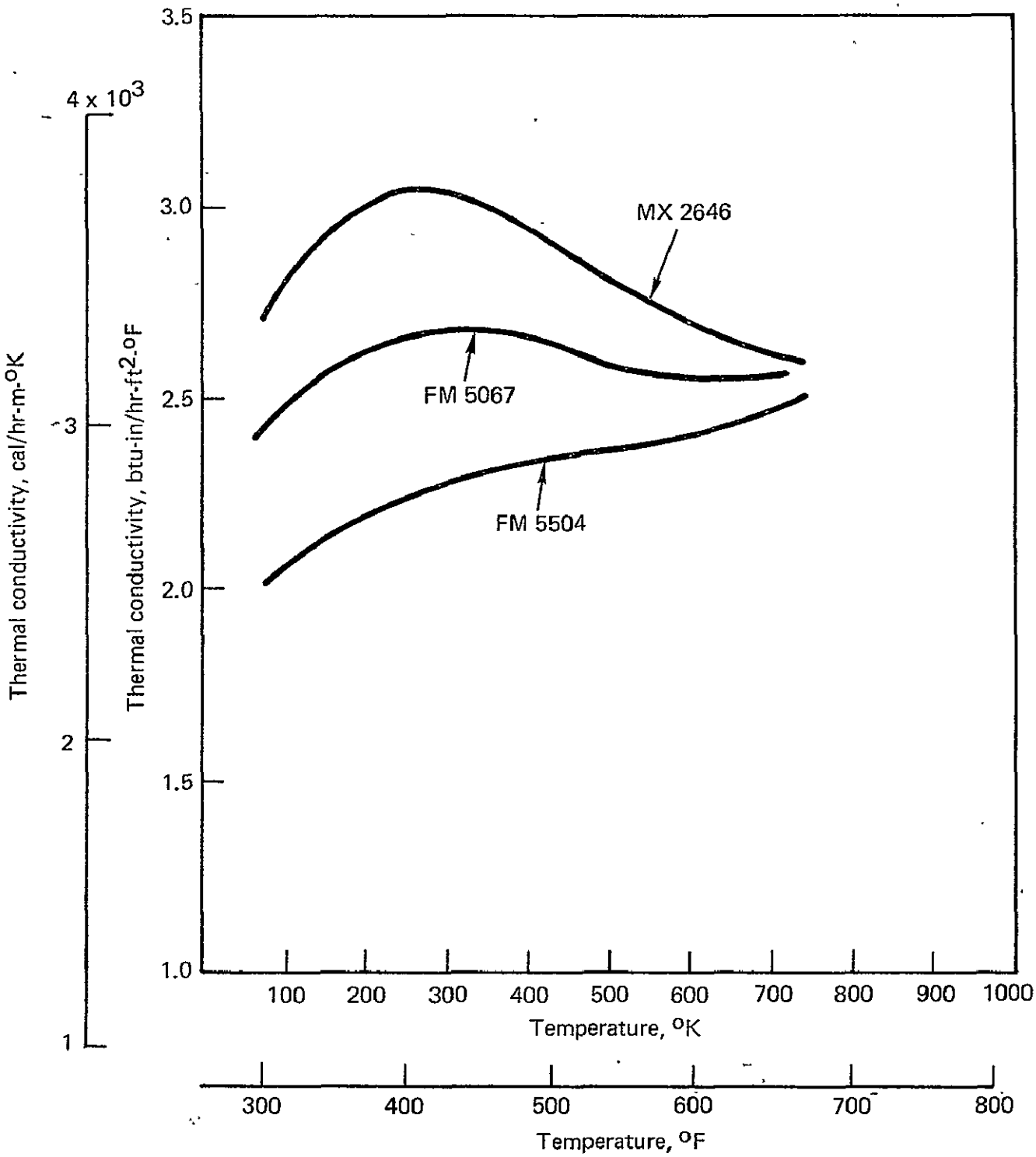

FIGURE A–3.4 THERMAL CONDUCTIVITY VERSUS TEMPERATURE OF SILICA REINFORCED COMPOSITES, ACROSS LAMINATE

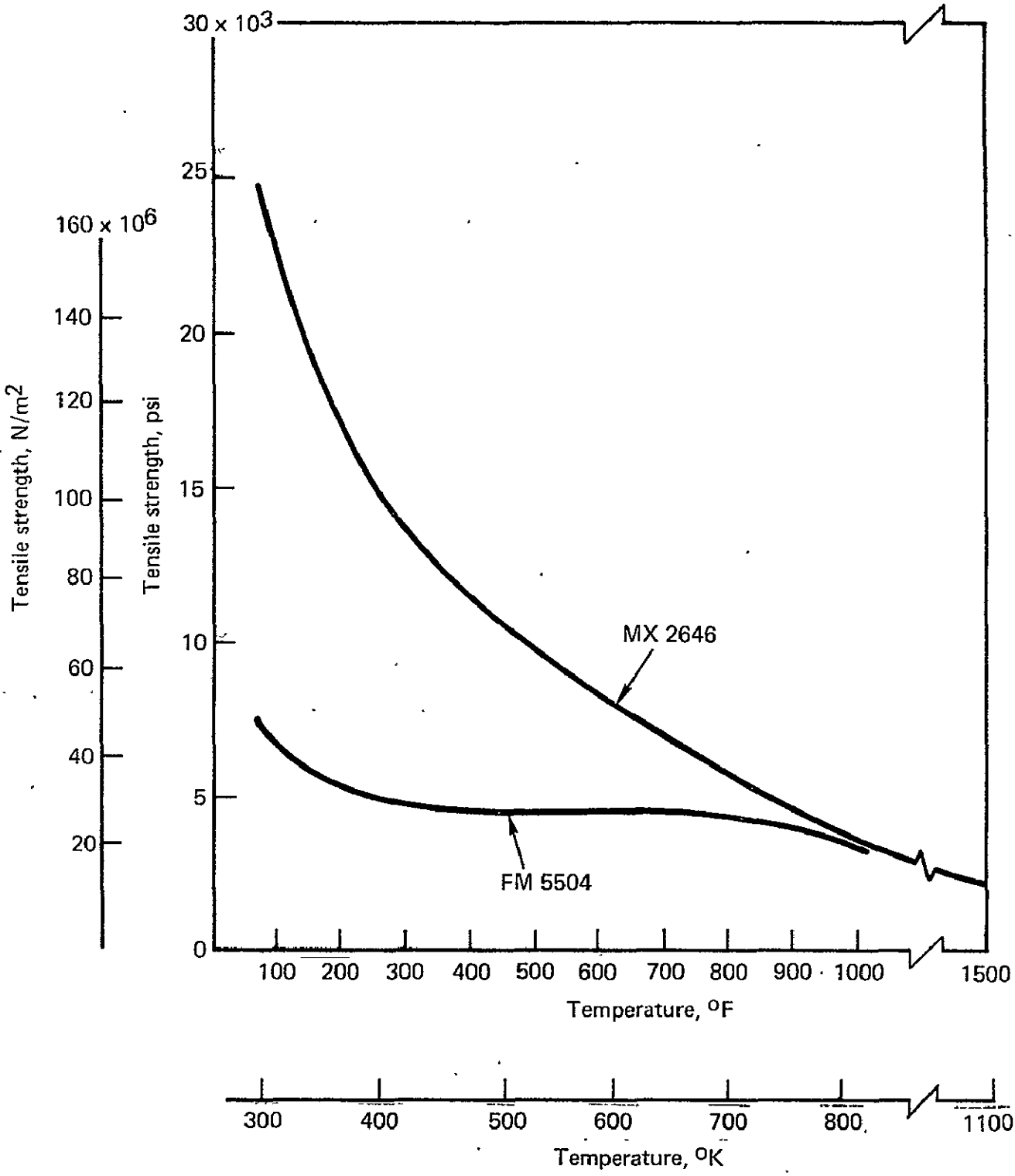

FIGURE A–3.5 TENSILE STRENGTH VERSUS TEMPERATURE OF SILICA REINFORCED COMPOSITES

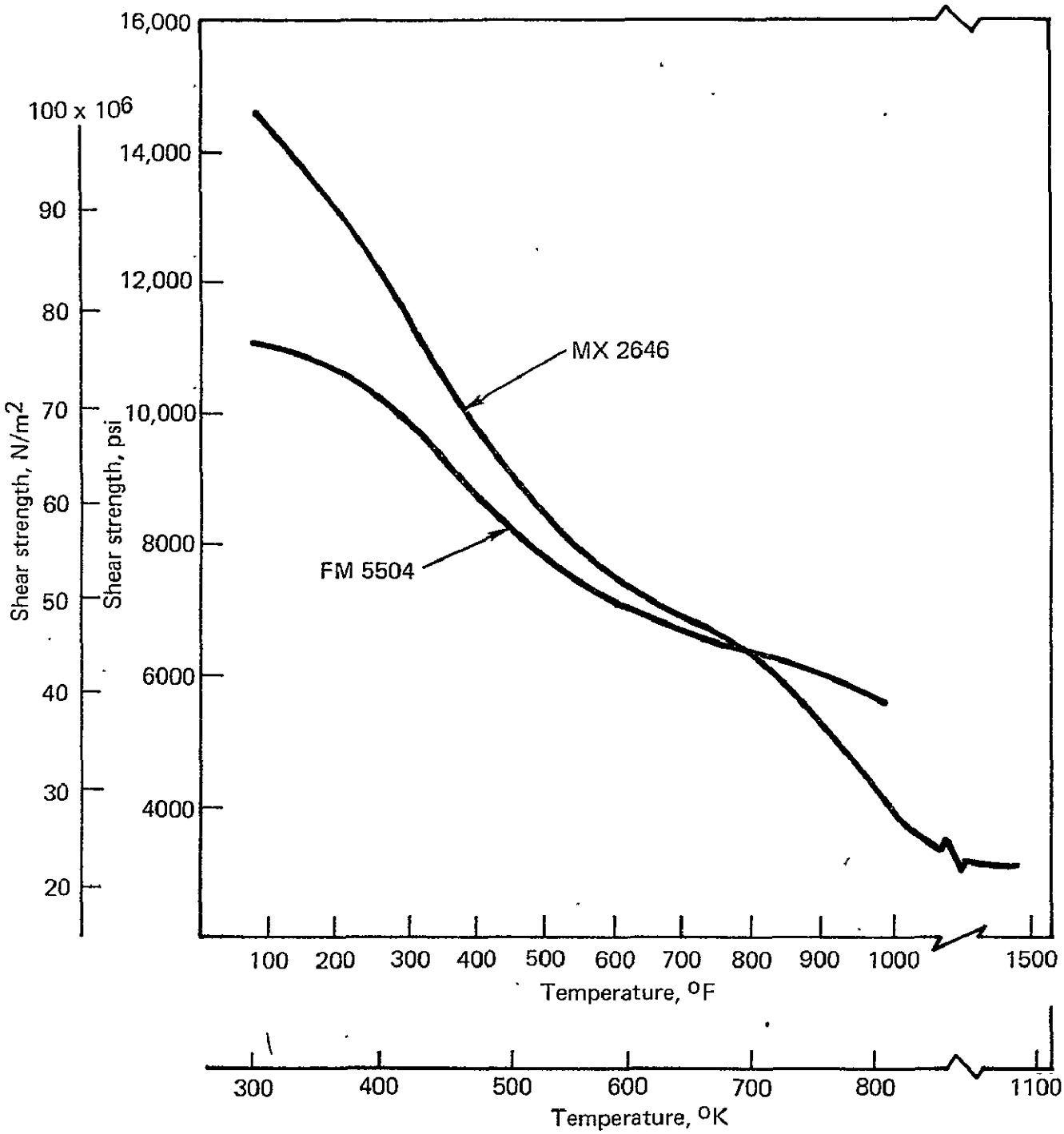

FIGURE A–3.6 SHEAR STRENGTH VERSUS TEMPERATURE OF SILICA REINFORCED COMPOSITES, ACROSS GRAIN

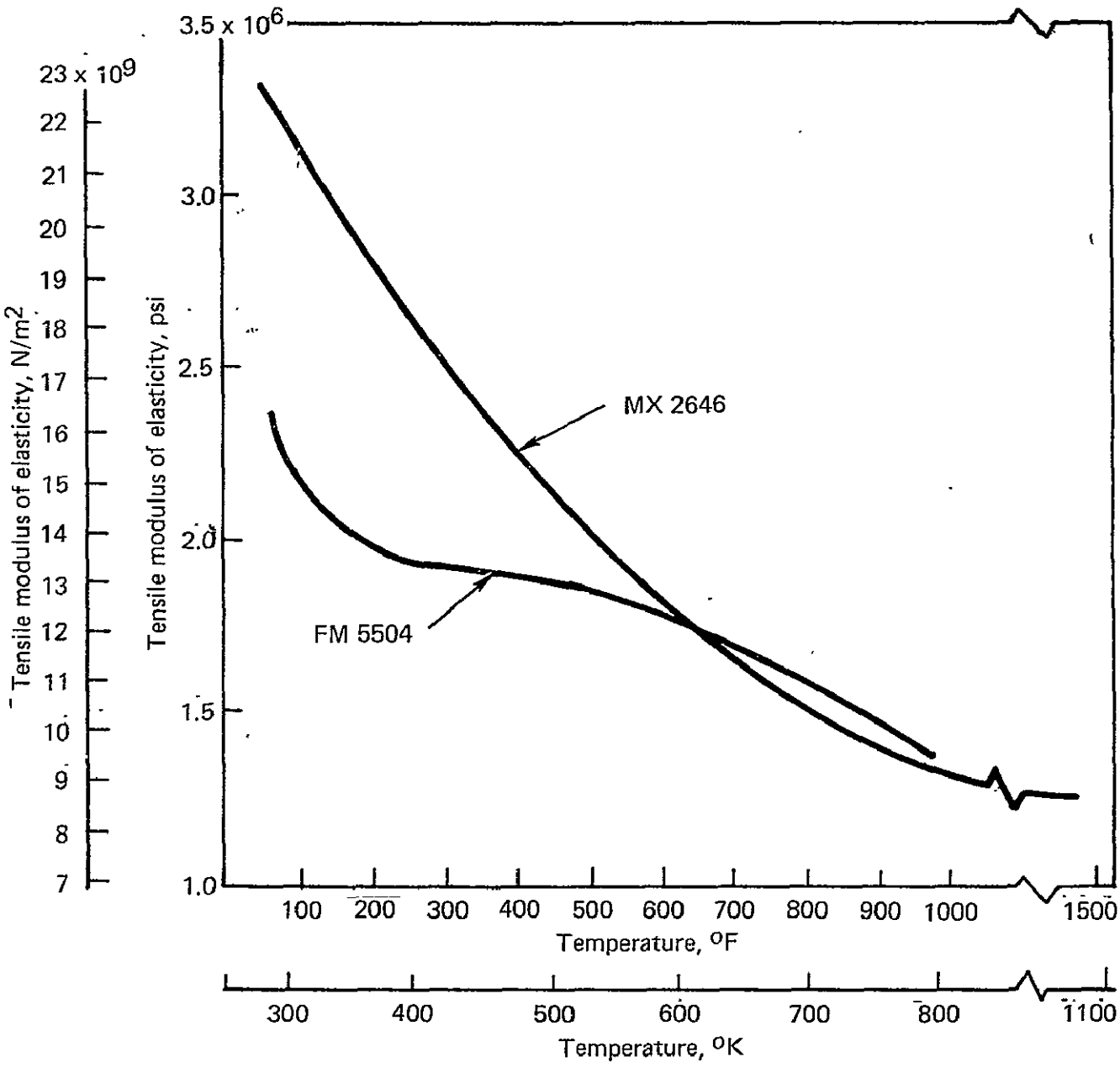

FIGURE A–3.7 TENSILE MODULUS OF ELASTICITY VERSUS TEMPERATURE OF SILICA REINFORCED COMPOSITES

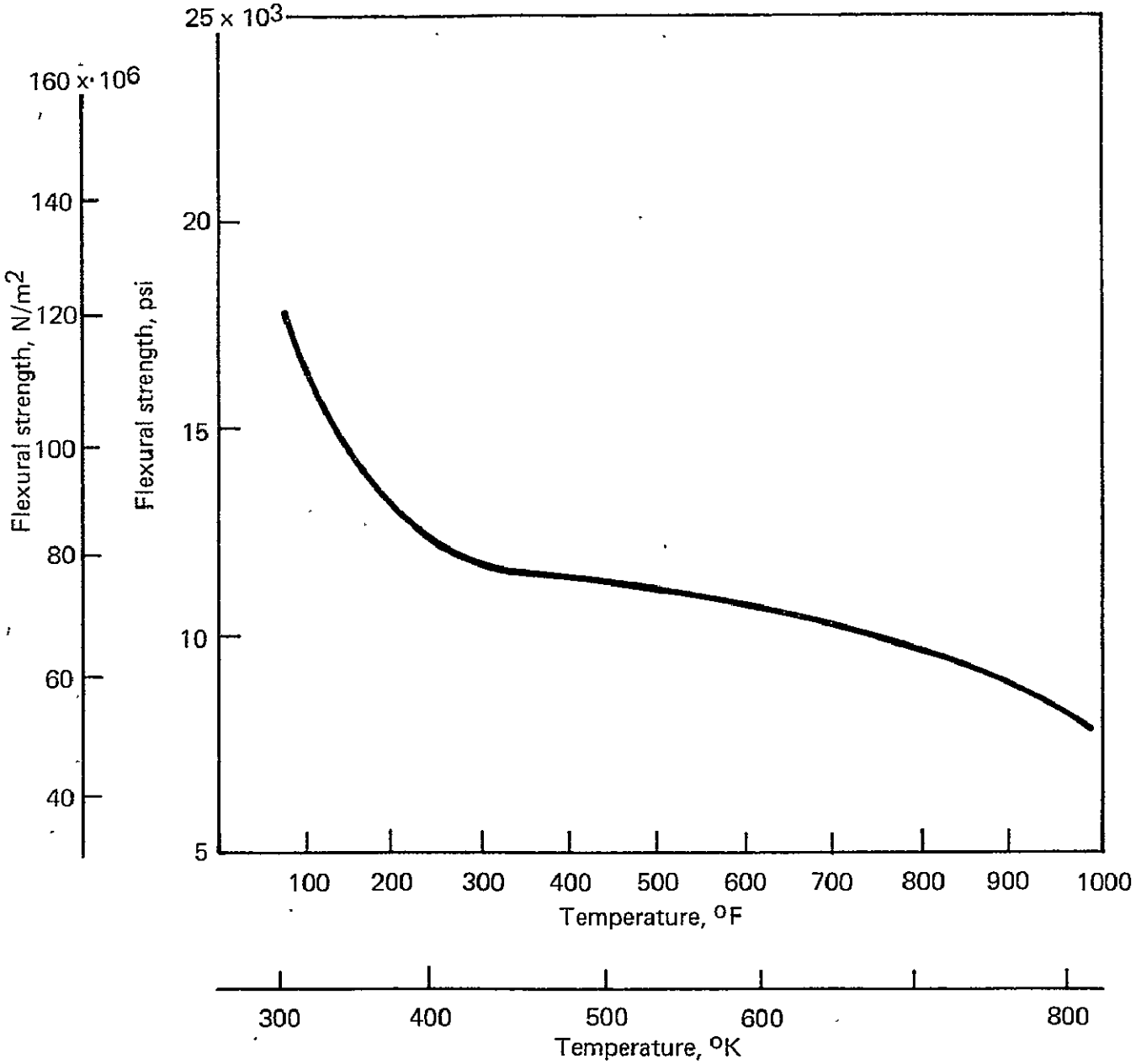

FIGURE A–3.8 FLEXURAL STRENGTH VERSUS TEMPERATURE OF FM 5504

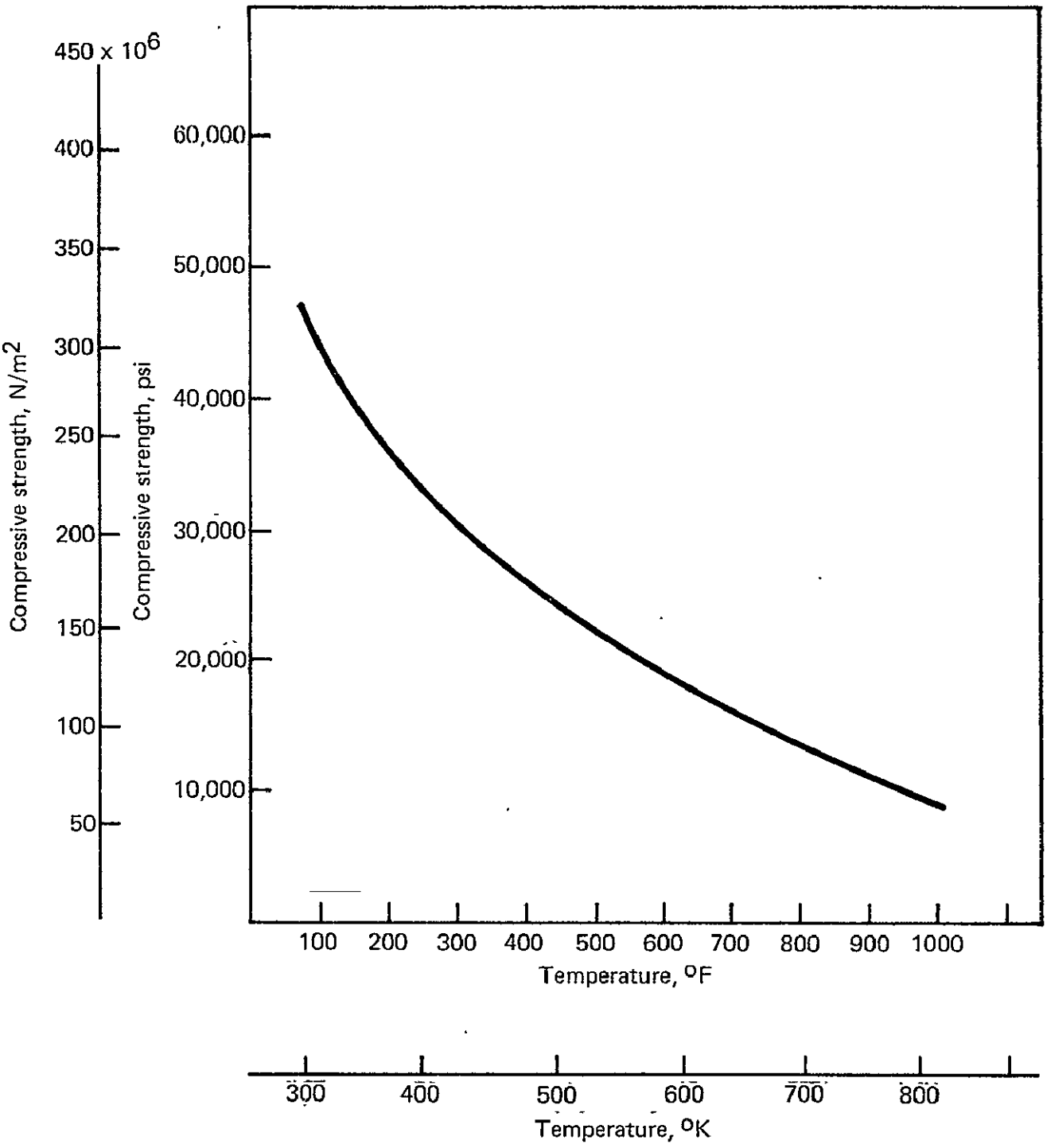

FIGURE A–3.9 COMPRESSIVE STRENGTH VERSUS TEMPERATURE OF FM 5504

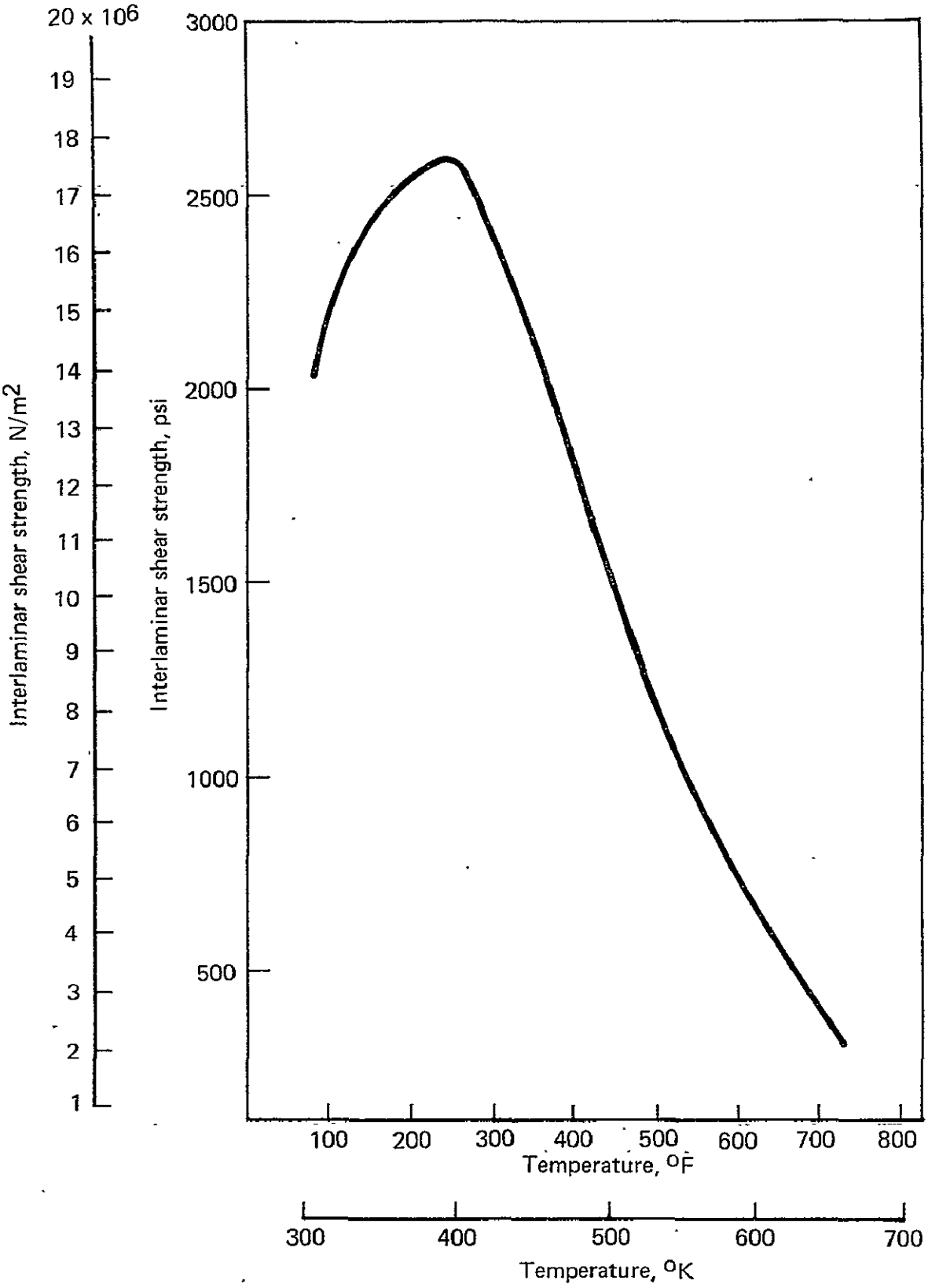

FIGURE A–3.10 INTERLAMINAR SHEAR STRENGTH VERSUS TEMPERATURE OF MX 2646

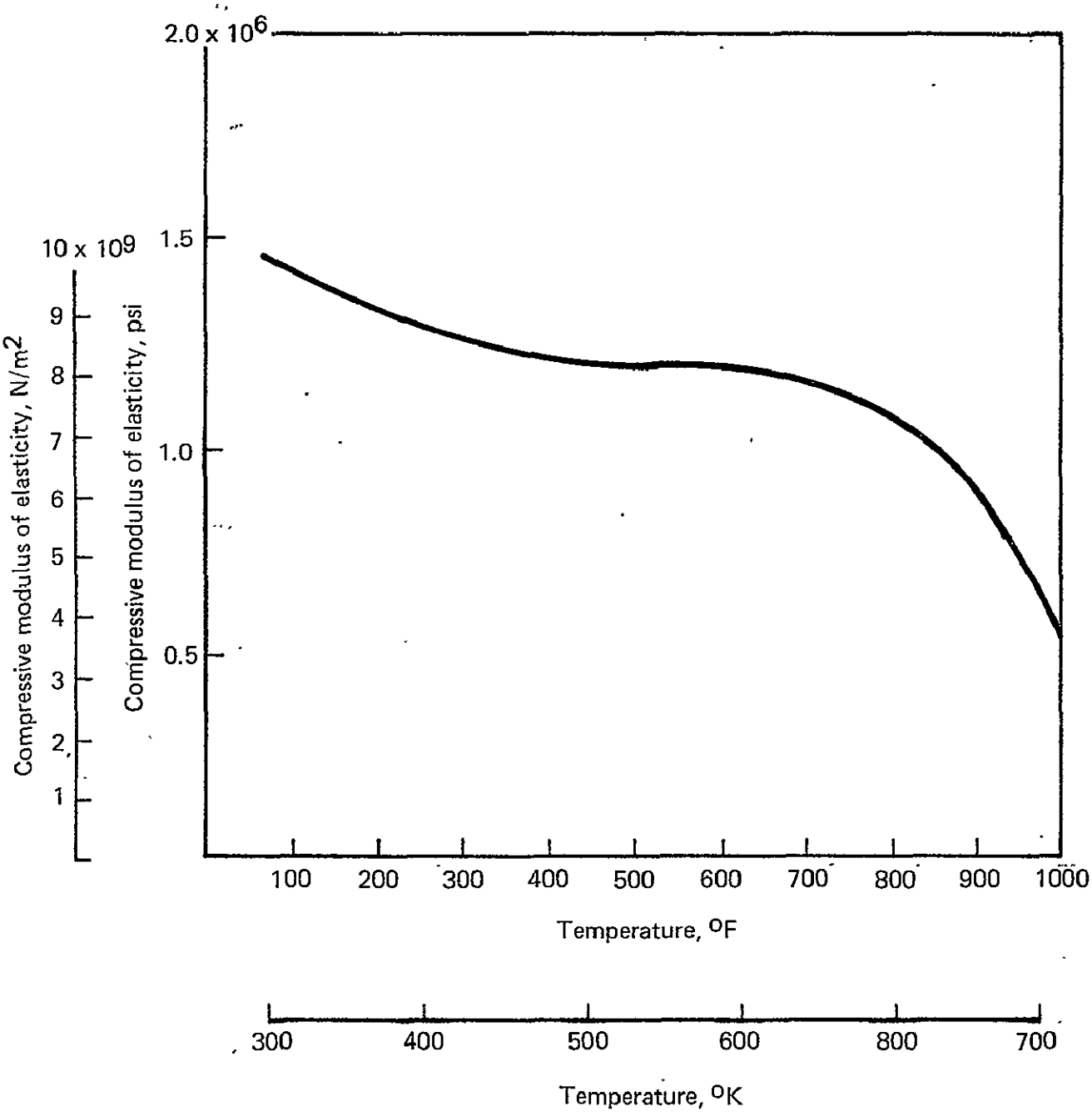

FIGURE A–3.11 COMPRESSIVE MODULUS OF ELASTICITY VERSUS TEMPERATURE OF FM 5504 ACROSS LAMINATE

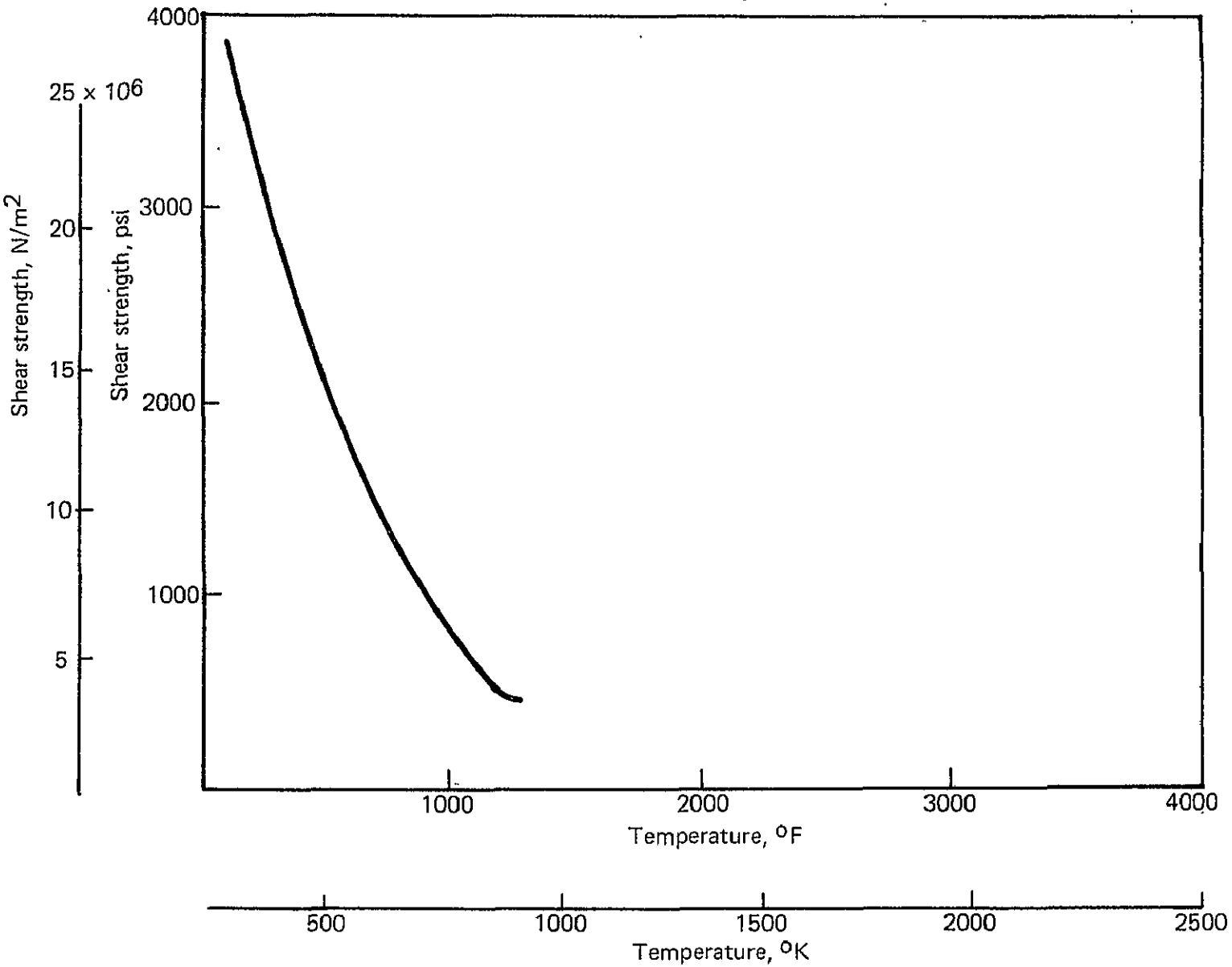

FIGURE A–4.1 SHEAR STRENGTH VERSUS TEMPERATURE OF HT-424 ADHESIVE

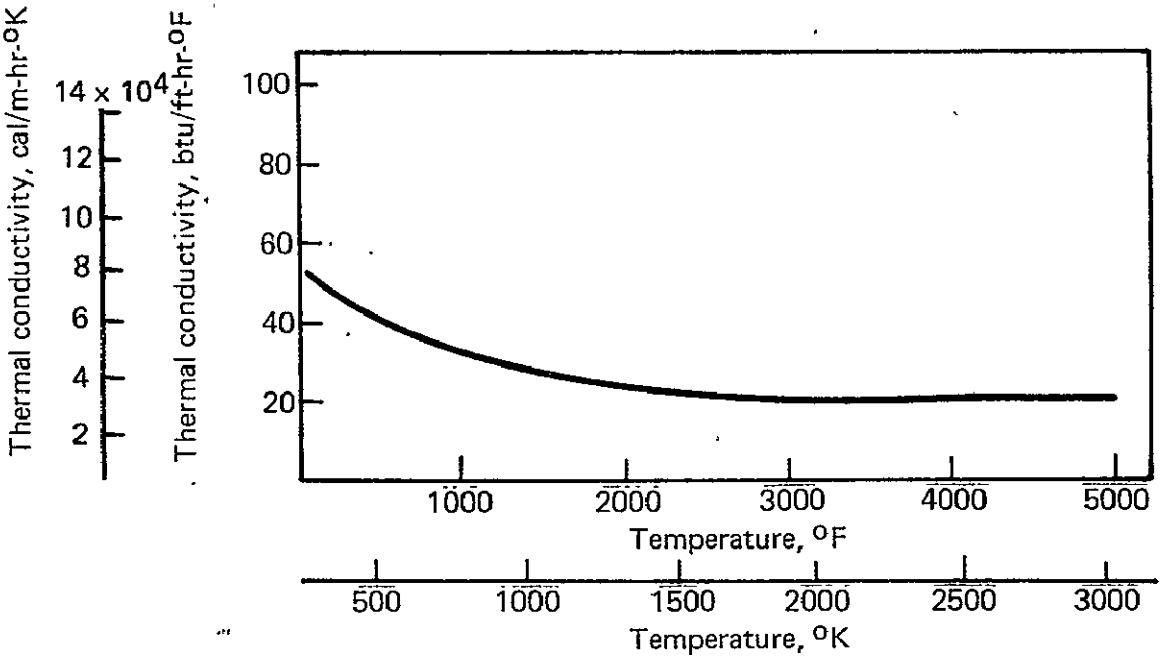

FIGURE A–5.1 THERMAL CONDUCTIVITY VERSUS TEMPERATURE OF ATJ GRAPHITE ACROSS GRAIN

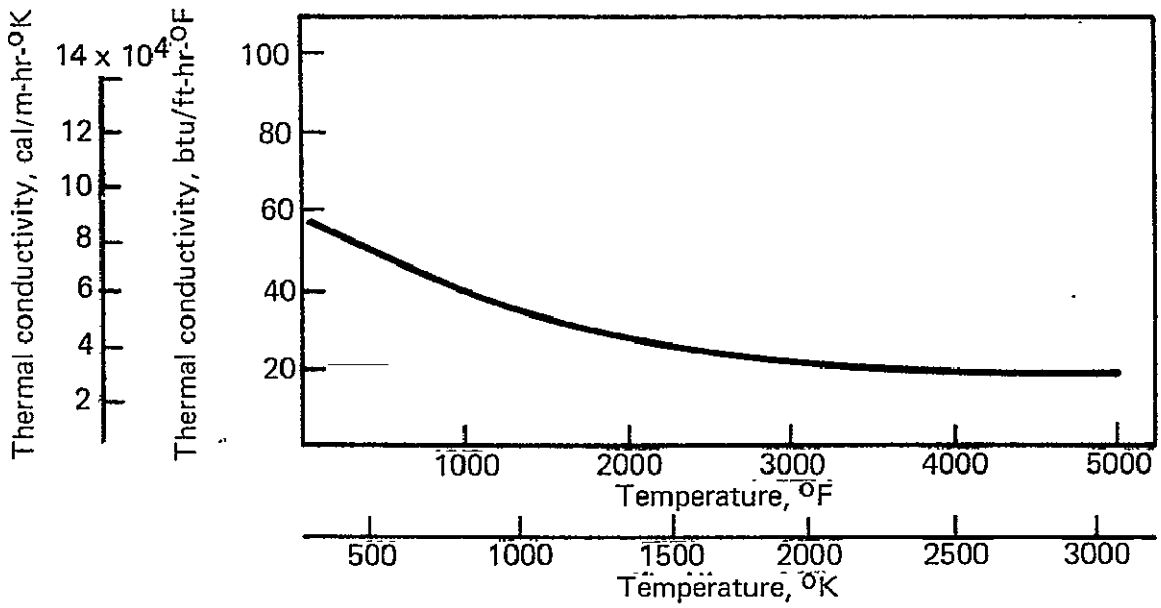

FIGURE A–5.2 THERMAL CONDUCTIVITY VERSUS TEMPERATURE OF ATJ GRAPHITE WITH GRAIN

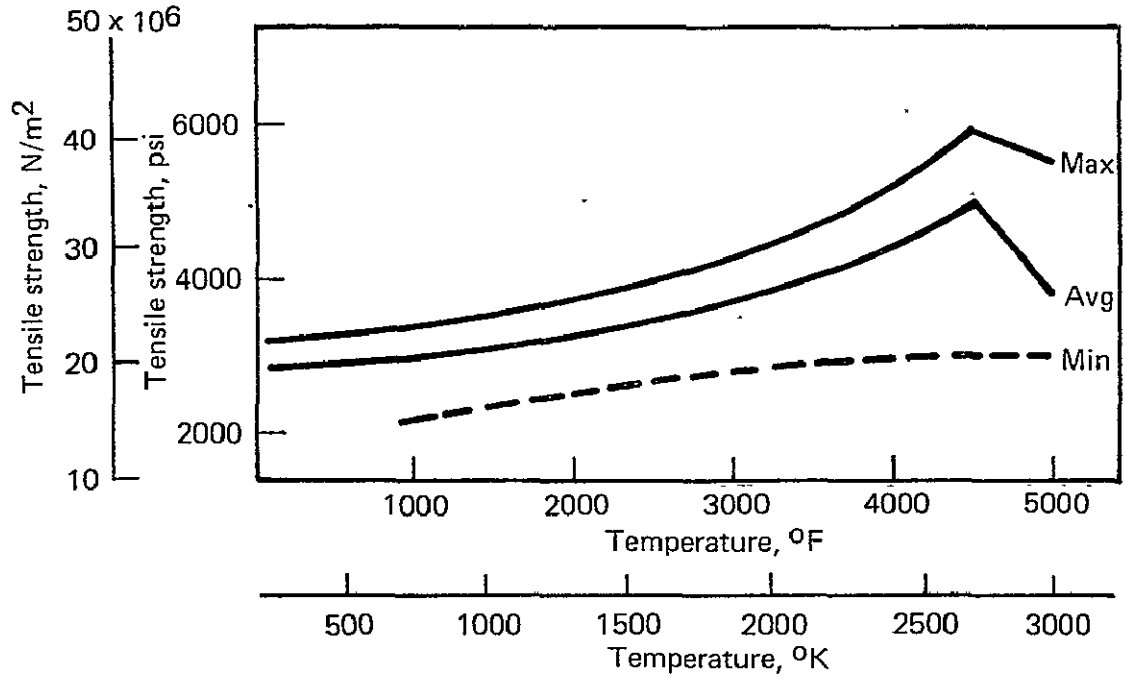

FIGURE A–5.3 TENSILE STRENGTH VERSUS TEMPERATURE OF ATJ GRAPHITE ACROSS GRAIN

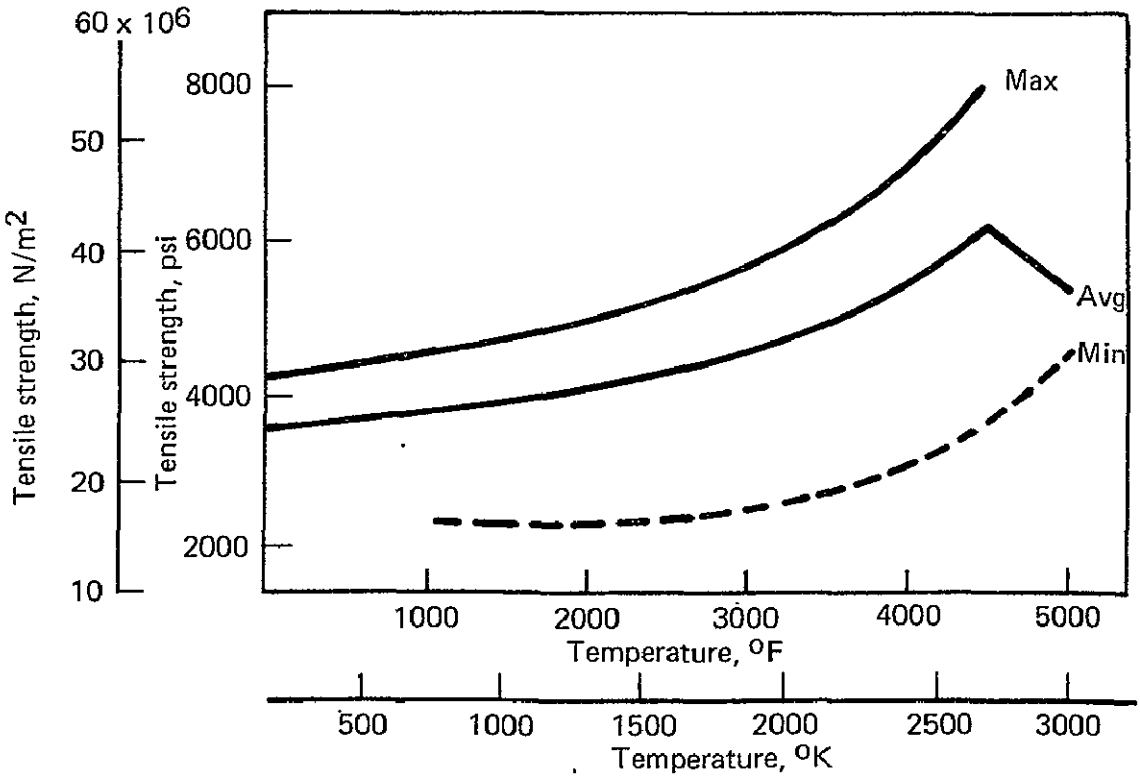

FIGURE A–5.4 TENSILE STRENGTH VERSUS TEMPERATURE OF ATJ GRAPHITE WITH GRAIN

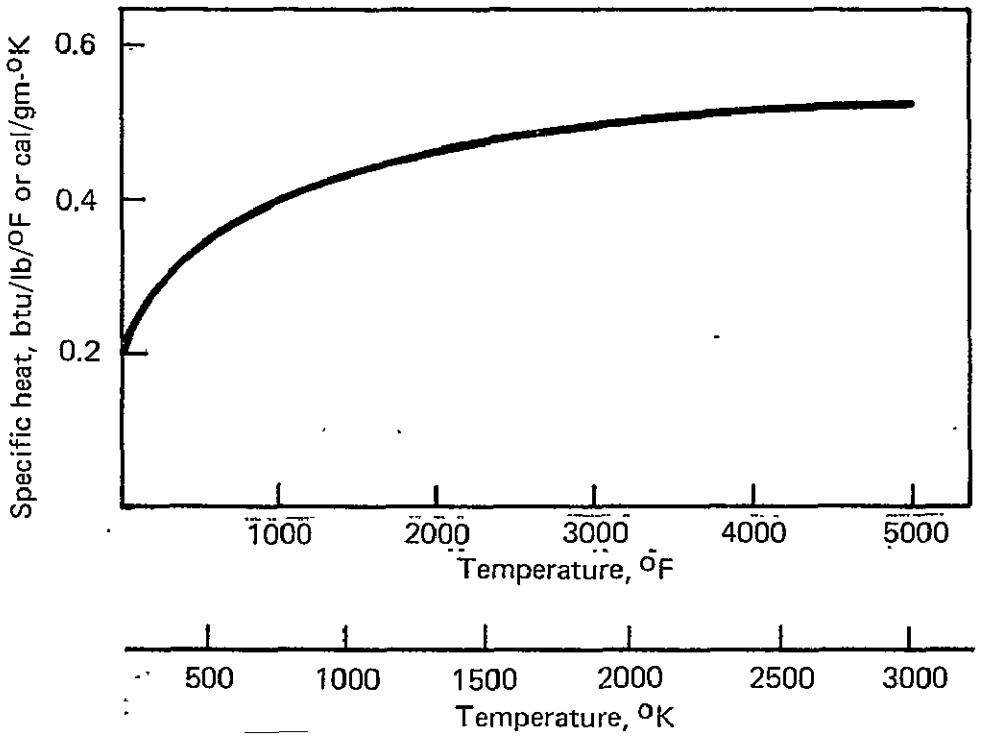

FIGURE A–5.5 SPECIFIC HEAT VERSUS TEMPERATURE OF ATJ GRAPHITE

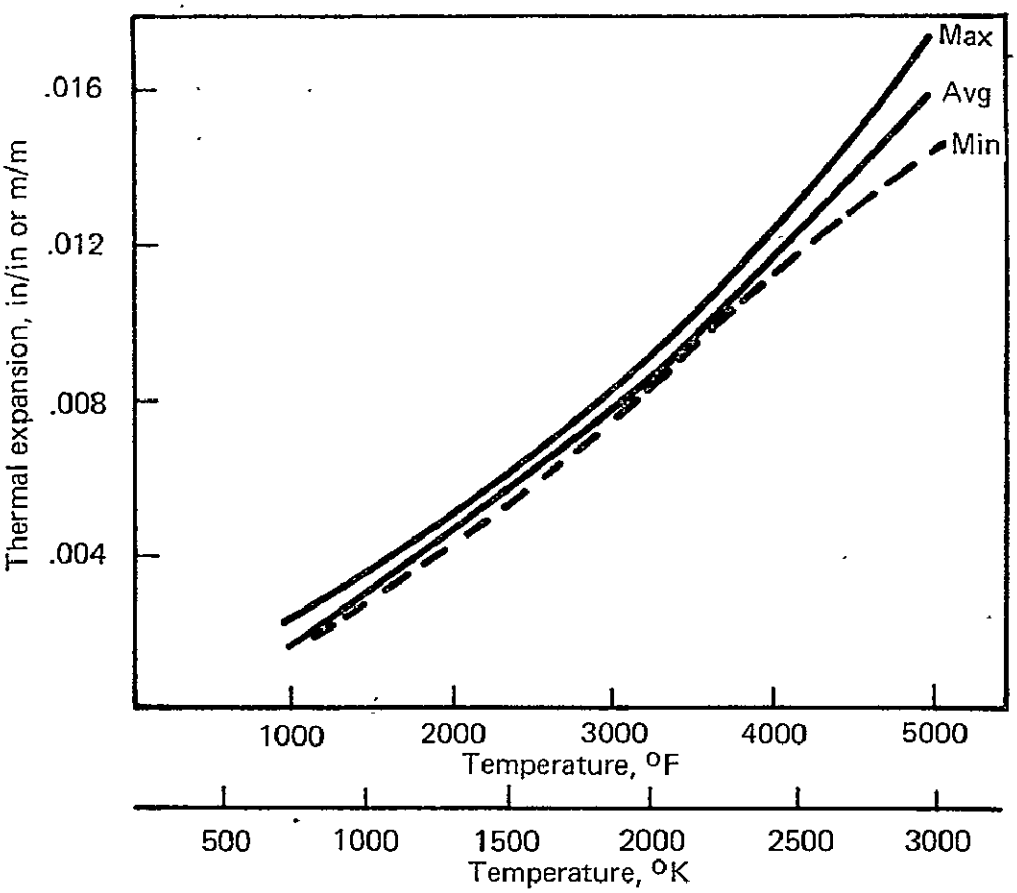

FIGURE A–5.6 THERMAL EXPANSION VERSUS TEMPERATURE OF ATJ GRAPHITE ACROSS GRAIN

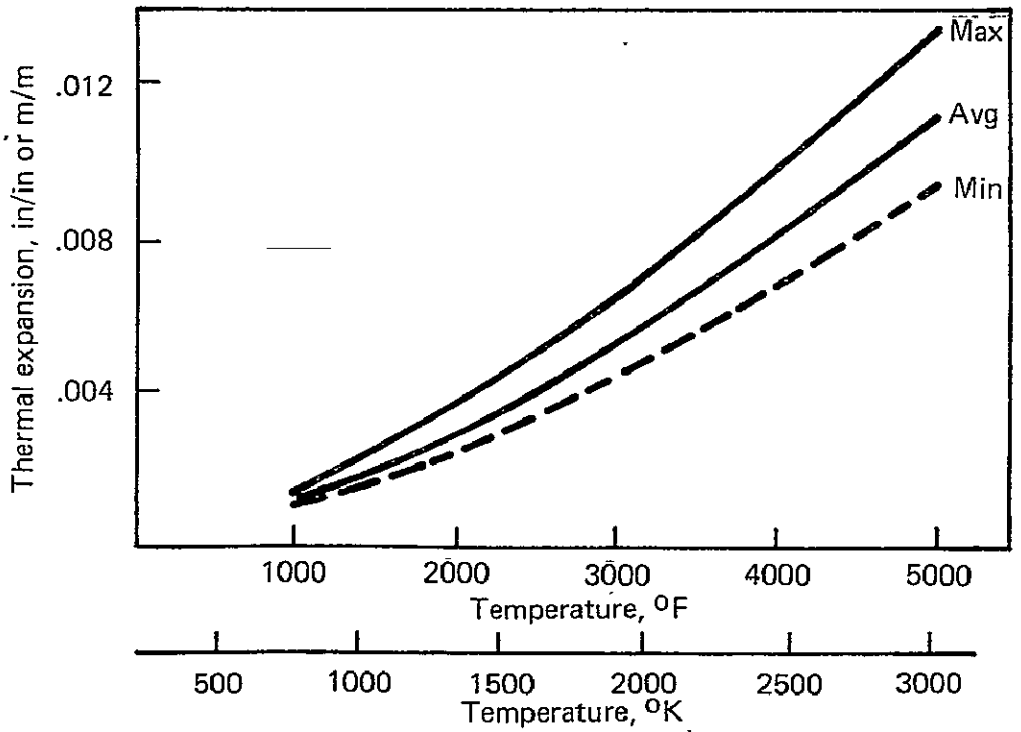

FIGURE A–5.7 THERMAL EXPANSION VERSUS TEMPERATURE OF ATJ GRAPHITE WITH GRAIN

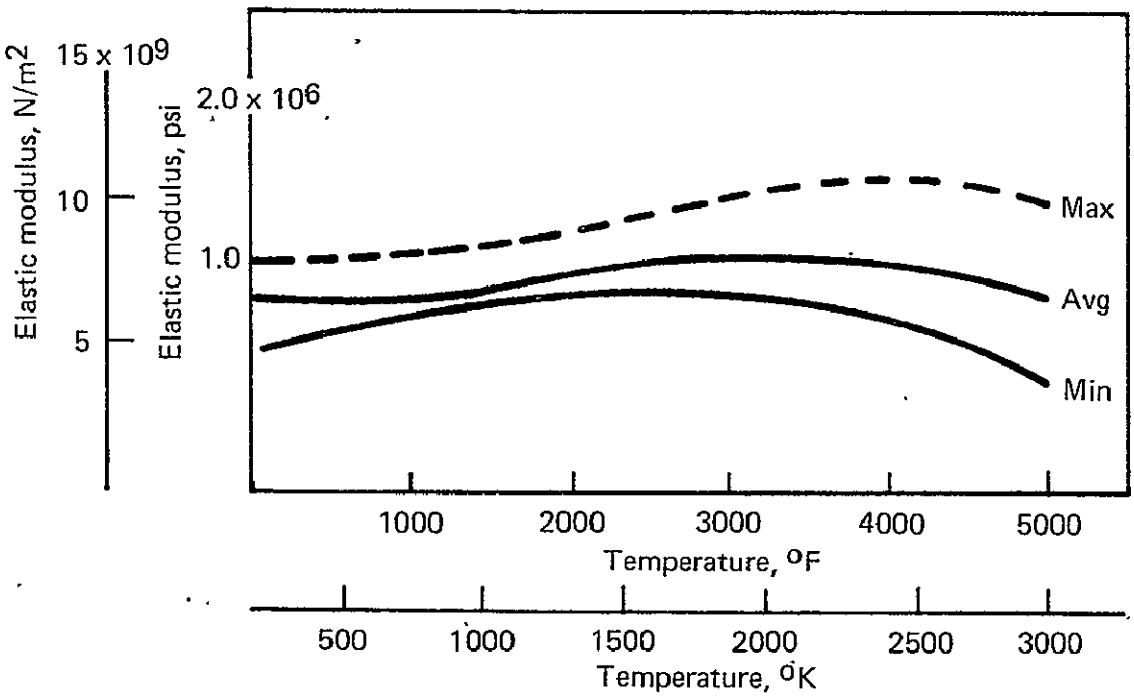

FIGURE A–5.8 ELASTIC MODULUS VERSUS TEMPERATURE OF ATJ GRAPHITE ACROSS GRAIN

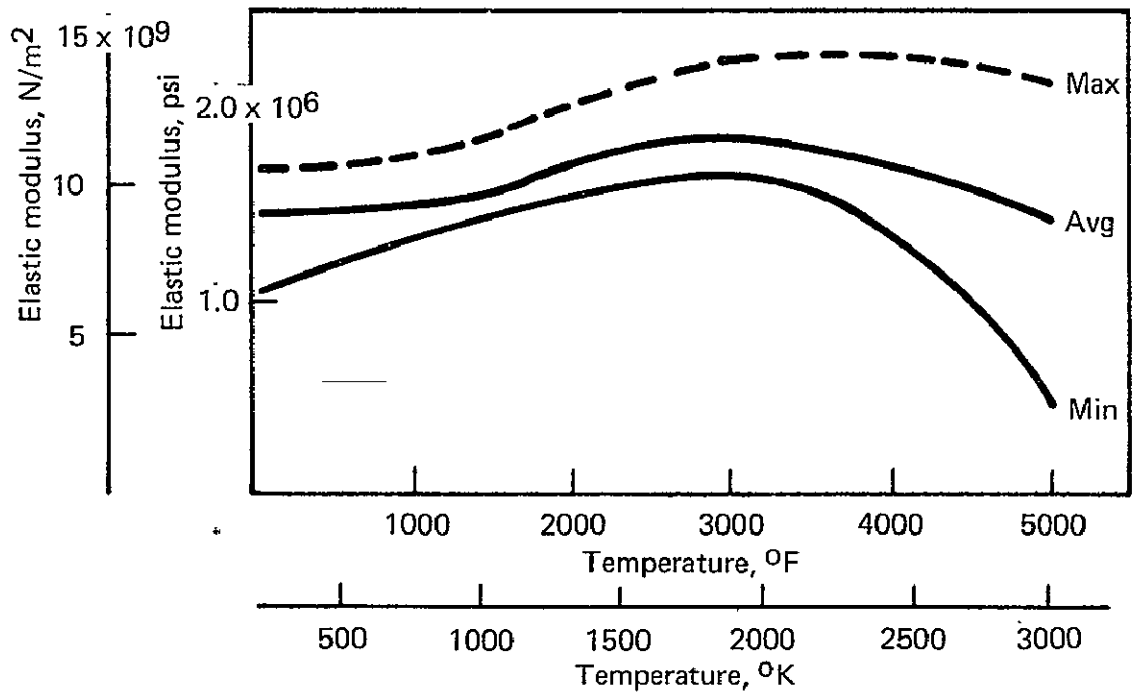

FIGURE A–5.9 ELASTIC MODULUS VERSUS TEMPERATURE OF ATJ GRAPHITE WITH GRAIN

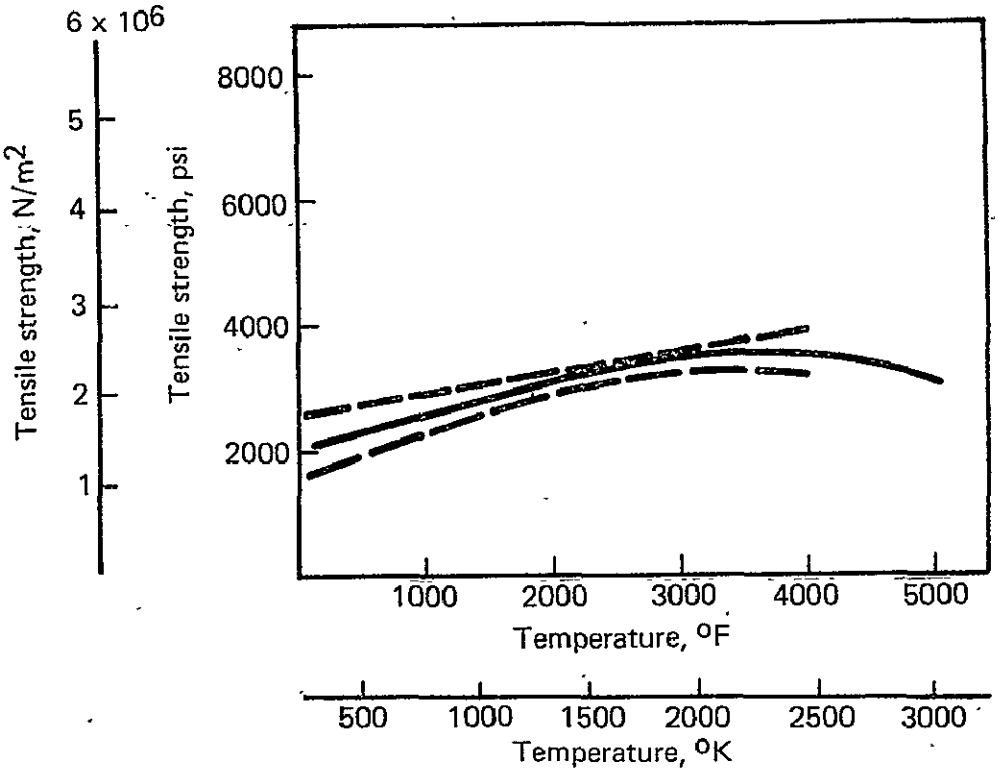

FIGURE A–6.1 TENSILE STRENGTH VERSUS TEMPERATURE OF GRAPHITE-G ACROSS GRAIN

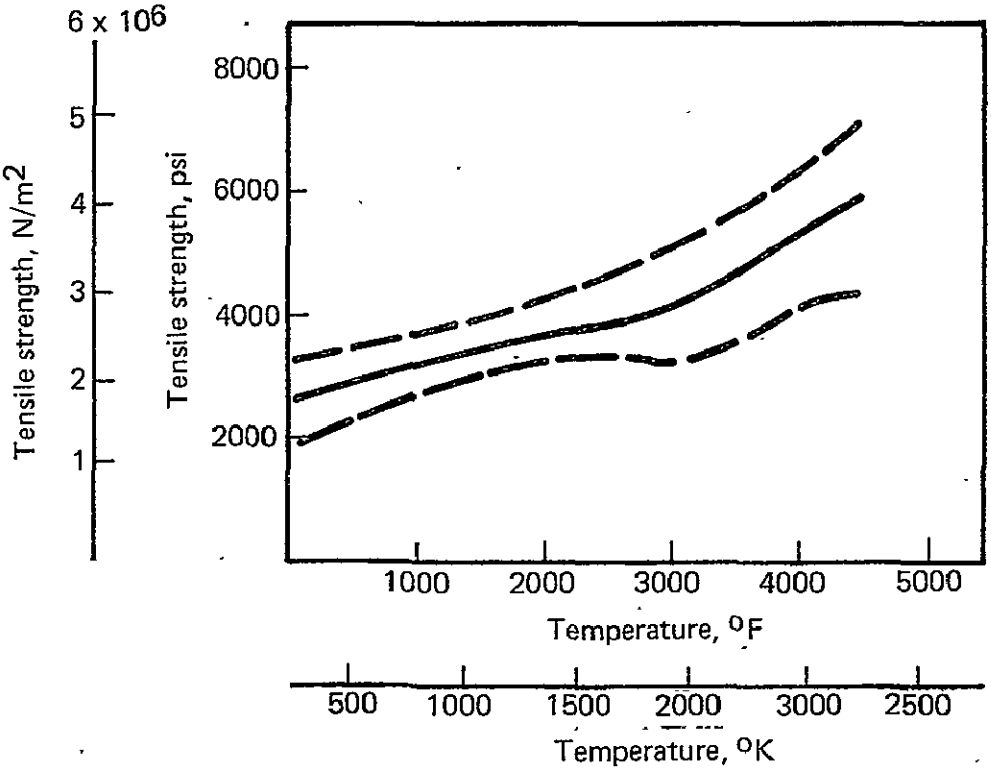

FIGURE A–6.2 TENSILE STRENGTH VERSUS TEMPERATURE OF GRAPHITE-G WITH GRAIN

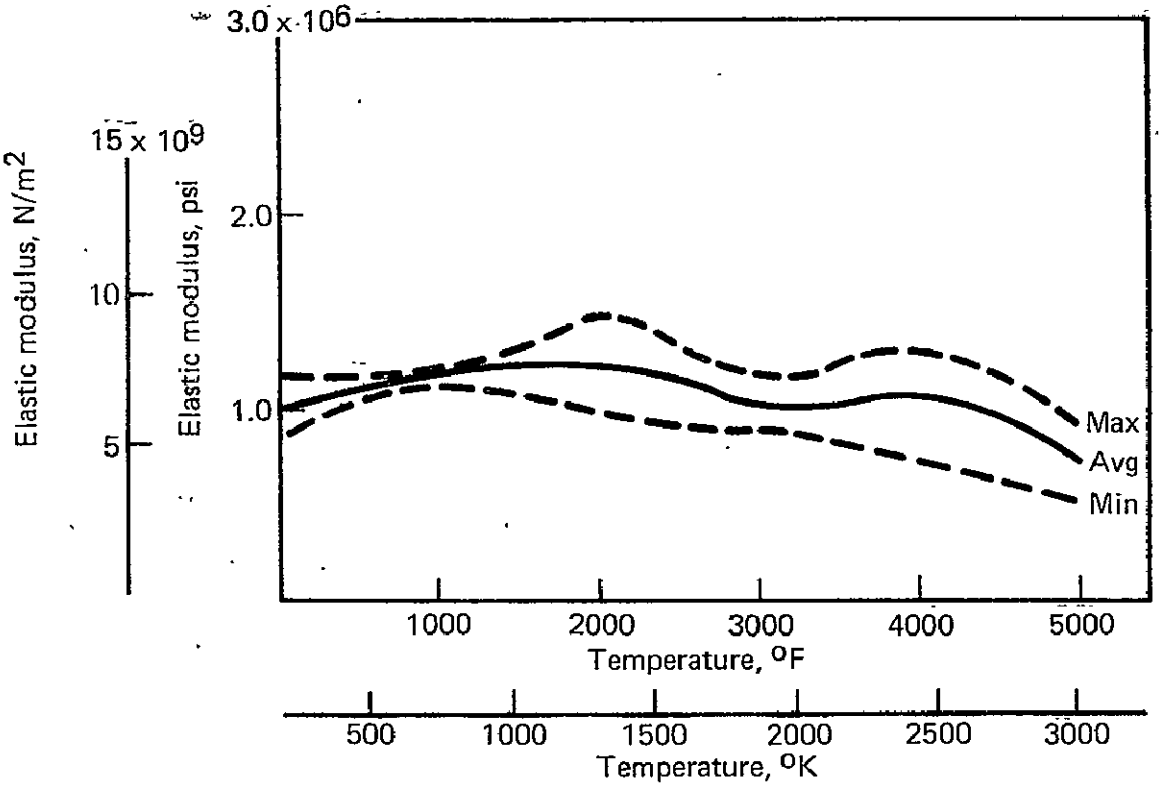

FIGURE A–6.3 ELASTIC MODULUS VERSUS TEMPERATURE OF GRAPHITITE-G ACROSS GRAIN

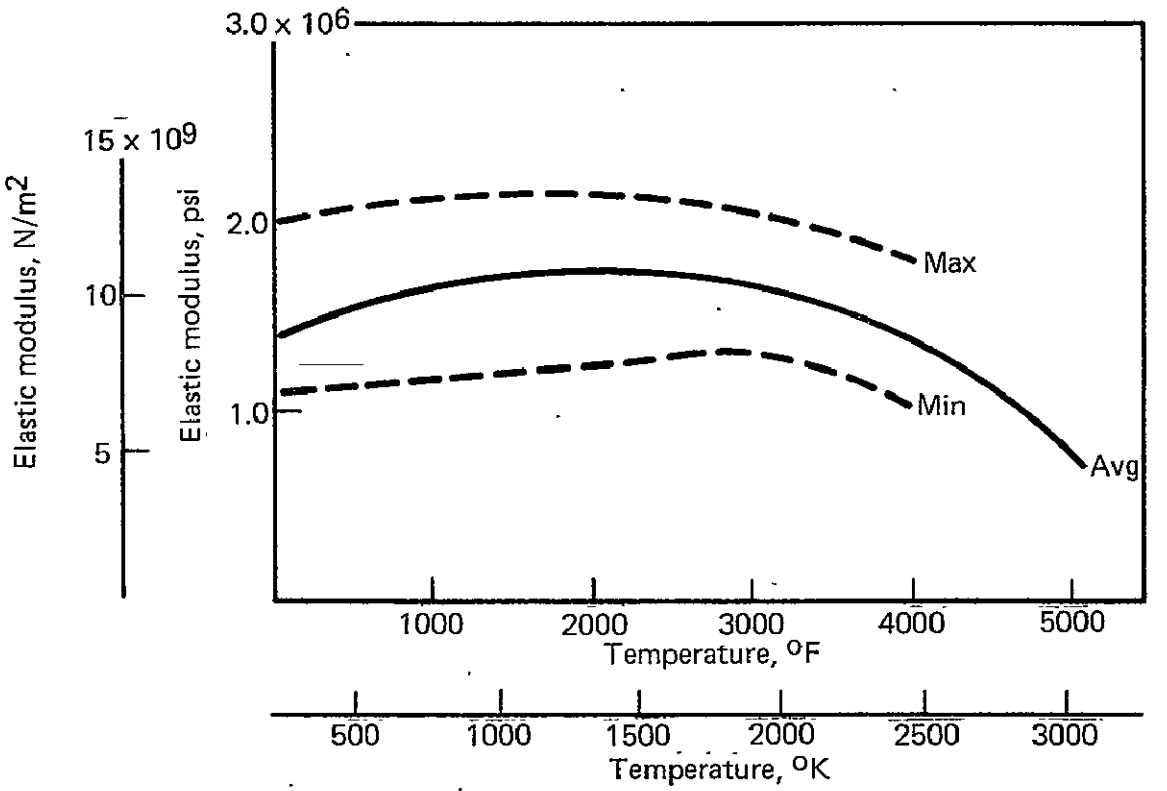

FIGURE A–6.4 ELASTIC MODULUS VERSUS TEMPERATURE OF GRAPHITITE-G WITH GRAIN

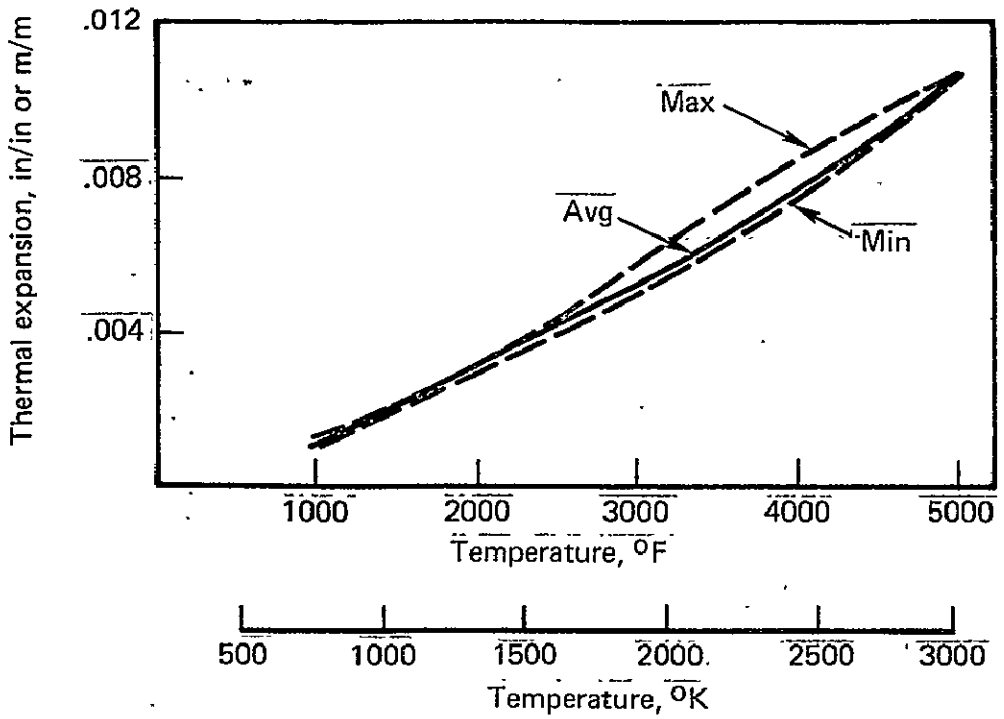

FIGURE A–6.5 THERMAL EXPANSION VERSUS TEMPERATURE OF GRAPHITITE-G ACROSS GRAIN

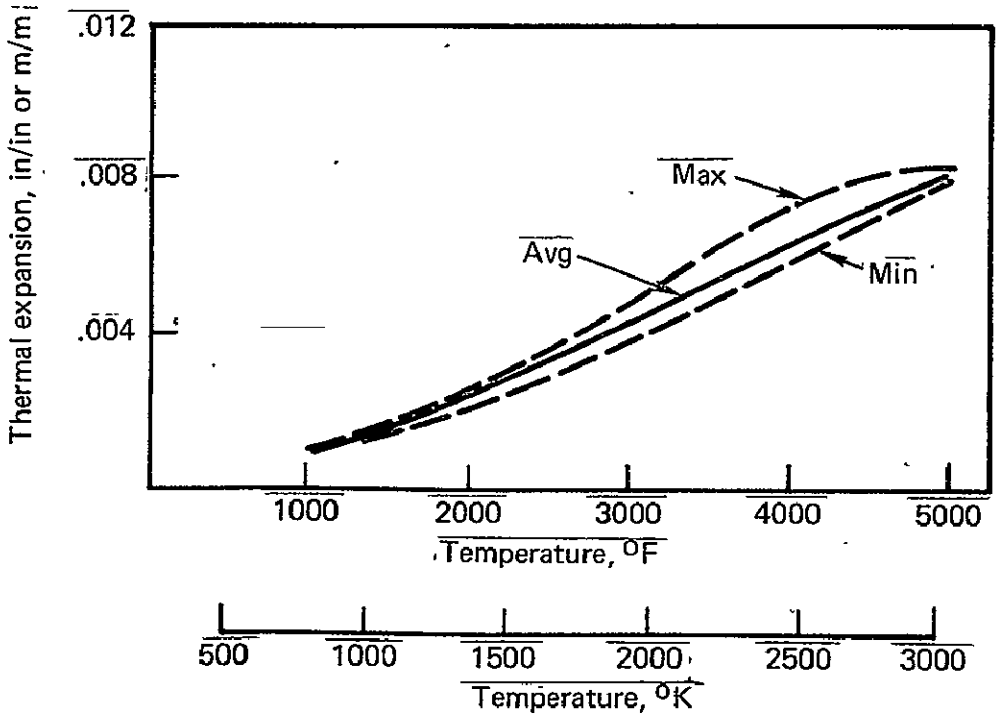

FIGURE A–6.6 THERMAL EXPANSION VERSUS TEMPERATURE OF GRAPHITITE-G WITH GRAIN

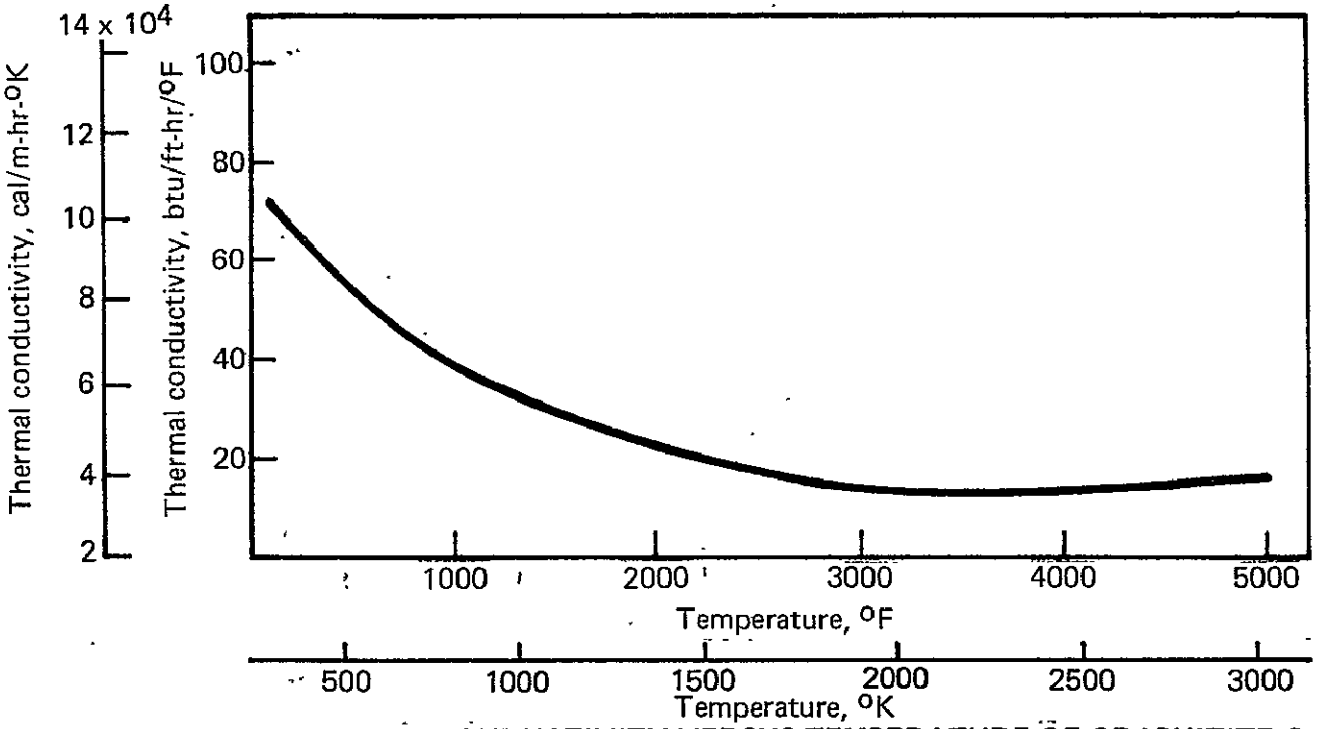

FIGURE A–6.7 THERMAL CONDUCTIVITY VERSUS TEMPERATURE OF GRAPHITITE-G ACROSS GRAIN

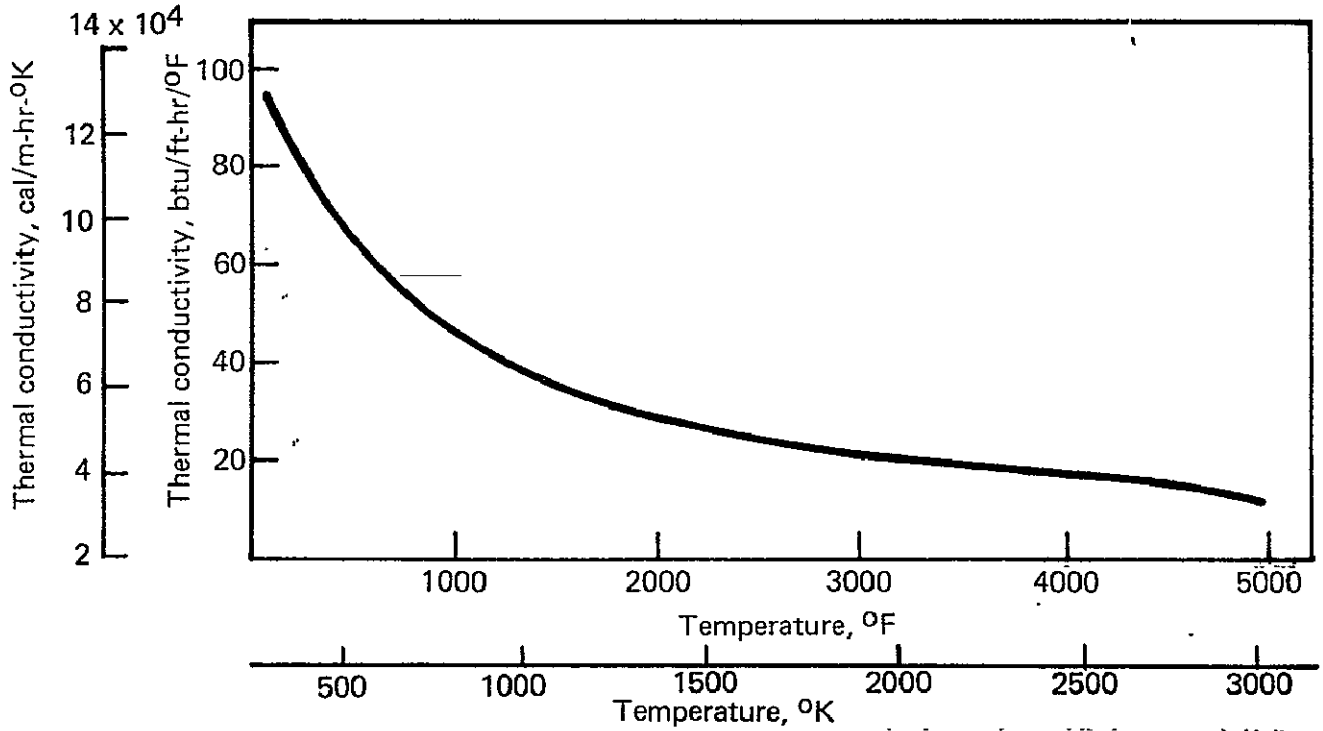

FIGURE A–6.8 THERMAL CONDUCTIVITY VERSUS TEMPERATURE OF GRAPHITITE-G WITH GRAIN

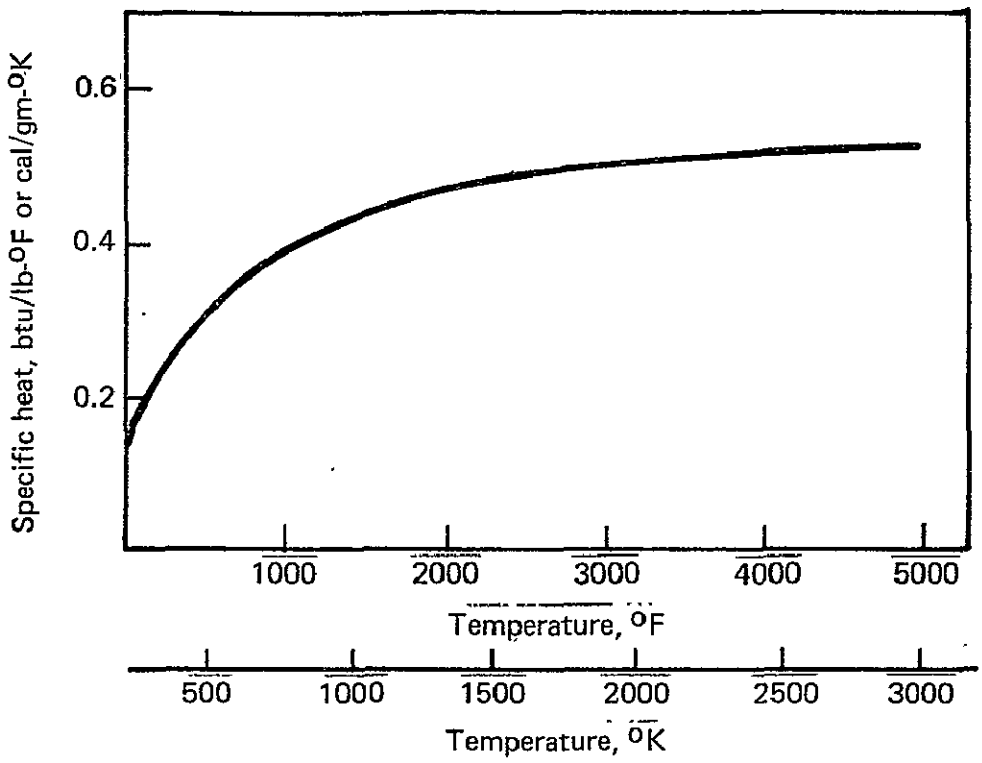

FIGURE A–6.9 SPECIFIC HEAT VERSUS TEMPERATURE OF GRAPHITE-G

TABLE A–I PHYSICAL AND MECHANICAL PROPERTIES OF SCOUT NOZZLE MATERIALS

		41 RPD					PA6					150 RPD				
		Temperature – °F					Temperature – °F					Temperature – °F				
		RT	250	500	750	1000	RT	250	500	750	1000	RT	250	500	750	1000
Density, gm/cm³ (lb/ft³)	With grain	1.86 (116)					1.70 (106)					1.76 (110)				
Thermal conductivity cal/m-hr-°K (btu/ft-hr-°F)	With grain						.108 (.0725)					.603 (.405)	.603 (.405)	.603 (.405)		
	Against	.46 (.308)	.48 (.325)	.52 (.35)												
Coeff. of thermal expansion, m/m-°K x10-6 (in/in-°F x10-6)	With grain		4.5 (2.5)	5.2 (2.9)	4.9 (2.7)	3.7 (2.03)	9.9 (5.5)					3.6 (2)				
	Against grain						15.8 (8.8)									
Modulus of elasticity N/m² x 10⁹ (psi x 10⁶)	With grain	34.79 (5.05)	34.45 (5.0)	36.52 (5 3)	31.01 (4.5)	16.54 (2.4)	22.74 (3.3)					15.71 (2.28)				
	Against grain						(2.1)									
Tensile strength, N/m² x 10⁶ (psi)	With grain	95.29 (13830)	76.79 (11145)	65.11 (9450)	48.23 (7000)		199.81 (29000)					(8800)				
	Against grain						121.26 (17600)									
Specific heat, cal/gm-°K (btu/lb-°F)		.3 (.3)					.27 (.27)					.27 (.27)				
Diffusivity, m²/hr (ft²/hr)								.00023 (.0025)								

TABLE A–I PHYSICAL AND MECHANICAL PROPERTIES OF SCOUT NOZZLE MATERIALS – Continued

		FM 5076					MX 2630 A					FM 5014				
		Temperature – °F					Temperature – °F					Temperature – °F				
		RT	250	500	750	1000	RT	250	500	750	1000	RT	250	500	750	1000
Density, gm/cm³ (lb/ft³)		1.70 (106)					0.71 (44)					1.44 (90)				
Thermal conductivity cal/m-hr-°K (btu/ft-hr-°F)	With grain	.31 (.208)						.72 (.483)	.69 (.463)			.72 (.483)				
	Against grain															
Coeff. of thermal expansion, m/m-°K x10⁻⁶ (in/in-°F x10⁻⁶)	With grain	(Note 1)	8.1 (4.5)	7.5 (4.2)	7.0 (3.9)	5.6 (3.1)			8.6 (4.8)			12.2 (6.8)				
	Against grain			-54 (-30)	-61 (-34)	-99 (-55)			106 (59)							
Modulus of elasticity N/m² x 10⁹ (psi x 10⁶)	With grain	20.67 (3.0)										11.02 (1.6)				
	Against grain															
Tensile strength, N/m² x 10⁶ (psi)	With grain	192.9 (28000)					241.1 (3500)					82.7 (12000)				
	Against grain															
Specific heat, cal/gm-°K (btu/lb-°F)		.22 (.22)					.24 (.24)					.23 (.23)				

Note (1) data from unfired Algol IIB nozzle.

TABLE A–I PHYSICAL AND MECHANICAL PROPERTIES OF SCOUT NOZZLE MATERIALS – Continued

		FM 5072					FIBERITE 4035					MX 2600				
		Temperature – °F					Temperature – °F					Temperature – °F				
		RT	250	500	750	1000	RT	250	500	750	1000	RT	250	500	750	1000
Density, gm/cm³ (lb/ft³)		1.39 (87)					2.00 (125)					1.75 (109)				
Thermal conductivity cal/m-hr-°K (btu/ft-hr-°F)	With grain	.45 (.3)											.35 (.233)	.31 (.208)		
	Against grain															
Coeff. of thermal expansion, m/m-°K x10-6 (in/in-°F x10-6)	With grain	5.8 (3.2)	27.7 (15.4)	15.5 (8.6)	10.8 (6.0)							9.9 (5.5)	9.9 (5 5)	9.9 (5.5)		
	Against grain											45 (25)	45 (25)	45 (25)		
Modulus of elasticity N/m² x 10⁹ (psi x 10⁶)	With grain	8.27 (1.2)	11.02 (1.6)	9.65 (1.4)	8.27 (1.2)							13.78 (2.0)				
	Against grain															
Tensile strength, N/m² x 10⁶ (psi)	With grain	77.17 (11200)	64.77 (9400)	57.19 (8300)	40.65 (5900)	27.56 (4000)	62.01 (9000)					96.46 (14000)				
	Against grain															
Shear strength, N/m² 10⁶ (inter laminar) (psi)		7.58 (1100)	6.89 (1000)	6.20 (900)	4.82 (700)							17.23 (2500)				
Specific heat, cal/gm-°K (btu/lb-°F)		.267 (.267)	.290 (.290)	.307 (.307)	.303 (.303)							.22 (.22)				

TABLE A-I PHYSICAL AND MECHANICAL PROPERTIES OF SCOUT NOZZLE MATERIALS – Continued

		FM 5504					FM 5067					MX 5707B			
		Temperature – °F					Temperature – °F					Temperature – °F			
		RT	250	500	750	1000	RT	250	500	750	1000	RT	500	750	1000
Density gm/cm^3 (lb/ft^3)		1.70 (106)					1.76 (110)					1.20 (75)			
Thermal conductivity cal/m-hr-°K x 10^3 (btu/ft-hr-°F)	With grain	.33 (.225)					.31 (.208)					.16 (.107)			
	Against grain	.25 (.167)	.28 (.186)	.29 (.196)	.31 (.210)		.29 (.198)	.33 (.222)	.32 (.215)	.32 (.215)					
Coeff. of thermal expansion, m/m-°K x 10^{-6} (in/in-°F x 10^{-6})	With grain						5.4 (3.0)	20.5 (11.4)	5.5 (3.05)	.7 (0.37)					
	Against grain														
Modulus of elasticity N/m^2 x 10^9 (psi x 10^6)	With grain	16.33 (2.37)	13.50 (1.96)	12.88 (1.87)	11.37 (1.65)	9.44 (1.37)						3.79 (.55)			
	Against grain														
Tensile strength, N/m^2 x 10^6 (psi)	With grain	51.68 (2500)	34.45 (5000)	31.01 (4500)	31.69 (4600)	21.36 (3100)	96.46 (14000)					33.76 (4900)			
	Against grain														
Specific heat, cal/gm-°K (btu/lb-°F)		.24 (.24)					.253 (.253)	.267 (.267)	.263 (.263)	.247 (.247)		.35 (.35)			
Diffusivity, m^2/hr (ft^2/hr)							.00067 (.0072)	.00070 (.0075)	.00067 (.0072)	.00071 (.0076)					

TABLE A–I PHYSICAL AND MECHANICAL PROPERTIES OF SCOUT NOZZLE MATERIALS – Concluded

		MX 2646					MX 2625				
		Temperature – °F					Temperature – °F				
		RT	250	500	750	1000	RT	250	500	750	1000
Density, gm/cm^3 (lb/ft^3)		1.78 (111)					1.80 (112)				
Thermal conductivity cal/m-hr-°K (btu/ft-m-°F)	With grain		.30 (.200)	1.26 (.175)				.29 (.197)	.26 (.173)		
	Against grain		.33 (.223)	.35 (.235)	.32 (.216)						
Coeff. of thermal expansion, m/m-°K x 10^{-6} (in/in-°F x 10^{-6})	With grain		20.5 (11.4)	9.0 (5.0)	4.9 (2.74)				4.7 (2.6)		
	Against grain								9.5 (53)		
Modulus of elasticity N/m^2 x 10^9 (psi x 10^6)	With grain	22.94 (3.33)	19.09 (2.77)	14.40 (2.09)	10.96 (1.59)	9.09 (1.32)	20.67 (3.0)				
	Against grain										
Tensile strength, N/m^2 x 10^6 (psi)	With grain	171.56 (24900)	105.42 (15300)	68.21 (9900)	45.47 (6600)	28.25 (4100)	58.57 (8500)				
	Against grain										
Shear strength, N/m^2 x 10^6 (psi) (inter laminar)		13.78 (2000)	17.91 (2600)	8.27 (1200)	2.07 (300)						
Specific heat, cal/gm-°K (btu/lb-°F)		.243 (.243)	.270 (.270)	.230 (.230)	.227 (.227)						
Diffusivity, m^2/hr (ft^2/hr)		.00075 (.0080)	.00077 (.0083)	.00084 (.0090)	.00082 (.0088)						

APPENDIX B

SUMMARY OF PHASE II REPORT

LTV Report 23.550, Final Report
Phase II Study of Improved Materials for Use on
SCOUT Rocket Motor Nozzles
13 April 1973

APPENDIX B

SUMMARY OF PHASE II REPORT

LTV Report 23,550, Final Report
Phase II Study of Improved Materials for
Use on Scout Rocket Motor Nozzles
13 April 1973

SUMMARY

A program, completed in 1973, to obtain nozzle material performance data and to determine the feasibility of using new materials on the SCOUT rocket motor nozzles was conducted by the Vought Systems Division.

The selection of materials used in full scale nozzle tests in this program was strongly influenced by data obtained in the Phase I study (Appendix A) and in NASA CR-112082 (reference 10). These materials are listed in Table I. The specific rationale for selecting these materials and for not selecting other Phase I candidates is as follows:

Throat Insert. - Reimpregnated reinforced carbon carbon materials can successfully be fabricated into throat insert billets. Predicted performance of these materials is superior to the graphite phenolic material tested. MXG-175 represents a reliable nozzle throat material that is adequate for an X259 or larger SCOUT motor. Only a small performance gain ($\sim$ 0.2%) in delivered Specific impulse is obtained by using the lower erosion rate graphite material. Based on the results of the Phase II program, an MXG-175 nozzle throat insert has been incorporated into the SCOUT X259 third stage motor design.

The erosion of Carbitex 700 is approximately fifty percent of the erosion of a graphite phenolic insert. However, Carbitex 700 and RPP-4 were eliminated from full scale motor testing as throat inserts because of high cost and the fact that those materials could not be bought to a controlled manufacturing specification (i. e., manufacturing would be proprietary). FM-5272 was also eliminated for the throat backup since predicted erosion was greater than desired. Carbitex 700 and RPP-4 throat insert billets were fabricated during this study but were not tested during this phase of the program. The Carbitex 700 billet was later machined and used as an insert in a similar test program.

Throat Backup Insulation. - The MX-4926 carbon phenolic backup insulation performed superior to the RPD-150 asbestos phenolic insulator presently being used in the X259 nozzle. A review of thermocouple data shows that the carbon phenolic insulation properties are sufficient to protect the aluminum attachment flange from excessive heating.

Throat Extension. - MX-4926 carbon phenolic performed as well as the throat extension liner in the exit cone.

Exit Cone Liner. - Low cost material such as paper and asbestos phenolic performed equal to the MX-2600 silica phenolic presently being used in the exit cone of the X259 nozzle. However, further investigation is warranted before the optimum material for this region can be identified.

The program included the following tasks:

Conducted stress and heat transfer analyses to aid in the selection of optimum materials for nozzle tests.

Fabricated two reimpregnated and graphitized RPP-4 and Carbitex 700 throat insert billets.

Dissection and measurement of char and erosion of two nozzles fired on X259 loaded cases. One of these nozzles used a graphite-phenolic ablative throat insert which was fabricated under this contract; the other unit was a standard X259 nozzle with a reduced area ATJ graphite throat insert (Figure 1).

A Hercules Incorporated X259 motor case was used as the test vehicle to obtain material performance data on two nozzles. The nozzle throats were designed to obtain average pressures above 4.14×10^6 N/m^2 (600 psi). The erosion and char depths for a nozzle fabricated by Haveg Incorporated with a graphite phenolic ablative throat and a modified X259 nozzle were obtained. Post-fire examination indicated material performance for the exit cone liners of the two nozzles were equivalent, however a carbon phenolic throat retainer performed superior to the molded asbestos phenolic being used in the present X259 nozzle. An erosion rate of

2.34×10^{-4} M/sec (9.15 mils/sec) was calculated for the ablative throat based on post-fire measurements.

The following materials were used in the materials demonstration nozzle:

TABLE I. - NEW MATERIAL USAGE IN TEST NOZZLE

Component	Material Type	Designation
Insert	Graphite Phenolic	MXG 175
Backup Insulation	Carbon Phenolic	MX 4926
Throat Extension	Carbon Phenolic	MX 4926
Exit Cone Insulation	Asbestos Phenolic	FM 5525

After selection of these materials, the program was redirected to include the fabrication of one complete test nozzle, the fabrication of components for another test nozzle and the post test analysis of two nozzles, one with a graphite phenolic ablative throat and a modified X259 nozzle.

The material performance data from two high pressure X259 motor firings, results of thermal and stress analyses, and fabrication of nozzles and components are discussed below.

Motor Test Data. - Motor burn time and pressures are shown in Table II for the two tests.

TABLE II. - MOTOR FIRING DATA

Nozzle Design	Modified X259	New Materials
Motor S/N	HIB 222	HPC 209
Throat Insert Material	ATJ (Graphite)	MXG 175 (Graphite Phenolic)
Burn Time, Sec	24.86	26.41
Avg. Burn Pressure, N/m^2	4.42×10^6 (641 psi)	3.97×10^6 (576 psi)
Web Time, Sec.	22.8	24.08
Avg. Web Pressure, N/m^2	4.63×10^6 (672 psi)	4.21×10^6 (611 psi)
Peak Pressure, N/m^2	5.11×10^6 (742 psi)	4.86×10^6 (706 psi)

Thermal Analyses. - Results of the thermal analyses were as follows:

The maximum temperature for the bond line between the throat insert and the throat backup insulation was calculated to be 2089°K (3300°F) for the Carbitex 700 and 922°K (1200°F) for RPP-4. The reason for the large difference in the predicted temperature is the much greater thermal conductivity for the Carbitex 700. Temperature measurements are listed in Table III.

The erosion of asbestos phenolic (FM 5525) was more than the cellulose phenolic (FM 5272) when used in the exit cone. For equal asbestos and cellulose thickness, bond line temperatures using the cellulose phenolic were approximately 45% of those using asbestos as an exit cone insulator.

TABLE III. - MEASURED TEMPERATURE INCREASE

Thermocouple Location	Modified X259 Nozzle on Motor S/N HIB 222	New Materials Nozzle on Motor S/N HPC-209
.0254 m (1 in) aft of nozzle attachment flange	20°K (35°F)	10°K (18°F)
.0763 m (3 in) aft of nozzle attachment flange	44°K (80°F)	14°K (25°F)
.0254 m (1 in) forward of nozzle exit plane	93°K (168°F)	25°K (45°F)

Carbon phenolic material erosion was predicted to be approximately .00051 m (0.02 in). Minimum required insulator thickness was calculated to be .00763 m (0.3 in). A comparison of measured erosion and char depths at selected locations in the two nozzles is listed in Table IV. Erosion and char profiles are shown in Figures 2 and 3.

TABLE IV. - MEASURED EROSION AND CHAR

Distance Forward of Exit Plane, m (a)	Ablative Throat Nozzle		ATJ Throat Nozzle	
	Erosion, m	Char, m	Erosion, m	Char, m
.0025 (.1 in)	.0013 (0.5 in)	.0028 (.11 in)	.0038 (.15 in)	.0061 (.24 in)
.0254 (1 in)	.0020 (.08 in)	.0025 (.10 in)	.0028 (.11 in)	.0038 (.15 in)
.0763 (3 in)	.0025 (.10 in)	.0023 (.09 in)	.0041 (.16 in)	.0031 (.12 in)
.1781 (7 in)	.0041 (.16 in)	.0020 (.08 in)	.0013 (.05 in)	0
.3817 (15 in)	.0076 (.03 in)	0	.0013 (.05 in)	0
.5089 (20 in)	.0013 (.05 in)	0	.0008 (.03 in)	0
.5471 (21.5 in)	.0028 (.11 in)	.0109 (.43 in)	.0010 (.04 in)	0
.5598 (22 in)	.0031 (.12 in)	.0117 (.46 in)	0	0
.5852 (23 in)	.0018 (.07 in)	.0130 (.51 in)	.0028 (.11 in)	.0038 (.15 in)
.6107 (24 in)	.0043 (.17 in)	.0132 (.52 in)	.0071 (.28 in)	.0079 (.31 in)

(a) Distance to aft edge of carbon phenolic liner = .1654 m (6.5 in).
Distance to aft edge of insert = .5471 m (21.5 in).
Distance to leading edge = .6590 m (25.9 in).

Stress Analysis. - A finite element computer analysis was performed. Calculated maximum stresses are shown in Table V for thermal gradients which exist at 26 seconds after ignition. These stresses were not excessive and no structural problems were found based on this analysis.

TABLE V. - THERMAL STRESSES FOR ABLATIVE THROAT DESIGN

	Graphite Phenolic Insert	Carbon Phenolic Overwrap	Carbon Phenolic Aft of Throat Insert
Direction	Max Stress, N/m^2	Max Stress, N/m^2	Max Stress, N/m^2
Radial	-8.67×10^6 (-1259 psi) .32 (+46 psi)	-29.06×10^6 (-4128 psi) 32.76 (+4755 psi)	-23.98×10^6 (-3480 psi) 32.23 (+4678 psi)
Axial	-13.25 (-1923 psi) 3.54 (+514 psi)	-15.71 (-2280 psi) 19.88 (+2886 psi)	-26.29 (-3816 psi) 38.04 (+5521 psi)
Hoop	-15.49 (-2248 psi) 5.35 (+776 psi)	-19.51 (-2832 psi) 1838 (+2668 psi)	-14.39 (-2088 psi)
Bondline Shear	3.86 (560 psi)	NA	NA

Fabrication Problems. - Problems encountered during fabrication of the nozzles included limited production of selected materials, cracking in FM 5272 material and wrapping the throat billets at 90° to centerline.

Limited production of some of the materials used for component fabrication resulted in long lead times for delivery and additional cost on the per pound use basis. It was determined that many materials, for example FM 5072LD, identified in material suppliers catalogs are manufactured on request with quantities around 2224 N (500 lb) required for a production run. The user either has to purchase the entire lot or pay a premium price for the materials.

Another problem was encountered in machining the FM 5272 Kraft Paper phenolic material. When the final exit cone outside diameter

was being machined a crack was initiated which propagated to the carbon-phenolic liner. Further review indicated that the crack was caused by high internal stresses built into the part by the wrapping and curing processes. When a groove was machined in the material during final machining operations, the groove caused a stress riser which caused the material to crack. The part was repaired by machining a Vee groove in the center of the delaminated area down to the carbon phenolic approximately .0064 m (.25 in) wide and wrapping FM 5272 in the Vee groove area. After machining flush, MXB 6001 glass cloth and E 801 glass roving were applied over the repaired area. It is believed that cracking could be eliminated by proper machining methods.

VSD had planned to have the ablative throat billets wrapped at 90° to centerline. However, because of the small ratio between outside and inside of the part, this could not be done without excessive wrinkling. After several attempts this wrap angle was revised to 45° and the parts were fabricated without difficulty.

Conclusions

The following conclusions were derived from this program:

The MX 4926 carbon phenolic backup insulation performed superior to the RPD 150 asbestos-phenolic insulator presently being used in the X259 nozzle. A review of thermocouple data shows that the carbon phenolic insulation properties are sufficient to protect the aluminum attachment flange from excessive heating. Additional investigations show that there are high reject rates in the fabrication of the molded RPD backup insulation. In addition, the MX 4926 carbon phenolic performed well as the throat liner in the exit cone. Based on information in the Phase I study which shows the use of carbon phenolic as a throat insert material, it is predicted that this material may also be used as a throat insert with equivalent performance as obtained from the MXG 175 tested under this program. Since one of the objectives of this program was to identify a

material which may be used in several locations in the nozzle, further investigation of incorporating this material or a similar material in the high erosive regions of the nozzle is recommended. The objective of this investigation would be to determine the feasibility from a fabrication, cost, design and performance standpoint of using a two-material nozzle design in the SCOUT rocket motors.

Low cost material such as paper and asbestos phenolic can be successfully fabricated. The asbestos phenolic performed equal to the MX 2600 silica phenolic presently being used in the exit cone of the X259 nozzle. However, further investigation is warranted before the optimum material for this region can be identified.

Reimpregnated reinforced carbon-carbon materials can successfully be fabricated into throat insert billets. Predicted performance of these materials is superior to the graphite phenolic material tested. The erosion rate of RPP 4 is predicted to be approximately 4 mils/sec which is less than half of that experienced in the graphite phenolic throat insert tested.

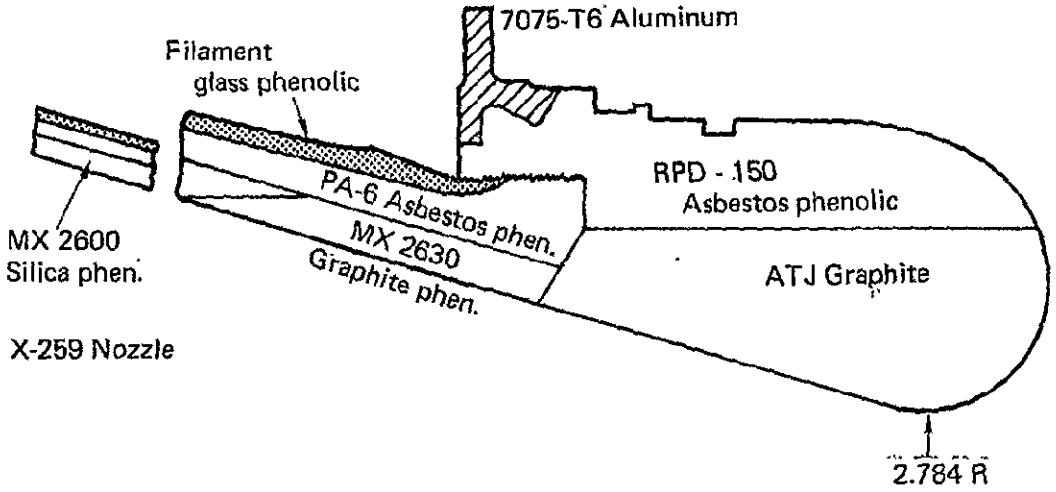

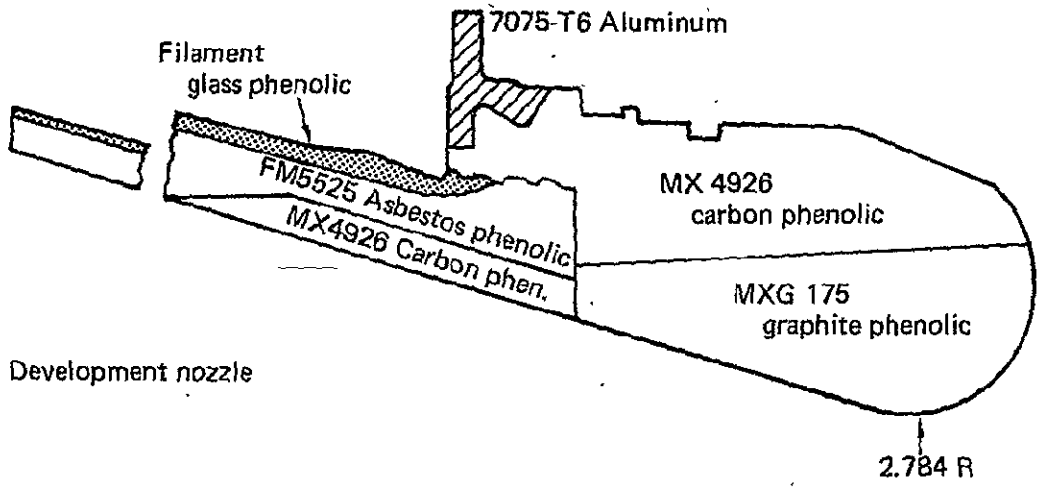

FIGURE 1.–TEST CONFIGURATIONS

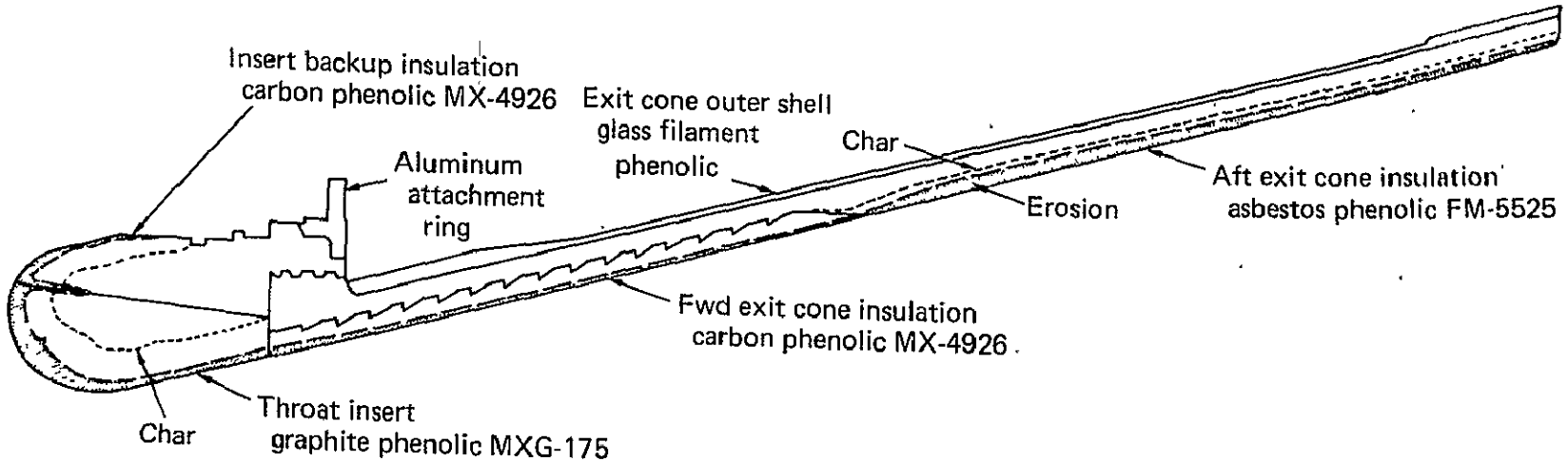

FIGURE 2. – X259 ABLATIVE THROAT POST FIRE RESULTS

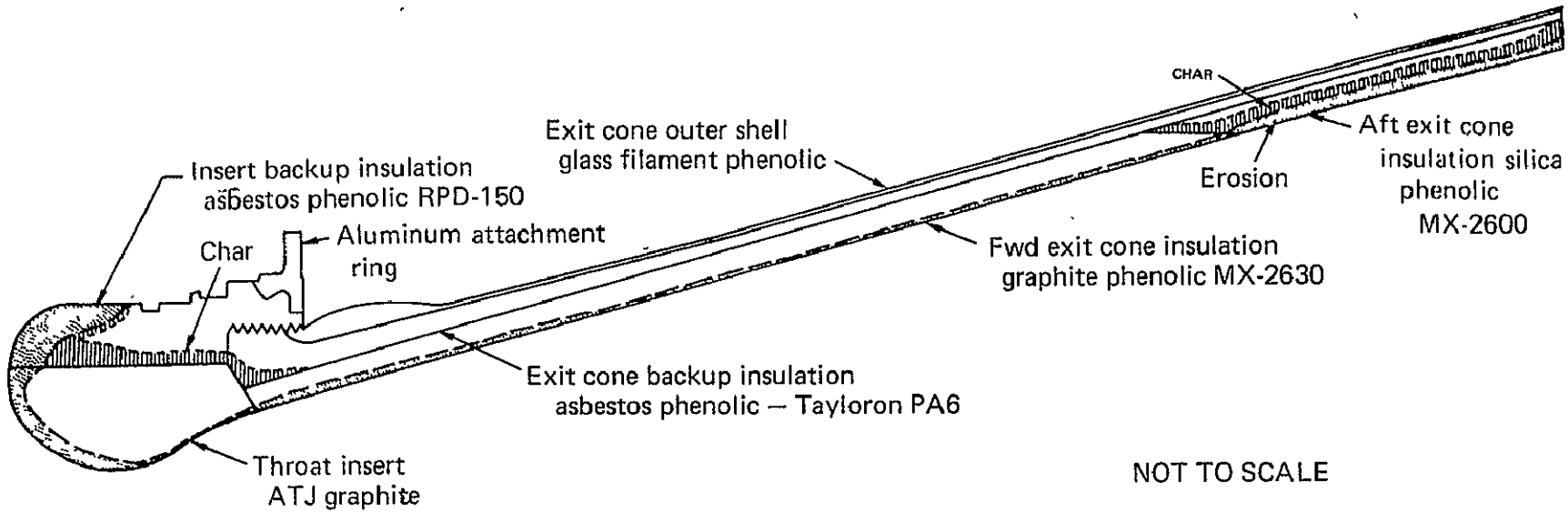

FIGURE 3. – X259 ATJ THROAT POST FIRE RESULTS

APPENDIX C

ANTARES IIB MOTOR NOZZLE DESCRIPTION

APPENDIX C

ANTARES IIB MOTOR
NOZZLE DESCRIPTION

ANTARES IIB

Introduction. - The Antares IIA (X259-B3) motor nozzle has had over 200 successful firings in its production history. Although lightweight by design, components had relatively high margins of safety and exhibited high reliability. To improve Scout system payload capability the motor was replaced by the Antares IIB (X259-B4) in 1972. Major component changes included: substitution of graphite phenolic for the ATJ graphite insert, reduction of throat area to raise the MEOP value from 2.87 X 10^6 n/m^2 (416 psi) to 4.75 X 10^6 n/m^2 (690 psi); the use of 0.0084 m (5/16 in) instead of 0.0067 m (1/4 in) nozzle attach bolts and substitution of a lightweight igniter.

A brief description of the effort performed to demonstrate the feasibility of the Antares IIB motor is as follows:

Hercules Inc./Bacchus Works performed a preliminary design review of a high pressure X259 motor. Results of the review indicated the design was feasible.

Two X259 motors were static fired at the Hercules Inc./ABL Facility to demonstrate the Antares IIB motor design feasibility. The nozzle on one of these motors, HIB-222, was a standard X259 nozzle with the ATJ graphite throat diameter reduced to obtain the desired operating pressure. The second nozzle, fired on X259 motor HPC-209, was fabricated by Haveg for Vought under a nozzle materials evaluation program. This nozzle had an MXG-175 graphite phenolic throat and a carbon phenolic (MX-4926) retainer ring.

Both motors and nozzles performed successfully. Since the erosion rate was acceptable for the MXG-175 graphite phenolic throat, and the phenolic inserts are generally less susceptible than monolithic graphite inserts to catastrophic failures, the MXG-175 was approved for the nozzle insert in the Antares IIB motor.

Following the demonstration firings, the design of the Antares IIB motor was finalized and nine (9) motors fabricated. One of these motors (S/N HIB-403) was selected as a lot acceptance round and successfully static fired under simulated altitude conditions at the Arnold Engineering Development Center (AEDC). This firing completed the effort to qualify the Antares IIB motor for use on Scout. Before the first Scout flight with an Antares IIB occurred, however, the failure of a modified Antares IIB nozzle on another program resulted in additional evaluation and test of the Antares IIB nozzle. A discussion of this failure, additional evaluation and test is discussed under "Problem Areas".

Nozzle geometry and materials are shown in Figures C-1 and C-2. Table C-I lists alternate qualified materials for each component in this nozzle.

Performance Data. - This SCOUT third stage motor has a maximum expected operating pressure (MEOP) of 4.75 X 10^6 N/m^2 (690 psi) and a flame temperature of 3802°K (6384°F). The CYI-75 modified double base propellant is the same as was used in the Antares IIA third stage motor. Motor performance parameters which affect the nozzle environment were obtained from the Model Specifications and are summarized in Table C-II. Time dependent variations in chamber pressure are shown in Figure C-3. Because this is a fairly new motor, the pressure-time curve is based only on AEDC simulated altitude tests.

Material Description. - The materials used in the Antares IIB nozzle (Figure C-2 & Table C-I) are described in this section. The temperature dependent material properties were obtained from Reference (5). Temperature dependent material properties are shown in Table C-III.

RPD-150 (retainer ring) is a general purpose molding compound of long spinning grade chrysotile asbestos fibers, grade AAAA, impregnated with a high temperature phenol-formaldehyde resin, B staged and then mascerated into a molding compound. The material may be molded at pressures of 13.78×10^6 N/m^2 (2000 psi) and greater at temperatures between 408 to 436°K (275 to 325°F). Post cure is recommended to obtain optimum properties.

MXG175 or FM 5014 (throat insert) is a graphite fabric impregnated with a high temperature phenolic resin. The graphite reinforcement is Hitco G 1550 or WCA manufactured by Union Carbide Corporation woven as a plain (square) weave and supplied by National Carbon Company. The high temperature phenolic resin is a MIL-R-9299 Type II phenolic. A filler in the resin is composed of zirconia refractory fines which pass through a 325 mesh screen.

MX 2600 (aft exit cone liner) is a silica fabric impregnated with a high temperature phenolic resin containing silica reinforcement. The phenolic resin must meet specification MIL-R-9299 Type II phenolic resin. The silica fabric is Sil Temp 84 or Hitco C100-48. The reinforcement, or filler, is silica dioxide of 98% purity.

MX 2630A (exit cone liner is a graphite fabric impregnated with a high temperature phenolic resin containing refractory reinforcement. The graphite fabric is WCA grade woven as a plain (square) weave. The graphite fabric resin is a MIL-R-9299 Type II phenolic. The filler in the resin is composed of refractory zirconia fines which pass through a 325 mesh screen.

Tayloron PA-6 (exit cone insulation) is an asbestos paper impregnated with a high temperature phenolic resin that conforms to MIL-R-9299, Type II, Class 2. The asbestos paper is Microasbestos paper supplied by the John Mansville Corporation.

ECG140-801 (filament wound glass rovings) is impregnated with Epon 828 resin system and B-staged at room temperature and cured at 311°K (100°F) for four hours and then at 344°K (160°F) for two hours.

Armstrong A-2 (adhesive) is a white epoxy adhesive that has a low coefficient of thermal expansion, making it quite suitable for bonding ceramic type materials. It has excellent wetting properties and it also provides exceptionally strong bonds to rigid materials such as phenolics. Activator A (or curing agent A) offers short time room temperature cures. The adhesive is prepared by mixing 4 parts of curing agent A to 100 parts of A-2 epoxy resin. Bond lap shear strength at room temperature is 2900 psi. No elevated temperature data is available.

The following percentages of solids, resins and volatiles for the plastic laminate nozzle materials were obtained from vendor catalogs and are used as acceptance criteria at room temperature.

Material	Resin Solids %		Resin Filler %		Volatiles %	
	Min	Max	Min	Max	Min	Max
RPD-150	38	43	-	-	3	12
MX 2630A	36	40	--	--	3	7.5
MX 2600	29	33	6	10	3	7
Tayloron PA-6	41	47	--	--	7	12

Drawings and Specifications. - Table C-IV lists the Antares IIB nozzle drawing and material specifications. Component fabrication procedures are identical to those listed for the IIA motor for the exit cone and similar for the remaining components.

Fabrication and Process. - The fabrication and inspection procedures are summarized for each component of the Antares IIB nozzle in Figure C-4. That figure briefly summarizes the fabrication procedures and quality inspections for each nozzle component.

Thermal Data

The Antares IIB thermal data was obtained from flight and ground test data supplemented with analytical data for times at which such data cannot be readily measured.

Antares IIB nozzle (S/N EII-1047) was attached to HIB-211 motor and a static firing of 30.2 seconds was performed at the Hercules Incorporated, Cumberland, Maryland (ABL) facility on 1 May 1974. For this ground firing test the exit cone was cut-off at an expansion ratio of 7.79. Post-fire examination indicated that the motor and the nozzle both were in excellent condition and all test objectives were met.

Char and Erosion. - Expected erosion profiles are shown in Figure C-5. Char depths in the exit cone are similar to those for the Antares IIA nozzle. In the insert maximum erosion depth was .0171 m (.674 in) and char depth was .0126 m (.295 in) after static firing (Reference 23).

Temperature Distribution. - Figures C-6 through C-8 present analytically determined isotherms at 5, 10, and 27 seconds after ignition. The 5 and 10 second plots show maximum thermal gradients and the 27 second plot indicates the maximum temperatures which the nozzle attains during firing.

Figure C-9 presents the analytically determined adiabatic wall temperature as a function of nozzle area ratio.

Figures C-10 and C-11 present the nozzle exit cone O.D. temperatures. Figure C-11 presents the nozzle exit cone O.D. temperatures obtained during the flight of SCOUT S-191C. Figure C-10 presents nozzle exit cone O.D. temperatures obtained in static test firing at the AEDC simulated altitude chamber. The test temperatures are lower due to a cooling effect from natural convection and better radiation cooling due to the absence of the nozzle shroud which is present during flight. Maximum observed external nozzle temperature occurred during flight and was 630°K (675°F).

All measured and analytically determined thermal parameters are within acceptable limits and the Antares IIB nozzle has not encountered a thermally related problem in two static tests and flights S-191 and S-194. However, there was an apparent nozzle failure on flight S-196 on 5 December 1975. Results of the related failure investigation are summarized under "Problem Areas".

Structural Analysis

Finite element thermal and structural analyses were performed by the motor vendor to aid in the design, optimization and evaluation of the Antares IIB high pressure nozzle. Initial analyses showed that the modified nozzle would perform adequately with the increased chamber pressure. Subsequent analyses have shown a marginal condition in the insert at 8 seconds after ignition.

Loads.- Chamber pressure variation during firing is shown in Figure C-3. Pressure distribution around the nozzle retainer ring and exit cone liner is shown in Figure C-12.

Nozzle proof test pressure is 3.69×10^6 N/m^2 (536 psi). This condition was not considered critical and not analyzed in Reference (5). During proof test the nozzle is in an intermediate configuration as shown in Figure C-13.

Environment. - Analytically determined temperature distributions in the nozzle and pressure distributions around the nozzle at specified times were used to determine maximum stresses in each component of the nozzle. Neither storage nor proof test environments were considered to be critical.

Factors of Safety. - A factor of safety of 1.0 was used in the design and analysis of this nozzle. Results of the stress analysis are reported as Margins of Safety (M.S.) where they are calculated as follows:

$$M.S. = \frac{\text{Strength}}{\text{Stress}} - 1$$

Strength represents the tensile ultimate strength or maximum shear strength of the material at temperature. Maximum principal tensile stresses in the radial-axial plane and circumferential hoop tensile stresses were compared to tensile strength; maximum shear stresses in the radial-axial plane were compared to shear strength. When loaded in compression, composite nozzle material failures appear as shear failures; therefore, shear stresses were used to judge reliability rather than compressive stresses.

Based on the above considerations, any positive margin of safety was considered acceptable in the analysis of this nozzle.

Results of Analysis. - The analysis of Reference (5) was performed in 1973. In that analysis hoop stresses in the insert were generally compressive during the entire motor action time. By the end of firing moderate tensile principal stresses were calculated near the hot surface. A minimum margin of 0.8 based on shear was reported at 15 seconds, but occurred in the forward region of the insert. Minimum margin of safety in the exit cone liner was 0.35 at 20 seconds after ignition. These results are shown in Tables C-V thru C-VII.

As part of the failure investigation for vehicle S-196, the nozzle was reanalyzed. Two unfired nozzles were dissected and samples from components were characterized at room temperature. Elevated temperature properties were adjusted to agree with trends indicated at room temperature. The major improvement in material property information was a better definition of coefficients of thermal expansion as a function of local heating rates in nozzle components. Information from the Poseidon investigation (described in the Trident section of this report, Page 156) was used to determine these values. Heating rate dependent properties are shown in Figure C-14 and are reported in Reference (16).

Results of the later analysis showed marked differences from the previous analysis (Ref. 5). Based on nominal properties a minimum margin of safety of 0.054 was calculated in the aft region of the insert at 8 seconds after ignition due to maximum principal stresses and using distortional energy failure criteria.

At this same time a minimum margin of safety of 0.033 was calculated in the same area based on across ply tension and maximum stress failure criteria. These results are in good agreement with the most probable cause of failure conclusions. Minimum margins of safety for all components at five times during firing are shown in Tables C-V through C-VII. Table C-VIII provides minimum margins of safety from the final (Reference 16) analysis.

Estimated Accuracy of the Antares IIB Nozzle Analysis. - The Antares IIB nozzle insert (graphite phenolic) and retainer ring (asbestos phenolic) have approximately the same relative stiffness. This provides better continuity of strains and probably better analytical accuracy than a nozzle such as the Antares IIA which has a relatively hard ATJ insert and a less stiff retainer ring. In addition, there have been a number of instrumented static firing tests which have provided measured radial deflections, temperatures and erosion profiles. This test data has been used to provide empirical correction factors which are used in the nozzle analyses and improved accuracy results.

Nozzle analyses may be separated into three groups: erosion, thermal and structural. Estimated accuracy for these analyses are approximately as follows:

Erosion Analysis: $\pm$ 10%

Temperature Analysis: $\pm$ 20%

Stress and Strain Analyses: $\pm$ 100% (throat)

$\pm$ 30% (attach ring)

Material property values at elevated temperatures are the leading cause of inaccuracies in the nozzle structural analysis. The effect of heating rates on coefficient of thermal expansion is shown in Figures 68 and 69. Variations in this property have linear effects on calculated strains, but there is no evidence available that thermal conductivity or specific heat exhibit similar changes. As a result, greater accuracy is to be expected in the erosion and temperature calculations than for determination of stresses and strains.

Problem Areas. - The process problems discussed for the Antares IIA (RPD-150 asbestos phenolic) retainer ring are applicable to this nozzle. To resolve this potential problem area, serious consideration has been given to the use of a carbon phenolic tape-wrapped retainer ring.

The retainer ring has always had sixty .00159 m (.063 in) diameter holes in two rows drilled through the ring to provide relief passages for volatiles. The presence of "voids" in the bond layer between insert and retainer, combined with the presence of the vent holes, may have caused a nozzle burn-through failure of a IIB nozzle during a special high energy propellant (XLDB) demonstration test. To eliminate this possibility, the drilled holes in the retainer ring have been eliminated by filling with EA-946 epoxy resin.

Sectioned nozzles after firing have shown indications of locally high erosion and scalloped material in the liner over a distance of about six inches aft of the insert. This is considered an acceptable condition for this nozzle since there still remains sufficient insulative material to thermally protect the outer structural members.

The first IIB nozzle failure, during static test in February 1974, was on a motor using XLDB propellant instead of standard Antares IIB propellant (CYI-75). The more severe combustion and gas environment imposed by the high energy XLDB propellant was suspected as the primary cause of failure at that time. For that test the standard X259-B4 (Antares IIB) nozzle was used. In this test the nozzle throat diameter was slightly smaller than the standard Antares IIB design and the exit cone was cut short for ground firing conditions. Nozzle burn-through was detected approximately 12 seconds after ignition. Failure was attributed to either severe spalling or "chunking" of the throat material or leakage through retainer ring vent holes. Details of the test are reported in Reference (6).

As a result of the XLDB failure, the following actions were taken to qualify the IIB nozzle for Scout.

(a) A design review of the IIB nozzle was performed.

(b) IIB nozzle fabrication procedures and documentation were reviewed.

(c) IIB nozzles in inventory were reinspected and a low pressure leak test of bondlines performed.

(d) The vent holes in the RPD-150 retainer ring were plugged with EA-946.

(e) One of the reinspected and reworked nozzles was successfully tested on Antares IIB motor S/N HIB-211.

After two successful SCOUT flights with the Antares IIB nozzles, failure of flight S-196 on December 5, 1975, was attributed to this nozzle. Post-flight analysis indicated evidence of progressive failure which started as early as seven seconds after ignition. It was concluded that the most probable cause of failure was delamination in the aft region of the insert. The reason for this delamination is not known positively, but recent finite element analyses indicate a marginal condition due to negative calculated margins of safety in this area. These thermoelastic stresses may have caused a delamination failure along the 45° plies in the aft end of the insert, resulting in loss of a portion of the insert. This would have exposed the forward face of the exit cone with resulting thermal degradation and burn-through.

As part of the S-196 failure investigation seven unfired Antares IIA nozzles were examined by X-ray. Except for the ATJ insert and the aft insert face angle, these nozzles are identical. Two of the nozzles had circumferential cracks progressing aft from the forward edge of the exit cone insulation to a maximum length of .024 m (0.9 in). There was also a small radial crack in one of the ATJ inserts (in addition to the cracked insulation) which originated in this same area. These cracks are attributed to residual stresses in the exit cone materials. The presence of these residual stresses in combination with high thermoelastic stresses during firing substantiate the conclusions of the S-196 failure investigation.

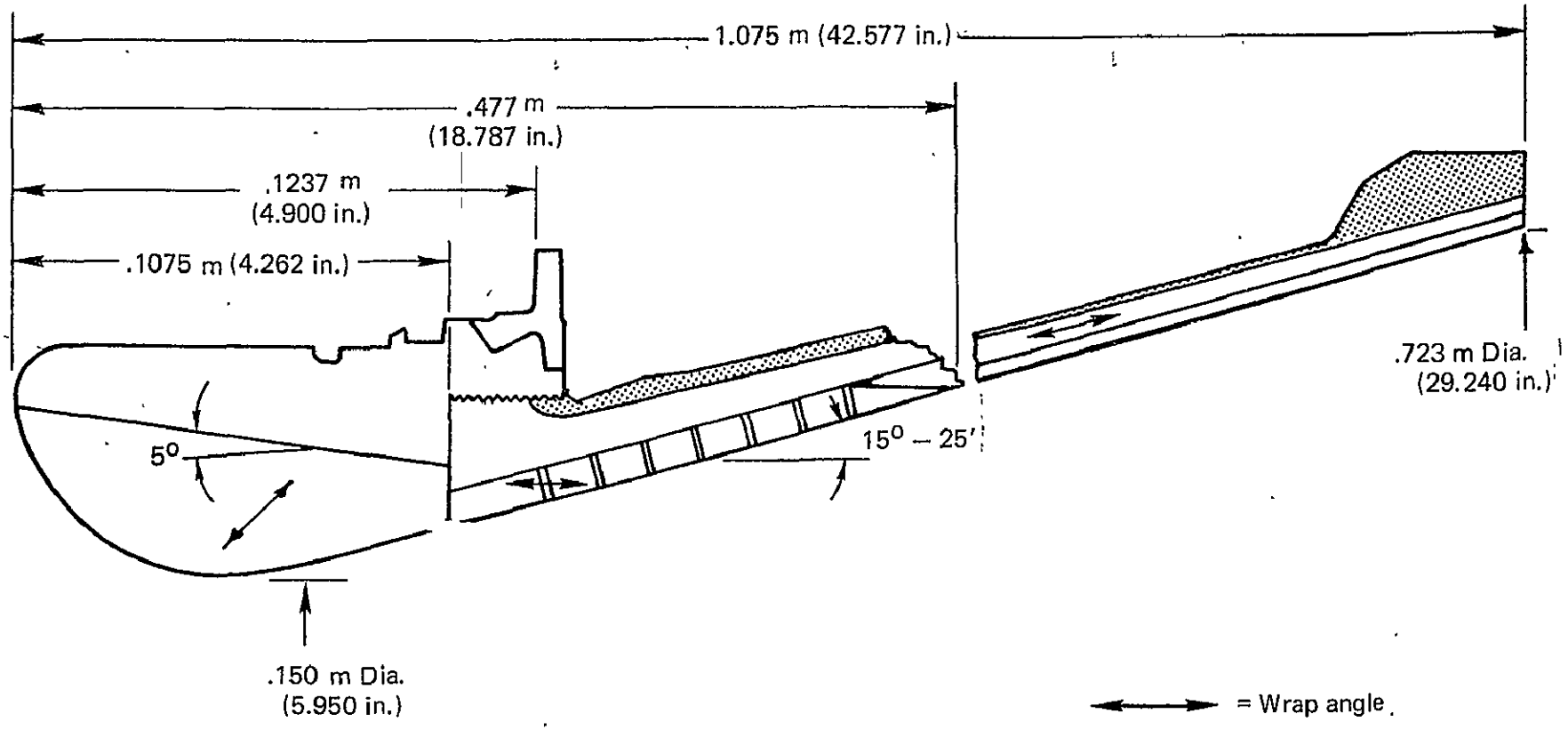

FIGURE C–1. – ANTARES II B NOZZLE GEOMETRY

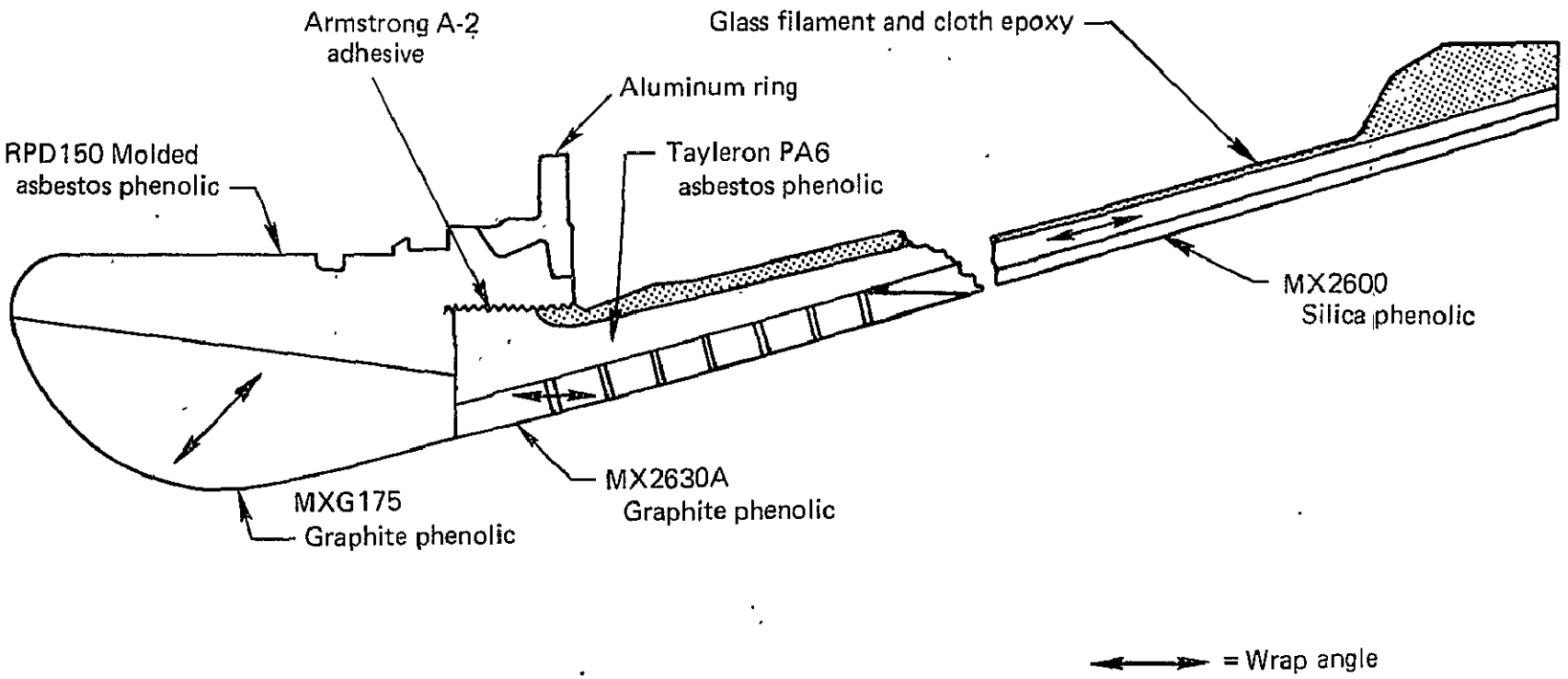

FIGURE C–2. – ANTARES IIB NOZZLE MATERIALS

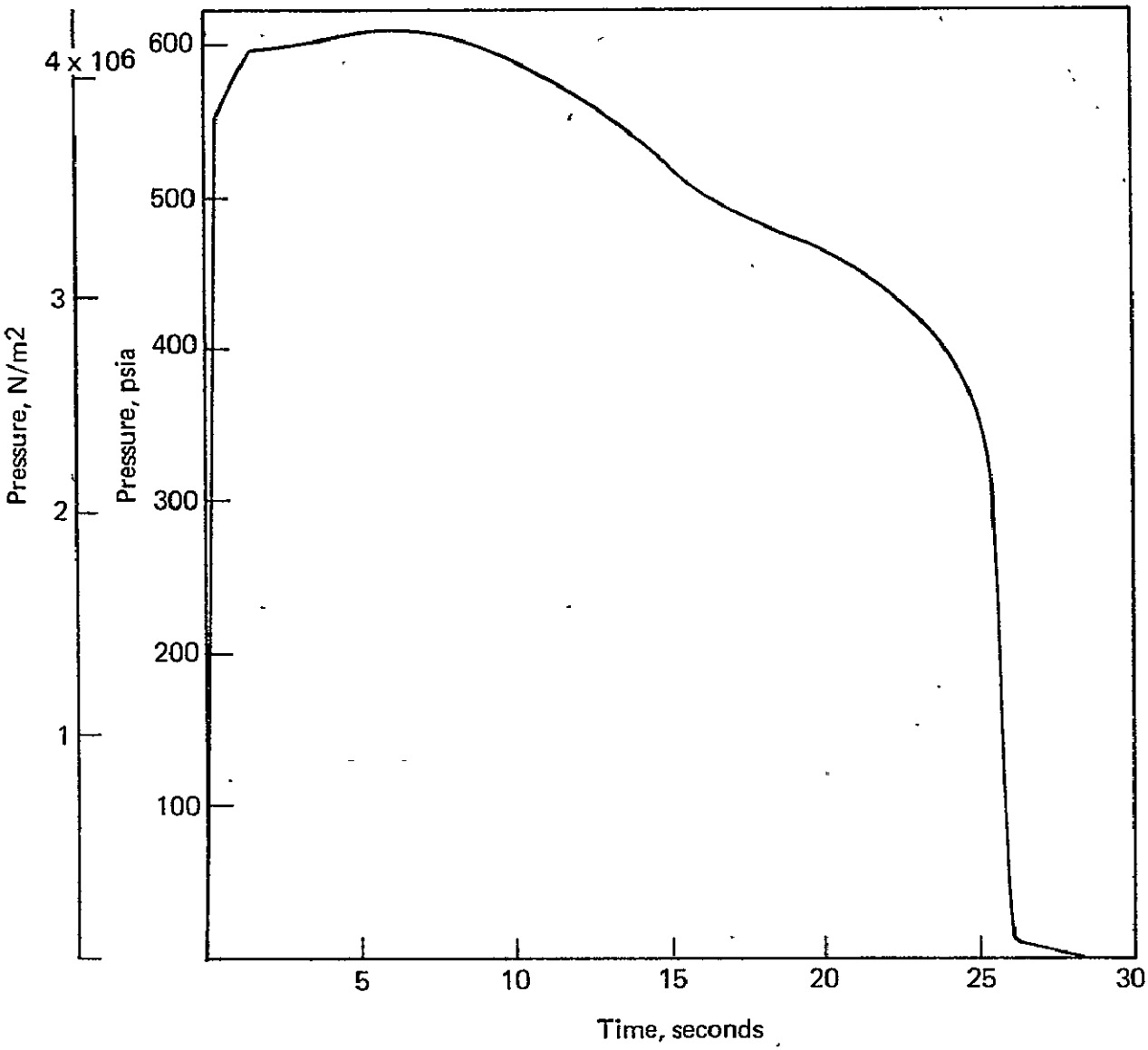

FIGURE C–3. – ANTARES II-B PRESSURE vs TIME

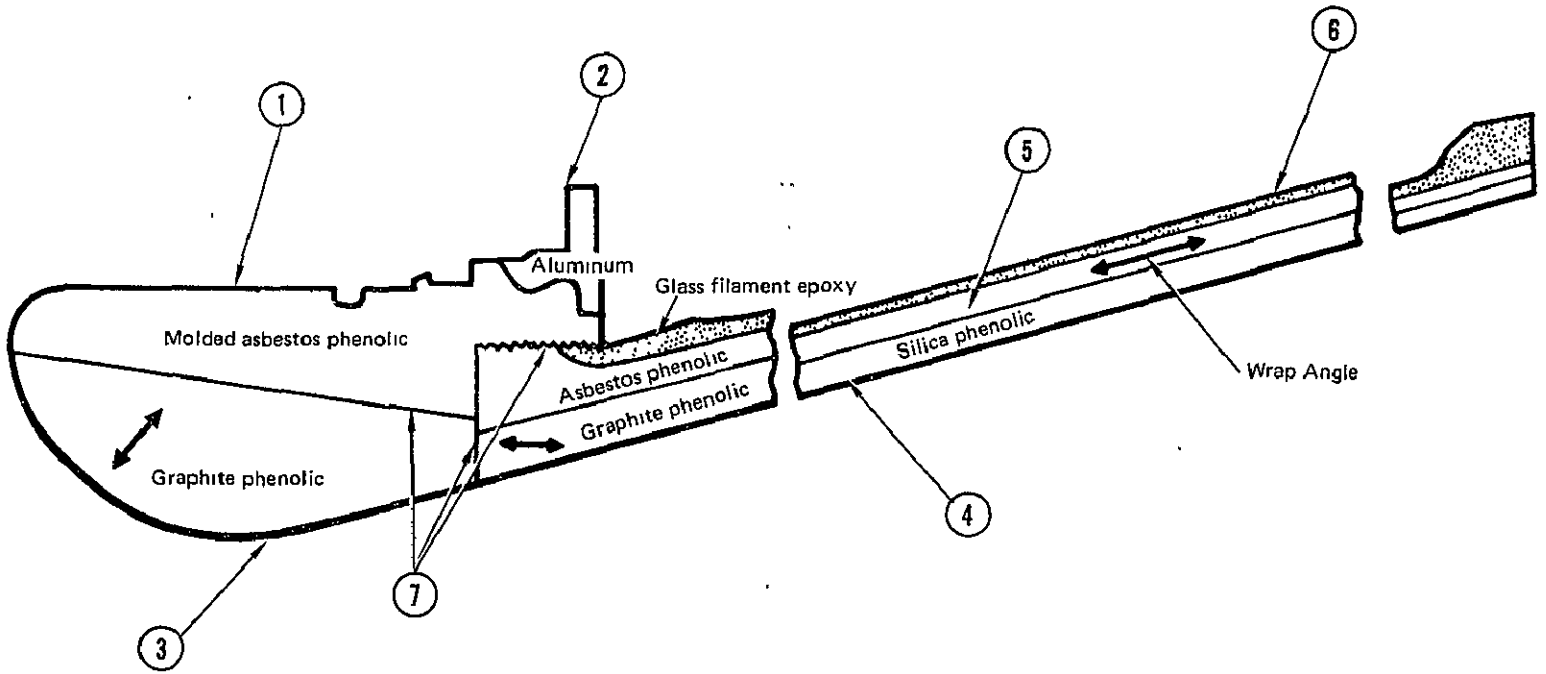

Item	Name	Material	Fabrication/inspection
1	Throat insert retainer ring molding	RPD 150 Asbestos phenolic per HS 259-2-166	The RPD 150 asbestos phenolic throat insert retaining ring and the 7075-T6 nozzle attach ring (item 2) are molded into an assembly in a hydraulic press using the following procedure. A weighed amount of macerated RPD 150 asbestos phenolic fiber is compressed in a cylindrical die at room temperature, ejected from the mold and preheated to 367°K (200°F) in a dielectric oven and then placed into a 423°K (300°F) preheated molding die. The 7075-T6 attach ring is also preheated to 423°K (300°F) and placed on top of the heated preform of RPD 150 just prior to closing the mold The two materials are cured at 423°K (300°F) at a pressure of 39.4 x 10^6 N/m^2 (5700 PSI). After ejection from the mold the assembly is post cured for 80 hours at 423°K (300°F) in an air oven. The molded assembly is visually and radiographically inspected for external and internal defects. All molded assemblies are final machined to drawing configuration.
2	Nozzle attachment ring	7075-T6 Ring forging per QQ-A-367	The ring forging is ultrasonically inspected for internal defects prior to machining into an attach ring. The machined attach ring is dye penetrant inspected prior to use in the retainer ring molding operation.
3	Throat insert	MXG 175 Graphite phenolic per HS 259-2-183	The graphite phenolic (MXG 175) throat inserts are fabricated by tape wrapping the MXG 175 bias tape material on a steel mandrel with the plies oriented 45° to the nozzle centerline. The outside diameter of the wrapped billet is machined to fit into a steel mold. The billet is then placed in the mold and cured in a steam heated hydraulic press at 423°K (300°F) under 27.6 x 10^6 N/m^2 (4000 psi) pressure. A test ring is cut off one end of the cured billet for test specimens. In-process tests are made to determine resin content, volatile content, degree of cure (acetone extraction) specific gravity, flexural strength, and horizontal shear. An alcohol wipe and radiographic inspection of the machined insert is made before it is bonded into a nozzle assembly

FIGURE C-4. – ANTARES II-B FABRICATION AND INSPECTION

Item	Name	Material	Fabrication/inspection
4	Exit cone liner Forward Aft	MX 2630A Graphite phenolic tape per HS 259-1-97, Type II MX 2600 Silica phenolic tape per HS 259-1-195, Type II	The exit cone liner is fabricated from two tape wrapped materials: graphite phenolic cloth (MX 2630A) in the forward portion and silica phenolic (MX 2600) in the aft portion. The two materials are tape wrapped parallel to the nozzle centerline on a common mandrel, vacuum bagged and partially cured in a hydroclave at 6.2×10^6 N/m^2 (900 psi). The partially cured assembly is then coated with phenolic resin (MIL-R-9299 Class 2, Type II) and overwrapped with asbestos phenolic tape (RPD-41, Type 9582) parallel to the liner surface. This assembly is hydroclave cured at 6.2×10^6 N/m^2 (900 psi) and then post cured in an oven. A ring of graphite phenolic is removed from the exit cone during facing operations for a density measurement test. .00158 M (1/16 in.) diameter holes are drilled in the graphite phenolic material to the asbestos phenolic interface to permit outgassing of volatile material during motor firing. 48 longitudinal grooves are equally spaced circumferentially in the PA-6, covered with acetate tape and overwrapped with glass filament epoxy for additional venting of outgassing volatiles
5	Exit cone liner backup insulation	Tayloron PA-6 asbestos phenolic tape per HS 259-2-185	
6	Exit cone outer shell	Filament wound glass rovings, ECG 140-801 per HS 259-1-211 181 Glass cloth, thalco glass per MIL-C-9084, Type VIII	The exit cone is covered with one layer of glass cloth (MIL-C-9084, Type VIII) impregnated with epon 828/ Metaphenylene diamine resin system and "B" staged at room temperature for 6-12 hours One ply of glass roving using the same epoxy resin system is wound circumferentially over the exit cone After "B" staging for 6-12 hours, a second ply of glass rovings is wrapped over the exit cone and again "B" staged for 6-12 hours at room temperature The large end of the exit cone is built up of alternate layers of glass cloth and circumferential winding plies. The exit cone is then oven cured for 4 hours at 311°K (100°F) followed by 2 hours at 344° K (160°F). One layer of Y9040 aluminum foil tape is bonded over the exit cone exterior surface to minimize heat radiation to the surrounding vehicle structure.
7	Adhesive	Armstrong A-2 epoxy with curing agent A per HS 259-1-186, Comp 4	The exit cone is machined and then bonded to the throat insert retainer molding using Armstrong A-2 epoxy with curing agent A. The assembly is oven cured at 325°K (125°F) for one hour. A thin layer of A-2 epoxy/curing agent A adhesive is applied to the I.D. surface of the retainer ring molding and similarly cured. This operation is performed to seal off the vent holes to prevent adhesive from extruding into them during bonding of the graphite throat insert. The MXG 175 graphite phenolic throat insert is bonded into the retainer ring/exit cone assembly using A-2/curing phenolic agent A epoxy adhesive and cured at 325°K (125°F) for one hour. The bonding surfaces of both the asbestos phenolic retainer ring and the MXG 175 throat insert are alcohol wipe inspected prior to bonding.

FIGURE C–4. – ANTARES II-B FABRICATION AND INSPECTION – Concluded

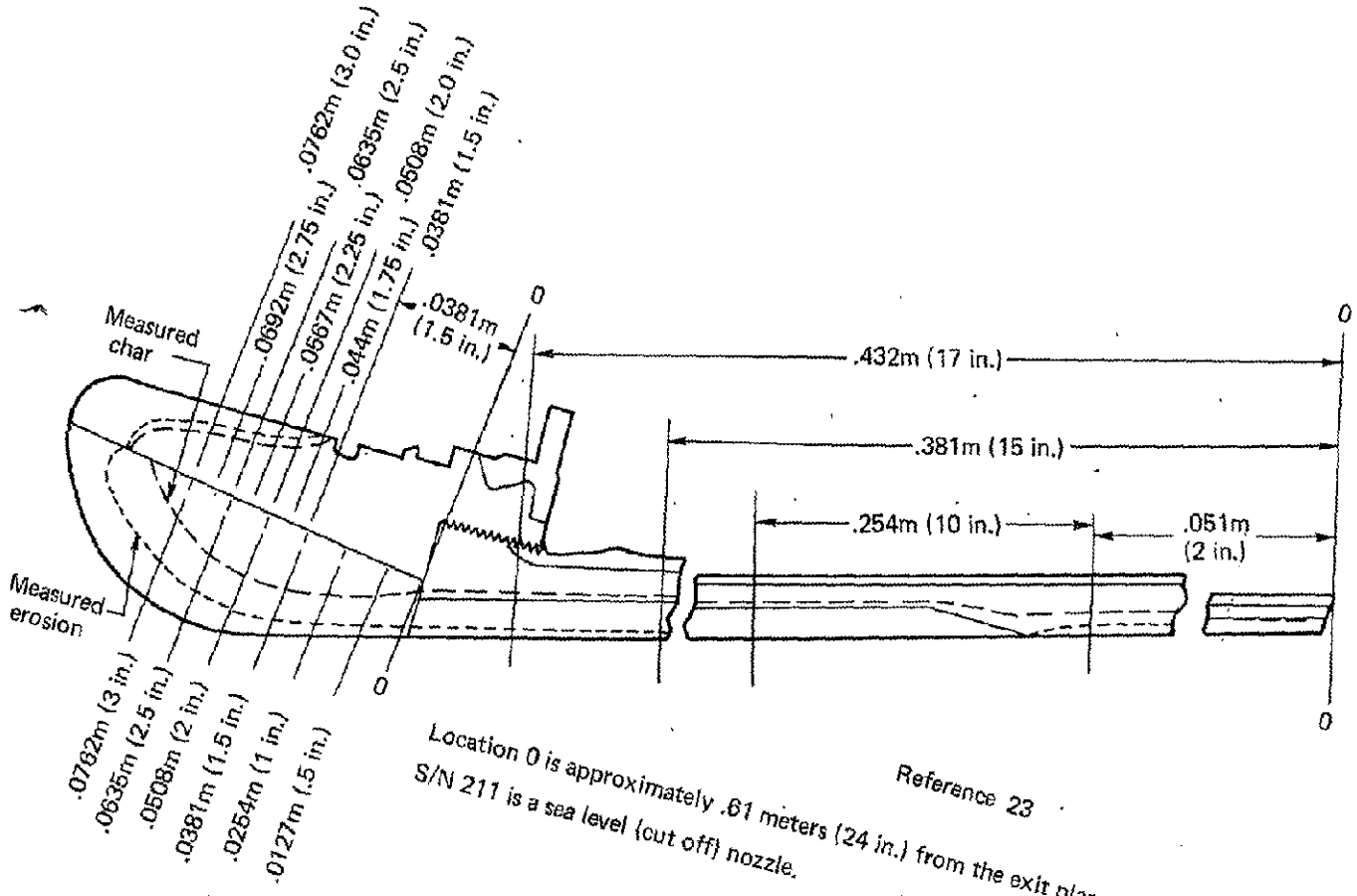

Location 0 is approximately .61 meters (24 in.) from the exit plane of a flight nozzle.
S/N 211 is a sea level (cut off) nozzle.

Reference 23

FIGURE C–5. – ANTARES II-B MEASURED CHAR AND EROSION

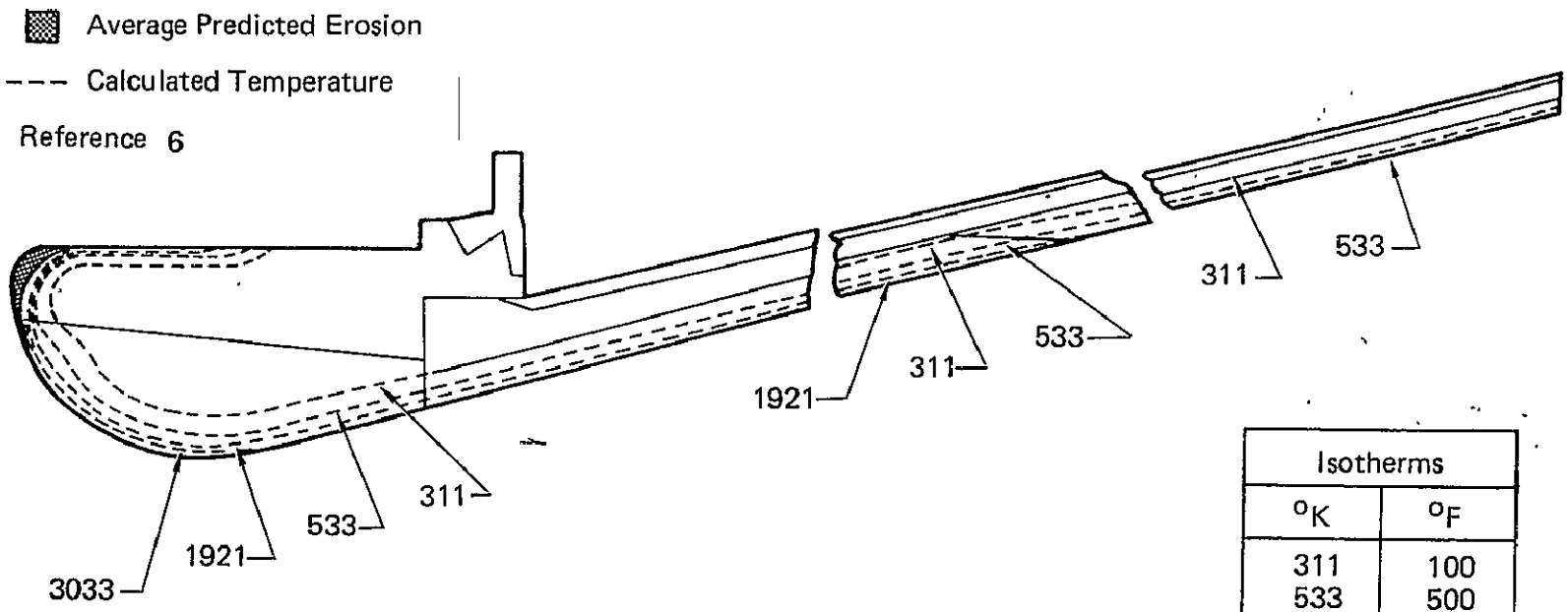

Isotherms	
^{o}K	^{o}F
311	100
533	500
1921	3000
3033	5000

FIGURE C–6. – TEMPERATURES IN THE ANTARES II-B NOZZLE AT 5 SECONDS

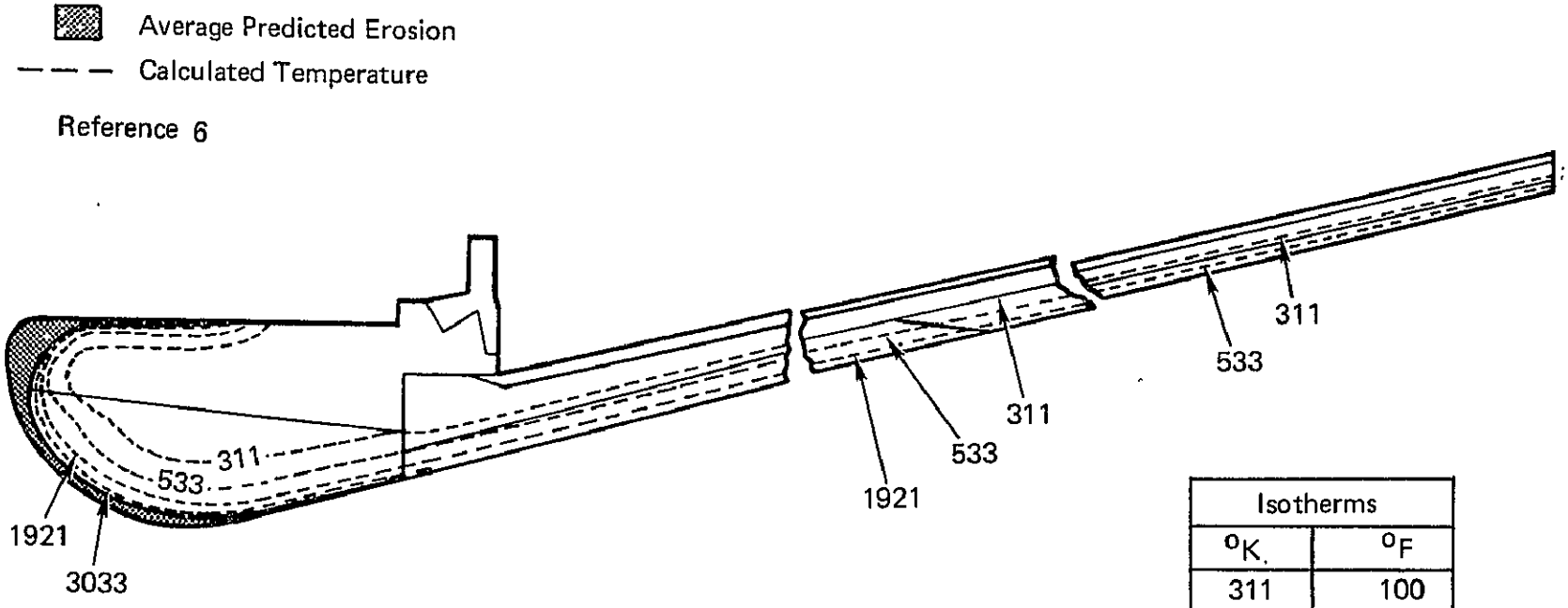

Isotherms	
^{o}K	^{o}F
311	100
533	500
1921	3000
3033	5000

FIGURE C–7. – TEMPERATURES IN THE ANTARES II-B NOZZLE AT 10 SECONDS

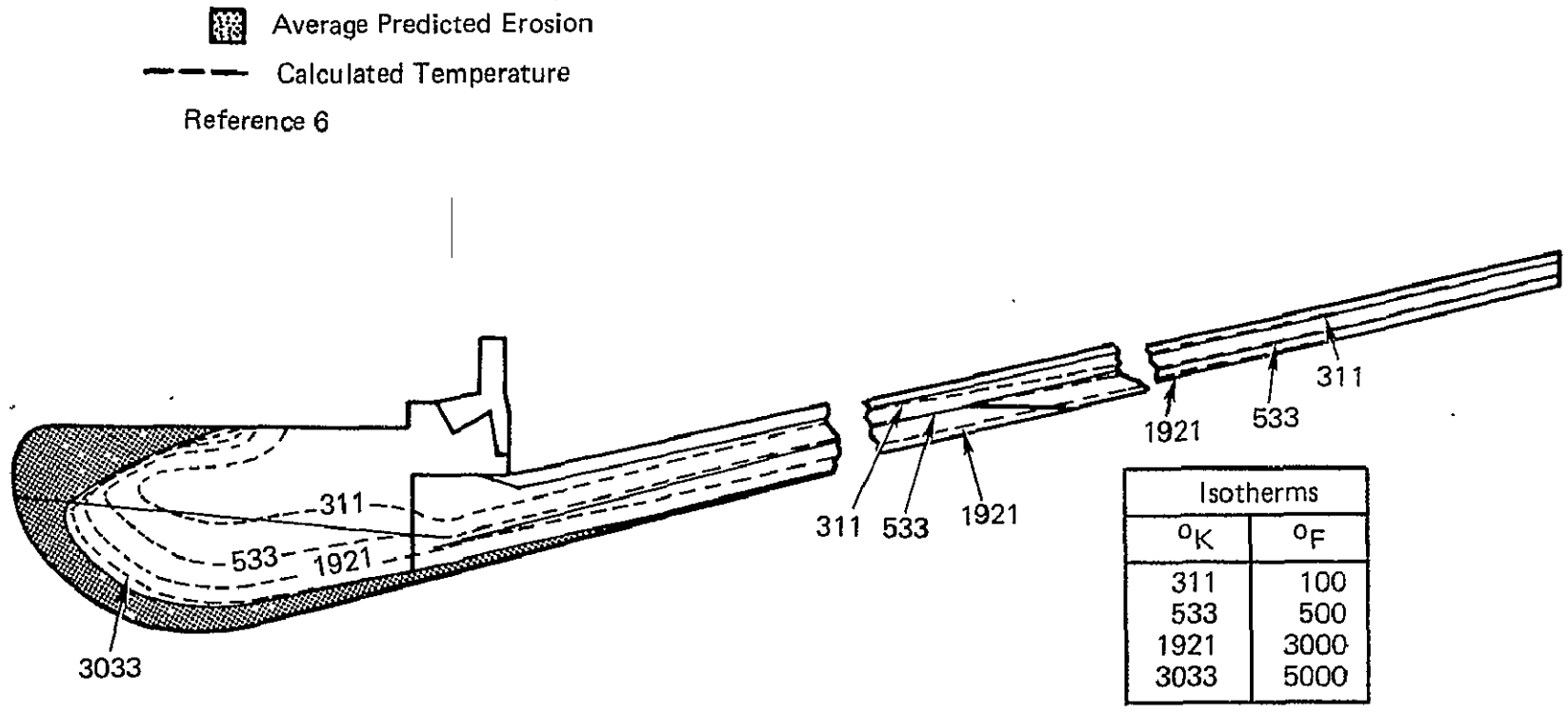

FIGURE C–8. – TEMPERATURES IN THE ANTARES II-B NOZZLE AT 27 SECONDS

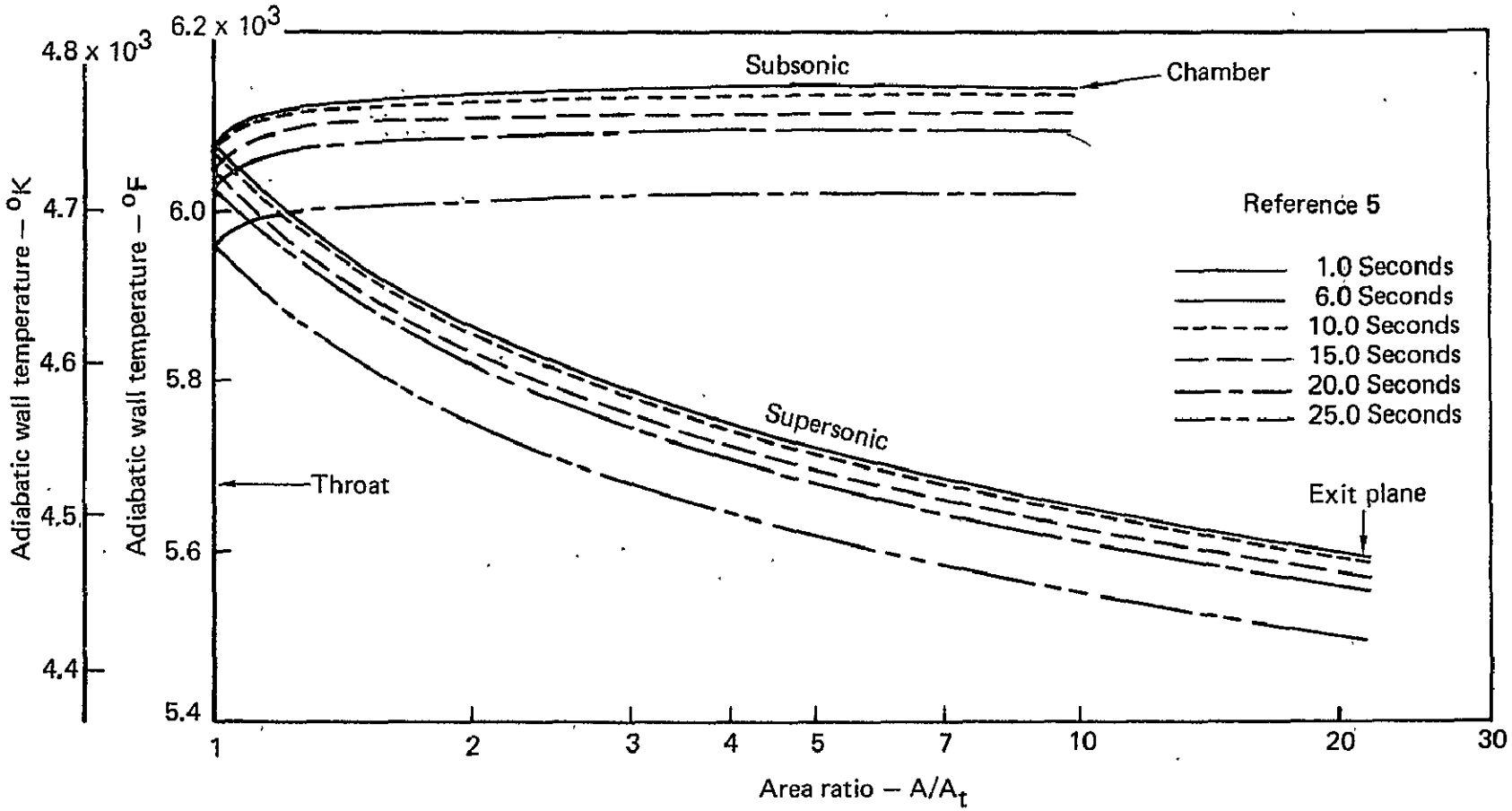

FIGURE C–9. – ADIABATIC WALL TEMPERATURE AS A FUNCTION OF NOZZLE AREA RATIO FOR THE ANTARES II-B NOZZLE

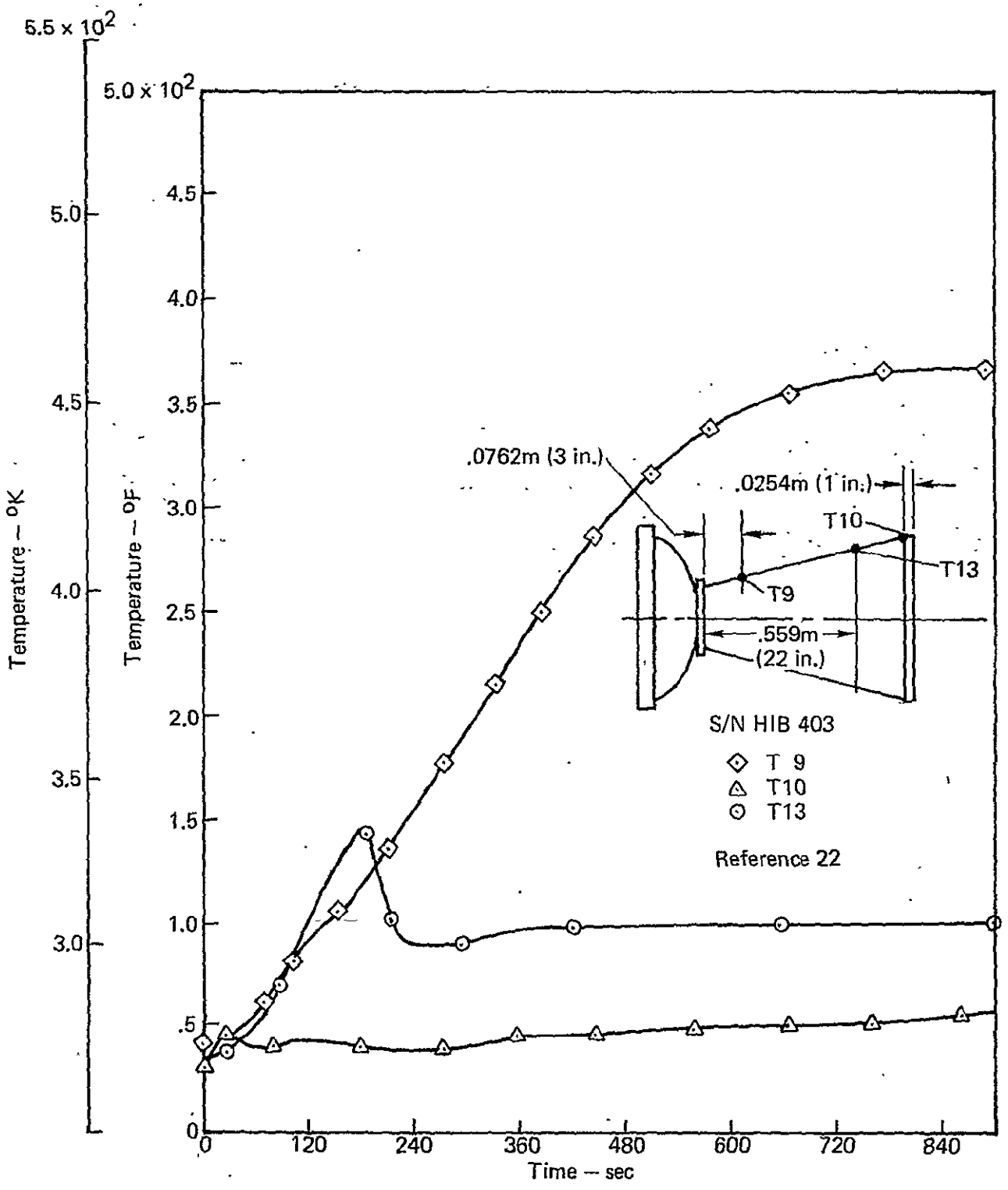

FIGURE C–10. –ANTARES II-B NOZZLE EXTERIOR TEMPERATURES VS TIME (AEDC TEST)

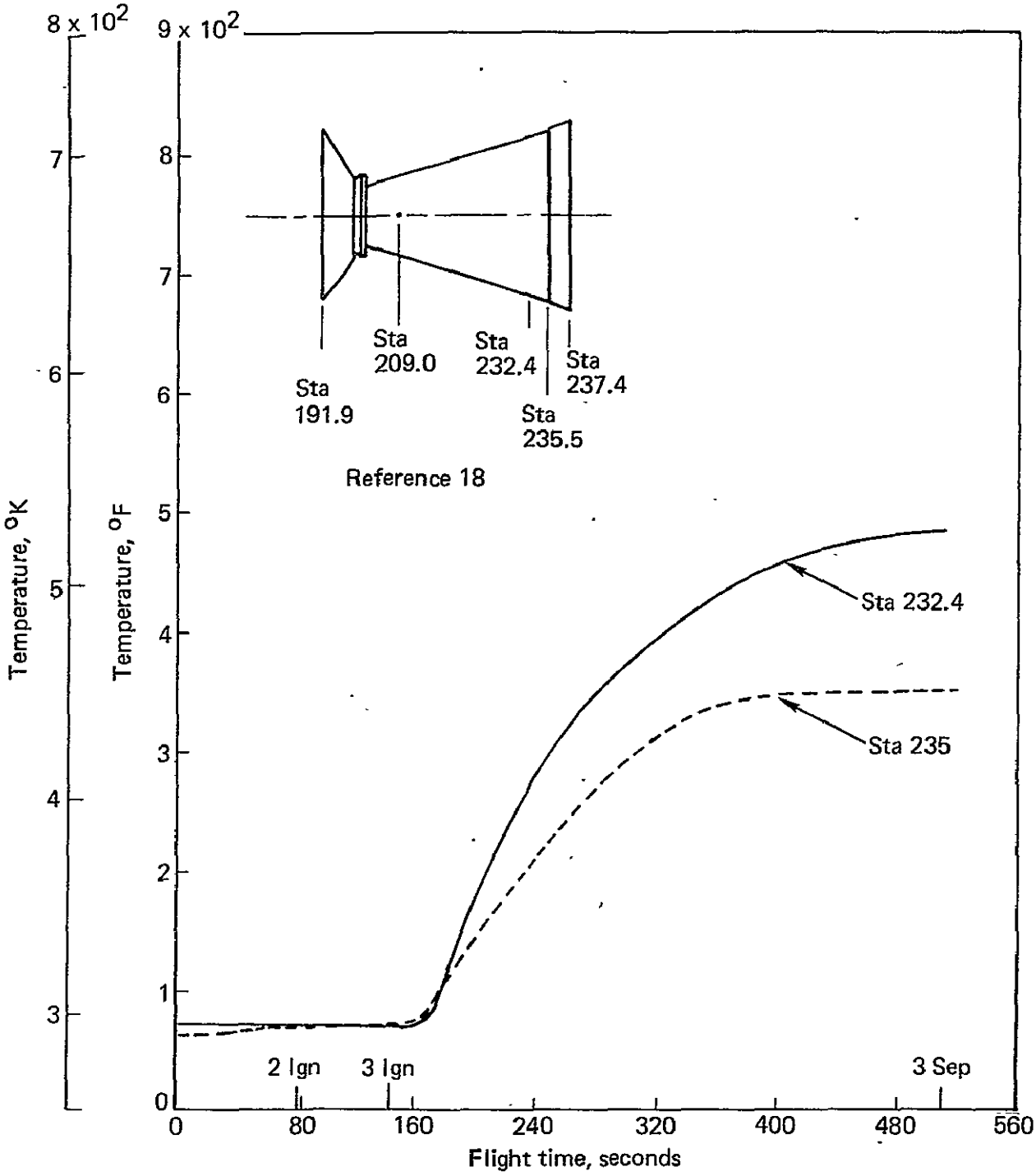

FIGURE C–11. –ANTARES II-B NOZZLE EXTERIOR TEMPERATURES (S191 FLIGHT DATA)

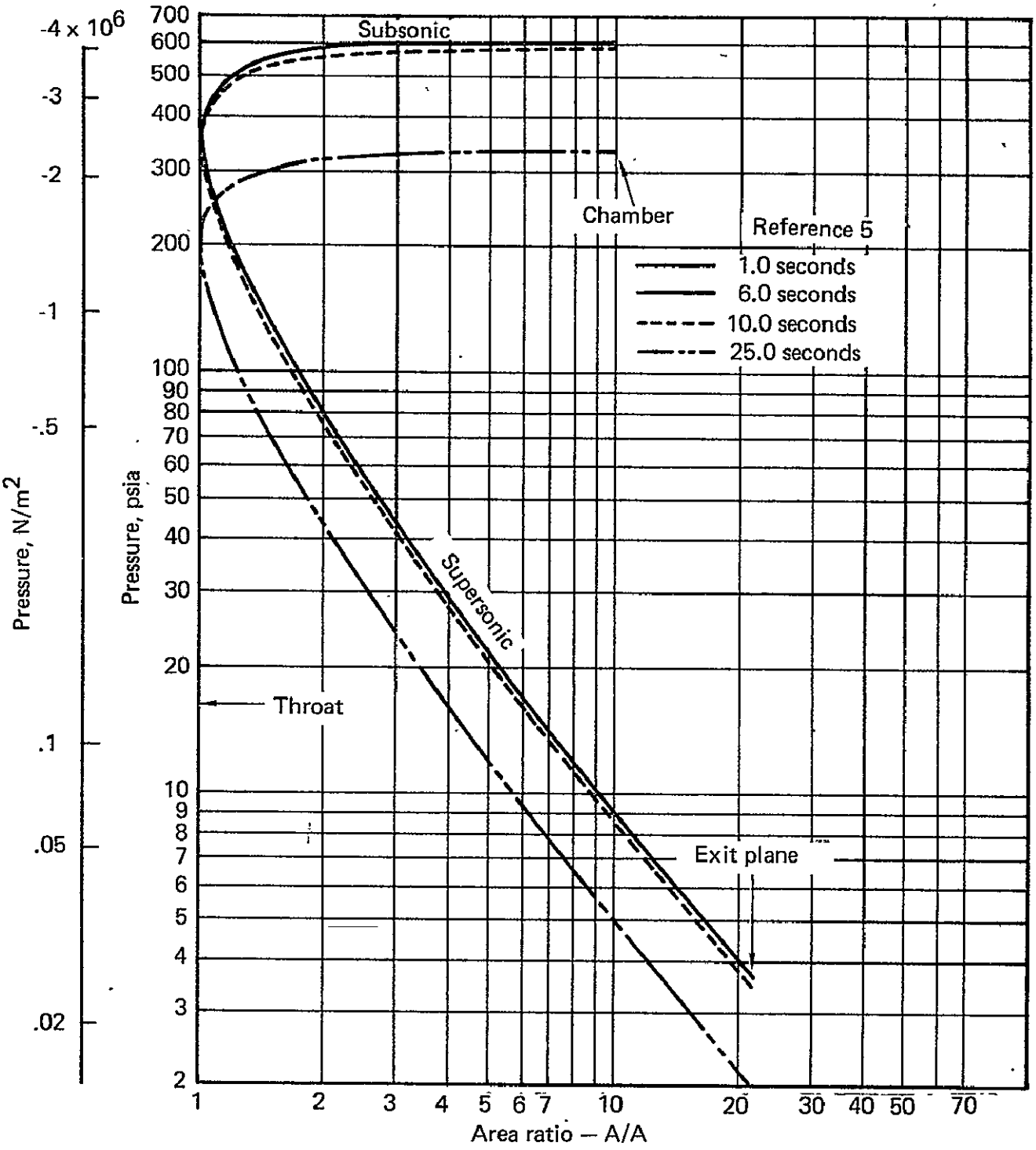

FIGURE C–12. – GAS PRESSURE AS A FUNCTION OF NOZZLE AREA RATIO

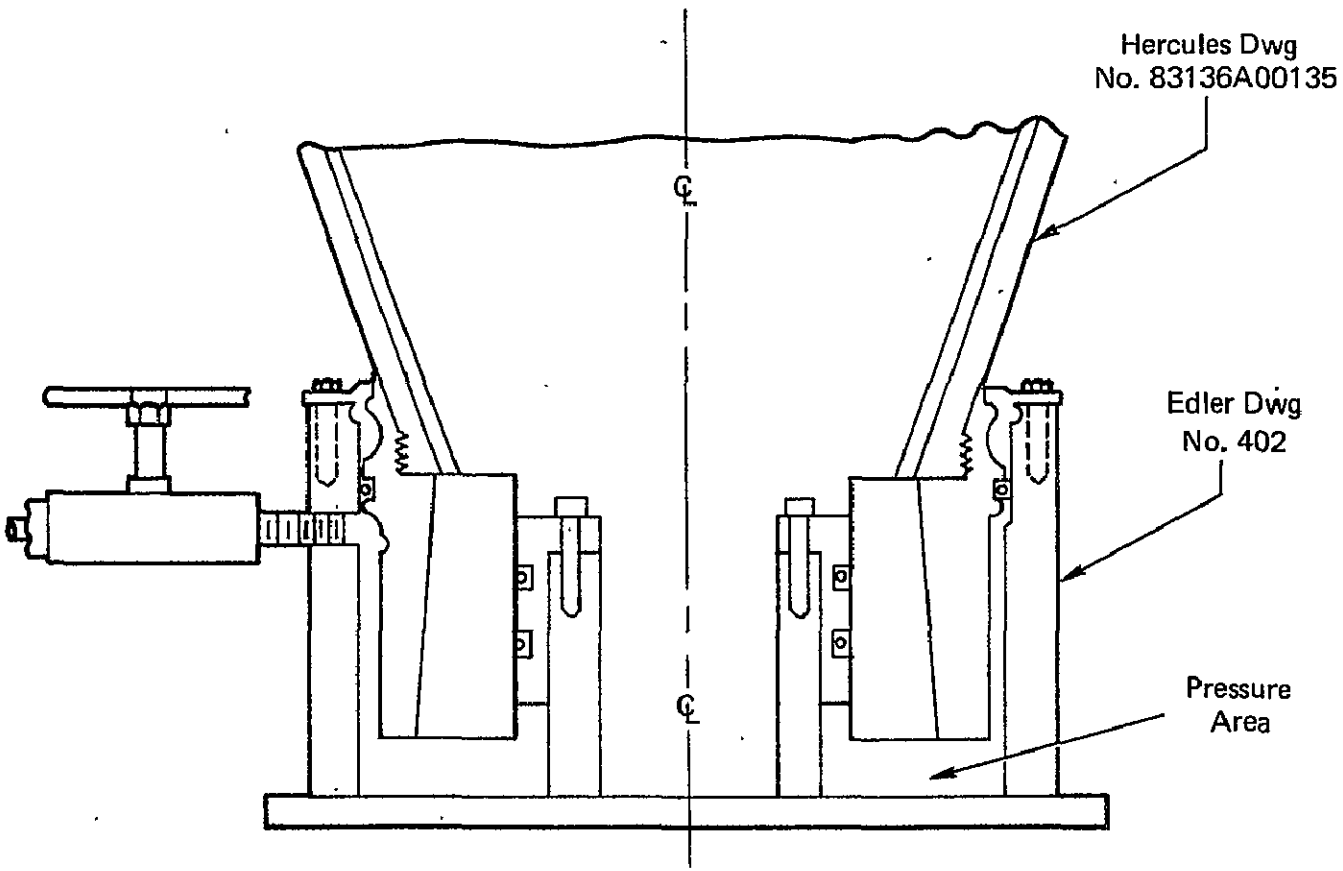

FIGURE C–13. – PROOF PRESSURE TEST ARRANGEMENT

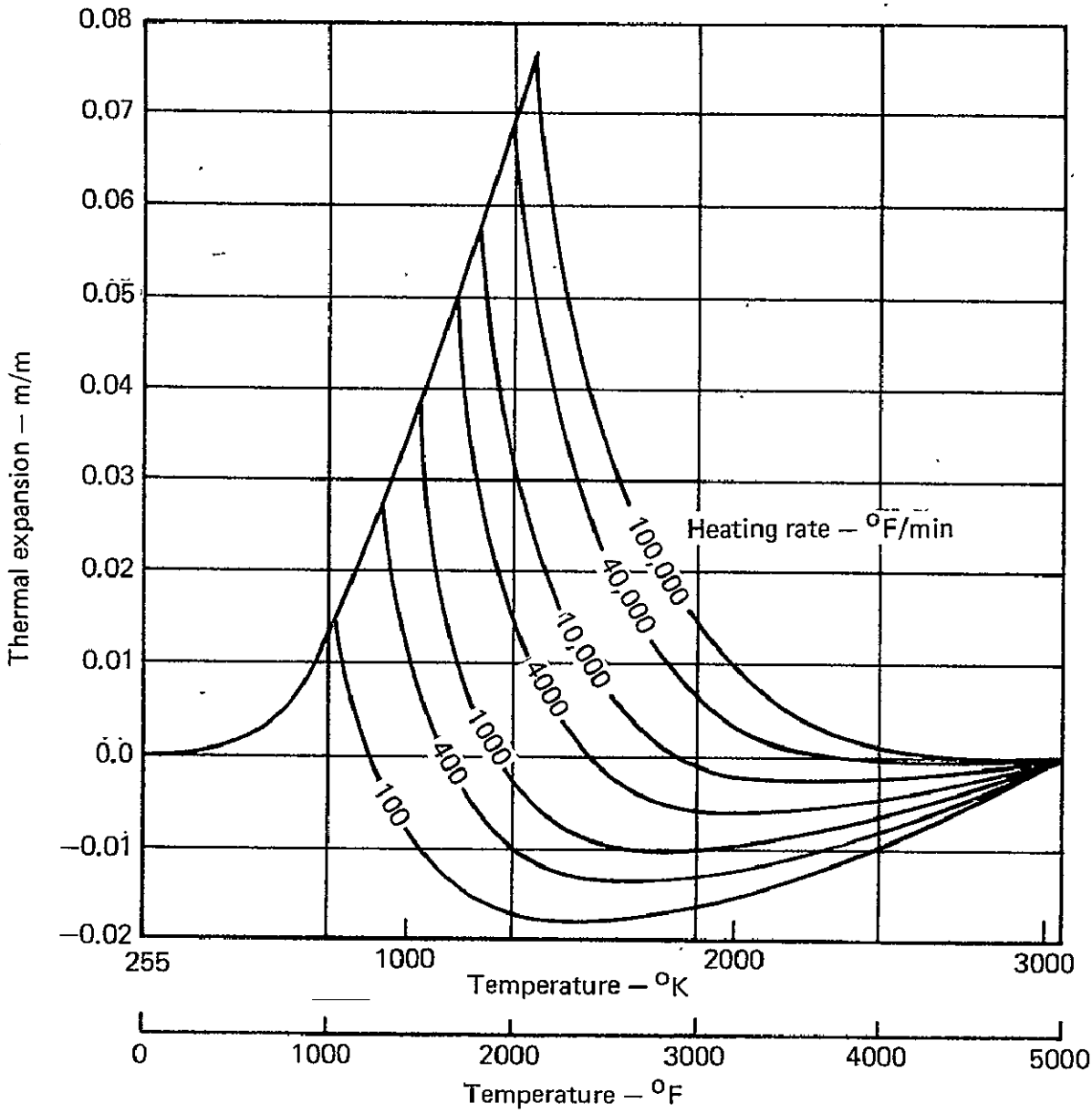

FIGURE C-14. — ESTIMATED HEATING RATE EFFECT ON THE THERMAL EXPANSION OF GRAPHITE PHENOLIC TAPE IN THE ACROSS PLY DIRECTION

TABLE C–I. – ANTARES IIB NOZZLE MATERIALS

Component	Material	Vendor designation	Procurement specification
Retainer ring	Asbestos phenolic	RPD 150	HS-259-1-166
Attach ring	7075 T6	Aluminum	QQ-A-367
Throat insert	Graphite phenolic	MXG 175 FM 5014	HS-259-2-183
Fwd exit cone liner	Graphite phenolic	MX 2630 A	HS-259-1-97
Aft exit cone liner	Silica phenolic	MX 2600 MX 2625	HS-259-1-195
Exit cone insulation	Asbestos phenolic	Tayleron PA–6	HS-259-1-111
Outer exit cone structure	Glass filament/ cloth/resin	ECG-140, 12 end with 801 sizing/ 181 glass cloth Epon 828 resin	HS-259-1-69 (Type I Class I), HS-259-1-211, MIL-C-9084 (Type VIII)
Adhesive	Epoxy	Armstrong A–2/curing agent A	HS-259-1-186

TABLE C–II. – ANTARES II-B MOTOR CHARACTERISTICS

Propellant property	Type/Designation
Propellant Designation	CYI-75
Propellant Type	Composite Modified Double Base
Grain Configuration	Cylindrical 4 pointed gear bore in aft end with a cylindrical bore in forward end.
Propellant Gas Properties: (Chamber)	
Specific Heat Ratio (γ)	1.15
C_p, cal/gm-^oK	0.425
Molecular Weight	19.3
C*, m/sec	1618 (5300 ft/sec)
Flame Temp, ^oK (at 525 psi)	3138 (6108^oF)

Motor performance	
Avg. Web Thrust Vacuum, N	126830 (28514 lb)
Total Motor Weight, Kg	1270 ± 12 (2800 ± 27 lb)
Consumed Weight, Kg	1171 (2582 lb)
Propellant Weight, Kg	1163 $^{+11}_{-7}$ (2565 $^{+25}_{-15}$ lb)
Specific Impulse Vacuum (Sec)	284.95
Total Burn Time (Sec)	28.9
Action Time (Sec) @ 297^oK	26.0 ± 3.3
Pressure, Action Average, N/m^2 @ 297^oK	3.62 x 106 (525 psi)
MEOP, N/m^2	4.75 x 106 (690 psi)
Proof Pressure N/m^2	Case: 5.17 x 106 (750 psi) Nozzle: 3.69 x 106 (536 psi)

Reference 16.

TABLE C–III. – ANTARES IIB NOZZLE MATERIAL PROPERTIES

Material: Asbestos phenolic (RPD-150)

Property	Temperature, °K (°F)				
	300°K (75)	811°K (1000)	1366°K (2000)	1782°K (2750)	3870°K (6500)
Modulus of elasticity $N/m^2 \times 10^9$ ($psi \times 10^6$)	14.9 (2.17)	6.8 (0.98)	2.3 (0.34)	0.2 (0.025)	0.2 (0.025)
Shear modulus $N/m^2 \times 10^9$ ($psi \times 10^6$)	6.0 (0.87)	2.6 (0.38)	0.9 (0.13)	0.07 (0.01)	0.07 (0.01)
Poisson's ratio	0.256	0.3	0.3	0.3	0.335
Coeff of expansion $m/m\text{-}^oK \times 10^{-6}$ ($in./in.\text{-}^oF \times 10^{-6}$)					
Hoop and axial	12.9 (7.2)	16.2 (9.0)	3.6 (2.0)	1.8 (1.0)	0.0 (0)
Radial	15.8 (8.8)	32.4 (18.0)	1.8 (1.0)	– .9 (–0.5)	–1.8 (–1.0)
Tensile strength $N/m^2 \times 10^6$ (ksi)	62.0 (9)	22.0 (3.2)	4.5 (0.66)	1.4 (0.21)	0.7 (0.10)
Shear strength $N/m^2 \times 10^6$ (ksi)	46.8 (6.8)	15.1 (2.2)	1.9 (0.28)	0.4 (0.06)	0.2 (0.03)
Thermal conductivity $cal/m\text{-}hr\text{-}^oK \times 10^3$ ($B\text{-}in./ft^2\text{-}hr\text{-}^oF$)	.55 (4.5)	.55 (4.5)	.55 (4.5)	.55 (4.5)	.55 (4.5)
Specific heat ($cal/gm\text{-}^oK$)	.27	.27	.27	.27	.27

Reference 5

TABLE C–III. – ANTARES IIB NOZZLE MATERIAL PROPERTIES–Continued

Material: graphite phenolic (MXG 175 or FM 5014)

		300°K R.T.	395°K (250°F)	533°K (500°F)	811°K (1000°F)	1366°K (2000°F)	1922°K (3000°F)	2478°K (4000°F)
Thermal conductivity, cal/m-hr-°K x 10^3 (B-in./ft^2-hr-°F)	With lam.	3.28 (26)	3.34 (27)	3.67 (30)	4.36 (35)	5.9 (48)	7.64 (61)	9.9 (80)
	Against lam.	1.15 (9)	1.15 (9)	1.22 (9)	1.6 (13)	3.28 (27)	5.78 (47)	8.83 (71)
Coeff of thermal exp. M/M-°K x 10^{-6} (in./in.-°F x 10^{-6})	With lam.	–	12.6 (7)	7.2 (4)	1.8 (1)	1.8 (1)	1.8 (1)	2.7 (1.5)
	Against lam.	–	23.4 (13)	–14.4 (–8)	.9 (.5)	3.6 (2)	3.6 (2)	3.6 (2)
Modulus of elasticity N/m^2 x 10^9 (psi x 10^6)	With lam.	13.1 (1.9)	11.0 (1.6)	8.3 (1.2)	0.7 (1)	2.75 (0.4)	2.4 (0.35)	2.1 (0.3)
	Against lam.	2.8 (0.4)	2.1 (0.3)	1.4 (0.2)	0.7 (0.1)	0.35 (0.05)	0.35 (0.05)	0.35 (0.05)
Tensile ult strength N/m^2 x 10^6 (psi x 10^3)	With lam.	55 (8)	45 (6.5)	34 (5)	20 (3)	13 (1.9)	13 (1.9)	13 (1.9)
	Against lam.	5.1 (0.74)	5.0 (0.73)	4.3 (0.63)				
Interlaminar shear strength N/m^2 x 10^6 (psi x 10^3)		13 1.85	10 1.52	7.5 1.10	2.8 0.4	1.6 0.24	1.6 0.24	1.6 0.24
Specific heat cal/gm-°K		0.23	0.32	0.37	0.43	0.48	0.5	0.5
Poisson's ratio, μ		–	–	–	–	–	–	–

Reference 5

TABLE C–III. – ANTARES IIB NOZZLE MATERIAL PROPERTIES – Continued

Materials: Graphite phenolic (MX-2630A)

Temperature ^{o}K (^{o}F)	Thermal conductivity Cal/m-hr-^{o}K X 10^3 (BTU-in/ft2-hr-^{o}F)		Specific heat Cal/gm-^{o}K	Emissivity	Density GM/cc
	Perpendicular	Parallel			
295 (70)	1.09 (8.8)	3.28 (26.5)	.24	.78	1.44
478 (400)	–	–	–	.78	–
589 (600)	1.2 (9.7)	3.66 (29.5)	.88	.78	1.39
728 (850)	1.19 (9.6)	3.5 (28.2)	.93	.78	1.36
866 (1100)	1.19 (9.6)	3.65 (29.5)	.88	.79	1.35
1366 (2000)	1.78 (14.4)	5.37 (43.4)	.49	.82	1.20
1922 (3000)	2.08 (16.8)	6.1 (49.4)	.50	.88	1.20
2478 (4000)	2.36 (19.2)	7.0 (56.5	.50	.91	1.20
3033 (5000)	2.74 (22.1)	8.22 (66.5)	.50	.95	1.27
3860 (6500)	4.02 (32.5)	11.87 (96.0)	.50	.95	1.28
4140 (7000)	4.02 (32.5)	11.87 (96.0)	.50	.95	1.28

Reference 5

TABLE C–III. – ANTARES IIB NOZZLE MATERIAL PROPERTIES – Continued

Material: Graphite phenolic (MX 2630A)

	Temperature, °K (°F)						
Modulus of elasticity N/m2 x 109 (psi x 106)	295 (70)	533 (500)	811 (1000)	1366 (2000)	1922 (3000)	2478 (4000)	3033 (5000)
Warp Dir.	9.9 (1.44)	5.2 (.75)	4.1 (.60)	5.3 (.77)	6.0 (.87)	3.9 (.56)	1.4 (.20)
Fill Dir.	8.0 (1.16)	2.8 (.40)	2.2 (.32)	3.4 (.50)	3.0 (.44)	2.0 (.29)	.7 (.10)
Across Dir.	5.2 (.75)	2.1 (.30)	1.4 (.20)	.9 (.13)	.6 (.08)	.3 (.05)	.1 (.02)
Interlaminar Shear Modulus N/m2 x 109 (psi x 106)	3.1 (.45)	.8 (.11)	.8 (.12)	1.0 (.15)	.9 (.13)	.6 (.09)	.2 (.03)
Poisson's Ratio							
Warp-Fill	.16	.14	.13	.11	.16	.21	.25
Across-Warp	.05	.04	.02	.01	.01	.01	.01
Across-Fill	.05	.04	.02	.01	.01	.01	.01
Coef. of Thermal Exp., m/m-°K x 10^{-6} (in/in.-°F) x 10^{-6}, Warp	14.4 (8.0)	24.6 (13.7)	12.6 (7.0)	1.8 (1.0)	0 (0)	0 (0)	0 (0)
Fill	19.1 (10.6)	25.2 (14.0)	13.5 (7.5)	1.44 (.8)	– .9 (–.5)	– .9 (–.5)	– .9 (–.5)
Across	24.6 (13.7)	85.5 (48.0)	360 (200)	– 10.8 (–6.0)	– 7.2 (–4.0)	– 3.6 (–2.0)	0 (0)
Tensile Strength N/m2 x 106 (psi x 103) Warp	164 (23.8)	118 (17.1)	50 (7.2)	54 (7.8)	58 (8.5)	72 (10.5)	48 (7.0)
Fill	83 (12.0)	58 (8.5)	37 (5.3)	32 (4.6)	39 (5.7)	30 (4.3)	12 (1.8)
Across	11 (1.6)	4 (.6)	1 (.2)	2 (.3)	2 (.3)	.7 (.1)	.3 (.05)
Shear Strength N/m2 x 106 (psi x 103) Warp	69 (10.0)	34 (5.0)	10 (1.5)	10 (1.5)	10 (1.4)	9 (1.3)	7 (1.0)
Fill	41 (6.0)	21 (3.0)	7 (1.0)	6 (.86)	6 (.84)	6 (.85)	5 (.70)
Across	41 (6.6)	21 (3.0)	7 (1.0)	6 (.86)	6 (.84)	6 (.85)	5 (.70)

Reference 5

TABLE C–III. – ANTARES IIB NOZZLE MATERIAL PROPERTIES – Continued

Material: Silica phenolic (MX 2600)

Temperature ^{o}K (^{o}F)	Thermal conductivity cal/m-hr-^{o}K x 10^3 (BTU-in/ft2-hr-^{o}F)		Specific heat Cal/gm-^{o}K	Emissivity	Density GM/cc
	Perpendicular	Parallel			
295 (70)	.31 (2.5)	.68 (5.5)	.20	.78	1.77
478 (400)	.31 (2.5)	.67 (5.4)	.29	.78	1.74
589 (600)	.3 (2.4)	.65 (5.3)	—	.78	1.70
728 (850)	.3 (2.4)	.62 (5.0)	—	.78	1.59
866 (1100)	.3 (2.4)	.64 (5.2)	—	.79	1.52
1366 (2000)	.85 (6.9)	1.81 (14.6)	.40	.82	1.45
1922 (3000)	1.09 (8.8)	2.33 (18.8)	.49	.88	1.37
2478 (4000)	1.26 (10.2)	2.8 (22.6)	.49	.91	1.17
3033 (5000)	1.46 (11.8)	3.33 (26.9)	.53	.95	1.23
3860 (6500)	1.57 (12.7)	3.64 (29.4)	.57	.95	1.28
4140 (7000)	1.57 (12.7)	3.64 (29.4)	.57	.95	1.28

Reference 5

TABLE C–III. – ANTARES IIB NOZZLE MATERIAL PROPERTIES – Continued

Material: Silica phenolic (MX2600)

	Temperature, °K (°F)						
Modulus of elasticity $N/m^2 \times 10^9$ (psi x 10^6)	295 (70)	533 (500)	811 (1000)	1366 (2000)	1922 (2000)	2478 (4000)	3033 (5000)
Warp Dir.	(3.3)	(1.5)	(1.2)	(1.3)	(.03)	(.03)	(.03)
Fill Dir.	(1.1)	(.6)	(.4)	(.8)	(.02)	(.02)	(.02)
Across Dir.	(.9)	(.5)	(.4)	(.5)	(.09)	(.09)	(.09)
Interlaminar Shear Modulus $N/m^2 \times 10^9$ (psi x 10^6)	(.47)	(.26)	(.21)	(.31)	(.01)	(.01)	(.01)
Poisson's Ratio							
Warp-Fill	.25	.27	.29	.30	.30	.30	.30
Across-Warp	.02	.03	.03	.06	.06	.06	.06
Across-Fill	.02	.03	.03	.06	.06	.06	.06
Coef. of Thermal Exp., m/m-°K x 10^{-6} (in/in.-°F) x 10^{-6}, Warp	12.6 (7.0)	15.1 (8.4)	16.2 (9.0)	5.04 (2.8)	1.8 (1.0)	0 (0)	0 (0)
Fill	12.6 (7.0)	15.1 (8.4)	16.2 (9.0)	5.04 (2.8)	1.8 (1.0)	0 (0)	0 (0)
Across	16.2 (9.0)	23.4 (13.0)	32.2 (17.9)	1.8 (1.0)	– .9 (–.5)	– 1.8 (–1.0)	– 1.8 (–1.0)
Tensile Strength $N/m^2 \times 10^6$ (psi x 10^3)							
Warp	(24.)	(10.)	(5.)	(2.)	(.3)	(.2)	(.1)
Fill	(10.)	(7.)	(1.5)	(1.2)	(.3)	(.1)	(.1)
Across	(2.5)	(1.0)	(.3)	(.2)	(.05)	(.01)	(.01)
Shear Strength $N/m^2 \times 10^6$ (psi x 10^3)							
Warp	(7.)	(3.)	(.6)	(.6)	(.1)	(.08)	(.05)
Fill	(7.)	(3.)	(.6)	(.6)	(.1)	(.08)	(.05)
Across	(16.)	(5.8)	(3.0)	(1.0)	(.1)	(.08)	(.05)

Reference 5

TABLE C–III. – ANTARES IIB NOZZLE MATERIAL PROPERTIES – Continued

Material: Asbestos phenolic (PA–6)

		300°K R.T.	533°K (500°F)	811°K (1000°F)	1366°K (2000°F)	1922°K (3000°F)	2478°K (4000°F)
Thermal conductivity, cal/m-hr-°K X 10^3 (B-in./ft^2-hr-°F)	With lam.	.21 (1.7)	.22 (1.8)	.21 (1.7)	.65 (5.3)	1.2 (9.4)	1.25 (10.1)
	Against lam.	.28 (2.3)	.3 (2.4)	.27 (2.2)	.68 (5.5)	1.0 (8.4)	1.25 (10.1)
Coeff of thermal exp M/M-°K x 10^{-6} (in./in.-°F x 10^{-6}	With lam.	12.6 (7.0)	15.1 (8.4)	16.2 (9.0)	5.1 (2.8)		
	Against lam.	16.2 (9.0)	23.5 (13.0)	32.3 (17.9)	1.8 (1.0)		
Modulus of elasticity N/m^2 x 10^9 (psi x 10^6)	With lam.	22.6 (3.28)	10.54 (1.53)	8.54 (1.24)	9.23 (1.34)		
	Against lam.	5.86 (0.85)	3.10 (0.45)	2.96 (0.43)	3.38 (0.49)		
Tensile ult strength N/m^2 x 10^6 (psi x 10^3)	With lam.	108.17 (15.7)	102.66 (14.9)	50.99 (7.4)	17.91 (2.6)		
	Against lam.	12.75 (1.85)	6.34 (0.92)	1.03 (0.15)	1.03 (0.15)		
Interlaminar shear strength N/m^2 x 10^6 (psi x 10^3)		42.03 (6.1)	35.14 (5.1)	38.58 (5.6)	65.46 (9.5)		
Specific heat cal/gm-°K		0.19			0.14	0.31	0.50
Poisson's ratio μ		0.018	0.029	0.031	0.063		

Reference 4

TABLE C–III. – ANTARES II-B MATERIAL PROPERTIES – Concluded

Material: Fiberglass (ECG 140-801/Epon 828)

	Temperature °K (°F)	
Modulus of elasticity N/m2 x 109 (psi x 106)	295 (70)	533 (500)
Warp Dir.	48 (7.0)	21 (3.0)
Fill Dir.	28 (4.0)	14 (2.0)
Across Dir.	14 (2.0)	7 (1.0)
Interlaminar Shear Modulus N/m2 x 109 (psi x 106)	12.4 (1.8)	6.2 (.9)
Poisson's Ratio		
Warp-Fill	.10	.10
Across-Warp	.07	.07
Across-Fill	.10	.10
Coef. of Thermal Exp., m/m-°K x 10^{-6} (in/in.-°F) x 10^{-6}, Warp	3.6 (2.0)	3.6 (2.0)
Fill	9.0 (5.0)	9.0 (5.0)
Across	18.0 (10.0)	18.0 (10.0)
Tensile Strength N/m2 x 106 (psi x 103)	138 (20.)	103 (15.)
Fill	69 (10.)	48 (7.)
Across	14 (2.)	3 (.5)
Shear Strength N/m2 x 106 (psi x 103 Warp	34 (5.)	7 (1.)
Fill	34 (5.)	7 (1.)
Across	83 (12.)	69 (10.)

Reference 5

TABLE C–IV. – ANTARES II-B NOZZLE DRAWINGS AND SPECIFICATIONS

Number	Title
83136D00056	Nozzle Filament Wound Exit Cone Machining
83136D00132	Nozzle Final Machining
83136D00134	Motor Assembly 259-B4
83136D00135	Nozzle Exit Cone, Retainer Ring and Throat Insert Assembly and Machining
83136D00136	Nozzle Exit Cone and Retainer Ring Assembly and Machining
83136D00137	Nozzle Throat Insert Billet and Preliminary Machining
83136D00138	Nozzle Retainer Ring Machining
83136D00139	Nozzle Retainer Ring Molding
83136D00007	Nozzle Altitude Exit Cone Filament Winding
83136D00008	Nozzle Altitude Exit Cone Liner Machining
83136D00009	Nozzle Altitude Exit Cone Liner Molding
83136D00012	Nozzle Attachment Ring
83136D00013	Nozzle Attach Ring Forging
Spec HD-259-1-801	Nozzle Exit Cone, Tape Wrapping and Molding
Spec HD-259-1-802	Nozzle Exit Cone Filament Winding
Spec HS-259-2-186	Model Specification 259–B4
Spec HS-259-1-205	Graphite Molded for High Temperature Application
Spec HS-259-1-97	Fabric, Graphite, Impregnated Resin and Filler
Spec HS-259-1-195	Fabric, Silica, Phenolic

TABLE C-IV. – ANTARES II-B NOZZLE DRAWINGS AND SPECIFICATIONS

Number	Title
Spec HS-259-1-111	Tape, Asbestos Paper Impregnated with Phenolic Resin
MIL-A-22771	Attachment Ring
Spec HS-259-1-186	Adhesive, Thermosetting, Epoxy, Resin Base
Spec HD-259-2-168	Adhesive, Epoxy Resin, Structural Bonding
Spec HS-259-2-166	Asbestos Phenolic Compound (Compression Molded)
Spec HS-259-2-159	Cloth, Graphitized
Spec HS-259-2-158	Fabric, Woven, Vitreous Fiber, for Plastic Laminates
Spec HS-259-1-211	Roving, Glass, Continuous Filament, Twelve End
Spec HS-259-1-69	Adhesive Systems, Epoxy Resin Base
MIL-C-9084	181 Glass Cloth

TABLE C–V. – MARGINS OF SAFETY FOR PRINCIPAL STRESSES (1973 ANALYSIS)

Component (material)	Time (sec)	Principal stress (psi)	Beta (1) (deg)	Temp (°F)	Strength (psi)	Margin of safety
Throat Insert (Graphite Phenolic Tape)	5	985	14.4	73	6,000	5.1
	10	1,040	9.6	80.8	5,900	4.7
	15	850	8.8	118	5,600	5.6
	20	510	– 7.6	85.4	3,500	5.9
	27	1,710	–12.0	2022	2,300	1.4
Throat Back-up Retainer Molding (Molded Asbestos Phenolic)	5	1,620	40.7	81.7	8,900	4.5
	10	3,650	31.7	126.5	8,700	1.4
	15	4,500	18.3	197	8,300	.84
	20	3,630	1.8	108	8,800	1.4
Exit Cone Insulation (Asbestos Phenolic Paper Tape)	5	1,340	48.3	70	4,000	2.0
	10	1,345	46.5	70	4,000	2.0
	15	1,310	45.5	70	4,000	2.0
	20	1,250	43.7	70	4,000	2.2
Exit Cone Overwrap (Glass Filament and Cloth, Epoxy Resin	5	2,820	–51.8	70	4,000	.42
	10	2,760	–45.0	70	4,000	.45
	15	2,700	–41.6	70	4,000	.48
	20	2,800	–39.2	70	4,000	.43
	27	2,980	–41.1	70	4,000	.34
Exit Cone Forward Liner (Graphite Phenolic Tape)	5	630	22.5	4085	1,500	1.4
	10	1,120	22.8	3694	1,700	.52
	15	1,140	27.0	3225	1,900	.67
	20	1,040	35.5	2873	2,000	.92
	27	830	42.5	3124	1,500	.81
Exit Cone Aft Liner (Silica Phenolic Tape)	5	740	–86.1	112	2,600	2.5
	10	790	17.0	96	8,000	9.1
	15	960	14.2	89	8,500	7.9
	20	790	16.7	116	8,000	9.1
	27	690	32.3	173	5,000	6.2
Attach Ring (Aluminum)	5	17,960	87.5	70	38,000	1.1
	10	17,700	87.6	70	38,000	1.1
	15	17,420	87.5	70	38,000	1.2
	20	17,150	87.5	70	38,000	1.2
	27	16,950	87.5	70	38,000	1.2

(1) Direction of principal stress with respect to axial direction; counter clockwise is positive.

Reference 5

TABLE C–VI. – MARGINS OF SAFETY FOR SHEAR STRESSES (1973 ANALYSIS)

Component (material)	Time (sec)	Shear stress (psi)	Temp (^{O}F	Shear strength (psi)	Margin of safety
Throat Insert (Graphite Phenolic Tape)	5	2500.	520	2950.	.18
	10	1880.	667.	2500.	.32
	15	2350.	646	2550.	.08
	20	2150.	491.	3000.	.40
	27	2280.	567.	2900.	.27
Throat Back-Up – Retainer Molding (Molded Asbestos Phenolic)	5	2150.	70.	6800.	2.2
	10	2290.	283.	5250.	1.3
	15	2300.	462.	4350.	.89
	20	1750.	517.	4150.	1.4
	27	1420.	452.	4350.	2.1
Exit Cone Insulation (Asbestos Phenolic Paper Tape)	5	975.	70.	6100.	6.3
	10	1000.	70.	6100.	5.1
	15	980.	70.	6100.	5.2
	20	940.	70.	6100.	5.5
	27	940.	70.	6100.	5.5
Exit Cone Overwrap (Glass Filament and Cloth, Epoxy Resin)	5	990.	70.	5000.	4.1
	10	1005.	70.	5000.	4.0
	15	980.	70.	5000.	4.1
	20	920.	70.	5000.	4.4
	27	910.	70.	5000.	4.5
Exit Cone Forward Liner (Graphite Phenolic Tape)	5	860.	367.	4000.	3.7
	10	860.	495.	3000.	2.5
	15	780.	773.	1800.	1.3
	20	740.	1200.	1000.	.35
	27	580	3124.	850.	.46
Exit Cone Aft Liner (Silica Phenolic Tape)	5	190.	73.	7000.	.10
	10	210.	96.	6900.	10
	15	240	106.	6600.	10
	20	150.	148.	6300.	10
	27	90.	233.	5000.	10
Attach Ring (Aluminum)	5	6300.	70.	25000.	3.0
	10	6230.	70.	25000.	3.0
	15	6150.	70.	25000.	3.1
	20	6090.	70.	25000.	3.1
	27	6040.	70.	25000.	3.1

Reference 5

TABLE C–VII. – MARGINS OF SAFETY FOR HOOP STRESSES (1973 ANALYSIS)

Component (material)	Time (sec)	Hoop stress (psi)	Temp (°F)	Hoop strength (psi)	Margin of safety
Throat Insert (Graphite Phenolic Tape)	5	20	2978	8,500	10
	10	40	74	23,000	10
	15	135	73	23,000	10
	20	490	382	17,150	10
	27	230	92	22,500	10
Throat Back-up Retainer Molding (Molded Asbestos Phenolic)	5	1500	70	9,000	5.00
	10	870	71.5	9,000	9.3
	15	1430	77	9,000	5.3
	20	1740	108	8,800	4.1
	27	1800	92	8,850	3.9
Exit Cone Insulation (Asbestos Phenolic Paper Tape)	5	1640	70	15,700	8.6
	10	2130	70	15,700	6.4
	15	2500	71	15,700	5.3
	20	2500	75.3	15,700	5.3
	27	2350	77.7	15,600	5.6
Exit Cone Overwrap (Glass Filament and Cloth, Epoxy Resin)	5	3275	70	20,000	5.1
	10	4380	70	20,000	3.6
	15	5400	70	20,000	2.7
	20	5600	70	20,000	2.6
	27	5580	72.5	20,000	2.6
Exit Cone Forward Liner (Graphite Phenolic Tape)	5	Compression	–	–	–
	10	Compression	–	–	–
	15	Compression	–	–	–
	20	Compression	–	–	–
	27	1010	3016	7,200	6.1
Exit Cone Aft Liner (Silica Phenolic Tape	5	900	70	24,000	10
	10	1170	75	24,000	10
	15	1330	89	23,500	10
	20	1230	116	22,500	10
	27	670	173	20,500	10
Attach Ring (Aluminum)	5	10,400	70	38,000	2.7
	10	10,700	70	38,000	2.6
	15	10,920	70	38,000	2.5
	20	11,260	70	38,000	2.4
	27	11,600	70	38,000	2.3

Reference 5

TABLE C-VIII. – X259 ANTARES IIB NOZZLE ANALYSIS MINIMUM MARGIN OF SAFETY SUMMARY WITH NOMINAL PROPERTIES FOR FINAL ANALYSIS

Part/material	Time (sec)	Minimum margins of safety				
		Major principal (de failure criteria) (1)	Circumferential (max stress failure criteria)	Parallel-to-plies (max stress failure criteria)	Across-plies (max stress failure criteria)	Interlamination shear (interlaminar shear criteria)
Throat/insert/ MXG-175	2	1.266	Compressive	276.841	1.293	5.853
	5	1.108	Compressive	56.699	1.164	6.689
	8	0.054	Compressive	35.590	0.033	5.409
	20	0.380	Compressive	34.815	0.255	5.507
	27	– 0.270	119.137	24.456	–0.281	3.509
Forward exit cone liner/ MX2630A	2	38.350	34.523	61.287	Compressive	5.298
	5	Compressive	108.143	Compressive	Compressive	5.262
	8	0.420	Compressive	85.649	0.419	4.880
	20	Charred	Charred	Charred	Charred	Charred
	27	Charred	Charred	Charred	Charred	Charred
Throat retainer/ RPD-150	2	0.537	3.138	0.289	1.781	0.383
	5	1.353	3.379	4.818	2.022	0.816
	8	2.000	3.448	4.819	2.237	0.518
	20	2.711	4.081	4.878	3.428	0.576
	27	2.200	4.266	1.569	2.692	1.107
Exit cone insulation/ Tayleron PA-6	2	1.162	7.110	17.020	1.151	11.269
	5	1.435	7.440	9.746	1.408	10.198
	8	1.802	7.344	9.758	1.726	9.474
	20	0.521	5.617	5.548	0.568	4.478
	27	0.162	5.969	5.693	0.171	3.136
Exit cone overwrap/ glass-epoxy filament wound	2	– 0.230	4.079	2.078	– 0.233	2.864
	5	–0.156	4.224	2.702	– 0.160	3.258
	8	–0.099	2.679	2.413	– 0.116	3.408
	20	1.221	0.290	– 0.070	0.083	3.975
	27	1.612	– 0.054	– 0.484	0.572	5.798
Attach ring/ aluminum	2	4.305	5.637	4.114	3.003	5.899
	5	4.403	5.770	4.194	3.084	6.021
	8	4.500	5.784	4.307	3.166	6.174
	20	6.023	7.054	5.965	4.379	8.379
	27	8.598	9.919	8.530	6.361	11.850
Aft exit cone liner/MX2600	2	5.235	33.751	19.776	21.142	4.336
	5	3.791	30.155	17.675	9.284	4.269
	8	1.120	36.494	366.677	2.833	3.438
	20	0.443	Compressive	Compressive	0.927	1.580
	27	0.284	Compressive	Compressive	1.025	1.462

Reference 16

(1) de = distortional energy (failure criteria)